Peer-to-Peer Trading for Enhancing Electric Vehicle Charging with Renewable Energy

HUW ROBERT THOMAS

Peer-to-Peer Trading for Enhancing Electric Vehicle Charging with Renewable Energy

Huw R. Thomas

A Thesis presented for the degree of
Doctor of Philosophy

Department of Engineering
Durham University
United Kingdom

May 2023

Peer-to-Peer Trading for Enhancing Electric Vehicle Charging with Renewable Energy

Huw R. Thomas

Submitted for the degree of Doctor of Philosophy

May 2023

Abstract: Electric vehicles (EVs) are rapidly increasing in popularity as greater attention is paid to climate change and decarbonisation, however the environmental benefits that EVs offer can only be fully realised through the use of renewable energy for their charging. Smart charging solutions are essential for managing the impact of EVs and increasing the utilisation of renewable energy, however, questions remain over whether low-voltage distribution networks can accommodate the upcoming increases in EV charging demand.

This thesis addresses both the challenge of increasing the utilisation of renewable energy for EV charging and also the importance of ensuring safe operation of low-voltage distribution networks with the integration of EV charging, distributed renewable energy generation, battery storage and vehicle-to-grid technologies.

Chapter 3 examines a scenario where houses equipped with solar photovoltaic panels and EV charge points endeavour to sell surplus solar energy and the use of their EV charge point to visiting EVs that require charging. A peer-to-peer auction is proposed, with a novel matching mechanism presented to increase the amount of EV charging completed using solar energy without any knowledge about future EV arrivals.

Chapter 4 presents a full peer-to-peer trading model of Network Impact Tokens and Phase Impact Tokens between houses in a low-voltage network. The Impact Tokens guarantee that all EV charging and renewable energy generation does not cause the network to exceed its voltage, current or transformer loading limits, while ensuring each house retains control over its energy usage, requiring no real-time monitoring or sensors in the network, and no privacy issues are encountered.

The Network and Phase Impact Token approach is further verified in Chapter 5, as it forms the basis of a novel approach for Distribution System Operators to evaluate the maximum EV hosting capacity of their networks in conjunction with renewable energy generation and battery storage. The maximum EV capacity results are verified by an alternate Optimisation approach and the maximum EV penetration is evaluated for a number of scenarios.

Declaration

The work in this thesis is based on research carried out in the Department of Engineering at Durham University. No part of this thesis has been submitted elsewhere for any degree or qualification.

This thesis is dedicated to

Mum and Dad

For all the love, encouragement
and support that you have given,
and that I know you always will.

Acknowledgements

This PhD has probably been the toughest four years of my life, and I couldn't have accomplished everything if it wasn't thanks to a number of people.

Firstly, to my supervisor, Professor Hongjian Sun. Back in the Summer of 2017, when I suddenly had to pick a new project for my Master's dissertation a month before starting, if you hadn't agreed to take me as an extra student working with you on an electric vehicle charging project, I would almost certainly be doing something completely different right now. Since then, you have given me the opportunities to pursue the topics I was most passionate about and the freedom to achieve a PhD that I can be really proud of. Your support, guidance, willingness to listen to my ideas and problems and help to keep everything on track has been invaluable.

Also, to Dr Kazemtabrizi, as the topic of my research evolved into the analysis of power networks, your expertise in the field, the feedback and encouragement you have given has been essential and especially welcomed.

To all of my friends and colleagues in the Engineering department, it has been so great to getting to know all of you, and having people to talk to about both the best and worst parts of the PhD! The opportunities to discuss ideas, hear about everyone's work and study alongside all of you have had a profound impact on my own work, helping me to develop my own ideas and really get the most from my time here. Many thanks to the Hamilton HPC service at Durham University, with the use of Hamilton essential to the completion of this thesis.

I would like to thank Josephine Butler College for making my time in Durham so

enjoyable. From all the friends I've made, to all the opportunities that I have been lucky to receive in my nine years at Durham, Josephine Butler College has been the foundation of my favourite memories. The chance to play and enjoy so much lacrosse and badminton, and the opportunity to work alongside college and university staff and make a real difference to the experiences of other students through the role of MCR president have given me skills and experiences I will remember forever.

To Rob and Melonie, the last few years have been so tough, thank you for all the support and everything you do to help. Finally, to my parents, I couldn't have done any of this without the love, support, advice and encouragement that you gave. Thank you for helping me to pursue my own dreams, to stay true to myself and make the best decisions in life. I know how proud you would be.

Contents

Abstract **iii**

List of Figures **xvii**

List of Tables **xxiii**

1 Introduction **1**

1.1 Research Challenges 1

1.2 Key Contributions and Thesis Outline 3

1.3 Thesis Publications 7

2 Background and Literature **9**

2.1 Background to Electric Vehicle and Charging Technology and Challenges 9

2.1.1 Carbon Emissions, Climate Change and Government Policy . 10

2.1.2 Introduction to Electric Vehicles 12

2.1.3 EV Charging 14

2.2 The Grid 18

2.2.1 Grid Structure 18

2.2.2 The Distribution Network 19

2.2.3 Solving Network Power Flow with the Backward-Forward Sweep 21

2.2.4 The Future Grid 25
2.3 Smart Charging 27
2.3.1 Key Concepts 29
2.3.2 Smart Charging Objectives 34
2.3.3 Maximising EV Penetration in the Distribution Network . . 41
2.3.4 Summary 46
2.4 Peer-to-Peer Energy Trading 47
2.4.1 P2P Trading and Network Constraints 49
2.4.2 Facilitating Peer-to-Peer Trading Through Auctions . . . 51
2.4.3 Peer-to-Peer Trading with Electric Vehicles and Renewable Energy 56
2.4.4 Summary 58
2.5 Conclusion 59

3 Closest Energy Matching Mechanism 63

3.1 Introduction 63
3.2 Double Auction Matching Mechanisms 66
3.2.1 One-to-One Matching vs Many-to-Many Matching 69
3.2.2 Determining the Bid and Ask Price 70
3.2.3 Auction Matching Mechanisms 76
3.3 Solving the Mechanism Optimisation Problems 83
3.3.1 MARMES 83
3.4 Results and Discussion 86
3.4.1 Case Study 86
3.4.2 Results 89
3.5 Conclusion 98

4 Peer-to-Peer Trading of Impact Tokens for Managing Network Capacity 101

4.1 Introduction 102

4.2 Network Models, Load Profiles and Study Parameters 104

4.2.1 Distribution Network Models 104

4.2.2 Load Profiles 105

4.2.3 Study Design 106

4.3 Fundamental Concepts 107

4.3.1 Network Initialisation and Power Flow Studies 108

4.3.2 Network Load Capacity 111

4.3.3 Impact Values and Impact Tokens 113

4.3.4 NITs and PITs Used in P2P Trading 118

4.4 Peer-to-Peer Trading Methodology 119

4.4.1 Energy Resource Planning 120

4.4.2 P2P Market Structure 130

4.4.3 Submitting Bids and Asks 132

4.4.4 P2P Market Mechanism and Matching Result 133

4.4.5 Market Operator Trades 137

4.4.6 Transaction Log 138

4.4.7 Finalise Energy Resource Usage 140

4.4.8 Seller-Led Market 141

4.4.9 Buyer-Led Market 144

4.4.10 Summary 147

4.5 Results and Discussion 147

4.5.1 Analysis of Network Limits 148
4.5.2 Comparison with Uncontrolled Loads and Generation . . . 150
4.5.3 Load and Generation Profiles 152
4.5.4 Economic Analysis 155
4.5.5 Analysis of Seller-led and Buyer-led Markets 157
4.5.6 Successful EV Charging with Varying DG Penetration . . . 160
4.5.7 Comparison with Alternative Approaches 163
4.6 Conclusion 165

5 Determining the Hosting Capacity of Electric Vehicles 169

5.1 Introduction 170
5.2 Optimisation Approach 171
5.2.1 Optimisation Problem 172
5.3 Network Impact Token Approach 178
5.3.1 Network and Phase Impact Tokens for Calculating the Maximum EV Penetration 179
5.4 Network Models, Load Profiles and Study Parameters 180
5.4.1 Distribution Network Models 180
5.4.2 Load Profiles 182
5.4.3 Study Design 186
5.5 Results and Discussion 188
5.5.1 Network 1: Verification of Network Impact Token Approach 188
5.5.2 Network 1: Speed Comparison Between Optimisation and NIT Approaches 192
5.5.3 Network 1: Comparison in EV Hosting Capacity Calculation Methods 196

5.5.4 Network 1: Other Results 198

5.5.5 Network 2: NIT Verification Results 205

5.6 Conclusion 208

6 Conclusions **213**

6.1 Achieved Research Goals 214

6.1.1 Chapter 3 214

6.1.2 Chapter 4 216

6.1.3 Chapter 5 218

6.2 Future Research 220

6.2.1 Inclusion of Reactive Power into Impact Values/Tokens . . 220

6.2.2 Further Improvement to EV Charging Success in P2P Impact Token Approach 220

6.2.3 Implementation of P2P Trading of Impact Tokens in Multi-Feeder Networks 221

6.2.4 Dealing with Error in Energy Usage Prediction and Missed Communication 222

6.2.5 Improving the Accuracy of the NIT Approach for Calculating the Maximum EV Penetration at Higher Penetrations of DG 222

List of Figures

1.1 This flowchart presents the key concepts introduced in each chapter of this thesis and explores the links between each concept 4

2.1 A simple 6 bus, 5 line radial network 20

2.2 Current and impedance diagram for nodal analysis of a network bus 22

2.3 Examples of domestic baseload without EV charging, valley filling and peak shaving 36

2.4 Example supply and demand curves constructed from double auction bids and asks. The dotted lines show the auction clearing price and clearing quantity 52

3.1 Effect of bid price on buyer gain for three different values of buyer valuation v_i 75

3.2 Schematic representation of the case study 88

3.3 Distribution of departure SoC gain showing the percentage of EVs departing with SoC gain in different ranges for each of the 5 mechanisms based on charging from the available solar energy. It is clear from the light blue bars that the majority of EVs will depart with all required energy for all mechanisms 90

3.4 Grid energy required at each repeat to satisfy all EV charging requests 92

3.5 Sensitivity analysis showing the effect of incorrect solar energy prediction and varying the ratio of EVs to houses on the average solar charge gained by EVs 93

3.6 Percentage of the total surplus solar energy available from houses traded through the auction using each mechanism 95

3.7 Average trade price agreed under each mechanism 96

3.8 Average cost per buyer to fully charge EV, and average profit per seller with each auction mechanism 97

4.1 Line diagram of the low-voltage distribution network used in this study 105

4.2 The proposed P2P trading approach of Network and Phase Impact Tokens is presented schematically, including the DSO initialisation stage and P2P trading stages 108

4.3 Flow diagram showing the sources and usage of each of the optimisation variables used in the energy resource planning stage. Pink lines identify variables representing power (kW), blue lines identify NITs and green lines identify PITs 122

4.4 Comparison of intersection scenarios 1 and 2 134

4.5 Transformer loading, line currents and node voltages from scenario 1 showing that the proposed P2P trading approach ensures that each is kept within its permitted limits 149

4.6 Transformer loading, line currents and node voltages from scenario 2 150

4.7 Transformer loading, line currents and node voltages from scenario 3 151

4.8 A comparison of the transformer loading, line currents and node voltages between the P2P trading of Impact Tokens and uncontrolled loads and generation, showing the importance of managing load in a network 152

4.9 Total power generation and consumption in the network for Summer and Winter scenarios 153

4.10 Power generation and consumption for two individual houses showing the different load profiles achieved through the P2P trading of Impact Tokens 154

4.11 Total daily cost or income of each houses through P2P trading, with houses categorised by types of DERs 156

4.12 Stacked bar chart showing the number of NITs and PITs offered for sale on seller-led market and number of ITs traded at each timestep 158

4.13 Stacked bar chart showing the number of NITs and PITs requested on buyer-led market and number of ITs traded at each timestep . . 159

4.14 Percentage of EVs meeting their desired SoC goal at their departure with varying penetrations of EV and DG 161

4.15 Comparison of the percentage of EVs which acheive their departure SoC as the penetration of EVs increases under three different control strategies: P2P trading of Impact Tokens, ESPRIT network monitoring and a centralised optimisation 164

5.1 Line diagram of the IEEE Low Voltage Test Feeder 181

5.2 Line diagram of Network 2 182

5.3 Distributions of Summer energy resource profiles 185

5.4 Distributions of Winter energy resource profiles 186

5.5 Distribution of maximum penetration of EVs calculated in Monte Carlo simulation with no houses equipped with solar PV or battery storage 188

5.6 Distribution of maximum penetration of EVs with V2G enabled and 50% of houses equipped with solar PV and battery storage 189

5.7 Distribution of maximum penetration of EVs with 100% of houses equipped with solar PV and battery storage 189

5.8 Distribution of difference in EV penetration calculated between Optimisation and NIT approaches for 0% DG scenario 192

5.9 Distribution of difference in EV penetration calculated between Optimisation and NIT approaches for 50% DG & V2G scenario . . . 193

5.10 Distribution of difference in EV penetration calculated between Optimisation and NIT approaches for 100% DG scenario 193

5.11 The maximum EV penetration of the network calculated using three different methods is compared for increasing levels of DG penetration 197

5.12 Comparison of the maximum EV penetration calculated through the three approaches with increasing penetration of solar PV but no battery storage 199

5.13 The maximum EV penetration for the network is calculated as the penetration of houses equipped with solar PV and battery storage increases from 0% to 100%, both with and without the use of V2G . 200

5.14 The maximum EV penetration for the network is calculated for both Summer and Winter load and PV data as the penetration of houses equipped with solar PV and battery storage increases 201

5.15 Varying the capacity of the house's installed battery if equipped with solar PV panels can have a big impact on the maximum EV hosting capacity in Summer 202

5.16 With Winter solar energy generation, the benefit of increasing the house's battery capacity on the EV capacity is reduced 203

5.17 Increasing the maximum transformer power and line current ratings can have a substantial impact on the maximum EV penetration . . 205

5.18 Colour coded map of Network 1 highlighting the houses with highest and lowest EV charging success from Monte Carlo simulation . . . 206

5.19 Distribution of maximum EV penetrations from Monte Carlo simulation for Network 2 without solar PV and battery storage 207

5.20 Distribution of maximum EV penetrations for Network 2 with 50% of houses equipped with solar PV, battery storage and the use of V2G 208

5.21 Distribution of maximum EV penetrations for Network 2 with 100% of houses equipped with solar PV and battery storage 209

List of Tables

2.1 UK EV Charging Standards 17

3.1 ILP solver algorithm comparison 86

3.2 Simulation Parameters 87

3.3 EV charge gained by departure. For each mechanism, the mean charge of all EVs on departure is shown, along with the percentage of EVs that depart with SoC gain in three specified ranges 91

3.4 Financial benefit of P2P trading 98

4.1 Network Constraints 105

4.2 P2P planning optimisation variables - χ_{P2P} 124

4.3 EV Charging Success, With and Without Buyer- and Seller-led Markets 157

5.1 Network 1 Constraints 181

5.2 Network 2 Constraints 182

5.3 Key statistics from EV penetration calculations 191

5.4 Average time per repeat of Monte Carlo simulation for Optimisation and NIT approaches 194

5.5 Run time and memory usage comparison for 1000 repeat Monte Carlo simulation 195

5.6 Network 2 verification of maximum EV penetration calculated by NIT approach 210

Chapter 1

Introduction

1.1 Research Challenges

Back in 2018, at the start of the research for this PhD Thesis, there were 45,000 electric vehicles (EVs) registered in the UK. Now, four years later there are 494,000, and the numbers continue to grow at an ever increasing pace. Unprecedented rises in carbon dioxide, nitrous oxide and other greenhouse gas emissions over the past hundred years have resulted in noticeable changes to our planet's climate and environment, and increasing awareness and concern for the future has necessitated a shift in government policy and consumer mindset towards more sustainable zero-emission vehicles. With over 6 million UK households planning to purchase an EV by 2030, and the sale of new petrol and diesel vehicles banned from the same year, the number of electric vehicles on the roads is set to increase exponentially [1][2]. Significant research is required in order to overcome the technical and societal challenges that will be faced in order to achieve the largest transportation revolution in a century.

EV charging increases the power demand on electricity generation and distribution networks to levels far in excess of their initial design specifications. The energy distribution landscape is rapidly evolving, with the implementation of smart grids, islanded microgrids, and an increasing penetration of distributed energy resources

(DERs), such as small-scale solar photovoltaic (PV) panels and battery storage. An increase in renewable energy generation, through DERs, large solar farms, off-shore wind farms and hydroelectricity plants are essential for fulfilling the green credentials of EVs and accomplishing the decarbonisation objectives. More research is needed into new methods of managing EV charging and maximising the utilisation of existing grid infrastructure and renewable energy generation for the uptake of EVs to be successful.

A key concern is that people will return home from work and all plug their EVs in to charge at the same time, leading to a huge spike in power which can cause serious problems for electricity networks. Smart charging techniques are essential for maximising the amount of EV charging that can take place, and have been widely studied across existing literature. Smart charging objectives can include minimising the total charging cost, maximising the utilisation of renewable energy generation or providing support to the grid, such as through the shifting of loads to off-peak times, frequency response or maximising the amount of charging that can be completed. With the driving range of EVs and lack of charging infrastructure among the key concerns of potential consumers, it is essential that additional research is conducted to ensure that the power networks can accommodate the required EV charging in order to alleviate these concerns [3].

While centralised and decentralised optimisation based systems can maximise the EV charging completed and usage of electrical networks and renewable energy, the loss of autonomy through having loads centrally controlled, and loss of privacy through the required sharing of load information can be problematic. Peer-to-peer (P2P) trading is able to solve some of these issues by offering a decentralised platform where participants retain more control over their power usage, while also helping to preserve privacy.

This thesis explores the benefits that P2P trading can provide to EV charging, from how solar energy consumption can be increased, to how the use of low-voltage networks can be managed in order to ensure that EV charging doesn't exceed network

operating limits. The main research questions that this thesis aims to address are as follows:

1. How can DERs such as solar PV generation, battery storage and V2G be utilised to maximise the amount of EV charging that can be successfully accommodated by a low-voltage distribution network?

2. How can the impact of EV charging be quantified to facilitate novel load management strategies and the calculation of the EV hosting capacity subject to all network limits?

3. What EV smart charging solutions can be developed to support network operation without resulting in a loss of autonomy or privacy for individual energy prosumers, while maintaining real-world viability, including the use of online information, decentralised computation and minimised hardware deployment?

4. What advantages can peer-to-peer trading offer to support EV charging and DER integration offer over alternative centralised and decentralised approaches?

1.2 Key Contributions and Thesis Outline

The main body of this thesis is divided into five chapters, with the main topics of each chapter and the key contributions each makes towards solving the aforementioned challenges expressed here, and shown in Figure 1.1.

Chapter 2 - Background and Literature

Chapter 2 contains an introductory synopsis of the key topics followed by a detailed literature study of relevant research. Background information is provided on electric vehicle charging, the UK's electrical distribution networks and the environmental and legislative factors behind this transition to zero-emission vehicles as a basis for understanding and explaining the challenges explored in the current literature and the shortcomings contained.

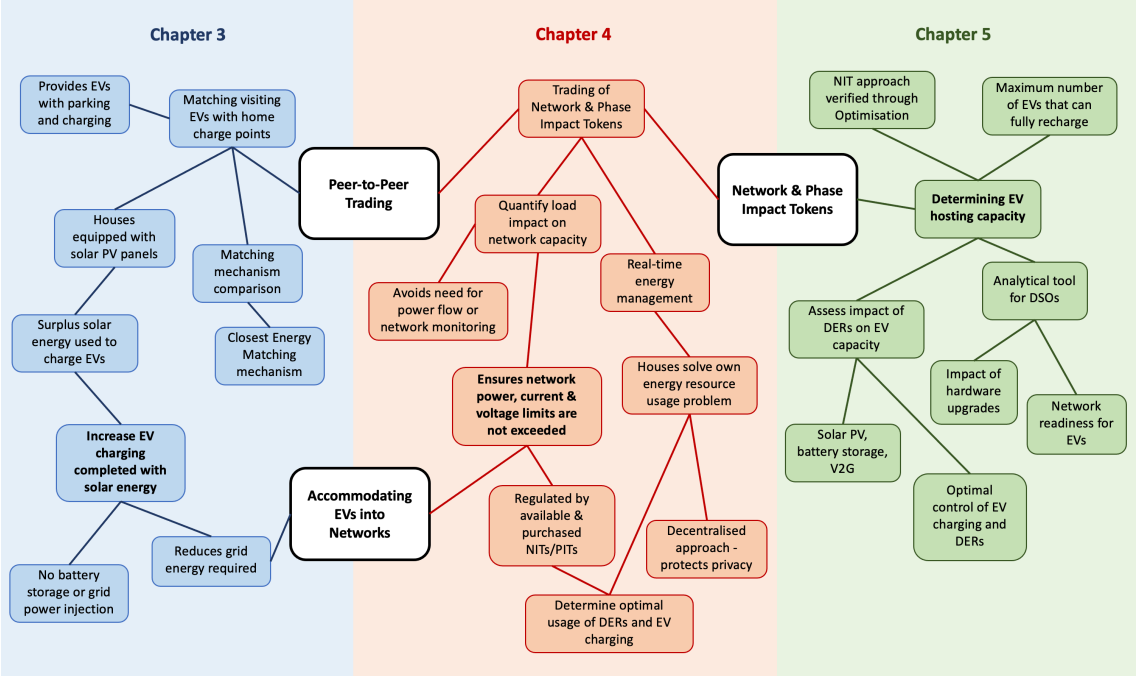

Figure 1.1: This flowchart presents the key concepts introduced in each chapter of this thesis and explores the links between each concept

Chapter 3 - Closest Energy Matching Mechanism

This chapter introduces the idea of visiting EVs using vacant home charge points during the day to provide a charging solution while also utilising any solar energy produced by the home's solar PV panels. A peer-to-peer trading problem is presented for matching the visiting EVs with home charge points. A detailed comparison is made between the proposed Closest Energy Matching mechanism and four other mechanisms to evaluate its performance for both buyers and sellers in terms of energy traded, EV charge achieved and economic benefit.

- A novel double auction matching mechanism, Closest Energy Matching (CEM), is developed to match EV owners requiring charging with households selling surplus solar energy. The matching algorithm benefits both energy producers and EV owners by maximising the amount of charge EVs receive from renewable energy and increasing seller profits

- One-to-one matching is enforced as each house is only able to charge a single

EV, and therefore the quality of the matching has significant impact on the amount of solar energy a house sells and the charge an EV receives. The CEM mechanism results in more optimal matchings for houses and EVs during an auction without any knowledge of future EV energy requests in later timesteps

Chapter 4 - Peer-to-Peer Trading of Impact Tokens for Managing Network Capacity

The concept of Network Impact Tokens and Phase Impact Tokens are introduced in this chapter which represent the capacity to accommodate load in the entire network and on each phase. The P2P trading of these Impact Tokens between houses in a network is proposed, which allows houses to manage their electricity consumption and generation while taking into account their impact on the network. Studies are conducted to evaluate the ability of the proposed P2P trading to increase EV charging while ensuring that no grid voltage, current or transformer limits are exceeded.

- The novel Network Impact Token (NIT) and Phase Impact Token (PIT) approach is introduced to quantify the effects of power generation and consumption on a low-voltage distribution network based on the load capacity of the network

- Peer-to-peer (P2P) trading of the NITs and PITs is proposed which allows houses to manage their impact on the network from baseload usage, EV charging, solar energy generation, battery storage and vehicle-to-grid (V2G)

- It is shown that the trading of Impact Tokens ensures that the network does not exceed its permitted bus voltage, line current or transformer loading limits, while maintaining privacy and ensuring houses retain significant control over their own electricity consumption and generation

Chapter 5 - Determining the Hosting Capacity of Electric Vehicles

This chapter expands on the use of the Network and Phase Impact Tokens introduced in Chapter 4 by using the concept in order to calculate the maximum penetration of EVs that could be accommodated within a distribution network given the network's voltage, current and power limits. A Monte Carlo simulation is performed to evaluate the network's representative maximum penetration as baseload, EV charging requirements and solar energy generation varies. The results from the NIT approach are compared with those generated by an equivalent optimisation problem including all network constraints for two separate networks, which verifies the accuracy and validity of the NIT approach. Analysis of one network is completed to show how the maximum EV hosting capacity is influenced by the amount of installed solar generation and battery storage, the seasonal effect on baseload and solar generation as well as the current and power limits of the installed network hardware.

- The NITs and PITs are used as the basis of a novel approach allowing network operators to calculate the maximum penetration of electric vehicles that can be accommodated in a network, including the use of solar energy generation, battery storage and V2G. The NIT approach is verified by an equivalent Optimisation approach, and is shown to calculate accurate results for two different networks
- Detailed analysis of the maximum EV penetration of a network is presented, including the maximum penetration as the amount of installed solar generation and battery storage varies, the impact of loads and solar generation in Summer and Winter, in addition to the effect of upgrading the transformer power or line current limits

Chapter 6 - Conclusion

Chapter 6 offers a conclusion to this thesis by summarising the main challenges, developed research contributions and key results, and suggests additional extensions

for future study.

1.3 Thesis Publications

- Closest Energy Matching: Improving peer-to-peer energy trading auctions for EV owners. H. Thomas, H. Sun, B. Kazemtabrizi. IET Smart Grid, Vol 4, 2021
- Calculating the Maximum Penetration of Electric Vehicles in Distribution Networks with Renewable Energy and V2G. H. Thomas, H. Sun, B. Kazemtabrizi. 2023 IEEE Innovative Smart Grid Technologies (ISGT), Abu Dhabi, Middle East, 2023

Chapter 2

Background and Literature

This chapter provides essential background theory around the challenges with electric vehicle charging, and a thorough examination of current literature on the key topics tackled by this thesis. This chapter is split into four sections: Section 2.1 provides a background to the reasons necessitating the switch to zero-emission EVs, current EV trends, and the basics of EV charging. The structure of the electricity grid is presented in 2.2, including a derivation of the power flow equations. Smart grids, distributed energy resources and other technologies are introduced in more detail, and the impacts of EV charging on the grid are analysed. Section 2.3 explains the concept of EV smart charging and evaluates the key developments and shortcomings in current literature. Section 2.4 introduces peer-to-peer (P2P) trading and auction mechanisms for facilitating trades.

2.1 Background to Electric Vehicle and Charging Technology and Challenges

This section explores the global climate crisis and the role that transport plays within it, and examines resultant government policies that are driving the switch to EVs. A brief overview of EV technology is provided along with discussion about key

trends within the market, the challenges holding back uptake, and future growth. Finally, EV charging is introduced and the main technological and behavioural aspects discussed.

2.1.1 Carbon Emissions, Climate Change and Government Policy

Increasing evidence of climate change and growing concerns for the future welfare of our planet are leading calls for faster and more significant action to reduce global warming. The Intergovernmental Panel on Climate Change's 2021 Sixth Assessment Report concluded that it is "unequivocal that human influence has warmed the atmosphere, ocean and land", with global surface temperatures in the past decade over 1°C higher than at the end of the 19th century, and that global warming will exceed 2°C by the end of the 21st century unless significant reductions in emissions occurs [4].

Emissions of greenhouse gases, such as carbon dioxide (CO_2), methane (CH_4) and nitrous oxide (NOx) become trapped in the Earth's atmosphere, and are widely attributed as the primary cause of climate change [5]. CO_2 emissions have been rising globally since the industrial revolutions in the 1800s, before peaking in the UK around 1990 and have since fallen to about 60% of this peak value. However, global CO_2 emissions are still rising in some parts of the world, such as in Asia, which currently contributes over 55% of total global emissions [6].

With 27% of the UK's annual CO_2 emissions produced by transport, and cars alone accounting for 15%, it is recognised that the decarbonisation of transport is a significant factor in tackling carbon emissions [7][8].

While EVs are zero-emission at the point of use, additional electricity generation is required for their charging, and using non-renewable forms of energy generation instead results in a shift of emissions from vehicle exhaust pipes to the sites of power generation. In addition, the extraction and processing of lithium and rare-earth

metals used in EV batteries and motors has detrimental environmental impacts. Numerous studies have tried to assess the relative environmental impacts of EVs against internal combustion engine vehicles (ICEVs). A 2021 study by the International Council on Clean Transportation showed that in Europe, EV life-cycle emissions are currently 66-69% lower than that of an equivalent ICEV. However, in countries with a heavier reliance on coal for electricity generation such as India and China, the reduction in emissions can be as little as 20-45% [9]. The UK is making progress with the decarbonisation of its electricity generation: in 2000, the UK generated 31% of its electricity from coal, 39% from gas, and only 2% from hydro, wind and solar, whereas by 2021, this had become <2% from coal, 38% from gas and 37% from renewables (excluding nuclear) [10]. As renewable energy generation increases, the switch to EVs will provide greater reductions in emissions.

Ambitious targets have been set to limit climate change. The Paris Agreement, signed between 196 parties in 2015, is a legally binding international treaty with the goal of limiting global warming to below 2 degrees through individually agreed goals and actions [11]. In 2021, the UK set into law the world's most ambitious climate change policy, through the Sixth Carbon Budget, with the goal to cut emissions by 78% from 1990 levels by 2035 and achieve net zero by 2050 [12].

To accomplish these goals, a number of policies regulating the use of ICEVs have been instigated. Low, Ultra Low and Zero Emission Zones have been introduced in some of the UK's major cities including London, Oxford, Birmingham and Bath, to reduce traffic and emissions through a daily charge, and an upcoming ban on the sale of new ICEVs has been announced. Over 20 countries have announced forms of limitations or bans on the sale of new ICE vehicles between 2025 and 2040. Norway has one of the most aggressive strategies for transitioning to EVs, being the first country to ban the sale of all new petrol and diesel cars from 2025, and has seen considerable EV uptake, with EVs comprising 54% of new vehicle sales in 2020 [13]. In the UK, a ban on the sale of petrol and diesel vehicles, including hybrids, is in place from 2030, although the sales of hybrids capable of travelling a "significant"

distance with zero emissions can continue until 2035 [2].

2.1.2 Introduction to Electric Vehicles

In this thesis, the term *electric vehicle* refers to fully electric cars, typically parked at home overnight and used for social, domestic and commuting purposes. While the electrification of other road vehicles, including motorcycles, commercial vans and heavy goods vehicles is progressing, these are beyond the scope of this thesis. Similarly, while other forms of electrification exist, including electrical assistance (mild hybrid), and vehicles that can travel short distances on electricity alone, with ICEs for longer journeys (hybrid and plug-in hybrid), only fully electric battery EVs are considered here, as their lack of ICE makes them completely zero emission.

With a typical battery capacity of 50-120 kWh, EVs can have a range of up to 450 miles [14], although ranges of 220-320 miles are currently most common. EVs can regain charge through regenerative braking, where by changing the quadrant of motor operation from I to II, the motor acts as a generator, recharging the battery and slowing the vehicle through the conversion of kinetic energy, however, dedicated EV charge points are essential for recharging EV batteries in an appropriate time frame.

In the UK, car travel accounts for 79% of the 328 billion vehicle miles travelled in 2019 [15], with over 78% of households in the UK owning a car [16], so this represents the greatest opportunity for transport decarbonisation yet also offers some of the biggest challenges, opportunities and solutions that can revolutionise the generation and consumption of energy in future.

The transition to EVs is well underway, with electric vehicles accounting for 11.5% of all new UK car registrations in 2021, compared to just 0.7% in 2018 [17]. However, this still represents just 1.2% of the total number of cars on the road [18], showing that there is still a long road to fully decarbonise transport. With the number of EVs on the road set to grow exponentially over the coming years, the challenges

surrounding their implementation and utilisation could be further exacerbated.

Research by Ofgem has shown that 6.5 million UK households (∼25%) plan to buy an EV or hybrid within the next five years, while 38% say that they would not consider an EV, primarily as costs are currently perceived to be too high [1]. With the EV's battery accounting for around 30% of its total cost, reducing the cost of batteries is essential to achieving EV affordability and increasing uptake further. Many experts put the average price of a battery pack to achieve price parity with an equivalent ICEV at $100/kWh. Between 2010 and 2020, BloombergNEF have found that the cost of a lithium-ion battery pack has decreased by 89%, from $1,110/kWh to $137/kWh, with the price of $100/kWh expected to be reached between 2023 and 2024 [19]. In order for the UK to meet its Sixth Carbon Budget emission reduction obligations, it is estimated that there would need to be at least 23.2 million EVs on UK roads (55% of all vehicles), and all new vehicle sales must be zero-emission by 2032. To achieve net zero targets by 2050, all 49 million vehicles would have to be zero emission [20].

Whilst the popularity of EVs is undoubtedly growing, key customer perceptions still hold back their uptake. Research from Deloitte shows that driving range, lack of charging infrastructure and time to charge are the greatest concerns for consumers, accounting for 71% of surveyed consumers' concerns [3].

EV development is rapidly advancing, and ranges greater than 300 miles are now common among premium vehicles, with the Mercedes EQS currently offering the longest range available of 450 miles [14]. However, these quoted ranges are often optimistic based on real life driving conditions and can be reduced significantly during cold weather, through the usage of HVAC or at higher motorway speeds due to increased drag. Whilst a range of 200 miles is sufficient for >94% of daily company car journeys in the UK [21] (note: this percentage would be even higher for private vehicle use - only 0.87% of annual car journeys are longer than 100 miles [22]), there is still hesitancy around EV ranges for longer journeys.

2.1.3 EV Charging

Rapid development and growth of charging networks is required to sustain higher penetrations of EVs. The Competition and Markets Authority predict that up to 480,000 public charge points will be needed by 2030, a significant increase on the 25,000 currently installed, and the installation rate of new chargers currently lags the uptake of EVs [23]. However, it is not only the number of charge points that must increase to accommodate more EVs. As there are limits on the extent to which the efficiency of EV drivetrains can be increased, battery capacity must be increased in order to offer longer ranges, which results in longer charge times or requires more powerful chargers. Whilst the rate at which EV batteries can be charged is increasing as the technology develops, rapid charging requires high current and increasing power demand on the grid: a 350 kW charger draws as much power in one hour as the average UK house uses in a month. New technologies have to be implemented to ensure that the electricity supply and distribution infrastructure can manage the increased power demand, and provide efficient use of resources.

Currently, around 80% of charging takes place at home [24] as EV owners offset the long charge times by utilising the 10-12 hour window overnight for charging to take place. This enables smart charging to create more flexibility and provide opportunities to support the grid, for instance, the vehicle could be charged continuously for that entire period at a low power, or multiple vehicles could be staggered throughout the night and charge at a higher power when base load demand is lower, whilst still meeting the owners' EV battery state of charge (SoC) requirements by morning.

Home charging typically uses a dedicated EV charge point, which can supply 3.6 kW or 7.2 kW single phase AC. The UK Government offers a subsidy of up to 75% or £350 off the cost of a home charge point to help cover the costs of installation [25], and has proposed new legislation to ensure that all new houses are fitted with electric vehicle charge points.

With reduced infrastructure costs and lower electricity rates than at commercial

charge points, home charging can be the cheapest way of charging an EV, particularly if renewable energy generated from household solar panels can be utilised, and offers significant savings over the comparable cost of refuelling an ICEV. Octopus Energy's Intelligent tariff offers electricity at just 10 p/kWh (pence per kWh, 1 p = £0.01) between the hours of 23:30 and 05:30 to encourage EV charging overnight. With the average annual mileage driven by a car in the UK being 7,400 miles [26], this tariff has the potential to provide sufficient energy for a years' driving for less than £250, less than a fifth of the cost in a comparable petrol or diesel vehicle.

However, home charging is often impractical for many people without access to off-street parking, or who park in communal car parks. Although 72% of drivers across the UK have access to off-street parking, this number drops to just 48% in London, and between 60-65% in other major cities [27]. To counter this issue, a number of schemes are being trialled to install on-street chargers with minimal disruption to existing infrastructure. For example, Oxford City Council trialled the 'OxPops' project in 2019 involving the installation of EV chargers that retract into the street when not in use to avoid taking up space on pavements [28]. Ubitricity and Siemens have partnered to install over 1300 charge points across London connected to existing lampposts, sharing an electricity connection and avoiding taking up additional space on the street [29].

With over 250,000 private charge points already installed in the UK, sharing these home charge points can be another good way to ensure sufficient charging infrastructure and efficient usage for EV drivers. Many home charge points are often vacant during the day whilst the owner is at work, and are not necessarily used every night depending on the distance their owner travels. Co Charger [30] is a new app that allows private charge point owners to share their charge point with their local community to provide solutions for people who are not able to charge at their home.

EV charging can use either AC or DC power, with AC commonly used for low-powered single or three-phase charging at home or work, and DC typically used for high-power rapid charging, and is classified into three modes, depending on the

power and hardware used. Table 2.1 lists the main charging standards used in the UK [31].

Mode 2 enables charging from a standard plug socket as a control unit built in to the charging cable provides the communication signals and protection required by the EV to charge. However, due to the limited current supplied through a standard socket, recharge times are too long for many vehicles, but its practicality makes it a suitable emergency back-up when no dedicated charging points are available. Mode 3 is most commonly used for EV charging, using a dedicated EV charge point to supply power, with in-built protection and communication to control charging with the EV. Home charging points have typically used 3.6 kW AC Mode 3 charging, although 7.2 kW home charge points are becoming more common. While few domestic properties have three-phase connections, 11 kW and 22 kW AC charge points may be found at commercial and industrial locations.

Despite commonly being referred to as "chargers", an AC charge point does not charge the EV's battery directly, but instead controls the supply of energy to the vehicle's on-board charger, where power factor correction and AC to DC conversion takes place before the appropriate current and voltage is supplied to the battery. Because of this, AC charge points are often named Electric Vehicle Supply Equipment (EVSE).

Mode 4 uses an external rapid DC charger to supply high power DC direct to an EV's battery, bypassing the on-board charger. An external charger allows for larger AC-DC converters, capable of delivering higher power to the EV battery, resulting in faster charging.

In both AC and DC charging, the actual power supplied to the EV battery is limited to the lower value of the power allowed by the EV and the power that the charge point is able to supply. For instance, an EV with a maximum DC charge rate of 100 kW connected to a 300 kW charger will only charge at a maximum of 100 kW, and an EV that can accept 11 kW AC but is connected to a 3 kW charge point will only charge at 3 kW.

Table 2.1: UK EV Charging Standards

Standard	Power	Voltage / Current	Connection
Slow (Mode 2)	3 kW AC	230 V 13 A, 1 ph	Domestic plug socket through In-Cable Control & Protection Device to EV Type 2 socket
Fast (Mode 3)	3.6 kW AC	230 V 16 A, 1 ph	Dedicated EV charge point to EV Type 2 socket
Fast (Mode 3)	7.2 kW AC	230 V 32 A, 1 ph	Dedicated EV charge point to EV Type 2 socket
Fast (Mode 3)	11 kW AC	230 V 16 A, 3 ph	Dedicated EV charge point to EV Type 2 socket
Fast (Mode 3)	22 kW AC	230 V 32 A, 3 ph	Dedicated EV charge point to EV Type 2 socket
Rapid (Mode 4)	50-500 kW DC	<1000 V 500 A	CCS2 connector

A 1 kHz, ± 12 V, pilot signal is used for communication between the EV and charge point, which enables the EV to communicate its readiness for charging, to show voltage can be safely applied by the charge point, as well as the charge point indicating the maximum current that can be supplied [32].

The maximum rate at which an EV can be charged varies with the state-of-charge (SoC) of the battery. Typically, batteries can be charged the fastest when the SoC is between 10% and 80%, with the maximum charge rate slowing significantly after the SoC reaches 80% to avoid exceeding cell voltage safety limits [33]. This is why the time to charge an EV battery at a rapid charger is often specified from 10% to 80% SoC, rather than the time to full charge. One of the most commonly used methods for charging EV batteries is the constant current - constant voltage (CC-CV) protocol [33]. This involves initially charging the battery at a constant current whilst the battery voltage increases, before holding the voltage at its peak value until the current decreases to zero while the battery completes charging. As the

current decreases during the latter stage of the protocol, this results in longer charge times, and slower charging at a higher SoC. However, this decrease in charge speed is most notable when connected to high powered DC chargers, the EV can sustain the power supplied through AC home charge points for far longer, and as a result, AC charging is typically modelled as constant power.

2.2 The Grid

This section provides an introduction to the UK's electricity grid from transmission to distribution, focussing in detail on the structure of the distribution network. The power flow equations for analysing the voltage and current within a network are derived, and the backwards-forwards sweep approach for solving the power flow problem is presented. As the grid is constantly evolving, some of the future opportunities and challenges for the grid are presented, and the specific challenges that EV charging can cause are explored.

2.2.1 Grid Structure

The electrical grid, or network, refers to the interconnected power lines and services that deliver electricity from where it is generated, to where it is used by consumers. There are three main aspects of the electrical grid: electricity generation, transmission and distribution.

Traditionally, electricity has been generated in large, centralised power stations, using a mixture of natural gas, coal and nuclear, as well as increasing amounts of wind turbines, solar panels, hydroelectric plants and other renewable forms of energy. Increasing prevalence of renewable energy generation is also leading to a shift towards a higher number of generation sites distributed throughout the network, with smaller generating capacity at each site.

All generators connected to the electrical grid are synchronised to operate at the same frequency to ensure that frequency is constant across the country. The nominal frequency in the UK is 50 Hz, with the maximum allowable variation to not exceed ±1% [34]. Grid frequency is stabilised by matching electricity demand and generation, if demand exceeds generation the frequency falls, and if generation exceeds demand the frequency rises. There are approximately 5,400 miles of cable that form the electricity transmission network in England and Wales. This network, owned and operated by National Grid, is responsible for transmitting electricity long distances across the country at high voltages (400 kV and 275 kV) from where it is produced to substations that reduce the voltage ready for onward distribution [35]. Distribution networks then take the electricity and deliver it at appropriate voltage to end consumers. There are 8 distribution network operators (DNOs) that own and manage the distribution networks across the UK, from major distribution lines down to the individual cables and connections that supply households.

2.2.2 The Distribution Network

The distribution part of the electrical grid is a vast, complex network that encompasses all cables and transformers that take three-phase electricity at 132 kV right down to 230 V for use in residential buildings. In this thesis, it is the final low-voltage (LV) sections of the distribution network that are analysed.

Unlike the transmission network, where transmission lines form a mesh with closed loops, the distribution network typically has a radial, or 'tree' topology [36][37]. Electricity cables ('lines') connect nodes ('buses') on the network, to which loads are connected. A simple five-line, six-bus radial network is shown in Fig. 2.1. Although the distribution system is a three phase network, only a single line is shown here for simplicity.

Also, as opposed to a three-phase network with balanced loads, the load in a LV distribution network is often unbalanced between the three phases, as each household

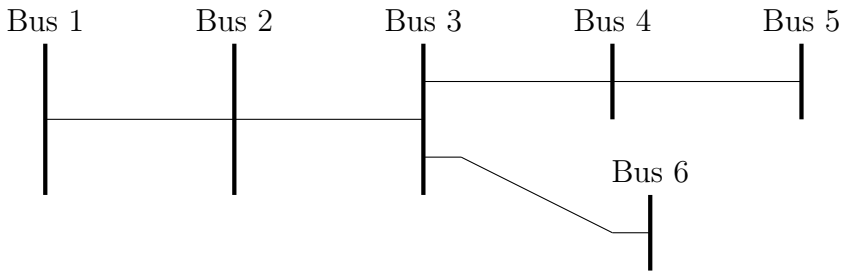

Figure 2.1: A simple 6 bus, 5 line radial network

consumer is typically only connected to a single phase. This requires that all three phases of the network must be analysed to account for all loads in the network and the effects of voltage sensitivity of a load on the other phases of a network [38]. The authors of [37] showed that unequal phase loading meant that houses of different phases at the same location in the network experience different voltages and even if the voltage has fallen below the minimum threshold in one phase, applying additional load to another phase can rebalance the network and bring the voltage back to within acceptable limits.

With the increasing implementation of small-scale solar and other renewable generation distributed throughout the distribution network, analysis of the network must also consider the injection of power at buses where these generators are connected. Typically, distributed generation (DG) can be modelled as either PV or PQ buses [39]. For a PV bus, the active power and voltage magnitude are known, and the appropriate reactive power generation and voltage phase angle can be calculated, so this type of bus is used for traditional generators in a network. With a PQ bus, the active and reactive power are known, and the generation is modelled as a negative load, injecting current into the bus [40]. In this thesis, renewable DG is modelled as a PQ bus.

2.2.3 Solving Network Power Flow with the Backward-Forward Sweep

This section presents the power flow equations that are solved with the backward-forward sweep approach to calculate the values of voltage and current throughout the network. Power flow analysis is essential for network modelling to ensure that it operates within its technical limits. In the UK, voltage must remain within the region of 230 V +10%, -6%, and there will also be thermal limits on the allowable power through the transformer and line currents to avoid damage to the network [38][41]. As distribution networks typically carry electricity at a low voltage over short distances, the short line model can be applied for analysis of the distribution network. This model is applicable to lines under 80 km long, and allows the shunt capacitance to be neglected and the resistance and reactance of the line to be modelled as a lumped load. This means that the impedance of the line is $Z = R + jX$, where R is the resistance of the line, X is the reactance and $j = \sqrt{-1}$.

Any network bus, generalised here as bus n, where $n > 1$, is shown in Figure 2.2. Bus 1 is the slack bus corresponding to the transformer, and is modelled with no upstream buses, no current flowing into the bus, no load current, and with a constant, known voltage. With radial topology, there is a single line into bus n from upstream in the network (closer to transformer), and D lines connecting to downstream buses (away from the transformer), where $D \geq 0$. Although only a single line is shown, each line carries 3 phases. The upstream bus is denoted u_1, and downstream buses denoted $d_1 - d_D$. Voltages at bus n are denoted V_{n_ϕ}, while currents are given by I_{n_ϕ} and the load current is given by $I^L_{n_\phi}$.

For bus n and phase ϕ of the network, the complex voltage is expressed as:

$$V_{n_\phi} = \left|V_{n_\phi}\right| e^{j\theta_{n_\phi}} \tag{2.2.1}$$

where $\left|V_{n_\phi}\right|$ is the voltage magnitude, and θ_{n_ϕ} is the phase angle. Ohm's law allows

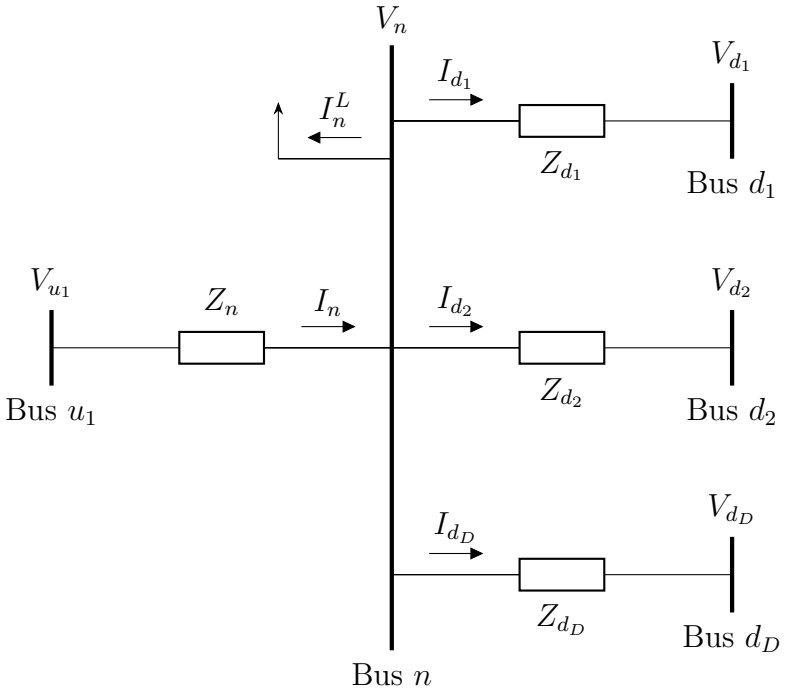

Figure 2.2: Current and impedance diagram for nodal analysis of a network bus

the voltage drop over a line to be calculated by: .

$$V = IZ \tag{2.2.2}$$

Kirchoff's Current Law (KCL) states that the current flowing into a bus must equal the current flowing out of the bus:

$$I_n = I_n^L + \sum_{i=1}^{D} I_{d_i} \tag{2.2.3}$$

The complex power at node n is given by:

$$S_n = V_n {I_n^L}^* = P_n + jQ_n \tag{2.2.4}$$

where * denotes the complex conjugate value and P_n, Q_n are the active and reactive load powers at bus n.

The backward-forward sweep is an iterative approach designed for radial networks, using (2.2.2) - (2.2.4) to calculate values of the voltage and current in the network. Although a number of iterative approaches exist to solve the power flow, including the

Gauss-Seidel method, the Newton Raphson method, fast decoupled power flow and DC approximation load flow [42], the radial topology of a distribution network, the relatively high R/X ratio on lines and the three-phase unbalanced nature means that these methods are not well suited for solving power flow problems in a distribution network as they will not converge [43]. As a result, the backward-forward sweep is one of the most popular approaches for solving power flow problems in low-voltage networks, and is utilised in the remainder of this thesis [44][45].

The three-phase backward-forward sweep is conducted as follows:

1. Initialise voltages at all buses in the network $n = 2, 3, ..., N$ and phases a, b, c as the voltage at the transformer V_{trans}, where here N refers to the total number of buses in the network.

$$\begin{bmatrix} V_{n_a} \\ V_{n_b} \\ V_{n_c} \end{bmatrix} = \begin{bmatrix} V_{\text{trans}} \angle 0° \\ V_{\text{trans}} \angle -120° \\ V_{\text{trans}} \angle 120° \end{bmatrix} \quad \forall n = 1, 2, \ldots, N \tag{2.2.5}$$

2. Initialise iteration $k = 1$

3. Calculate the load current I_n^L for all buses for iteration k, treating distributed generation as a negative power using (2.2.4). If in the initial iteration ($k = 1$), use the assigned voltage from step 1

$$\begin{bmatrix} I_{n_a}^{L\ (k)} \\ I_{n_b}^{L\ (k)} \\ I_{n_c}^{L\ (k)} \end{bmatrix} = \begin{bmatrix} \left(\left(P_{L_{n_a}} + jQ_{L_{n_a}}\right) / V_{n_a}^{(k-1)}\right)^* \\ \left(\left(P_{L_{n_b}} + jQ_{L_{n_b}}\right) / V_{n_b}^{(k-1)}\right)^* \\ \left(\left(P_{L_{n_c}} + jQ_{L_{n_c}}\right) / V_{n_c}^{(k-1)}\right)^* \end{bmatrix} \quad \forall n = 2, 3, \ldots, N \tag{2.2.6}$$

4. Starting from the most downstream buses of the network, i.e. those furthest from the transformer, perform the backward sweep to calculate the currents in the line segment connecting into the bus. This uses the load current at bus

n calculated in the previous step and the sum of currents leaving the bus from additional downstream branches to calculate the current flowing into the bus through (2.2.3). The end buses of the network have no downstream branches, so the line current calculated here is equal to the load current at the bus.

$$\begin{bmatrix} I_{n_a}^{(k)} \\ I_{n_b}^{(k)} \\ I_{n_c}^{(k)} \end{bmatrix} = \begin{bmatrix} I_{n_a}^{L\ (k)} \\ I_{n_b}^{L\ (k)} \\ I_{n_c}^{L\ (k)} \end{bmatrix} + \begin{bmatrix} \sum_{i=1}^{D} I_{d_{ia}} \\ \sum_{i=1}^{D} I_{d_{ib}} \\ \sum_{i=1}^{D} I_{d_{ic}} \end{bmatrix} \tag{2.2.7}$$

where I_{n_ϕ} is the current flowing into bus n in phase ϕ and $I_{d_{i\phi}}$ is the current flowing from bus n to connecting downstream bus d_i in phase ϕ

5. Perform the forward sweep starting from the first bus in the network down every branch to calculate an updated bus voltage based on the line currents calculated above. The updated bus voltage at bus n is equal to the voltage at upstream bus u_1 minus the voltage drop over the line segment (2.2.2). The Z matrix contains the self and mutual impedances of the distribution line connecting into bus n [43].

$$\begin{bmatrix} V_{n_a}^{(k)} \\ V_{n_b}^{(k)} \\ V_{n_c}^{(k)} \end{bmatrix} = \begin{bmatrix} V_{u_{1a}}^{(k)} \\ V_{u_{1b}}^{(k)} \\ V_{u_{1c}}^{(k)} \end{bmatrix} - \begin{bmatrix} Z_n^{aa} & Z_n^{ab} & Z_n^{ac} \\ Z_n^{ba} & Z_n^{bb} & Z_n^{bc} \\ Z_n^{ca} & Z_n^{cb} & Z_n^{cc} \end{bmatrix} \begin{bmatrix} I_{n_a}^{(k)} \\ I_{n_b}^{(k)} \\ I_{n_c}^{(k)} \end{bmatrix} \quad \forall n = 2, 3, \ldots, N \tag{2.2.8}$$

6. Calculate the voltage error $e_n^{(k)}$ in the voltages evaluated in (2.2.8) between iteration k and iteration $k-1$ for all phases at every bus. If the voltage error at any bus is above a desired accuracy threshold ε, increase $k = k+1$ and repeat steps 3-6.

$$e_n^{(k)} = \max\left(\left|V_{n_a}^{(k)} - V_{n_a}^{(k-1)}\right|, \left|V_{n_b}^{(k)} - V_{n_b}^{(k-1)}\right|, \left|V_{n_c}^{(k)} - V_{n_c}^{(k-1)}\right|\right) \quad \forall n = 2, 3, \ldots, N \tag{2.2.9}$$

$$e_{\max}^{(k)} = \max\left(e_2^k, e_3^k, \ldots, e_N^k\right) \tag{2.2.10}$$

if $e_{\max}^{(k)} \leq \varepsilon$ $\rightarrow$ convergence

else repeat steps 3-6.

2.2.4 The Future Grid

The electrical distribution system is rapidly evolving as technology develops and consumer habits change. Grids are getting smarter, where the flow of both electricity and data can make the grid more resilient, efficient and enable the implementation of new technologies such as distributed energy resources (DERs) for small-scale generation, energy storage and islanded microgrids which operate independently from the main grid. DERs and microgrids can increase the resilience of the distribution network through self-sufficiency, with distributed generation and storage, allowing supply and demand to be balanced on a local basis. Enabled by the extensive monitoring, communication and control networks embedded in a smart grid, households equipped with DERs, such as rooftop solar photovoltaic (PV) panels, integrated energy storage and smart appliances can act as both consumers and producers of energy (prosumers) allowing them to play a more active role in their usage of energy and interaction with the grid [46].

DNOs are currently undergoing a transition to become Distribution System Operators (DSOs) to adapt to this new distribution network operational paradigm. To facilitate the new flexible modes of operation, DSOs must take a more active role in the monitoring and management of distribution networks on a local level, for instance through the management of DERs and ensuring that supply and demand can be balanced [47].

The increasing penetration of distributed renewable generation also causes several challenges for DSOs to manage. A key challenge with solar and wind generation is its intermittent nature, as frequent changes in cloud cover and wind speed can cause significant and unpredictable fluctuations in the power generated on a rapid

timescale. This can cause a number of problems within the network, including difficulty balancing supply and demand in small networks and rapid variation in voltage [48][49]. High penetrations of generation within the network can also cause issues with reverse power flow or the bus voltage rising above the allowable limit. This issue can be more severe when the generation is located at the end of long feeders [50][51], and can often require the curtailment of generation, which wastes valuable renewable resources or costs the network operator significant amounts of money in compensation.

A DSO can counter some of the challenges arising from electricity supply and demand in a smart grid through demand response techniques. Rather than controlling the supply of energy, demand response, or demand side management, incentivises consumers to modify their demand profile in response to current grid conditions to balance supply or manage their impact on the grid [52]. Demand response is often considered at times of peak load, when the grid may be approaching transformer or line loading limits to reduce demand on the grid by shifting load to a time of greater grid capacity or through load shedding. One common demand response technique is time-of-use (ToU) tariffs, which offer lower electricity rates at times of low average load, such as overnight, as an incentive for consumers to shift their flexible load demand, including EV chargers, washing machines and heaters, to these periods [52][53]. Alternatively, prices can be lowered at times of high renewable generation to maximise consumption [54], or to prevent transformer overloads [55].

Electric vehicles can also offer a number of services to the grid, both by adjusting their charging load, but also through vehicle-to-grid (V2G) or vehicle-to-home (V2H), by discharging their batteries to feed energy back into the grid or to provide power a building. The large batteries in EVs offer the grid a significant amount of connected distributed energy storage which can be utilised by the grid for support. As well as incentivising EV charging away from times of peak load to reduce the impact on the network, it can also be encouraged at times of high energy supply, particularly from renewable generation which would otherwise have to be curtailed [56]. For instance,

some Octopus Energy customers were paid to charge their EVs in May 2020 as a result of low demand and increasing renewable energy production [57]. Additional benefits that the charging of EVs can provide will be explored in greater detail in section 2.3.

The provision of grid services through the discharging of electric vehicle batteries has been extensively researched in literature and includes uses such as:

- Peak shaving - where the peak load in the grid is reduced through the discharging of electric vehicle batteries [58]
- Reducing network losses and voltage deviation to increase the permissible capacity of installed distributed generation [59]
- Primary frequency response services to provide rapid injection of energy into the grid in the event of a sudden loss of generation to stabilise frequency [60]
- Off-line uninterruptible power supply (UPS) to restore power to a home or other building in the event of power loss from the main grid [61]
- Providing reactive power compensation - EV charging points can operate at a leading power factor to inject reactive power to the grid, which can increase voltage when approaching lower grid limits [62]

2.3 Smart Charging

Despite the benefits that EV charging can offer the network, it also poses a number of significant challenges that must be overcome in order to successfully accommodate high penetrations of EVs in the grid, especially if EV charging is uncontrolled. Uncontrolled charging refers to the scenario where the EV will charge as soon as it is plugged in, at the maximum possible charge rate until fully charged. The distribution networks were designed based on the typical load value for consumers, known as the after-diversity maximum demand (ADMD). A number of studies have shown that

the ADMD of networks with EV charging can be significantly higher. The 2014/15 My Electric Avenue study showed that even if home charging is limited to 16 A (3.6 kW), the ADMD resulting from uncontrolled EV charging increases from 0.8 kW to 2 kW at peak times and at least 30% of low voltage (LV) distribution networks would need upgrading [63]. The Electric Nation Smart Charging Trial found that the ADMD of a 11 kV feeder could be over 30% higher with EV charging than under typical winter load, exceeding the network capacity limits. They concluded that charging an EV is equivalent to adding an additional house to the network [64].

J. Quirós-Tortós et al. analysed the effect of increasing penetrations of EV charging on the transformer loading, feeder current utilisation factor and voltage violations, and showed that transformer and feeder utilisation could exceed the thermal limit of the installed hardware, whilst also increasing the probability and extent of voltage problems. However, the constraint that limits the implementation of additional EV charging differed between networks, with some networks experiencing voltage issues first at high EV penetrations, whereas other networks overload transformers or lines before experiencing voltage issues [38]. In addition to the above factors, [41] also considered the impact of EV charging on network losses, showing that a high penetration of EVs could increase losses by a factor of 5, compared to without EV charging. Increased loading on distribution transformers can cause overheating in the transformer, leading to accelerated ageing, and increased costs of maintenance and replacement [65].

Smart charging describes a wide range of methods for controlling the time, duration and power of EV charging in an attempt to alleviate the challenges on the network, and provide greater benefit to EV owners, such as through reduced charging costs. Since 2019, all UK Government funded EV charge points must feature smart charging technology, with the ability to be accessed remotely and respond to external signals [66]. The actual implementation of smart charging can range from simple ToU tariffs or load balancing for sharing the available power capacity between charge points to more sophisticated algorithms developed in current literature which benefit the grid

as well as EVs.

This section contains an exploration of the key concepts of smart charging from current literature and analysis of the main drawbacks and research opportunities.

2.3.1 Key Concepts

Centralised, Decentralised and Distributed Charging Strategies

The majority of the smart charging algorithms presented in current literature involve the solving of an optimisation problem to maximise the benefit of the charging scheme based on information related to the EVs that need to charge, the state of the network, price signals or other data. The collection and communication of this data in addition to the computation of the optimisation problem means that smart charging strategies can typically be classified into three categories: centralised, decentralised or distributed.

In a *centralised* system [44], [67]–[70], computation is handled by a single central processor or server, sometimes referred to as an aggregator. All participants, e.g. houses or EV charging points, must communicate directly with the central processor to provide information relating to the EV's energy requirement, arrival and departure times or other loads in the network that the processor requires to calculate the optimal charging schedule for each connected EV, before communicating the results back to each charge point for the charging to be completed. Centralised systems have the advantage of perfect information, as the central processor knows everything about the EVs and grid, so the true optimal solution is calculated. In addition, they are easy to design and construct, as there only has to be communication between a charge point and the central controller, so the network can be expanded without it impacting on the already installed charge points. However, there are a number of significant disadvantages. In large networks with high numbers of EVs, solving complex optimisation problems becomes significantly more computationally challenging, requiring expensive hardware or impractically long computation time,

and the system architecture with a single central controller means that any issues with the controller or communication channel can disrupt the entire system. Because the optimal charging schedule is determined by the central controller, individual EVs lose autonomy over their charging, and the sharing of information presents a number of privacy issues [71]–[73].

To overcome the challenges with centralised charging schemes, academic research has focused on *decentralised* systems. There are typically two system architectures considered in decentralised charging literature. The first divides the electrical network or entire set of charging EVs into smaller groups with each group managed by its own controller, which reduces the problem complexity compared with a fully centralised system [68], [74]. The controllers of each group can then collaborate to achieve specific goals on a system-wide scale, so these systems can be considered as a centralised system within each group, and a decentralised system on the larger scale when the entire network is considered. The second decentralised structure still involves communication between each charge point and a central operator, but the calculation of optimal charge schedule is completed by the charge point, rather than the operator. This preserves privacy as less data must be shared between charge point and operator and gives the EV a greater ability to set its own charging schedule. This is commonly achieved through iterative communication between operator and charge point, for instance in [36] where EVs transmitted their scheduled charging to the operator which then calculated a new signal to be broadcast back to the EV charge points for them to update their charge profiles until there was convergence between subsequent iterations. Valley filling was achieved in [75] through EVs choosing when to charge based on a cost signal, which was then updated for the next time step based on allocated charging load, over time flattening the load. A similar approach was presented by Xing et al. [76], where a water-filling algorithm was solved by EVs at each iteration. A multi-agent system is presented in [59], where individual EVs were managed by vehicle controller agents which interact with aggregating microgrid aggregator and regional aggregation agents. Vehicle agents respond to a virtual price

signal corresponding to network load variance and based on the vehicle's response, the regional agent updated the price signal for the next iteration. In [77] each EV chose a start time and reported to the transformer aggregator which sent the total load to all EVs. In turn each EV was able to update its start time with a round of communication with the transformer between each update to determine its own charge schedule in a round-robin manner.

Distributed strategies increase the level of decentralisation even further than those described above, by removing the central operator and interconnecting every charging point on the network for communication between all charge points. Charge points each determine their own optimal charging strategy depending on the behaviour of the other charge points in the network. There are fewer examples of true distributed charging schemes, but [65] and [52] do not require any communication so cannot be classified as either centralised or decentralised. The authors of [65] presented vehicle-directed smart charging strategies such as the proposed Random-In-Window strategy which required no outside information as an alternative to centralised schemes to minimise transformer aging. A fuzzy controller was developed in [52] which received a ToU price signal, the owners' EV power requirement and a measurement of grid voltage as inputs to determine charge rate.

Offline vs Online Methods

Depending on the availability of information and the time at which the problem is solved, charge scheduling approaches can be classified as either offline or online.

An *offline* approach means that the charge scheduling takes place in advance of the charging, with the resulting charge profile then subsequently being implemented [68], [69], [76], [77]. Full information is required about all EVs and grid base load for the duration of the charge scheduling in order to calculate the optimal schedule and it cannot adapt to changes in the planned EV charge schedule or grid load once the scheduling has taken place. Another form of offline strategy is through day-ahead

scheduling [73], [78] where day-ahead energy prices can be used to minimise energy cost, however good knowledge or forecasting ability is required of future demand in order to utilise such a scheme.

Alternatively, *online* approaches operate in real-time, with the charge scheduling updating multiple times throughout the considered period to take account of unknown future load or EV arrivals [67], [70], [74], [75], [79], [80]. Online methods offer the greatest flexibility as they can adapt to unknown future information and realistically reflect the real-time knowledge of information in the real-world, but typically do not provide the same level of optimality that can be achieved in an offline schedule. One common approach for implementing an online algorithm is through a sliding window [67], [74], [81], [82], which at each time step calculates the optimal solution for all time steps within the window based on information known at that point, but only implements the solution at the next time step, allowing the solution to be updated later on once additional data is available.

Some approaches attempt to factor in future EV arrivals or power demand that would affect the charge allocations, such as in [67] or [69] which included expected arrival times and initial SoC probability distributions in the scheduling which could be updated later once the EVs had arrived, or through forecasting base load for planning future time steps [75], [81].

However, a number of studies implementing either offline or online strategies require knowledge of some information in advance to perform charge scheduling, including knowledge of future EV arrivals, departures or energy requirements [76], [81], [83] and knowledge of the grid base load [36], [62], [82], [84]. For instance, in [81] EV owners were required to submit their arrival and departure times, initial SoC and desired charge level at the beginning of the control period for any charging they had planned that day, although small deviations from the submitted plans could be factored into the online charging stage once the EV had arrived. Both online and offline stages were implemented in [83], but grid load and EV information were required ahead of time to perform an offline algorithm to minimise variance between

network load and a target load profile, before controlling EV charging if required in real time to ensure the actual load matches the profile generated in the offline stage. In [84], the base load was assumed to be predictable so that it could be used as a signal by decentralised EV charge points to coordinate their charging.

Grid Constraints

It is important to consider the impact of scheduled EV charging on the distribution grid to ensure that none of the technical limits on the network's operation are violated. The key limits that are typically considered are transformer apparent power limits, bus voltage lower and upper bounds and line current capacity which are expressed through (2.3.1) - (2.3.3).

$$S_{tr,t} \leq S_{tr_{\max}} \quad \forall t \in 1 \dots T \tag{2.3.1}$$

$$V_{\min} \leq V_{i,t} \leq V_{\max} \quad \forall\, i \in 1 \dots N_{\text{bus}},\ t \in 1 \dots T \tag{2.3.2}$$

$$I^{\text{line}}_{l,t,\phi} \leq I^{\max}_{l,t,\phi} \quad \forall\, l \in L,\ t \in 1 \dots T,\ \phi \in 1, 2, 3 \tag{2.3.3}$$

A number of studies, such as [36], [37], [62], [67], [69], [78], [80], ensured that the grid limits are not violated by including them as constraints when the charge scheduling optimisation was computed. This adds significant complexity to the scheduling computation however, as power flow equations must be solved to calculate the impact of the charging on the network. In addition, it requires full knowledge of the network topology and line impedances. Sun et al. [69] calculated voltage and current sensitivity matrices showing the effect of a change in load at bus j on bus i. This created a linear power flow approximation that could be used to quantify the impact of EV charging and ensure that grid limits were not violated. Voltage and current probabilistic impact indices were presented in [85] as a method for evaluating the impact of EV charging on the network, requiring less data about the network than traditional load flow based approaches.

An alternative to constraining the grid limits in the scheduling stage is to implement

a real-time monitoring and control strategy to detect violations and apply remedial control actions to return within allowed limits. At each control cycle in [38], voltage, current and transformer loading data was collected from sensors throughout the network and if the limits have been violated, the controller calculated the number of charging EVs that must stop charging in order to rectify the issue. The EVs that must be disconnected were selected in order of charge time, with those that have been charging the longest being the first to disconnect. If the demand on the network later dropped sufficiently such that the measured parameters were below their limit plus an additional safety margin, EVs could be reconnected, with the EV with the shortest charging time reconnecting first. A real-time control algorithm was used to minimise total harmonic distortion (THD) of the current in [86], where if the system detected the THD has passed an upper limit, EVs were disconnected in order of the SoC, with the EV with the highest SoC being disconnected first, and reconnected last. However, such a scheme is challenging to implement, as EVs do not currently communicate their SoC to the charge point, which is why charge time is used as a substitute value above. However, as the size of EV batteries can vary significantly, an EV with a large battery that arrived empty could charge for a long time but have a lower SoC than an EV that has not been charging long but has a small battery that was almost fully charged on arrival.

2.3.2 Smart Charging Objectives

This section explores some of the most popular objectives of smart charging algorithms in current literature.

Load Shifting

One of the most commonly implemented objectives for smart charging is load shifting, such as shifting EV charging load away from times of peak demand, encouraging valley filling or for tracking a specific load profile. One of the primary uses of load

shifting is to achieve valley filling, or peak shaving when combined with V2G. The typical shape of the baseload peaks between 6pm and 10pm in the evening, before falling to a much lower level, the 'valley', between 12am and 6am. Valley filling aims to shift demand from peak times to these morning hours to flatten the overall demand profile. Figure 2.3 shows the typical load curve and an example of both valley filling and peak shaving.

Time-of-use (ToU) energy tariffs are one of the simplest strategies for load shifting [52], [53]. By offering higher electricity prices at times of high load, and lower prices when demand is expected to be lower, customers are encouraged to alter their demand to off-peak times to save money, reducing the impact on the network. However, while consumers are encouraged to wait until the cheaper electricity tariff starts before charging their EV, there is no incentive to wait until later in the period of cheaper electricity which leads to a significant and rapid spike in demand at the start of the cheap ToU period, and can lead to the network being under-utilised at later hours [53]. To overcome this, Faddel and Mohammed introduced a multi-group ToU tariff, which split the total group of consumers into multiple smaller subgroups, which had staggered ToU tariff times [52]. This resulted in the a smaller peak forming at the start of each ToU period than under the typical ToU tariff as there were fewer households and therefore less demand in each group.

A more sophisticated approach was used in [59], [74], [75], [87], [88] to overcome the issue. Firstly, the base load would be predicted for the coming day, and the value of the load converted to a continuous virtual price signal, with a higher virtual price at times of high predicted demand, and a lower price at times of low demand. Solving an optimisation problem where the virtual cost of charging is minimised resulted in EV charging scheduled at times of lower demand, such as overnight. A sliding-window was implemented in [74] to adjust the EV charging of a local group of EVs based on the forecasted baseload and EV load and account for new arrivals in each time period. If the virtual price signal was regularly updated with the scheduled EV load, the final load profile could achieve valley filling and also minimise variation

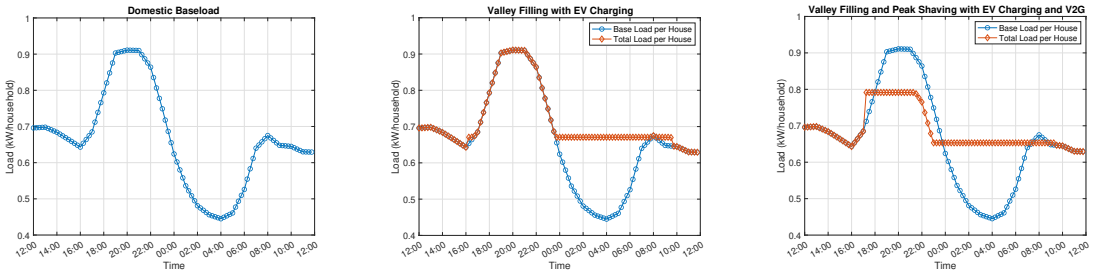

(a) Typical shape of UK domestic baseload without EV charging (b) Example of valley filling (c) Example of valley filling and peak shaving

Figure 2.3: Examples of domestic baseload without EV charging, valley filling and peak shaving

in load caused by the EV charging, as newly arriving EVs reacted to the updated signals. This required sufficient numbers of new EVs to arrive between price updates in order to flatten the load however, else new peaks could occur [75]. Zhang et al. recognised that if a valley occurred in the afternoon, it may not be filled as cars arriving ahead of the afternoon valley would instead prioritise charging overnight when the demand, and therefore the price, was lower. By the time sufficient numbers of EVs had scheduled their charging overnight to bring the virtual price up to the same level as the afternoon valley, the afternoon valley may already have passed, or there is insufficient flexibility in EVs to reschedule charging to that period. As a result, a weighting must be applied to artificially lower the price of the afternoon valley to encourage charging in that time [88].

Valley filling increases the number of EVs that can charge without violating grid limits, and reducing load variance can also make it easier for the power system operator and distributed generation owners to balance supply and demand within the system [75]. Liu et al. presented a decentralised approach including grid constraints using the Shrunken Primal-Dual Subgradient method that achieved valley filling overnight without violating grid limits [36].

Often, V2G discharging is also modelled so that both valley filling and peak shaving can be achieved [76], [89], [90]. Peak shaving is accomplished through the discharging of EV batteries at times of high load to satisfy electricity demand locally, reducing

the apparent load on the network.

Xie et al. focused on peak shaving and load flattening to completely flatten the load on the grid between 6pm and 3pm through a centralised, online approach. Fairness metrics were utilised so that the EVs with highest SoCs partook in the discharging stage, and were rewarded with higher priority for charging so charged faster than EVs that did not contribute [90]. Wang et al. presented an agent-based approach to determine the optimal EV charge profile and DG injection with the objectives of minimising wasted renewable energy, achieving sufficient EV SoC at departure, minimising charging cost and load flattening (valley filling + peak shaving) [89]. A water filling algorithm with V2G and smart charging was presented to achieve load flattening. With EVs initially discharging at peak times to reduce peak load, the time that discharging stopped and charging began was calculated to achieve a flat load throughout both peak and valley periods [76].

An extension to valley filling is load profile tracking, for instance if electricity has been purchased on a day ahead market and the network operator needs to ensure that the next-day consumption matches the purchased energy [91]. Rassaei et al. explored the reshaping of the electricity demand to minimise the cost of buying energy in the real-time market if consumption did not match the electricity purchased day-ahead [92].

Other Grid Protection and Ancillary Services

Smart charging can be used to support the grid in a number of different ways, such as through voltage regulation [44], [52], [93], reducing transformer ageing [65], [75], [77] and providing reactive power compensation [62].

With high penetration levels of EVs, the voltage drop could exceed grid limits, so the voltage profile was levelled in [44] by minimising the variance in the deviation in voltage from the nominal voltage at all nodes. A two stage control strategy was presented in [93] with centrally managed primary control adjusting the phase

connection of PV generation and nodes to minimise voltage imbalance and neutral wire current, and secondary control coordinating EV charging to compensate for the neutral current. The multi-group ToU tariff presented in [52] also reduced the voltage drop caused by EV charging, particularly on the more vulnerable downstream buses. The proposed strategy was also tested in conjunction with shunt capacitors for providing voltage support, which increased the charge rates of downstream EVs.

Beaude et al. utilised a game theoretic approach to solve a distributed EV charging problem to minimise a cost function incorporating transformer ageing, energy loss and EV charging cost [77]. The impact on transformer ageing of a range of vehicle-directed charging coordination methods were evaluated in [65]. These methods included uncontrolled charging, ToU tariff, charge by departure and random-in-window start time. The random-in-window approach resulted in a transformer ageing factor significantly lower that the other approaches, and only marginally higher than a centralised smart charging approach. A valley filling strategy was presented in [75] including a timeslot rejection modification to delay EV charging if the transformer load limit was exceeded. In addition, a forced cool down period could limit the power through the transformer to help prevent overheating, which had a significant impact on reducing loss-of-life.

EV charge points are also able to operate at a non-unity power factor to provide reactive power compensation to the grid through the consumption or injection of reactive power, which can increase the number of EVs that can charge in the network without violating grid limits and reduce charging cost [94], and improves the voltage profile by reducing deviation at EV nodes [62], [95].

Integration of Renewable Generation

EV smart charging solutions can be used to help support the integration of renewable energy by dealing with the intermittency of renewable generation [81], [83], supporting a higher penetration [59], [96] and maximising self-consumption of renewable energy [97], [98]. Bilh et al. presented a method of controlling EV charging

to minimise the fluctuations in renewable generation. An offline stage was solved ahead of time to minimise the difference between the predicted load and desired load profile, with an online stage controlling EV charging to account for fluctuations and deviation from the desired load profile [83]. A deterministic optimisation was developed in [81] for controlling EV charging and discharging in the presence of renewable energy in a microgrid. The optimisation was initially solved using forecast data for renewable output, but was updated in a real-time sliding window approach to adjust EV charging and discharging according to the actual output.

An agent-based smart charging and V2G strategy was presented in [59]. The EV charger aimed to minimise its virtual charging cost by charging at times of lower demand and higher renewable penetration. In comparison with other charging approaches, the proposed charging strategy enabled a significantly higher renewable generation hosting capacity. Xie et al. aimed to calculate the maximum capacity of renewable DG in a network with the presence of EVs, optimising network loss as an equivalent to decreasing the load variance which could help increase the DG penetration [96].

Increasing self-consumption - the amount of energy produced by a distributed generator that is utilised at source or in the surrounding network - is an important objective to ensure that renewable energy is not wasted. Van der Meer et al. proposed an Autoregressive Integrated Moving Average (ARIMA) model for forecasting solar energy generation. A cost minimisation problem encouraged use of produced renewable energy as the cost is lower [97]. Minimising the cost was also the objective used in [98] to maximise the consumption of solar energy, as it was cheaper than consuming energy from the grid. Two terms are used to define the solar energy: the total energy generated and the energy not consumed. By minimising the solar energy not consumed, the total cost of charging was also minimised.

Financial

Minimising cost is an important objective of many smart charging strategies, as financial benefits for consumers can increase participation in these schemes [55], [67], [69], [73], [99].

The charging of EVs was scheduled offline using a day-ahead price in [69], with the optimisation objective to minimise the total charging cost for all EVs taking into account grid constraints. Uncertainty mitigation was included to take into account the stochastic and unpredictable nature of EV arrivals and energy requirements, resulting in better performance than without the mitigation. Antúnez et al. also considered EV charging and discharging subject to grid constraints with the objective of minimising the cost of energy provided by the upstream grid. The use of DG and V2G could reduce the need for energy to be purchased and the cost of operation. A penalty was included for insufficient EV charge as otherwise providing the EV with less energy than it required would reduce the cost and hence improve the optimisation objective [67]. In [73], the total daily cost for energy consumed for household appliances and EV charging was minimised based on day-ahead prices received from the network operator. The discharging of EVs allows a number of other scenarios to be considered: vehicle-to-home (V2H), vehicle-to-grid (V2G), and vehicle-to-neighbour (V2N). The objective function in [99] also minimised the cost of energy purchased from the grid to charge and maximised profit from V2G or V2H. Minimising energy costs for a neighbourhood of smart households was considered in [55], where the optimisation objective was to minimise the cost of energy purchased by the smart grid and maximise the profit from selling energy, subject to transformer limits. A profit driven mechanism was presented in [78] for an aggregator to maximise profit while consumers minimise their costs. Based on forecast day-ahead prices, consumers optimised their demand to minimise their cost and submitted their demand profile to the aggregator. If grid limits could be violated based on the combined demand profiles, a sliding window rescheduling stage was

implemented, where the aggregator could offer incentives to consumers in exchange for modifying their demand.

2.3.3 Maximising EV Penetration in the Distribution Network

Whilst many of the the smart charging strategies explored above attempt to provide some benefit to the distribution network, none specifically attempt to evaluate or maximise the penetration of electric vehicles that can be hosted within the network. With the high load placed on the network by EVs, it is realistic that many networks would not be able to cope with an EV penetration of 100% or higher, i.e. every house has at least one EV to charge. In fact, several of the studies do not even attempt to constrain grid limits or monitor operation to ensure that the smart charging strategies can be safely accommodated.

Reducing EV Charging Impact on the Grid

A decentralised fuzzy controller was developed in [100] to minimise the impact of EV charging by controlling the EV charge current based on grid voltage. The lower the grid voltage, the greater the reduction applied to the charging current by the controller to avoid exacerbating voltage issues, unless SoC was extremely low, when the current was not adjusted to ensure the EV could charge. At times of high voltage, the charging current could be increased as the increased load would reduce voltage. If an EV's SoC was already high, then the charging current should be decreased so that the available capacity could be utilised by other EVs that had a lower SoC. Shao et al. attempted to hide the charging of EVs in the network by setting a load limit on the network equal to the peak demand without EVs to ensure the original peak load on the network is not exceeded through the addition of EV charging. The household demand limit could then be maximised such that the sum of all household loads was equal to the network load limit [101]. Any households

with power consumption greater than the household demand limit were curtailed, however such a strategy is less fair on larger households with greater energy demand as they would be curtailed more regularly. Impact indices for voltage and current were proposed in [85] to assess the impact of EV charging on the grid. Load flow data was used to calculate a centralised index for bus voltages and line currents as a function of base load, EV charging and renewable generation. The impact indices could be used for monitoring grid operation, forecasting future grid impact and for scheduling EV charging. However, it was found that only 60-70% of the energy required for EV charging could be accommodated by the network, the multi-stage charging process required centralised computation with lots of information sharing, and the flexibility of EV charging was limited by predetermining charging rate based on the EV's SoC.

The Distribution System Loading Margin (DSLM) was used in [102], defined as the amount of extra load each node could accommodate before grid constraints were violated. A multi-objective planning problem was formulated to determine the allocation of public charging stations in order to maximise the extra load capacity for minimal impact on the network, minimise the cost of charging stations and minimise EV charging distance. A grid planning tool was presented in [103] which analysed the hosting capacity of distribution networks based on future forecasting. A Grid Needs Analysis was performed to evaluate each line and transformer in the network against the forecast load and generation and network constraints.

Determining the Maximum Allowable EV Penetration

A number of studies explore the determination of the maximum penetration of EVs that can be charged within a distribution network without violating any operating limits [70], [95], [104]–[107]

Aravinthan and Jewell used a two-stage approach for scheduling EV charging, with day ahead and real-time stages that attempted to calculate the optimum and maximum numbers of EVs that could be connected to charge at each hour considering

CO_2 emissions and transformer ageing [104]. Two smart charging strategies were presented in [70] to minimise total cost and peak-to-average ratio (PAR). An iterative approach was taken to determine the maximum EV penetration that could be accommodated before violating a voltage or load constraint. Results showed that minimising the PAR achieves load flattening and that the network could accommodate an EV penetration six times higher than through minimising total cost, showing that the optimisation objective can play a significant role in determining the maximum permissible EV penetration. A water cycle algorithm was implemented in [95] with the aim of minimising cost, voltage deviation and PAR. The maximum penetration of EVs that can be hosted without overloading the transformer was found when EVs partake only in charging, and when EVs can both charge, discharge and provide reactive power compensation. It was found the use of V2G could increase the maximum penetration of EVs from 60% to 80%. Zaidi et al. took a probabilistic approach to determining the maximum EV penetration. Monte Carlo simulations were used to account for the stochastic variations of load and EV profiles to produce cumulative distribution functions for differing EV penetrations. Analysis of these results enabled the maximum EV penetration to be determined, and the likelihood of voltage unbalance or under-voltage conditions occurring to be calculated, however no charge scheduling was attempted to adjust the charging profiles of EVs [105].

For simulations involving complex load flows or multiple Monte Carlo analyses of stochastic variables, computation time can be a significant limiting factor. Parallel computing was used in [106] to solve the problem simultaneously on different processing cores, which greatly reduced the computational time. A logarithmic search algorithm was performed to find the maximum penetration of EVs that could be accommodated within grid limits, which was verified through a power flow study, but smart charging of EVs was not considered. An alternative approach to maximising EV penetration was considered in [108]. The objective function aimed to maximise the Distribution System Loading Margin (DSLM), a measure of how much additional EV charging load could be supported by the network, considering both

uncontrolled and smart charging implementations. The maximum permissible EV penetration and expected EV charging load profile for uncontrolled charging could be calculated each hour based on the DSLM using a Monte Carlo simulation. Based on this profile, an optimisation problem determines the maximum penetration of EVs with smart charging and reactive power compensation. Carrión et al. considered the reactive power voltage control that EV charge points could provide and constructed an optimisation problem to maximise the number of charge points that could simultaneously operate at peak load subject to network constraints [62]. The hosting capacity of extremely fast EV chargers was evaluated in [109] against constraints of voltage and thermal limits at peak load. The amount of additional load that the network could accommodate was calculated by raising the load at each node in turn by a set amount and performing a power flow study to determine whether any grid limits were violated, while all other nodes were held at peak load. While this would calculate the additional amount of load each node could accommodate above the peak load, it doesn't take into consideration additional load at the other nodes, which means the calculated capacity is only valid while the load at other nodes is the peak value or lower. A multi-feeder study was conducted in [110], evaluating the maximum penetration of residential EV charge points that could be simultaneously operated per phase across the multiple feeders before an under-voltage condition occurred.

Whilst evaluating the hosting capacity with simultaneous charging at peak load can provide a worst case scenario, research into smart charging shows that controlling the charging of EVs can enable significantly more EVs to be accommodated, leading to an underestimation of the network's actual EV hosting capacity.

Rather than attempting to calculate the maximum EV penetration, the following studies maximised the EV hosting capacity. For instance, Shaaban et al. used a genetic algorithm to plan the optimal location and size of distributed generation facilities with the aim of maximising the permissible EV penetration level without violating grid limits. It was shown that the integration of DG could increase the

permissible EV penetration by up to four times during the worst case scenario at peak load and all EV chargers operating simultaneously [111]. The concept of the EV chargeable region - the amount of EV charging load that can be accommodated into a distribution network - is proposed in [107]. A two-stage approach was considered where the distribution network cost was minimised in the first stage by optimising variables of shunt capacitors, chargeable region and distribution network operation, with the worst case scenario checked in the second stage. Uncontrolled charging was compared with a price-based charging strategy, which resulted in a slightly higher allowable penetration, but no smart charging or DG was considered. The authors of [112] considered both EV charging and DG resources through the simultaneous estimation of the maximum capacities for EVs and DG in a network. An optimisation problem maximised installed DG capacity and EV charging demand while minimising energy loss. The EV charging was aggregator based with each aggregator selecting a population of EVs of different sizes in order to maximise the permissible charging. Deng et al. investigated the accommodation capability for EVs in a distribution network through a two-level optimisation problem. The first level attempted to maximise the EV capacity in terms of the total EV charging power, while the second level minimised the network operation costs through the control of DG resources. The accommodation capacity calculated was measured in MW, so the EV hosting capacity in terms of the number of vehicles would depend on the actual EV charge and travel profiles [113]. Interaction between the high voltage and medium voltage networks was considered in [114] due to the integration of EVs and solar PV. A scheduling based optimisation problem was formulated to maximise the hosting capacity of the network for EVs (measured in MW), by optimally utilising available resources and the flexibility of EVs to increase the number of EVs and PV that could be supported without violating network constraints. Some studies, including [115] also calculated the the maximum penetration by iteratively increasing the number of vehicles in the study until constraints were violated. A year long study was conducted with at each day an initial number of EVs chosen and an optimisation

problem solved to maximise the hosting capacity. If a feasible solution was found, the number of EVs was increased and the process repeated. Repeated over a number of years, an average hosting capacity could be calculated for each day. The final Expected Maximum Hosting Capacity was the minimum average daily capacity. This type of approach can be significantly slower than finding the maximum number as a single optimisation, as multiple power flow studies or optimisations must be solved before the maximum penetration is found. In addition, it can be very dependent on the load profiles selected. For instance, selecting a low number of profiles with abnormally high load will result in a significantly lower penetration being found than selecting a higher number of profiles with lower load.

2.3.4 Summary

Significant research has been devoted to the exploration of EV smart charging with a large focus on the benefits that EV charging can provide to the grid and consumers, for example through valley filling, supporting higher penetrations of renewable generation and lowering the cost of charging. However, the penetration of electric vehicles and the resulting challenges on distribution networks are rapidly increasing. The benefits that smart charging can offer are irrelevant if the distribution networks cannot accommodate the charging of a high penetration of electric vehicles.

Some studies have attempted to find the maximum allowable penetration of EVs that a network can support without violating grid limits, however it has also been seen that the approach to EV charge scheduling and the integration of renewable generation and voltage support can have a big impact on the maximum penetration. Distribution networks will upgrade components over time to improve the performance and capacity of the network, but this can be expensive and disruptive. There is limited research into the upgrades to a distribution network that can provide the greatest increase to EV penetration. Maximising the penetration of electric vehicles accommodated by a network is a challenging problem, as the number of EVs that

can charge is affected by all other loads and generation in the network, and therefore cannot be directly optimised.

As the number of EVs increases and charging demand grows, the additional computational complexity required to solve smart charging optimisation problems, coupled with increasing concerns about data protection and privacy is leading to a preference of decentralised and distributed solutions. However, all optimal solutions result in the individual EVs giving up some freedom to make their own charging decisions, particularly in the case of curtailment based strategies. There is little exploration of the ability to permit EVs to follow their own charging schedule if their impact can be mitigated, for instance through incentivising another EV to discharge at the same time.

2.4 Peer-to-Peer Energy Trading

With the increasing deployment of distributed energy resources (DERs), such as solar PV panels, battery storage and EVs, in addition to the decentralisation of electricity networks into smart and micro grids, peer-to-peer (P2P) energy trading is emerging as a key technology for power networks and smart grids.

P2P trading facilitates transactions of small quantities of any sort of item directly between prosumers in a network, with this section focusing on the trading of electricity. Energy producers can sell electricity directly to consumers, who avoid having to purchase electricity through the electricity supplier or network operator, and some of the traditional challenges of selling energy back to the grid are avoided, such as ensuring supply and demand are balanced. A P2P trading system typically consists of individual consumers and producers of electricity within an electricity network, a communication network to facilitate communication of available energy and trades and a market operator to coordinate transactions [116].

Peer-to-peer energy trading can offer a number of financial advantages for participants and the network operator as well as giving prosumers greater control over

how they consume and sell energy. A common issue addressed through P2P trading is economic dispatch [117], [118], where the trading of energy is used in conjunction with the control of loads and generation to minimise the overall cost for a micro or smart grid. It can also result in economic benefits for energy prosumers, as while energy companies such as E.ON Energy offer just 3 pence per kWh (p/kWh) to purchase energy from consumers through a Smart Export Guarantee (SEG) compared to their standard selling rate of over 18 p/kWh [119], a P2P trade can be agreed at a price beneficial to both parties. In addition, P2P trading can reduce the load on the grid by increasing the consumption and generation of locally sourced energy, rather than importing electricity from upstream networks.

P2P trading can be conducted in a centralised [117], [120], [121] or distributed [122]–[126] procedure. In a centralised trading framework, the control of the amount of energy traded and the price is managed by a central operator to achieve an overall system objective, whereas in a distributed framework buyers and sellers operate as individual entities to establish their own trades and prices with each other. Wang et al. [117] developed a centralised blockchain-based approach to P2P trading crowd-sourced energy. Sellers and buyers sent energy supply or demand requests for day-ahead trading to the utility, which solved an optimal power flow problem on a distribution network to minimise the generator cost function. The ECO-Trade algorithm was presented in [120] to coordinate P2P energy trading among households to solve an energy cost optimisation problem whilst ensuring fairness amongst participants. A Stackelberg Game approach was considered by [122]–[124] to coordinate P2P trading in a distributed manner. Liu et al. [122] considered a microgrid operator (MGO) which optimised energy sharing between solar PV prosumers. The MGO set internal prices for energy trading, and prosumers acted as followers to determine their energy consumption. Prosumers and the MGO chose strategies to maximise profit for the MGO and utility for prosumers. In [123], buyers and sellers in a community microgrid acted on non-cooperative and Stackelberg Game frameworks to select the trade to maximise their welfare, with

buyers iteratively selecting a seller to trade with based on submitted energy costs. Liu et al. also considered a game theory relationship between microgrids for distributed P2P trading. An iterative non-cooperative game was played among the energy sellers as they attempted to maximise their profits by selling energy to buyers. The relationship between buyers and sellers was then modelled as a Stackelberg Game to achieve equilibrium to determine the optimal pairing of buyers and sellers, and quantity of energy sold by the sellers [124]. A contract-based approach for energy trading was considered in [125]. Forward and real-time markets were considered, where agents could buy and sell energy contracts in the forward market based on predictions of cost and demand, before meeting their obligations in the real-time market. At each iteration of the market, each agent was offered a set of contracts by its neighbours. The objective of the market was to ensure that the agents chose a set of contracts that they do not wish to alter, through a distributed price adjustment process. Khorasany et al. [126] presented a distributed approach to maximising the welfare of all participants in the market. The market clearing problem was decomposed into local subproblems, which could be solved with limited information using the primal-dual gradient method. This maintains the privacy of participants and, by each participant solving their own welfare maximisation problem, the social welfare of the entire market can also be maximised. Two decentralised matching strategies to facilitate P2P trading between houses are presented in [127]. The first strategy matches houses based on their difference between solar generation and baseload deficit and surplus, while the second approach considers the distance between houses in the network to improve network efficiency through encouraging trading between more local houses.

2.4.1 P2P Trading and Network Constraints

One challenge of peer-to-peer energy trading is ensuring that the completed energy transactions do not cause any of the network's allowed limits on transformer loading, line utilisation, node voltages or power loss to be exceeded [116].

Consideration was given to the protection of the distribution network in [128], with the impact on the grid of energy transactions quantified using voltage sensitivity coefficients, power transfer distribution factors and loss sensitivity factors. After prosumers' bids and asks were matched in an auction, line loading and voltage was evaluated throughout the network using the above factors, with prosumers receiving an updated signal to inform whether they could continue to participate in the energy trading market without causing grid constraint violations, and an additional charge was incorporated into the transaction based on the congestion caused on the network. However, this approach requires real-time network monitoring for the operator to control trading, as all trades must be approved by the network operator. Trading between microgrids was analysed in [129]. Based on the outcome from the trading, the DSO would make adjustments to reconfigure the network topology or ask microgrids to reduce their power consumption if the network limits would be exceeded. Yao et al. analysed the trading between prosumers equipped with DERs. To account for the usage of the network infrastructure, prosumers were charged for investment and operation costs [130]. The operation costs incentivised transactions that support the network usage, and penalised unfavourable transactions, through marginal prices determined from a power flow analysis. These prices take into account line losses, node voltage limits and power limits. Jia et al. proposed a zero-sum settlement with a balance cost assigned to participants in the P2P market to account for any discrepancy in power supply and demand that arose through P2P trading [131]. A two-level trading problem was presented in [132], with trading between EVs and charging stations using V2G and renewable energy occurring at the first level, and then trading of energy between charging stations over the grid in the second level. The second level trading ensured the network limits are not violated, with the market clearing function performed by the network operator incorporating the power flow limits. The network limits were managed in [133] through the introduction of nodal agents. Each nodal agent performed energy management at its node of the network, and was responsible for voltage limits at the node and line current limits in adjacent

lines. However, this approach required each house to monitor the voltage and current at its node of the network in order to solve an optimal power flow problem. Feng et al. used sensitivity analysis to analyse the impact of P2P energy transactions on the network. The voltage sensitivity and power loss sensitivity resulting from a change in load was incorporated into the decentralised market clearing function to ensure the network limits are not violated. P2P trading between charging EVs and DERs was proposed by Yang et al. [134]. Two markets were implemented, an hour ahead market, which included constraints on all network limits, and a 5-minute real-time market, with both markets cleared using a decentralised approach.

While these works ensure that the network limits are not exceeded, all the above approaches require complex implementation. Network monitoring is required for the network operator or individual houses to have real-time knowledge of the voltages and currents in order to be able to solve power-flow based clearing mechanisms, or require the network operator to influence the actual P2P market in order to ensure that no network limits are exceeded.

2.4.2 Facilitating Peer-to-Peer Trading Through Auctions

Auctions are a popular method of facilitating P2P energy trading, and offer prosumers the ability to set their desired bid and ask prices, quantity of energy traded and participation.

The main types of auction structure include the forward auction, reverse auction and double auction. The forward auction can be considered the classic auction, where multiple buyers make bids to attempt to win the item from a single seller, typically with the buyer who bids the highest winning the goods. These types of auctions are common in markets with high demand and low supply, as the buyer-led approach gives power to the seller and will drive the price up, resulting in greater benefit for the seller. In a reverse auction, a single buyer wishes to buy a good or service offered by multiple sellers. Sellers present offers, herein referred to as

asks, for the price they would like to receive for the item. In response to other sellers in the market, a seller may lower its ask to drive the price down in hope of being picked by the buyer until a floor is reached at the minimum price a seller is willing to receive. This type of auction gives greater power to the buyer and results in a lower cost. The third common auction structure is the double auction, between multiple buyers and multiple sellers, where both buyers and sellers submit bid and ask prices, respectively [118], [135]–[140]. The submitted bids and asks form demand and supply curves based on price and quantity. The intersection point of these curves determines the quantity sold and the market clearing price, as shown in Figure 2.4 [118], [137]. At the end of the auction, buyers and sellers must be matched to determine the participants in each trade. In a classic double auction, buyers and sellers are typically matched according to price, where the highest bidder trades with the seller with the lowest ask [135], [140], until such time that there are no longer any bids higher than asks. This point is reached at the intersection of the demand and supply curves, and the dotted lines in Figure 2.4 signify the auction clearing price (y axis) and clearing quantity (x axis), which are the price at which trades occur and the total volume of items sold, respectively.

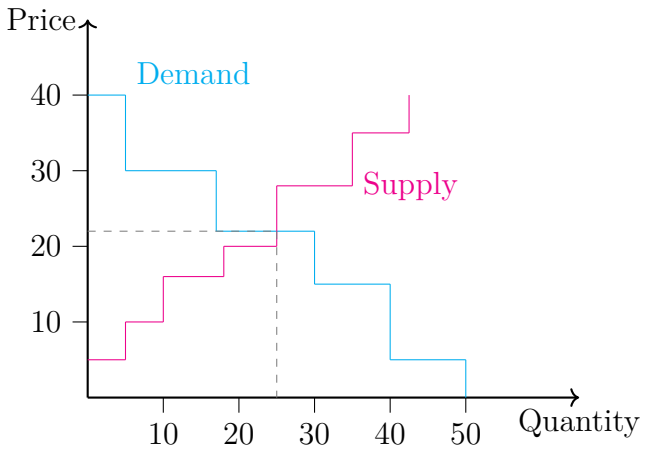

Figure 2.4: Example supply and demand curves constructed from double auction bids and asks. The dotted lines show the auction clearing price and clearing quantity

Auctions can also be classified as single-unit, or multi-unit. A single-unit auction is one where the buyers are bidding for a single item, such as a defined block of energy.

The winning buyer receives the single item from the seller. A multi-unit auction occurs when a seller has a higher quantity of an item to sell, and buyers also wish to purchase more than just a single unit. An example of a multi-unit auction would be the stock market, where a seller owns a number of shares S_{shares} and a buyer wishes to purchase quantity D_{shares}. Multi-unit auctions can be further classified in terms of the matching of multiple buyers and sellers into one-to-one, one-to-many, many-to-one and many-to-many matchings [141]. A one-to-one matching auction is where each buyer/seller only trades with a single seller/buyer. A one-to-many matching is the matching of a single buyer with multiple sellers. For instance, the buyer who bids the highest is first matched with the seller with the lowest ask. If this seller is unable to fulfil the buyers' demand, the buyer is then matched with subsequent sellers until the demand is fulfilled. The many-to-one matching is the reverse of this, where multiple buyers are able to match with the same seller. If a seller has a large quantity of an item for sale, then multiple buyers can trade before the supply is consumed. A many-to-many matching deals with the scenario where certain buyers will have demand greater than a single sellers' supply, and where some sellers with have greater supply than demand.

A key concept in auction theory is the idea of the participants' private valuations for the item in the auction, which are known only to the individual buyer or seller. A buyers' private valuation v_b is the highest price that the buyer is willing to pay for the item, whereas the sellers' private valuation v_s is the lowest price that the seller is willing to receive [138]. Buyers and sellers wish to maximise the gain they receive from the auction, which is the difference between their valuation and the actual trade price. A buyer would not bid in excess of their private valuation, and a seller would not ask for less than theirs to avoid receiving negative gain from the trade. However, buyers and sellers may bid dishonestly and bid a value that differs from their private valuation if they believe that this can maximise the gain they receive from the auction.

The method for determining which buyer and seller trade with each other in a double

auction is known as the auction matching mechanism. The key properties [138], [142] considered when evaluating a mechanism are:

- **Individual Rationality** - no participant should be negatively affected by taking part in the auction. Significantly, the price paid by a buyer should be at most equal to their private valuation $\pi_{\text{trade}} \leq v_b$, and the price received by a seller should at least exceed their private valuation $\pi_{\text{trade}} \geq v_s$
- **Budget Balance** - A strong balanced budget occurs if the auctioneer neither makes nor loses money as a result of the trades, that is the price paid by buyers is equal to the income received by sellers. A weak balanced budget relaxes this to state that the auctioneer should not lose money as a result of the trades, but can gain money.
- **Truthfulness** - The dominant strategy for buyers and sellers to take in a truthful auction is to bid and ask their true private valuations. The gain from the auction is lower when not bidding truthfully.
- **Economic Efficiency** - The trades made in the auction should maximise the utility of the participants and result in items purchased by buyers with the highest valuations.

As stated above, the traditional matching mechanism in a double auction is to order the bids from high to low, and order the asks from low to high, and the breakeven index k can be found at the intersection of demand and supply where there are no more bids that exceed the price of remaining asks. The first trade is between highest bidder and lowest asker at the market clearing price, the second trade is between the second-highest bidder and second-lowest asker, and final trade is between the k^{th} bidder and k^{th} asker. This can be applied in single-item and multi-item auctions, and with one-to-one and many-to-one matchings. In a multi-item, many-to-one auction, the highest bidder will trade with as many sellers as required to fulfil their demand, starting with the seller with the lowest ask price

and working their way through sellers in increasing ask price order until they have fulfilled their order. However, this mechanism does not result in truthful bidding as the k^{th} bidder and seller have an incentive to alter their bid and ask prices to improve their utility as their trade sets the auction price. If buyer k changes its bid $\pi_{\text{bid},k_{\text{new}}}$ such that $\pi_{\text{bid}_{k+1}} \leq \pi_{\text{bid},k_{\text{new}}} \leq \pi_{\text{bid}_k}$, they will remain the k^{th} highest bidder and still participate in the auction but would trade at a lower price, hence increasing their utility. This mechanism can be made truthful by only allowing the first $k-1$ buyers and sellers to trade at a price determined by the k^{th} buyer and seller, so none of the first $k-1$ participants have an incentive to misreport their price as it has no impact on the auction trade price. An extension on this is McAfee's mechanism [143] which will allow the first k buyers and sellers to trade if the trade price π_{trade} determined by the $k+1$ bid and ask is in the range between $\pi_{\text{ask}_k} \leq \pi_{\text{trade}} \leq \pi_{\text{bid}_k}$, where $\pi_{\text{trade}} = \frac{1}{2}\left(\pi_{\text{ask}_{k+1}} + \pi_{\text{bid}_{k+1}}\right)$. If the average price is outside of this range, then only the first $k-1$ participants can trade, with buyers paying price π_{bid_k}, and sellers receiving price π_{ask_k}, leading to a weakly budget-balanced auction where the auctioneer receives profit of $\text{Profit}_{\text{auctioneer}} = (k-1) \cdot (\pi_{\text{bid}_k} - \pi_{\text{ask}_k})$. However, there are also many other mechanisms for matching buyers and sellers. The Vickrey sealed bid mechanism [138], [144] can facilitate truthful bids, as the highest bidder wins the auction but pays second highest bid price. In [145], the difference between bid prices and market price was calculated, with the smaller the difference resulting in the higher the priority to trade, rewarding buyers who bid truthfully at market price. Kan et al. [139] determined trades through a combination of cost and the percentage of EV's energy need fulfilled, whereas [136] used a day-ahead auction with the goal of minimising impact on the grid through charging and discharging EVs. An Average Price Mechanism was compared with trading at the market clearing price in [138], the authors concluding that the Average Price Mechanism allowed more participants to trade. Rana et al. [146] considered auction matching mechanisms for P2P energy trading among EVs (V2V). They focused on a cloud-based server for communication between EVs, and considered the amount of energy each EV has

initially when determining the matching through a value known as the aspiration rate. The auction matching mechanism aimed for greater profit for all participants, and the matching of EVs was determined optimal if the sum of the gain (difference between bid and asks) was maximised.

2.4.3 Peer-to-Peer Trading with Electric Vehicles and Renewable Energy

EVs can also utilise P2P networks for the trading of energy. EVs with surplus energy in their batteries can sell energy directly to other EVs that require charging (V2V) [137], [139], [146], [147]. A double auction was implemented in [139] to allow multiple EVs to trade with each other through the discharging and charging of their batteries. Each EV traded to maximise their utility, with charging vehicles attempting to maximise their energy, and discharging EVs attempting to minimise their cost. Li et al. [137] also considered a multi-unit double auction approach in a parking lot for EVs to trade energy between themselves. Rana et al. [146] proposed a cooperative game to match charging EVs with discharging EVs to maximise social welfare, through a combination of bid prices and aspiration rates in order to minimise the sharing of private information. Liu et al. introduced a smart contract based reverse auction for EVs to trade energy between themselves at charging stations [147]. The energy stored in EV batteries can also be sold to the grid, for instance in [148], EVs acted as either buyers or sellers of energy with the grid, with the aim of regulating voltage deviations. The EVs submitted both bids and asks, with an auctioneer choosing which offer to accept. Another key implementation of P2P energy trading is for facilitating EV charging, where EVs can purchase energy to charge their batteries directly from distributed energy producers. Smart charging of EVs was considered in [87], where contracts were negotiated between EVs and aggregators to coordinate EV charging in a way that is beneficial to the grid. The aggregator attempts to maximise profits and, with the cost set as a function of base load, also resulted in

flattening of the total grid load. A multi-agent system was proposed in [149], where a local scheduling agent could optimise control of energy resources in the network, taking into account grid constraints. If there was an energy deficit, the additional energy could be procured through P2P trading. Buyers and sellers could negotiate temporary contracts for the sale and purchase of energy, including the ability to renegotiate the price.

P2P trading of surplus solar energy was covered in [121], [144], [150], [151]. In [121] prosumers could sell or buy solar energy depending on their net power. When purchasing energy, buyers looked to minimise their cost, and when selling energy, maximise their profit. A bi-level programming model was implemented, with the first stage determining an internal price for each prosumer depending on whether they are buying or selling energy in the time slot, and the second stage to maximise the benefit of all prosumers. The trading price of the surplus solar energy was calculated from the supply and demand ratio (SDR) in the market. In [150], PV owners submitted asks as they attempted to sell their surplus energy to flexible load users, such as EVs. The market mechanism aimed to maximise the PV revenue, taking into account the revenue from energy sold, positive deviation sold and reducing the costs of negative deviation. The PV offers were ranked low to high, and loads were matched with PV owners until there is no unmatched load remaining, with buyers paying the PV ask price. The uncertainty in solar PV forecasting was considered, with the proposed P2P system capable of consuming more PV energy locally than traditional market methods. Doan et al. presented a P2P system for houses with surplus solar energy production to sell energy to houses requiring energy, rather than selling energy with the main grid, with a blockchain implementation for preserving participant privacy [151].

In many energy auction studies, a seller is able to provide energy to multiple buyers, or a buyer is able to purchase energy from multiple sellers, simultaneously. However, in certain trading scenarios, the resources available do not cater to this. For instance, Schürmann et al. considered the limited availability of on-street charging for EVs

through incentivising cooperative handovers to encourage better utilisation of charging points, for instance in ensuring that charging points were vacated once the EV is fully charged [152]. The limited availability of parking spaces for EVs was also considered in [153] and [154]. Both used auction mechanisms with a limitation on the number of EVs that win in the auction to match the available resources (number of parking spots and charge points). In [154] and [155] the amount of energy available to a buyer was also limited. The energy available to each buyer was determined by the total energy available minus the amount requested by buyers offering a higher bid price. A blockchain-based auction system was presented in [144], where sellers offer a block of energy for sale via a blockchain platform. Unlike many other auction based energy trading studies, this was a forward auction rather than a double auction, as multiple buyers bid on individual items, in this case a block of energy, and under the Vickrey model, the highest bidder won the auction but paid the second-highest bid price, ensuring truthful bidding. In these works, the priority of obtaining the desired resource was based upon the bid price, with a higher bid price increasing the likelihood of trading the desired quantity of the resource.

2.4.4 Summary

Peer-to-peer trading is an important technology for the future implementation of smart grids, allowing greater implementation of distributed generation, less reliance on upstream parts of the network to provide power and additional financial benefits for participants. EVs can benefit from P2P energy trading to increase the amount of renewable energy consumed, to lower their charging costs or to sell surplus energy to houses or other EVs through V2G for a profit. Double auctions are a popular way to facilitate trading, giving participants greater autonomy over how much energy they trade and the price they are willing to pay or receive for it. However, the auction matching mechanism is an important tool for ensuring that the available resources are efficiently allocated and that buyers and sellers are not disadvantaged and must be given special consideration to ensure that the market objectives are achieved.

However, few existing studies explore the scenario where there is insufficient energy to meet all buyers demand in detail and the resulting complexity of designing the mechanism for maximising the benefit of all participants combined, versus prioritising the highest bidders. A number of existing P2P studies allow many-to-one matching in order to meet the needs of the highest bidder, but less attention is given to one-to-one matchings in continuous auctions. One-to-one matchings are an important class of auction, for example when the trade includes items that are geographically or time limited, where it is not possible to trade with multiple sellers, or in the energy market if selling energy produced by one distributed generator to another buyer through the grid could cause violation of grid limits, the energy could be consumed by an EV locally without violating the limits. One-to-one matching also introduces a number of interesting challenges for the matching mechanism that are not present in many-to-one and many-to-many matchings. The matching mechanism has to make the optimal choices for buyers and sellers based on the information known in the auction at the current time, without future knowledge of any new participants that could join the auction at a future time that would enable a higher utility for the participants, and to take into consideration that if the matched seller is unable to provide the quantity demanded by the buyer, then the buyer has no ability to get their deficit from another seller. The sale of solar energy is a particularly interesting case in this scenario as the generation is time-sensitive, for instance a seller may question if it is better to sell a small amount of energy straight away with lower chance of selling more later, or to wait and waste the solar energy produced until a consumer arrives looking to purchase a larger quantity of energy.

2.5 Conclusion

This chapter has presented an introduction to the transition toward zero emission vehicles, electric vehicle charging and the structure of low-voltage distribution networks, along with the backward-forward sweep power flow equations for analysing

the network. Current literature covering a broad range of topics within EV smart charging and peer-to-peer energy trading was then evaluated.

A significant amount of research on EV charging has focussed on the benefits that EVs can provide to the grid through smart charging, such as by peak shaving, valley filling or managing voltage levels. The key motivation behind these smart charging services is to reduce the impact of EV charging on the network, therefore increasing the number of EVs that the network can accommodate. Load shifting manages transformer loading and prevents the network from exceeding any power limits, however many of these studies do not include network voltage or current constraints, which are necessary to ensure that the EV charging can be successfully accommodated by the network. Where considered, the inclusion of voltage and current limits has typically been implemented either through power flow equations incorporated into the optimisation problem, or through real-time network monitoring. However, both approaches have significant drawbacks that limit their real-world implementation. Power flow based optimisations add significant computational complexity to the problem, and often require knowledge of all loads and generation throughout the network in order to compute the problem. This level of knowledge is unrealistic in a real-world application, as the required sharing of private load information would be prohibitive. Real-time monitoring requires the deployment of voltage and current sensors throughout the network in order to communicate the voltage and current values at all buses and lines in the network to the EV charging controller.

Increasing deployment of distributed energy resources including solar PV generation, home battery storage, vehicle-to-load (V2L) and vehicle-to-grid (V2G) can enhance EV charging by adding additional energy flexibility, offsetting increased charging load and furthering the decarbonisation of transport by supplying renewable energy for EV charging. Challenges surround maximising the consumption of generated renewable energy, dealing with generation intermittency and discrepancy between predicted and actual generation. By maximising the utilisation of renewable energy,

the benefit to EV charging can be maximised, and the hosting capacity of EVs increased.

In addition to ensuring that EV charging can be accommodated by the network while remaining within permitted voltage, current and power limits, there is a significant amount of research into calculating the maximum EV penetration that can be accommodated. This provides an analytical tool for network operators to assess the readiness of their networks for increasing numbers of EVs, and enables analysis of potential network upgrades and how the EV hosting capacity is affected. However, there is very little research on calculating the EV hosting capacity with the inclusion of DERs, which can be managed in order to increase the number of EVs that a network can accommodate.

The maximum EV hosting capacity requires optimal usage of all energy resources in order to be accommodated within the network, which can only be realised through a centralised control algorithm with control of all DERs. However, this results in a significant loss of autonomy for each house, who relinquish control over their energy generation and consumption, requires high levels of communication and privacy sharing, and leads to vastly increased computational complexity for large networks or complex optimisation algorithms. Therefore, with the increasing numbers of prosumers in modern distribution networks, alternative DER management strategies are required in order to support the network operation while also benefiting the individual prosumers. Peer-to-peer trading strategies offer a compelling decentralised option to support the management of DERs between houses in a network by hosting a market-based platform allowing houses with surplus renewable energy to sell this energy to other houses who wish to consume power. With a free market, such as through a double auction, houses can solve a cost-based optimisation problem in order to determine the optimal usage of their DERs, and whether to consume or sell generated energy by submitting bids and asks for their energy. However, a major issue with P2P trading is ensuring that the agreed energy trades do not violate any of the network voltage, current or power limits, and maximising the

benefit that can be achieved through the market. While a number of studies have included these limits into P2P trading, the same issues occur as with the inclusion into smart charging. There has been very little consideration of unorthodox P2P trading approaches that can offer the primary benefits of P2P trading to network operation and prosumer energy management, while providing simpler integration of network operation constraints.

In conclusion, there are still significant unsolved challenges with regards to the management of DERs for maximising EV charging, while promoting the autonomy of individual prosumers, supporting network operation and offering solutions conducive to real-world implementation.

Chapter 3

Closest Energy Matching Mechanism

Chapter Summary

The concept of matching EVs with vacant house charge points is introduced in this chapter to provide visiting EVs with charging solutions while maximising the consumption of solar energy produced by each house. This problem is presented through a peer-to-peer trading scenario and five auction matching mechanisms are compared, including the proposed novel Closest Energy Matching (CEM) to evaluate their performance in terms of the utilisation of renewable energy for EV charging. The proposed CEM mechanism is shown to perform better than the alternative matching mechanisms, facilitating a greater proportion of EV charging from renewable energy, reducing charging costs to EVs while increasing the consumption of generated renewable energy and profits for sellers.

3.1 Introduction

As the uptake of electric vehicles increases, charge point availability and driving range are still among the top concerns of potential EV buyers. Around 80% of EV

charging currently takes place at home, typically in the evening and overnight once EV owners have returned from work, meaning that there are already significant numbers of under-utilised private charge points, which will only increase as more people transition from ICEV to EV ownership [24]. Although currently around 90% of EV owners have access to private charge points at home or work, 43% of current car owners do not have a driveway or access to a private charger which will cause challenges for EV charging as the transition concludes [156]. These home charge points are often vacant during the day, with their house's EV parked elsewhere, such as at work. There is an emerging market for houses to allow visiting EVs to utilise their vacant charge points during the day, which can solve many of the challenges that EV drivers currently face. Introducing a reservation system for private charge points would alleviate EV owners' concerns over charge point availability, especially when travelling to a new location as public charge points cannot be booked. In addition, allowing other EVs to use private charge points would provide parking for visiting EVs, helping to alleviate parking and congestion difficulties. Distributed Energy Resources (DERs) such as residential solar panels are becoming increasingly popular as houses attempt to reduce their carbon footprint and energy bills. However, the times of peak solar generation typically coincide with lower baseload energy demand, and to maximise the benefit of the PV system, a house would ideally look to sell the energy to consumers at these times, such as visiting EVs, or store it in on-site batteries. The development of P2P trading provides a perfect platform for the implementation of such a charge point and solar energy sharing proposal. This can help increase self-consumption of its solar energy to avoid the need for battery storage, wasting renewable energy, or having to sell it through the local grid which can be problematic in residential distribution networks at times of low demand and high PV production. Commercial solutions already exist for facilitating the sharing of private parking spaces, including JustPark [157], YourParkingSpace [158] and Park on My Drive [159], and the sharing of private EV charge points through Co Charger [30] and Zapmap [160]. This chapter proposes an extension to these existing

schemes, combining the sharing of private parking spaces and EV charge points with surplus renewable energy generation, and providing a competitive, market-based approach and improved matching mechanisms to determine the optimal pairings of visiting EV and house charge point.

This study considers a scenario where a house or small-business, etc. (hereafter just referred to as houses), wishes to sell surplus solar energy produced by solar PV panels mounted on their building to a visiting EV that requires charging. It is assumed that the house owns their own EV and has a vacant EV charging point during the day for the visiting EV to use. A double auction platform is designed to host the P2P trading system, where houses can submit asks to sell their surplus solar energy and visiting EVs can submit bids to purchase this energy. In the auction, the winning houses will provide the winning EVs with a guaranteed parking space, EV charging point and the agreed amount of solar energy in exchange for the price determined from the bid and ask prices. Each EV can only trade with a single house as it is assumed that the EV would not want to relocate during the day, and as each house only has a single charging point, they can only charge one EV at any given time. In line with existing work, our auction ensures that participants are no worse off through participation in the auction, and buyers and sellers are free to individually determine their own bid and ask prices based on their own preferences. The primary contributions of this work are as follows:

1. Unlike many existing pieces of literature that assume that there is sufficient energy to ensure all EVs are able to fully charge, this study examines the scenario where there may be insufficient energy to complete all EV charging demands, and explores auction matching mechanisms that aim to maximise the amount of charge all EVs receive.

2. Electricity produced by house solar panels is fed directly to the house's charge point to charge the EV, rather than sold and distributed through the grid. This reduces system complexity and power issues resulting from the charging of EVs

or injection of DER-produced energy. Focusing on increasing the EV charge aids decarbonisation by increasing the amount of solar energy consumed.

3. One-to-one matching of EVs and houses is enforced to explore the effectiveness of different auction mechanisms for EV energy auctions under the scenario of limited solar energy and imperfect online information regarding the future needs of EVs. One-to-one matching is chosen for this paper because most houses have only a single EV charge point, meaning they can charge only one EV at a time, and in addition, house PV arrays may not generate sufficient energy to fully charge one EV, and are unlikely to have sufficient surplus solar energy to trade with multiple EVs. One-to-one matching is an interesting scenario to analyse as it increases the importance of the decisions made in a real-time auction matching mechanism with incomplete information.

4. A novel double auction mechanism, Closest Energy Matching (CEM), is proposed which aims to maximise the amount of charge EVs receive from solar energy, reduce the grid energy required for charging, reduce the EV's cost to charge and increase the profit made by sellers. The proposed CEM mechanism is described along with four other mechanisms in Section 3.2. Section 3.4 explains the case study used and the performance results for each of the presented auction mechanisms, showing that the Closest Energy Matching mechanism results in higher solar consumption, greater EV charge, increased revenue for houses, lower costs for EVs and a significant reduction in grid energy required to fully charge all EVs.

3.2 Double Auction Matching Mechanisms

The auction mechanisms presented in this chapter are based on the double auction premise: buyers submit a bid consisting of the price in p/kWh (1p = £0.01) that they are willing to pay for the energy, along with their departure time and amount of

energy requested in kWh; sellers submit an ask price in p/kWh and a vector of their predicted surplus energy available to sell throughout the day. The purpose of the auction matching mechanism is to match bids with asks to determine which buyers and sellers trade together. The mechanism should satisfy individual rationality (the participants are no worse off through participation in the auction), achieve a strong balanced budget (the auctioneer neither gains nor loses money as a result of a matching), and attempt to satisfy economic efficiency (maximise total social welfare). A major factor of the auction used in this scenario is that each buyer wishes to acquire a certain quantity of energy and each seller has a different amount of finite energy available. In addition, each buyer(seller) is only able to trade with a single seller(buyer). As a result, the sellers are non-homogeneous - the choice of seller affects both trade price and energy quantity - so the auction mechanism must take both price and energy quantity into account during the matching.

The objective of a buyer is to purchase their desired quantity of energy from a seller at the lowest possible total cost, while a seller aims to maximise the amount of energy they can sell and the price they receive for it. As the total cost/income is prioritised rather than the trade price, a house can achieve higher profit by selling a greater quantity of energy at a lower trade price than selling less energy at a higher trade price. Similarly, if it is assumed that the buying EVs will have to charge from the grid at a higher price if they are unable to purchase all their required energy from their matched house, then an EV that can purchase all of its required energy at a slightly higher trade price can have a lower total cost than an EV that was only able to obtain a portion of its required energy, even if it traded at a slightly lower price. With the purpose of this thesis to evaluate how renewable energy can improve EV charging, the primary objective that these markets are evaluated by is to maximise the amount of EV charging completed using solar energy. Therefore, unlike traditional double auctions that prioritise economic efficiency, where the goods are won by the buyers that value them the most, mechanisms 3-5 remove the constraint that only participants to the left of the supply and demand curve intersection can

trade, allowing any buyer to trade with any seller as long as their bid price is greater than the seller's ask price. This enables the market clearing mechanism to prioritise alternative objectives, with the overall goal of maximising participant welfare through increased EV charging.

In all of the tested mechanisms, the auction runs every 15 minutes. If the EV owner requires energy and is not already charging, they will submit their bid price and quantity of energy required. Similarly, if the house has surplus energy available and is not currently charging another EV, they can submit an ask price and their predicted surplus energy profile. Privacy issues are an important consideration with P2P trading systems for EVs. Buyers and sellers must submit private information relating to their energy demand and supply profiles, EV energy needs and driving patterns. The auction mechanisms presented in this chapter utilise a sealed-bid system, where the private information regarding the EVs and houses (energy profiles, departure times) is only visible to the auctioneer that conducts the matching mechanism. In addition, each buyer and seller are identified by a unique ID number which preserves privacy during the auction process. Once the auction matching process is complete, the private information of a house's location or EV information can be communicated directly with the matched buyer and seller, respectively. Although not within the scope of this work, the auction mechanism can be combined with a blockchain implementation, such as in [139], [140], [161]. Public-key encryption and the blockchain consensus procedure is used in [140] to validate transactions and discard any transactions created by dishonest partners within the network. Smart contracts are also used to deal with discrepancies between energy awarded in the auction and energy actually traded. A consortium blockchain is used in [139] to allow permitted aggregators to verify the energy trades. Public/private key encryption is again used to mask real identities and ensure all messages and transactions are legitimate. The authors of [161] present a privacy-preserving algorithm through the encryption of bids, with matching taking place over the blockchain through a smart contract and the masking of the identities of participants.

PV production and the house's energy requirement are assumed to be predictable, and therefore the house is able to broadcast their profile of surplus solar energy throughout the day to all buyers. A further assumption is that an EV owner would not wish to move their EV during the day. Therefore, a buyer can only match with at most one seller, regardless of whether or not that seller is able to provide sufficient energy to fully charge the EV. Most houses only have a single EV charging point so, until an EV departs from a seller, no other EVs can be charged. If a seller has insufficient solar energy production to meet the EV's demand, grid energy can be used to make up the shortfall.

3.2.1 One-to-One Matching vs Many-to-Many Matching

This paper proposes a one-to-one auction matching mechanism, where each buyer is only able to match with a single seller and vice versa. One-to-one matching has been chosen as the most suitable auction type in our scenario for the following reasons. Firstly, such a system can be easily implemented with existing hardware and technology, and is less computationally complex than a many-to-many matching system, making it more appropriate for use within low-powered hardware as may be used in an EV charging point. Secondly, it enables the house's charge point and solar panels to be isolated from the grid, enabling EV charging and use of DERs without concerns around transformer load and voltage deviation issues. Thirdly, EV energy requirements are high in comparison with the energy generated from domestic PV panels. A single house is unlikely to have sufficient surplus solar energy to charge multiple EVs and most houses only have a single charge point, so trading amongst multiple houses and EVs is not greatly beneficial in the scenario considered in this paper. By enforcing one-to-one matching, the auction mechanism must determine which house should charge each EV to ensure best consumption of solar energy and EVs achieving the greatest percentage of their required energy, without any information about future demand.

Alternatively, many current studies consider many-to-many matching, where each house can charge multiple EVs, and each EV can purchase energy from multiple houses [123], [136], [139], [149]. In certain scenarios, such a system could result in greater utilisation of renewable energy, or cheaper prices for consumers. Although this is beyond the scope of this paper, it is possible to adapt the proposed P2P trading to conduct many-to-many matching auctions. Auctions can be conducted in two rounds, with the first round matching each EV with a house where the EV can park and charge. The second round would be an energy-only round where, if an EV is unable to fulfil its charging requirements from the house that it has been matched with in the first round, it can make an energy bid to the other houses to supply its energy shortfall through the grid. If a house has additional surplus energy not already promised to a charging EV, they can submit an energy ask to sell this energy to another EV through the grid. This requires another round of communication to the auction but could result in more EVs achieving a full charge and houses selling more of their surplus solar energy. However, if a house that is not charging an EV opts to sell energy in the second round, it could reduce the chance of that house winning a more profitable future first-round auction, as it has already committed to sell some of its energy in future timesteps through the energy-only market. A comparison between the two auction types and EV charging performance is beyond the scope of this work.

3.2.2 Determining the Bid and Ask Price

Each buyer i and seller j has their own private valuation of the energy, which is the equivalent of the highest price they are willing to pay per kWh (denoted v_i) or lowest price they are willing to receive (v_j), respectively. This valuation is known only to the individual participant and is determined individually through a variety of factors. A buyer who requires a large quantity of energy may value it more highly than a buyer who requires less energy, but the valuation is also a factor of their own personal and economic situation - if the buyer has other EV charging alternatives

they would likely the value energy lower than a buyer who relies heavily on the energy they are bidding for. Likewise, a seller with a large quantity of energy may value it lower than a seller with less energy to sell. However, if battery storage is available to them, they may prefer to store the energy rather than sell it and would therefore value the energy they sell in the auction more highly. It is logical for a buyer to wish to trade at a price considerably lower than their valuation and a seller to wish to trade at a price higher than their valuation. The gain that a buyer receives from the auction matching is defined as the difference between their valuation and the price they pay for the energy, and the gain a seller receives is the difference between the price they receive for the energy and their private valuation [137], [162]. If buyer i bids lower than their true valuation they risk not receiving the full amount of energy they request if the only seller j with sufficient energy has an ask price $\pi_{\text{bid}_i} < \pi_{\text{ask}_j} < v_i$. However, because sellers are free to set their own ask price, and the award of energy through the auction mechanisms considered here is not directly proportional to the bid price, it is an appropriate assumption for the buyer and seller to choose their optimal bid and ask prices solely based on their expected gain per kWh. If buyer i and seller j are matched by the auction mechanism with bid and ask prices of π_{bid_i} and π_{ask_j} and trade at price $\pi_{\text{trade}_{ij}} = \frac{1}{2}\left(\pi_{\text{bid}_i} + \pi_{\text{ask}_j}\right)$, then the gain the buyer receives is given by:

$$G_i = v_i - \frac{1}{2} \cdot \left(\pi_{\text{bid}_i} + \pi_{\text{ask}_j}\right) \tag{3.2.1}$$

The maximum gain that a buyer can receive from that trade is:

$$G_{\text{max}_i} = v_i - v_j \tag{3.2.2}$$

which occurs when $v_j = \pi_{\text{ask}_j}$ and $\pi_{\text{bid}_i} = v_j$, i.e. when the seller asks for their true value and the buyer's bid is equal to the seller's true valuation. If both parties bid truthfully - $\pi_{\text{bid}_i} = v_i$ and $\pi_{\text{ask}_j} = v_j$ - the gain the buyer receives is given by:

$$G_i = v_i - \frac{1}{2} \cdot (v_i + v_j) = \frac{1}{2}(v_i - v_j) \tag{3.2.3}$$

The gain received by a seller is the difference between the trade price and their valuation:

$$G_j = \frac{1}{2} \cdot \left(\pi_{\text{bid}_i} + \pi_{\text{ask}_j}\right) - v_j \tag{3.2.4}$$

A seller will maximise their gain if their ask price is equal to the matched buyer's true valuation and the buyer bids their own true valuation:

$$G_{\text{max}_j} = \frac{1}{2} \cdot (v_i + v_i) - v_j = v_i - v_j \tag{3.2.5}$$

It can be seen from (3.2.2) and (3.2.5) that the maximum gain that a buyer and seller can achieve from a trade are equal, but cannot happen simultaneously, as they rely on opposite bidding strategies - a buyer requires the seller to bid truthfully while the buyer bids untruthfully, and the seller requires the buyer to bid truthfully while the seller bids untruthfully. If both parties bid truthfully, the gain of the seller is equal to the gain received by the buyer:

$$G_j = \frac{1}{2} \cdot (v_i + v_j) - v_j = \frac{1}{2}(v_i - v_j) \tag{3.2.6}$$

Therefore, if both parties bid truthfully, they will sacrifice half of their maximum possible gain that would have been achieved if one of the parties had bid untruthfully.

$$\begin{aligned} \Delta G &= G_{\text{max}_i} - G_i = (v_i - v_j) - \left(v_i - \frac{1}{2} \cdot (v_i + v_j)\right) \\ \Delta G &= \frac{1}{2}(v_i - v_j) \end{aligned} \tag{3.2.7}$$

It can been seen that a buyer will increase their gain from the auction if they bid untruthfully, however the following constraint must be satisfied to ensure that the trade price is lower than the trade price derived from truthful bidding:

$$v_i - \pi_{\text{bid}_i} > \pi_{\text{ask}_j} - v_j \tag{3.2.8}$$

This means that the difference between the buyer's actual bid price and truthful valuation must be greater than the difference between the seller's ask price and truthful valuation, that is the buyer must act more untruthful than the seller. If this constraint is not satisfied, then the trade price will be closer to the buyer's truthful

valuation, therefore resulting in a lower gain than if both parties bid truthfully. Similarly, a seller must ensure that they submit a more untruthful ask than the buyer, otherwise the trade price will be less than the achieved trade price from truthful bidding, which reduces the seller's gain:

$$\pi_{\text{ask}_j} - v_j > v_i - \pi_{\text{bid}_i} \tag{3.2.9}$$

In the case that $\pi_{\text{ask}_j} - v_j = v_i - \pi_{\text{bid}_i}$, the trade price will be equal to the truthful trade price, and neither party has increased their gain from submitting an untruthful bid or ask. There is also a limit to how untruthful each participant can act, as the buyer's bid price becomes higher than the seller's ask price and the buyer and seller are unable to trade if:

$$v_i - (v_i - \pi_{\text{bid}_i}) > v_j + \left(\pi_{\text{ask}_j} - v_j\right) \tag{3.2.10}$$

Therefore, a buyer (seller) can increase their gain from the auction by not bidding truthfully, as long as they bid more untruthfully than the seller (buyer), but not so untruthfully that their bid price exceeds the seller's ask (buyer's bid). Because neither buyer or seller are aware of the other's bid price, the incentive to not bid truthfully exists. If the buyer and seller are aware of each other's truthful valuation, then truthful bidding becomes a dominant strategy, as both parties would try to increase their gain by altering their offers until the point at which $\pi_{\text{bid}_i} = \pi_{\text{ask}_j}$ and each party's gain is equal to that from submitting truthful offers.

However, in the case of the sealed-bid market presented here, where the actions of other participants are unknown to each other, bidding truthfully is not a dominant strategy in the auction and, as such, the buyers and sellers must choose their bid and ask prices in order to try and maximise their gain. The optimal bid price for a buyer is derived as follows: It could be assumed that the asks are normally distributed as it is likely that participants will have past knowledge of the average trade price [163]. The majority of bids/asks will be distributed around the average price, with fewer offers at prices further from the average price. In this paper, the past data has been

estimated with $\mu = 11.5$ p and $\sigma = 1$. The buyer wishes to choose their bid price to maximise their gain against the expected ask price, but if they bid lower than the ask price then they will receive 0 gain. The expected gain that a buyer would expect to achieve based on their bid price, $G_{\exp_i}$, is given by (3.2.11):

$$G_{\exp_i} = \int_0^{\pi_{\text{bid}_i}} \left(v_i - \frac{1}{2} \left(\pi_{\text{bid}_i} + x \right) \right) \cdot f(x)\, dx \tag{3.2.11}$$

where $f(x)$ represents the normal distribution probability density function:

$$\mathcal{N}(\mu, \sigma^2) \text{ PDF:} \quad f(x) = \frac{1}{\sigma\sqrt{2\pi}} \exp\left[-\frac{1}{2} \left(\frac{x - \mu}{\sigma} \right)^2 \right] \tag{3.2.12}$$

Figure 3.1 shows the value of the buyer's expected gain calculated from solving (3.2.11) for a range of bid prices for three different valuations (v_i). It shows that the buyer can expect to obtain a higher gain by bidding a value lower than their true valuation, as expected from (3.2.7), but it also shows that their expected gain decreases if they bid too low as the probability of trading decreases. The optimal bid price ($\pi^*_{\text{bid}_i}$) to maximise the expected gain for each valuation is shown on the graph by the dotted lines corresponding to the maximum value. In order to maximise the expected gain, the buyer must choose a bid price that maximises the value of equation 3.2.11. To simplify the calculation, this integral is approximated as a Riemann sum using the midpoint rule, and the optimisation problem is presented as follows:

$$\underset{\pi^*_{\text{bid}_i}}{\arg\max} \sum_{k=1}^{n} \left(v_i - \frac{1}{2} \left(m_k + \pi_{\text{bid}_i} \right) \right) \cdot f(x) \cdot \Delta x \tag{3.2.13}$$

subject to

$$\Delta x = \frac{\pi_{\text{bid}_i}}{n} \tag{3.2.13a}$$

$$m_k = \frac{1}{2} \left(k\Delta x - (k-1)\, \Delta x \right) + (k-1)\, \Delta x \tag{3.2.13b}$$

$$\pi_{\text{bid}_i} \leq v_i \tag{3.2.13c}$$

where n is the number of intervals, m_k is the midpoint of interval k in the integration and Δx is the width of each interval. Each buyer can calculate their optimal bid price $\pi^*_{\text{bid}_i}$ by finding the value of π_{bid_i} that maximises the objective function (3.2.13).

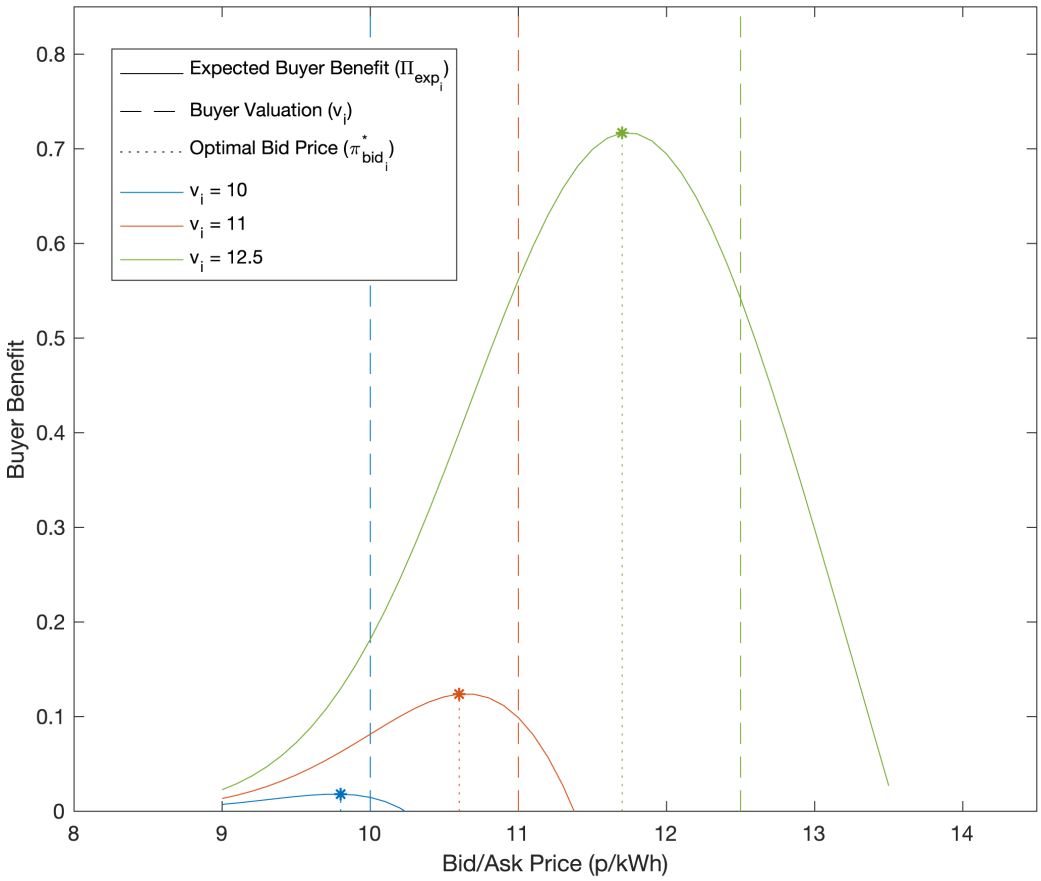

Figure 3.1: Effect of bid price on buyer gain for three different values of buyer valuation v_i

The derivation of the optimal ask price for a seller $\left(\pi^*_{\text{ask}_j}\right)$ is not shown here, but it can be obtained using the same procedure as above and is given by:

$$\underset{\pi^*_{\text{ask}_j}}{\arg\max} \sum_{k=1}^{n} \left(\frac{1}{2} \left(m_k + \pi_{\text{ask}_j} - v_j \right) \right) \cdot f(x) \cdot \Delta x \tag{3.2.14}$$

subject to

$$\Delta x = \frac{\pi_{\text{grid}} - \pi_{\text{ask}_j}}{n} \tag{3.2.14a}$$

$$m_k = \frac{1}{2} \left(k\Delta x - (k-1)\,\Delta x \right) + (k-1)\,\Delta x \tag{3.2.14b}$$

$$\pi_{\text{ask}_j} \geq v_j \tag{3.2.14c}$$

3.2.3 Auction Matching Mechanisms

Five mechanisms are explored below, each with a different strategy for matching buyers and sellers. The overall aims of a buyer are to maximise the amount of charge they receive for their EV and reduce the cost of the energy they buy, while sellers wish to maximise the amount of their surplus energy sold and increase their profit from selling energy. In each mechanism, the trade price is calculated as the mean of the matched bid and ask prices, resulting in buyers always paying the bid price or less, and sellers always receiving their ask price or greater.

Mechanism 1: Cheapest Ask

This is the classic double auction mechanism, as in [135] and [140]. Once buyers and sellers have submitted bids and asks, they are ordered according to natural ordering - bids are sorted from high-to-low, and asks from low-to-high. Each bid is taken in this order and matched with the lowest available ask. The corresponding house and EV are then matched and can trade. This mechanism only considers the bid and ask prices and not the amount of available energy.

Mechanism 2: Sufficient Energy/Cheapest Ask

Mechanism 2 is an adaptation of mechanism 1. Because the first mechanism did not consider the energy requirement of the EVs during the matching mechanism, it is possible that an EV will be matched to a house that is unable to provide the desired quantity of energy, when there may be an alternate house that could supply sufficient energy with little difference in price. This mechanism makes the following adjustments to the algorithm used in mechanism 1: Once the bids and asks have been sorted, each bid is taken in order. However, sellers that have insufficient energy to meet the EV's energy need are first removed from the list of asks before the cheapest ask remaining is matched. If there are no sellers available with sufficient energy, then the mechanism picks the cheapest ask, as per mechanism 1. Mechanisms 1 and

2 reward buyers who have bid the most by giving them priority in the matching, as in [154] and [155].

Mechanism 3: Minimise Cost

This mechanism attempts to minimise the total cost to buyers through solving the following optimisation problem. Similar cost minimisation strategies are popular in energy auctions, and can be found in [121], [145], [148], [164].

$$\min_{\boldsymbol{X}} \sum_{j=1}^{J} \sum_{i=1}^{I} \left(\pi_{\text{trade}_{ij}} E_{\text{trade}_{ij}} + \pi_{\text{grid}} E_{\text{grid}_{ij}} \right) \cdot x_{ij} \tag{3.2.15}$$

$$\text{s.t.} \quad E_{\text{trade}_{ij}} = \min \left\{ \sum_{t}^{T_{\text{D}_i}} E^{t}_{\text{av}_j}, E_{\text{req}_i} \right\} \tag{3.2.15a}$$

$$E_{\text{grid}_{ij}} = E_{\text{req}_i} - E_{\text{trade}_{ij}} \tag{3.2.15b}$$

$$\pi_{\text{trade}_{ij}} = \frac{1}{2} \left(\pi_{\text{bid}_i} + \pi_{\text{ask}_j} \right) \tag{3.2.15c}$$

$$\pi_{\text{bid}_i} > \pi_{\text{ask}_j} \tag{3.2.15d}$$

$$x_{ij} \in 0, 1 \qquad \forall i \in \{1 \dots I\}, \forall j \in \{1 \dots J\} \tag{3.2.15e}$$

$$\sum \mathbf{x}_i \leq 1 \qquad \forall i \in \{1 \dots I\} \tag{3.2.15f}$$

$$\sum \mathbf{x}_j \leq 1 \qquad \forall j \in \{1 \dots J\} \tag{3.2.15g}$$

where I, J are the number of buyers and sellers, respectively, $\pi_{\text{trade}_{ij}}$ is the agreed trade price, $E_{\text{trade}_{ij}}$ is the amount of solar energy traded, π_{grid} is the price to purchase energy from the grid, $E_{\text{grid}_{ij}}$ is the amount of energy that must be purchased from the grid to ensure EV i receives a full charge if trading with seller j. T_{D_i} and E_{req_i} are the departure time of, and amount of energy required by EV i, respectively. $E^{t}_{\text{av}_j}$ is the amount of surplus energy seller j has available at time t, and $\pi_{\text{bid}_i}, \pi_{\text{ask}_j}$ are the bid and ask prices of buyer i and seller j, respectively. The decision variable is $\boldsymbol{X}$ - a matrix with I rows and J columns, and x_{ij} is the value of $\boldsymbol{X}$ at position (i, j), where $x_{ij} = 1$ if buyer i trades with seller j, or else equals 0, I is the total

number of buyers, and J is the total number of sellers. If buyer i's bid price is not greater than seller j's ask price, they are unable to trade and $x_{ij} = 0$. Constraints (3.2.15e), (3.2.15f) and (3.2.15g) ensure that matrix $\boldsymbol{X}$ contains only 0s and 1s and has at most a single 1 in every row and column, to enforce one-to-one matching.

The problem considers both the cost to a buyer of purchasing solar energy from a seller and also the the cost of any additional energy that would be needed from the grid to enable the EV to depart with its required energy. By attempting to minimise the total cost, the mechanism encourages matching which will maximise the amount of renewable energy each EV purchases, as it is assumed that $\pi_{\text{trade}_{ij}} < \pi_{\text{grid}}$. Therefore a matching which increases the amount of EV charging completed with solar energy will be sought, as this reduces the total cost of energy required to fully charge the EVs. This increases the quantity of surplus solar energy sold, and thus the amount of charge received by the EVs, whilst also reducing the cost to the consumer.

Mechanism 4: Buyer/Seller Utility

To ensure that the auction mechanism is beneficial to both buyers and sellers, mechanism 4 considers the satisfaction of both buyers and sellers through a quantity known as the buyer's or seller's utility, which has been based on the work in [139]. A good matching for a buyer meets the following criteria:

- *Low Cost* - a buyer wishes to pay as little as possible for the energy
- *High Charge* - a buyer wishes to receive all of their required energy

Whereas sellers aim for:

- *Maximised Income* - a seller prefers to sell surplus energy at a higher price, as this increases their income
- *High Energy Utilisation* - a seller aims to sell all surplus solar energy

Despite each buyer and seller having two objectives, there is inherent equivalence, allowing them to be expressed as a single aim for a buyer and for a seller. Buyers wish to increase the amount of charge received and by doing so will also help the seller's aim of increasing the amount of solar energy sold. The utility that a buyer receives from a trade corresponding to their EV charging objective is given by:

$$U_{\mathrm{b}_{ij}} = \frac{E_{\mathrm{trade}_{ij}}}{E_{\mathrm{req}_i}} \tag{3.2.16}$$

The term "cost benefit" allows the second point for each participant to also be met [137], [154], [155]. The cost benefit for buyer i and seller j trading are defined as the difference between the trade price and the bid or ask price, respectively, as given in (3.2.17) and (3.2.18):

$$\beta_{\mathrm{buy}_{ij}} = \pi_{\mathrm{bid}_i} - \pi_{\mathrm{trade}_{ij}} \tag{3.2.17}$$

$$\beta_{\mathrm{sell}_{ji}} = \pi_{\mathrm{trade}_{ij}} - \pi_{\mathrm{ask}_j} \tag{3.2.18}$$

where $\beta_{\mathrm{buy}_{ij}}$ is the buyer's cost benefit and $\beta_{\mathrm{sell}_{ji}}$ is the seller's cost benefit. The use of subscript ij denotes the value from buyer i's point of view, and subscript ji is a value from seller j's view. For instance, $\beta_{\mathrm{buy}_{ij}}$ is the benefit buyer i receives if trading with seller j, whereas $\beta_{\mathrm{sell}_{ji}}$ is the benefit seller j receives if trading with buyer i. Based on the definition of $\pi_{\mathrm{trade}_{ij}}$, the buyer and seller cost benefits can be expressed as:

$$\beta_{\mathrm{buy}_{ij}} = \pi_{\mathrm{bid}_i} - \frac{1}{2}\left(\pi_{\mathrm{bid}_i} + \pi_{\mathrm{ask}_j}\right) = \frac{1}{2}\left(\pi_{\mathrm{bid}_i} - \pi_{\mathrm{ask}_j}\right) \tag{3.2.19}$$

$$\beta_{\mathrm{sell}_{ji}} = \frac{1}{2}\left(\pi_{\mathrm{bid}_i} + \pi_{\mathrm{ask}_j}\right) - \pi_{\mathrm{ask}_j} = \frac{1}{2}\left(\pi_{\mathrm{bid}_i} - \pi_{\mathrm{ask}_j}\right) \tag{3.2.20}$$

From (3.2.19) and (3.2.20) it can be seen that the buyer cost benefit is equal to the seller cost benefit. Therefore, increasing either the buyer or seller cost benefit also results in an increase to the other. This allows the financial objectives of both

buyers and sellers to be expressed through the seller utility, given in (3.2.21):

$$U_{\mathrm{s}_{ji}} = \left|\pi_{\mathrm{trade}_{ji}} - \pi_{\mathrm{ask}_j}\right| = \beta_{\mathrm{buy}_{ij}} = \beta_{\mathrm{sell}_{ji}} \tag{3.2.21}$$

The total utility of buyer i trading with seller j is the sum of both buyer and seller utilities:

$$U_{\mathrm{T}_{ij}} = w \cdot U_{\mathrm{b}_{ij}} + U_{\mathrm{s}_{ji}} \tag{3.2.22}$$

where $U_{\mathrm{T}_{ij}}$ is the total utility resulting from a trade between buyer i and seller j, $U_{\mathrm{b}_{ij}}$ is the buyer utility, $U_{\mathrm{s}_{ji}}$ is the seller utility and w is a unitless constant to adjust the relative importance of EV charging against cost benefit.

The utility that would be achieved for every combination of buyer and seller trading can be calculated at every time step using the submitted bids and asks. If a buyer and seller cannot trade, i.e. they are already partaking in a different trade, or the buyer's bid does not exceed the seller's ask, the total utility for that combination can be set to $-\infty$. Mechanism 4 matches buyers and sellers by solving optimisation problem (3.2.23) to maximise the total utility. The optimisation outputs matrix $\boldsymbol{X}$ which contains a 1 at position (i, j) if buyer and seller i and j should trade, or 0 otherwise. This is very similar to the approach used in [146], however, there it is assumed that the EVs will reach a full charge so the matching mechanism only includes (3.2.21) and not (3.2.16).

$$\max_{\boldsymbol{X}} \sum_{j=1}^{J} \sum_{i=1}^{I} U_{\mathrm{T}_{ij}} \cdot x_{ij} \tag{3.2.23}$$

$$\text{s.t.} \quad eqs.\ (3.2.15\text{d}) to\ (3.2.15\text{g}) \tag{3.2.23a}$$

$$x_{ij} \cdot U_{\mathrm{T}_{ij}} \geq 0 \qquad \forall i, j \tag{3.2.23b}$$

Mechanism 5: Closest Energy Matching

Whilst previous mechanisms can make optimal decisions based on the information known at the time each auction is run, they may not make the best matchings with

respect to unknown future EV arrivals. This disadvantage of mechanisms 3 and 4 can be demonstrated through the following simple example: There are two houses selling energy and two EVs wishing to charge, arriving at different times: *House A* has a total of 20 kWh of energy available to trade and asks for 11 p/kWh, and *House B* can offer a total of 50 kWh at a price of 10 p/kWh. *EV 1* arrives at 11am, requiring 15 kWh with a bid price of 12 p/kWh. Under mechanisms 3 and 4, *EV 1* would trade with *House B*. However, if *EV 2* then arrives an hour later at 12pm, requiring 30 kWh and bidding the same price, *House A* is its only option to trade, resulting in *EV 2* not receiving a full charge. It should be apparent that if *EV 1* had instead matched with *House A*, then *EV 2* would be able to trade with *House B*, resulting in both EVs receiving a full charge.

The concept of Closest Energy Matching attempts to rectify this problem by matching each buyer with the seller whose available surplus energy is closest to the amount requested by the buyer. In this context, the seller j with the closest available energy to buyer i is the seller whose total available surplus energy minus the buyer's requested energy results in a positive value closest to zero as in (3.2.24). As with the other mechanisms, a buyer can only be matched with a seller if the bid price is higher than the seller's ask.

$$\arg\min_{j} \left(\sum_{t}^{T_{\mathrm{D}_i}} E^{t}_{\mathrm{av}_j} - E_{\mathrm{req}_i} \right) \qquad \forall j \tag{3.2.24}$$

If there are no sellers for which this calculation results in a positive value, the seller with the closest energy is the one which has the highest negative value:

$$\arg\max_{j} \left(\sum_{t}^{T_{\mathrm{D}_i}} E^{t}_{\mathrm{av}_j} - E_{\mathrm{req}_i} \right) \tag{3.2.25}$$

The Closest Energy Matching mechanism matches buyers and sellers so that their energy difference is minimised, and the energy purchased/sold and cost benefit are maximised. Matching buyers and sellers by minimising the difference between the buyer's need and seller's surplus energy should result in a matching that not only

meets the buyer's energy needs but also considers potential future EV charging requests as it keeps houses with greater available surplus energy in reserve for the event that an EV with a greater energy requirement arrives. The optimisation problem includes both the energy difference and the total utility from mechanism 4, which incorporates the cost benefit and EV charge success into the problem.

The optimisation problem solved at time t by mechanism 5 is

$$\max_{\boldsymbol{X}} \sum_{i=1}^{I} \sum_{j=1}^{J} \left(E_{\mathrm{D}_{ij}} + U_{\mathrm{T}_{ij}} \right) \cdot x_{ij} \tag{3.2.26}$$

$$\text{s.t.} \quad eqs.\ (3.2.15\text{d}) to\ (3.2.15\text{g})$$

where

$$E_{\mathrm{D}_{ij}} = \begin{cases} w \cdot \frac{1}{E_{\mathrm{diff}_{ij}}} & \forall E_{\mathrm{diff}_{ij}} > 0 \\ \frac{w}{a} \cdot E_{\mathrm{diff}_{ij}} & \forall E_{\mathrm{diff}_{ij}} \leq 0 \end{cases} \tag{3.2.26a}$$

$$E_{\mathrm{diff}_{ij}} = \sum_{t}^{T_{\mathrm{D}_i}} E^{t}_{\mathrm{av}_j} - E_{\mathrm{req}_i} \tag{3.2.26b}$$

The two terms in the optimisation problem are $E_{\mathrm{D}_{ij}}$, which is a function of $E_{\mathrm{diff}_{ij}}$: the difference between seller j's available energy and buyer i's required energy, $U_{\mathrm{T}_{ij}}$ is the total utility from mechanism 4, which incorporates the cost benefit and EV charging success, and w and a are unitless constants to adjust the importance of closest energy matching against energy provided and cost benefit. For this study, values of $w = 5$ and $a = 100$ were found to maximise the amount of EV charge received from the solar energy, which is the purpose of this chapter.

3.3 Solving the Mechanism Optimisation Problems

3.3.1 MARMES

The optimisation problems in mechanisms 3-5 are from the class of integer linear programming problems, as the optimisation variable, $\boldsymbol{X}$, only contains zeros and ones. The problem being solved is to place ones in the matrix $\boldsymbol{X}$ to maximise the sum of the elements in $\boldsymbol{U*} = \boldsymbol{X} \cdot \boldsymbol{U}$, where $\boldsymbol{U}$ is a matrix containing the utility values from mechanism 4, the inverse of the cost function in (3.2.15), or the energy difference function from (3.2.26), calculated for each combination of buyer i and seller j. $\boldsymbol{U*}$ is a matrix containing the chosen elements from $\boldsymbol{U}$. The constraints (3.2.15f) and (3.2.15g) enforce that matrix $\boldsymbol{X}$ can contain at most one 1 in any row or column as each EV is only able to trade with a single house and each house can only trade with a single EV, all other values must be 0.

The problem can be generalised as follows:

$$\max_{\boldsymbol{X}} \sum_{m=1}^{M} \sum_{n=1}^{N} A_{mn} \cdot x_{mn} \tag{3.3.1}$$

$$\text{s.t.} \quad A_{mn} \in \mathbb{R} \qquad \forall m \in \{1 \dots M\}, \forall n \in \{1 \dots N\} \tag{3.3.1a}$$

$$x_{mn} \in 0, 1 \qquad \forall m \in \{1 \dots M\}, \forall n \in \{1 \dots N\} \tag{3.3.1b}$$

$$\sum \mathbf{x}_m \leq 1 \qquad \forall m \in \{1 \dots M\} \tag{3.3.1c}$$

$$\sum \mathbf{x}_n \leq 1 \qquad \forall n \in \{1 \dots N\} \tag{3.3.1d}$$

where $\boldsymbol{A}$ is a $M \times N$ matrix containing a set of real numbers and $\boldsymbol{X}$ is a matrix of equal size to $\boldsymbol{A}$ containing the output from the maximisation. Matlab supports the solving of this type of problem through its 'intlinprog' solver, however a new algorithm named MARMES (MAtrix Ranking for Maximising Element Selection) specifically designed for solving this problem is proposed here. MARMES solves

the problem faster than Matlab's solver and does not rely on Matlab functionality, making it more appropriate for use in a real-world application.

Algorithm 1 MARMES Algorithm for maximising the sum of chosen elements in a matrix

Input: $\boldsymbol{A}$

1: *Initialisation* : $iter \leftarrow 1$, $\boldsymbol{A}_{\text{ranked}} \leftarrow \boldsymbol{A}$, $\boldsymbol{X}^{(iter)} \leftarrow 0_{M,N}$
2: **for** $m = 1$ to M **do**
3: Replace numbers in row m of $\boldsymbol{A}_{\text{ranked}}$ with their rank, where highest number = 1, lowest number = N
4: Find location n of number with rank = 1 in row m and put a 1 in corresponding location m, n in $\boldsymbol{X}^{(iter)}$
5: **end for**
6: **while** there exists a column n where $\sum \mathbf{x}_n^{(iter)} > 1$ **do**
7: $iter \leftarrow iter + 1, \boldsymbol{X}^{(iter)} = \boldsymbol{X}^{(iter-1)}$
8: $\Omega_n \leftarrow n$ where $\sum \mathbf{x}_n^{(iter)} > 1$
9: **for** $n \in \Omega_n$ **do**
10: $\Omega_m \leftarrow m$ where $x_{m,n}^{(iter)} = 1$
11: **for** $m \in \Omega_m$ **do**
12: $R \leftarrow$ rank value from location m, n in $\boldsymbol{A}_{\text{ranked}}$
13: **if** $A_{\text{ranked}_{mn}} > 1$ (Current rank > 1) **then**
14: **if** columns containing higher ranked values in row m are empty in matrix $\boldsymbol{X}^{(iter)}$ **then**
15: Move 1 in $\mathbf{x}_m^{(iter)}$ from current position to higher ranked position, replace current position with 0
16: **end if**
17: **end if**
18: Calculate $A_{\text{diff}_m} = A_{mn} - A_{mn*}$ where $n*$ is the column containing rank $R + 1$ in row m of $\boldsymbol{A}_{\text{ranked}}$
19: **end for**
20: $A_{\text{diff}_{max}} \leftarrow$ row index in Ω_m corresponding to the greatest A_{diff}
21: **for** Each row in Ω_m, except $A_{\text{diff}_{max}}$ **do**
22: **if** Higher rank value not allocated in line 15 **then**
23: Move 1 in $\boldsymbol{X}^{(iter)}$ from current position in row to position corresponding to next highest rank - column $n*$
24: **end if**
25: **end for**
26: **end for**
27: **end while**
28: **return** $\boldsymbol{X}^{(iter)}$

The MARMES algorithm begins by ranking numbers in each row of the matrix $\boldsymbol{A}$, with the highest number given the rank 1, second highest rank 2, etc. Once all numbers have been ranked, it begins by selecting the highest number (rank = 1) in each row, by placing a 1 in the corresponding field in matrix $\boldsymbol{X}$. Given that there

can be, at most, one 1 in each column, the columns that contain more than one 1 are found. While there are any columns that contain more than a single 1, the following is repeated: for each of these columns (denoted by set Ω_n), the rows that contain the 1s are found (set Ω_m). In each of these rows the algorithm looks to see if the location of the 1 in that row of $\boldsymbol{X}$ corresponds to the highest rank (1). If not, it then checks to see if the higher ranked values in that row fall in columns of $\boldsymbol{X}$ that contain all zeros. If so, the location of the 1 in that row of $\boldsymbol{X}$ is moved from the current column to the empty column corresponding to the highest rank. If this is not possible, the difference between the values of the number in $\boldsymbol{A}$ in the current rank (position currently selected by 1), and the number in the next highest rank is calculated ($A_{\text{diff}_{m\in\Omega_m}}$). The row from set Ω_m containing the greatest difference is left unchanged, and in all other rows from this set, the location of the 1 in matrix $\boldsymbol{X}$ is moved to the position corresponding to the next highest rank. If there are still columns containing more than a single 1, then the iteration number increases and the algorithm repeats. Once a solution has been found that results in at most a single 1 in each row and column, the algorithm stops and outputs the current iteration of $\boldsymbol{X}$. The locations of 1s in this matrix show the chosen values that maximise the sum of $\boldsymbol{A}$, subject to the imposed constraints. The algorithm does not place a 1 in every row if there is no feasible solution - if there is no next highest rank available in line 23 of the algorithm, then this row would be left blank instead. If $\boldsymbol{A}$ contains negative numbers or other unwanted values, then these can be ignored by adjusting the ranking criteria in line 3, for example by only ranking positive numbers.

The performance of this algorithm is measured against that of the intlinprog solver in Matlab, which is assumed to be reliable in providing the optimum selection of values resulting in the highest possible total sum. The algorithm is compared with Matlab's solver through computation time - the time taken to find the optimum selection of values, and the solution accuracy - the ratio of the sum of values selected by the proposed algorithm, to the true maximum value computed by Matlab. To evaluate the performance, 1000 repeats are taken using a 50x50 matrix filled with a

random selection of numbers between 1 and 20 for input $\boldsymbol{A}$. The accuracy and the average time (ms) to compute the solution with each algorithm is shown in table 3.1.

The proposed algorithm solves the problem on average 93.5% faster than Matlab's intlinprog solver, whilst maintaining an average accuracy of 99.4%. For reference, an average accuracy of 100% would mean that the proposed algorithm reaches the exact same solution as Matlab's solver on every repeat. As it is assumed that Matlab's solver is the optimum solution, it is not possible to exceed an accuracy of 100%. Because of the success of this algorithm in reducing computation time without sacrificing result, this algorithm is used in the Closest Energy Matching mechanism to compute the optimal matching of buyers and sellers.

3.4 Results and Discussion

3.4.1 Case Study

The case study centres around the simulation of a 24-hour period, beginning and ending at midnight, using the parameters in table 3.2. Eighty EVs randomly arrive between 6am and 2pm and will make a request for the energy they require to fully recharge, a randomly selected value between 3 and 30 kWh. The EV will also announce its planned departure time, which will be no sooner than the soonest time that the EV could receive all of its required energy at the standard home charging rate of 7 kW. There are eighty houses equipped with EV charging points and rooftop solar PV panels ranging between 5 and 20 kWp capacity, with the percentage of

	Intlinprog	MARMES
Computation Time (ms)	22.73	1.46
Avg. Accuracy	100%	99.4%

Table 3.1: ILP solver algorithm comparison

No. EVs / houses	80 / 80
EV Energy Required	3 – 30 kWh (random uniform distribution)
Arrival Times	6am - 2pm (random uniform distribution)
Departure Times	Sufficient to fully charge EV at 7 kW
Solar PV Size (kWp)	5 (40%), 7 (20%), 10 (30%), 20 (10%)
Available Solar Energy	Expected PV data for 1st May [165]
Grid Energy Cost	14.37 p/kWh [166]
Charging Efficiency	90%

Table 3.2: Simulation Parameters

houses allocated each PV array capacity given in Table 3.2. Houses can sell their surplus solar energy (the difference between generation and the house's baseload consumption) to visiting EV drivers who require charging. The EVs can park at the house and use their charging point to recharge with the surplus solar energy. The information about EV arrivals/departures and energy needs are considered 'online' information, and are therefore not known ahead of their arrival.

If there are EVs that need to charge, prior to the auction each EV will each submit a bid consisting of their energy requirement, departure time and bid price. If a house is not currently charging an EV and has surplus solar energy available to trade, they can broadcast their available surplus energy profile for the day with an ask price they want to receive for their energy. It is assumed that a house can predict their solar energy generation and baseload consumption on a daily basis, but the procedure for this prediction is beyond the scope of this paper. The amount of energy that a house has available for trading is the minimum of either the available surplus solar energy, or the amount of energy that can be charged at a rate of 7 kW (maximum EV charge rate).

The energy trading auction takes place every 15 minutes using the bids and asks submitted in the prior quarter hour. The auction mechanism under study is used to match the bids and asks to determine which EVs and houses trade, and therefore

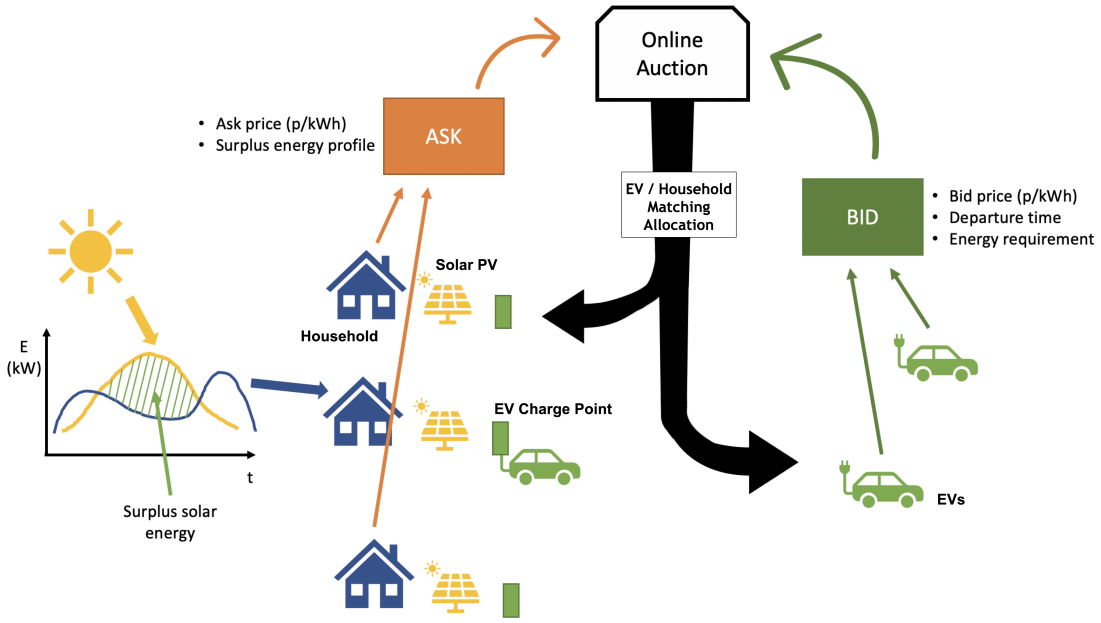

Figure 3.2: Schematic representation of the case study

where the EVs will go to park and charge. Once a house and EV have matched, the house will feed its surplus solar energy generated by its PV panels directly to its EV charge point, allowing the visiting EV to charge.

It is assumed that EVs will account for the charging efficiency during the trade – for instance if they require 18 kWh to fully recharge and the charging efficiency is 90%, then the EV will request 20 kWh.

As there is significant inherent variation in the selection of the random parameters, the simulation is repeated 1000 times for each of the five auction mechanisms studied in this paper. This ensures accuracy and reliability in the results and enables comparisons between the five mechanisms to be made unaffected by the randomness of the simulation parameters.

The described case study is shown schematically in Figure 3.2. It displays the process of houses submitting asks containing their surplus solar energy profile and EVs submitting their bid prices and energy requirements to the auction system, and the outcome of the matching algorithm confirming which house and EVs are matched.

3.4.2 Results

EV Charging Success

Of primary importance in an EV charging scenario is the amount of charge received by the EVs, as it is necessary to ensure that EVs receive sufficient charge for subsequent journeys. Increasing the amount of charge EVs receive from the solar energy can reduce the cost to the buyer, increase seller profits, assist with decarbonisation objectives and reduce the load on the grid, enabling a higher penetration of EVs to charge. It also enables communities to become more self-reliant, as is necessary in the case of islanded microgrids, by reducing the amount of additional energy that must be imported. Increasing consumption of solar energy is an incentive for further investment in new renewable energy sources and expands capacity for further DER integration and decarbonisation in the grid. However, it should be acknowledged that given the relative size of EV batteries to domestic PV installations, there is unlikely to be sufficient surplus energy produced by a single house to fully meet the needs of an EV. Therefore, it is important that the auction matching mechanism can make optimal usage of the available solar energy to ensure that EVs are allocated to charge in the most efficient way.

The SoC gained by the EV by its departure time resulting from the P2P trading matching is defined in (3.4.1). It gives the percentage of the EV's required energy that was successfully charged. For example, an EV with $SoC^{\text{gain}} = 100\%$ has successfully charged all of its required energy, while an EV with $SoC^{\text{gain}} = 50\%$ was only able to obtain half of the energy it needed. Therefore, the SoC^{gain} of an EV is given by:

$$SoC_i^{\text{gain}} = \frac{E_{\text{trade}_{ij}}}{E_{\text{req}_i}} \tag{3.4.1}$$

Figure 3.3 shows the distribution of the percentage of the EV's requested charge that has been fulfilled from solar energy by their departure, for all five auction mechanisms. Each bar in a group of 6 represents a range of EV SoC gain at departure, and the height of the bar signifies the percentage of EVs that depart with SoC gain in that

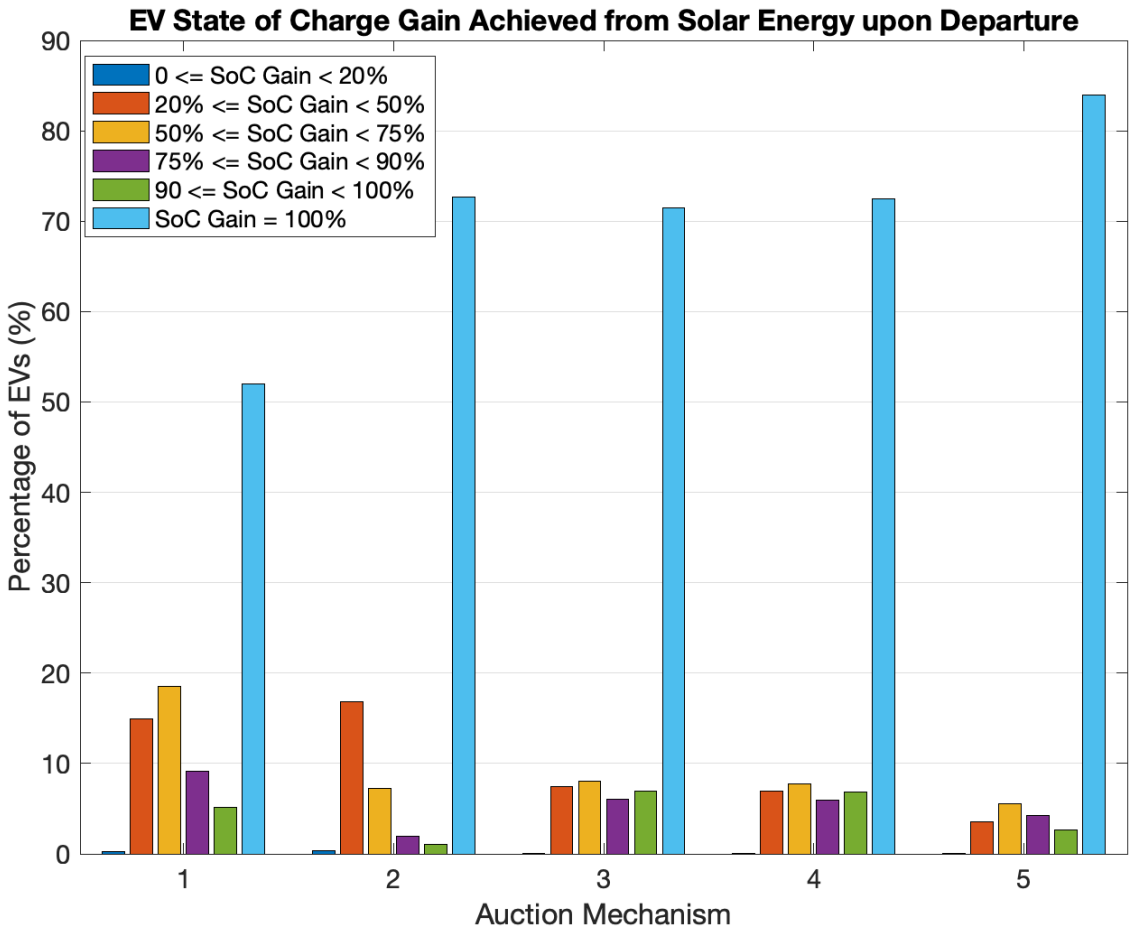

Figure 3.3: Distribution of departure SoC gain showing the percentage of EVs departing with SoC gain in different ranges for each of the 5 mechanisms based on charging from the available solar energy. It is clear from the light blue bars that the majority of EVs will depart with all required energy for all mechanisms

range. It is clear from the light blue bars that the majority of EVs will depart with 100% SoC gain, showing that the solar energy from the house the EV is trading with was able to completely satisfy the EV's charging requirement.

Table 3.3 displays the average charge achieved by EVs with each mechanism and the final 3 columns display the percentage of EVs departing with SoC gain specified by the three criteria. The mechanisms based on the standard double auction mechanism (1 & 2) result in lower SoC gain than are achieved through other mechanisms: 15.2% of EVs depart with 50% or less of their requested energy with mechanism 1, whereas mechanisms 3-5 see a significant improvement, with 7.5% of EVs departing with 50% or less with mechanism 3, and just 3.7% with Closest Energy Matching (mechanism

5). Mechanisms 3 and 4 both perform similarly, however there are clear improvements with the proposed Closest Energy Matching mechanism. There is a 16% improvement in the number of EVs that depart with full charge compared with mechanisms 2-4, with all other departure charge ranges seeing a decrease in the percentage of EVs departing with that range of charge. Only 13.4% of EVs depart with less than 90% of their requested charge, compared with over 20% of EVs using any of the other four mechanisms. The Closest Energy Matching mechanism also results in the highest average SoC gain at departure, with EVs departing with on average 94.8% of their requested energy, with mechanism 4 achieving the next highest average charge of 91.4%.

Mechanism	Mean SoC Gain	EV SoC gain <50%	EV SoC gain <90%	EV SoC gain 100%
1	81.7%	15.2%	42.9%	50.0%
2	85.8%	17.2%	27.4%	72.6%
3	91.0%	7.5%	21.6%	71.4%
4	91.4%	7.0%	20.7%	72.4%
5	94.8%	3.7%	13.4%	84.0%

Table 3.3: EV charge gained by departure. For each mechanism, the mean charge of all EVs on departure is shown, along with the percentage of EVs that depart with SoC gain in three specified ranges

Figure 3.4 quantifies the amount of grid energy that is required to fully charge all EVs in each mechanism. Despite there only being a 3% difference between the mean charge from solar energy of mechanisms 3, 4 and 5, this equates to a 36% reduction in required grid energy between mechanisms 4 and 5, and a 71.4% reduction in grid energy between mechanism 1 and the CEM mechanism. This means that the proposed Closest Energy Matching mechanism can reduce the load on the grid by over one-third, essential to increasing the penetration of EVs within existing grid limits.

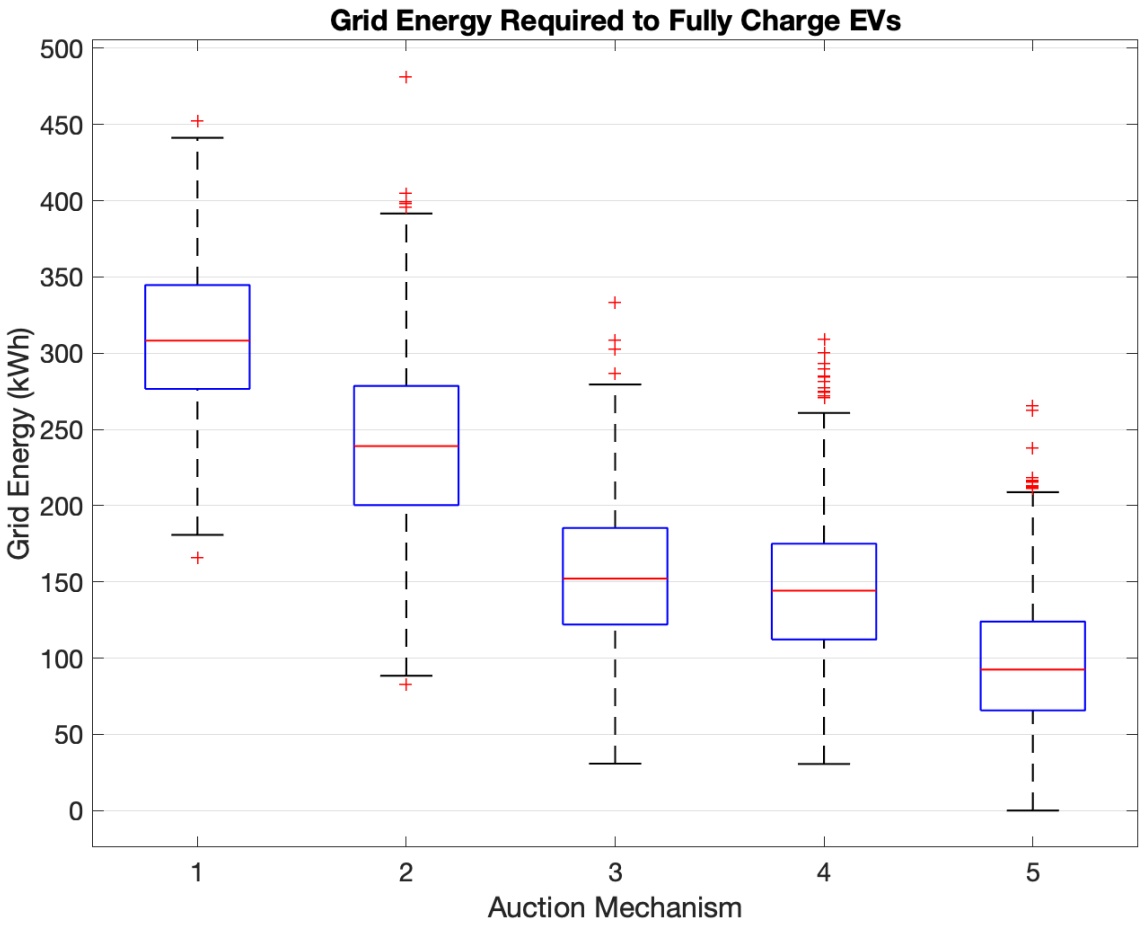

Figure 3.4: Grid energy required at each repeat to satisfy all EV charging requests

Figure 3.5 shows the results of a sensitivity analysis exploring the impact of incorrect solar prediction and a varying ratio of EVs to houses on the mean solar energy charge (mean SoC gain) of EVs. Whereas the previous results have used equal numbers of EVs and houses, this figure shows how varying the ratio of the number of EVs to houses from 1:4 (20 EVs, 80 houses) to 4:1 (80 EVs, 20 houses) affects the mean SoC gain at departure. In addition, the percentage error in solar energy prediction is also varied to evaluate the robustness of the CEM mechanism and its reliance on accurate solar predictions. The solar energy is predicted by the houses and this prediction is used in the auction matching, however the actual solar energy that can be sold to the EV is varied between 20% greater (+20%) and 20% lower (-20%) than the prediction. Under-predicting solar energy (percentage error +5% – +20%) results in a very slight increase in the mean departure charge (0.8 – 4%) as although the

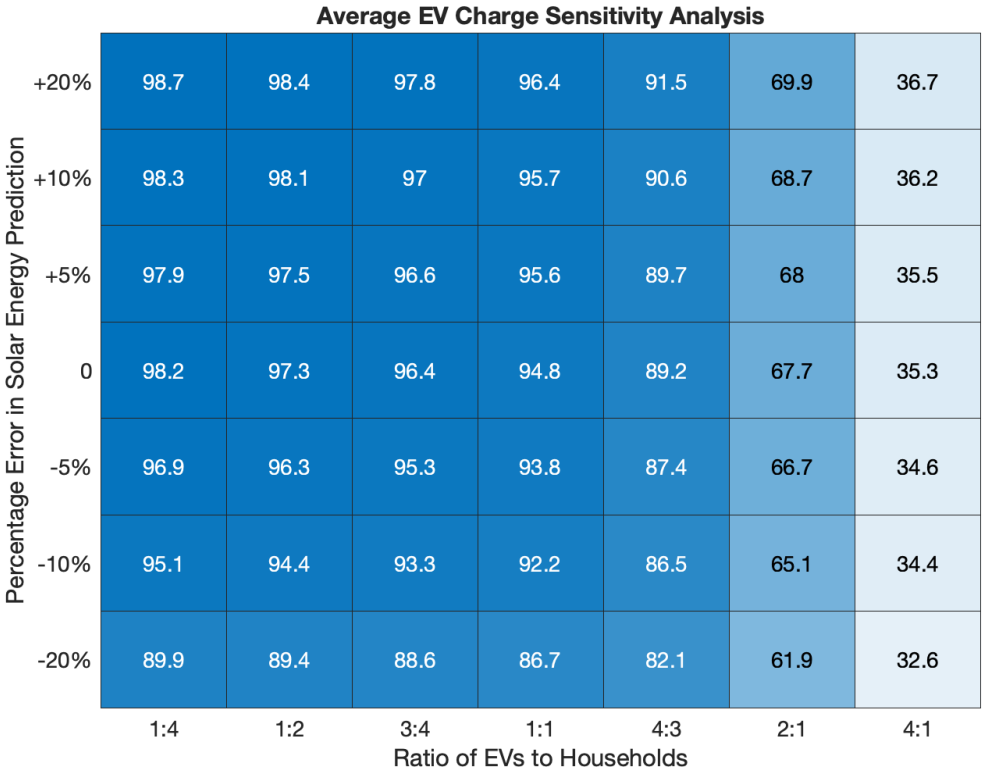

Figure 3.5: Sensitivity analysis showing the effect of incorrect solar energy prediction and varying the ratio of EVs to houses on the average solar charge gained by EVs

additional solar energy theoretically enables the EVs to depart with greater charge, the charge they receive is limited by the availability of houses with sufficient energy to meet every EV's requirement. If the solar energy is over-predicted by the house, and the actual solar energy that is traded is less than declared by the house during the auction process (percentage error -5% – -20%), there is a greater decrease in average charge. Over-predicting solar energy by 20% results in a decrease in SoC gain of between 8 and 9% compared with accurate solar predictions. This is not a huge decrease however, and shows the Closest Energy Matching auction mechanism to be fairly robust against deviations between predicted and actual solar energy production. Decreasing the ratio of EVs to houses also results in slight increases in mean SoC gain as there are more options for each EV, however, similarly to under-prediction of solar energy, there is a limit to the increase in mean SoC gain as there are inevitably EVs with energy requirements greater than can be fulfilled by house

solar energy. Increasing the number of EVs relative to the number of houses shows a more significant drop in the mean SoC gain. A ratio of 4 EVs to 3 houses still results in a relatively high SoC gain (89.2% compared with 94.8%), likely because there will be enough EVs departing fully charged early enough in the day to enable another EV to charge at the same house after it leaves. However, with double the number of EVs as houses or above, there is a significant reduction in the mean charge as there are increasing numbers of EVs that are unable to trade with any house as the demand greatly exceeds supply, and depart with a SoC gain of 0%.

Solar Energy Utilised

Figure 3.6 shows the amount of available surplus solar energy from all houses that is sold EVs through the P2P trading system for each auction matching mechanism. It can be seen that the proposed Closest Energy Matching mechanism results in the greatest utilisation of the available renewable energy, and whilst only around 45-50% of the solar energy is utilised in energy trades, over 90% of the total EV charging demand has been met through the proposed CEM mechanism.

To ensure fairness amongst sellers, the percentage of the 80 sellers that successfully sell energy in the P2P market under each mechanism must also be considered. Despite there being the same number of sellers as buyers, and every buyer receiving charge, it is possible for a single seller to sell to more than one buyer during the day: if the first buyer can arrives and departs early, a second EV can charge after. As a result, not every seller is guaranteed to sell energy through the auction. Mechanism 1 results in the highest percentage of sellers trading, with a median value of 73 sellers, mechanisms 2 and 5 have almost identical results with a median of 71 sellers, and mechanisms 3 and 4 are similar, with a median of 70 sellers trading. The differences between these results are too small for a conclusion that the choice of mechanism significantly affects the likelihood of a seller trading.

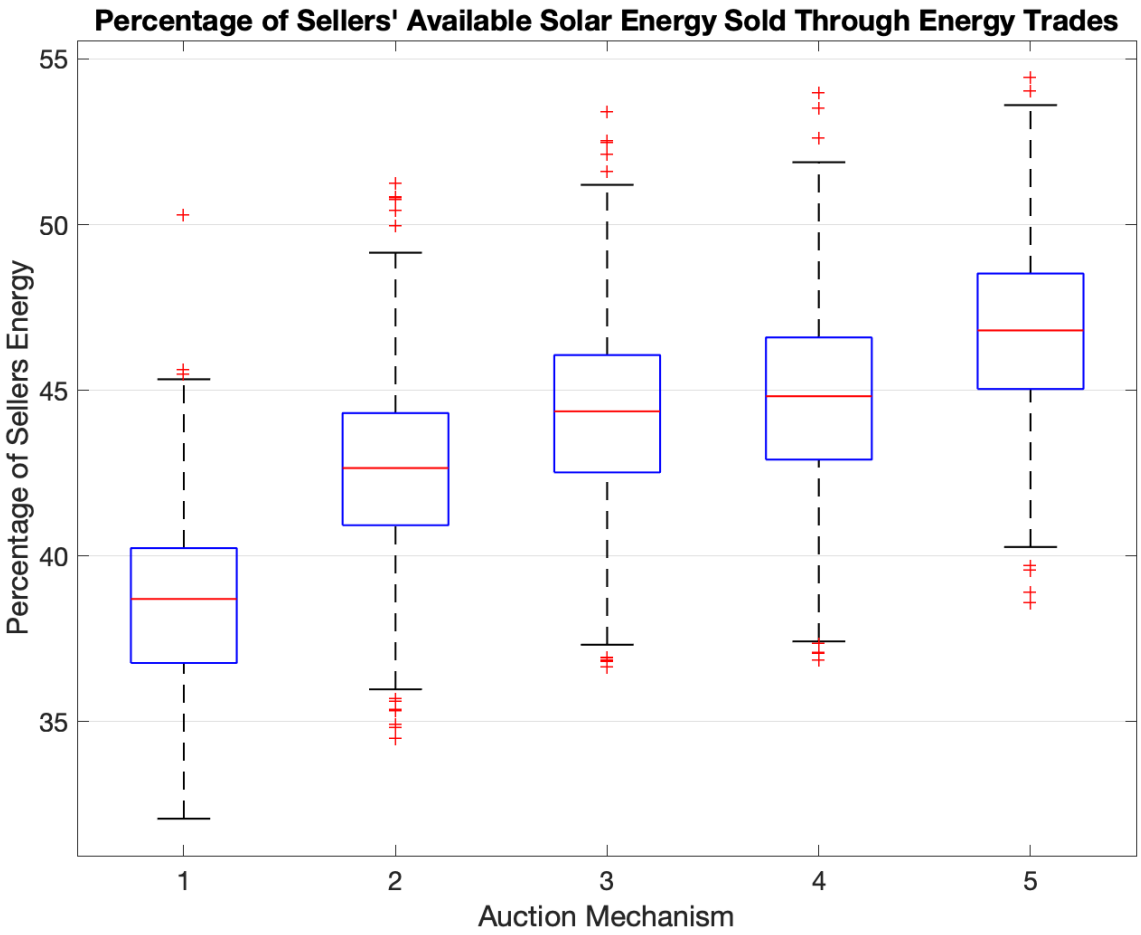

Figure 3.6: Percentage of the total surplus solar energy available from houses traded through the auction using each mechanism

Economic Analysis

Figure 3.7 displays the average trade price $\pi_{\text{trade}_{ij}}$ from each of the five auction mechanisms. It can be seen that mechanism 1 produces the lowest average trade price and mechanisms 2-4 result in very similar trade prices. Mechanism 5 is designed to prioritise charge received over cost benefit, and it does therefore result in higher trade prices, and therefore lower buyer/seller cost benefit. A higher trade price is closer to the upper end of the range of possible bid and ask prices, and therefore results in buyers receiving less of a discount and sellers receiving less of a bonus compared with their bid and ask prices than they would under other mechanisms. However, the median trade price from mechanism 5 is only 2% higher than mechanism 1, and 1% higher than mechanisms 3 and 4, so there is only a minor difference between the

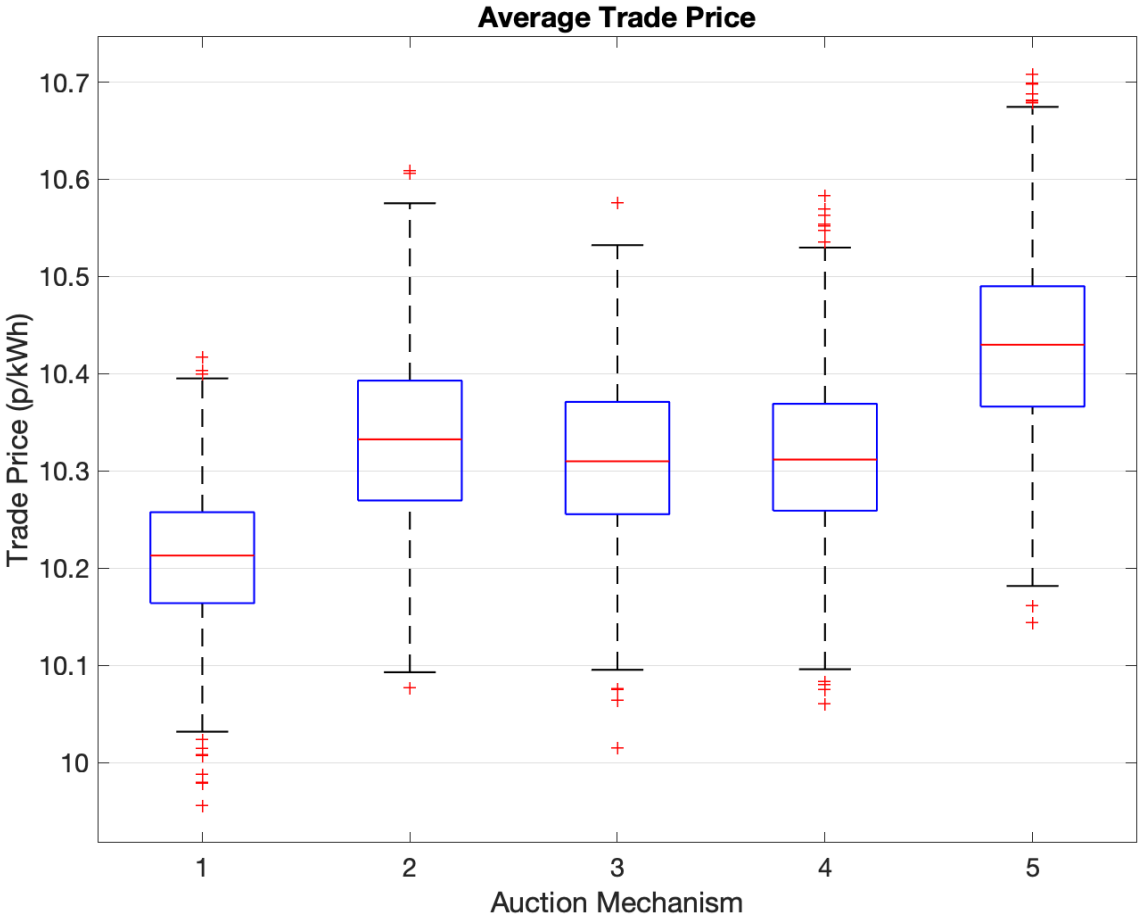

Figure 3.7: Average trade price agreed under each mechanism

mechanisms.

A higher trade price would appear to be more advantageous to sellers as selling surplus energy at a higher price will increase their profit, but would be detrimental to buyers as it means that they pay more per kWh than under a different mechanism. However, if it is assumed that the buyers would purchase the additional energy they require to ensure full EV charge by departure at standard grid energy prices, then the total cost incurred to buyers is not just the cost of buying the solar energy from the house but also the additional cost of the grid energy. Figure 3.8 shows the average cost per buyer and average profit per seller for each of the auction mechanisms.

Mechanisms 3–5 result in a very similar average cost per buyer, however despite the highest trade price, the Closest Energy Matching mechanism results in the lowest cost per buyer because of the increased amount of EV charging that is completed using solar energy, resulting in a greater reduction in the more expensive grid energy

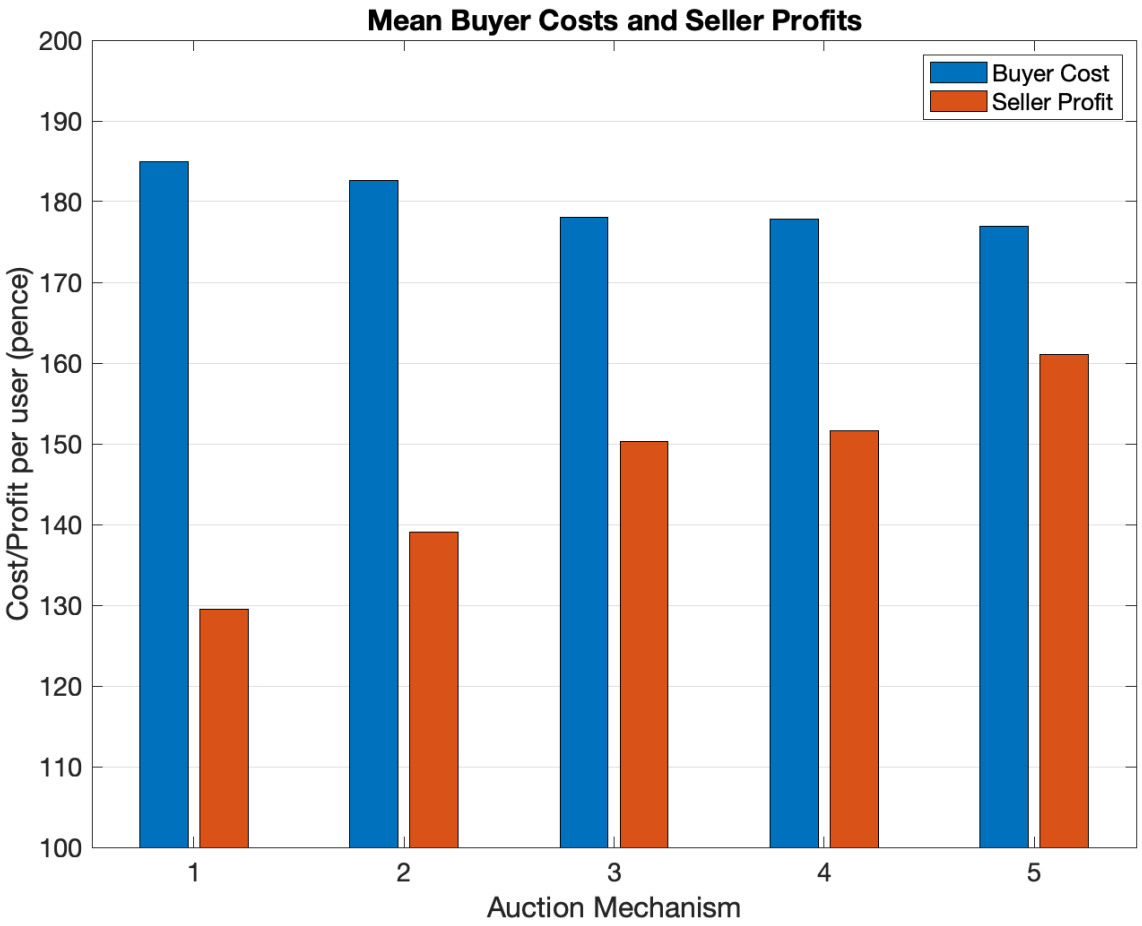

Figure 3.8: Average cost per buyer to fully charge EV, and average profit per seller with each auction mechanism

required to complete charging, equating to total costs 0.6% and 0.5% lower than mechanisms 3 and 4, respectively, and 4.3% lower than the most expensive mechanism (mechanism 1). Mechanism 1 provides the lowest trade price, and greatest cost benefit, but results in higher costs to buyers and lower seller profits because of the lower solar energy consumption and subsequent increase in grid energy required to fulfil all EV charging demand. Mechanisms 3 and 4 are a clear improvement over the first two mechanisms for seller profit, both averaging around 21 pence greater profit than mechanism 1. However, the Closest Energy Matching mechanism provides the greatest profit for sellers, with a 31.6 pence (24.4%) improvement over mechanism 1, and a 10.2 pence improvement over mechanisms 3 and 4 on account of the highest utilisation of solar energy.

The average buyer cost and seller profit using Closest Energy Matching (mechanism

5) are compared with a house that does not partake in P2P trading in table 3.4. Instead of selling energy to other EVs, the house instead sells all produced solar energy to the grid at Smart Export Guarantee (SEG) price of 3p/kWh [119], and the EV must purchase all required energy at grid price. To make this a fair comparison, the house partaking in P2P trading is also able to sell its un-traded solar energy to the grid at the SEG price, resulting in a seller profit greater than displayed in Figure 3.8.

	Trade w/ Grid	Mechanism 5	% Improvement
Avg. Cost per Buyer	233 p	177 p	24.0%
Avg. Seller Profit	101.9 p	237 p	132.6%

Table 3.4: Financial benefit of P2P trading

As the trade price is much lower than the standard grid electricity rate, the cost to a buyer using P2P trading with the CEM mechanism is around 24% lower on average than if purchasing energy directly from the grid. In addition, the price received through exporting energy to the grid through the SEG is significantly lower than can be obtained through P2P trading, with sellers able to achieve a 132% increase in income if using the CEM mechanism and P2P trading.

3.5 Conclusion

This chapter has presented and compared five different auction mechanisms for matching buyers and sellers in a P2P energy double auction. The specific scenario considered was where houses were able to utilise their vacant EV charge points during the day to sell surplus solar energy produced by the house's PV panels to visiting EV owners. It is in the interests of the EV owners to receive as much energy from the surplus solar energy sold as possible and reduce their costs to charge, and it is in the interests of the sellers to sell as much surplus solar energy as they

can, and to receive the maximum amount of income for doing so. The proposed Closest Energy Matching algorithm (mechanism 5) can be seen to offer the best performance of all considered auction mechanisms in relation to these objectives of buyers and sellers. It increases the percentage of EV charging completed using solar energy by matching EVs and houses from the P2P auction in a way that increases the satisfaction of participants in the current timestep, but also retains greatest flexibility for future timesteps with unknown EV charging demand, maximising EV charging performance across all timesteps. It therefore reduces the amount of grid energy required to fully charge EVs, facilitating the accommodation of higher EV penetrations and reducing CO_2 emissions. The total cost to buyers is decreased as more of the required charging is completed using cheaper solar energy from the P2P market, and the profit of sellers is increased through the greater solar energy utilisation.

Chapter 4

Peer-to-Peer Trading of Impact Tokens for Managing Network Capacity

Chapter Summary

This chapter presents a novel peer-to-peer trading approach for the trading of Network and Phase Impact Tokens, which correspond to use of the network's load capacity. Through the trading of these tokens, houses are able to secure the use of a portion of the network's capacity, allowing each house to add load or generation to the network without exceeding any of the transformer power, line current or node voltage limits. The proposed approach provides a real-time, decentralised method for managing EV charging, baseload and renewable energy generation without requiring any network monitoring. In addition, houses have the potential to reduce their energy cost or even profit from the P2P market, and efficient use of the network is encouraged.

4.1 Introduction

As discussed in Chapter 2, increasing penetrations of electric vehicle chargers are adding significant new loads to distribution networks, while distributed renewable energy generation, battery storage and V2G is adding generation into new parts of the networks. In particular, EV charging can push low-voltage networks to their limits, with significantly higher power usage than the networks were originally designed for. If left uncontrolled, the impact of these can lead to unsafe operation of the network with node voltage, line current and transformer power limits being exceeded [69]. Therefore, there has been significant research on suitable strategies for mitigating these risks while maximising the use of the network and ensuring that all houses are able to meet their required loads.

Ensuring that P2P trading does not exceed any of the network limits is becoming an increasingly researched problem [128]–[131]. However, these previous works focus on the trading of energy and require real time monitoring of the networks and complex integration of the network limits into the market clearing mechanism or intervention from the network operator to ensure that no limits are exceeded.

This chapter presents an approach to peer-to-peer trading with the objective of managing EV charging, baseload usage and renewable energy generation in real-time. Unlike other P2P trading studies that focus on the trading of energy, this chapter introduces the novel concept of trading tokens which correspond to the utilisation of network capacity. Houses are able to buy and sell the usage of portions of the network capacity, which ensures that load and generation can be managed without exceeding any network limits, while retaining each house's autonomy over the use of its loads and privacy, and without requiring real-time monitoring or sensors to be installed in the network. A three-phase LV distribution network is analysed here, with each house connected to one of the three phases. P2P trading is modelled for a 24 hour period, with trading taking place every 10 minutes.

The capacity of the network to accommodate load without exceeding any limits is

calculated through an optimisation problem, and is expressed in terms of Network Impact Tokens (NITs) and Phase Impact Tokens (PITs), which are tradeable tokens representing the utilisation of the total capacity of the network, and the capacity of the individual three phases of the network, respectively. If a house wishes to add a load to the network, they must possess the number of NITs or PITs equivalent to the magnitude of the load to compensate for its utilisation of the network's capacity. Similarly, if a house injects power to the network from renewable energy generation or battery discharging, the house will create additional NITs and PITs for the network which can be used for further loads, offset by the power generation.

During a one-time initialisation stage, the DSO calculates the total number of NITs and PITs that correspond to the overall capacity of the network. The total network capacity is assumed to be time-invariant, and is only determined by the network topology and hardware. Timesteps of 10 minutes are considered here, with all loads assumed to be constant during the timestep. This means that at any timestep, the network can accommodate the same total load. Because of this nature, the network capacity only needs to be calculated one time, unless changes to network hardware or topology occur. The number of NITs and PITs corresponding to the capacity of the network and each phase are allocated equally to all houses by the DSO, with the same number of tokens allocated in every timestep. If a house wishes to add a load to the network that corresponds to a greater number of NITs than they were allocated, then the house can attempt to purchase the additional tokens on the P2P market. If a house does not require all of their allocated tokens for their planned load, or will generate additional tokens through power injection, the house can sell their surplus tokens on the P2P market to increase their revenue.

This Chapter first presents the network model and key parameters of the P2P implementation. Fundamental concepts required for the understanding of the proposed Impact Token P2P approach are then introduced, in addition to the initialisation stage that must be completed by the DSO, including power flow studies to analyse the behaviour of the network, the calculation of a house's impact on the network,

the determination of the network's load capacity and the Network and Phase Impact Tokens. Subsequently the P2P trading approach for the Impact Tokens is then presented, and the chapter concludes with full analysis of the proposed approach.

4.2 Network Models, Load Profiles and Study Parameters

4.2.1 Distribution Network Models

A real, three-phase low-voltage distribution network from North West England, UK has been selected for this study. While the proposed P2P trading approach is tested on this specific network, the methodology can be applied to any distribution network, consisting of a single or multiple feeders, providing a power flow study can be completed. This network consists of a single feeder serving 159 houses connected across three unbalanced phases. The network has a radial topology and a three-phase transformer reduces the voltage at the head of the feeder from 11 kV to the network's nominal phase-to-phase voltage of 416 V.

The chosen distribution feeder is shown in Figure 4.1, with the locations of the houses and the phase of the network that they are connected to shown by the coloured circles, and the transformer location marked with a black square.

Constraints on the node voltages, line currents and transformer loading are imposed on power networks to guarantee safe and reliable operation. Table 4.1 gives the values of these constraints. An additional 5% safety margin is further added to ensure the network does not operate right at its limit to avoid any risk of violations and unnecessary component aging.

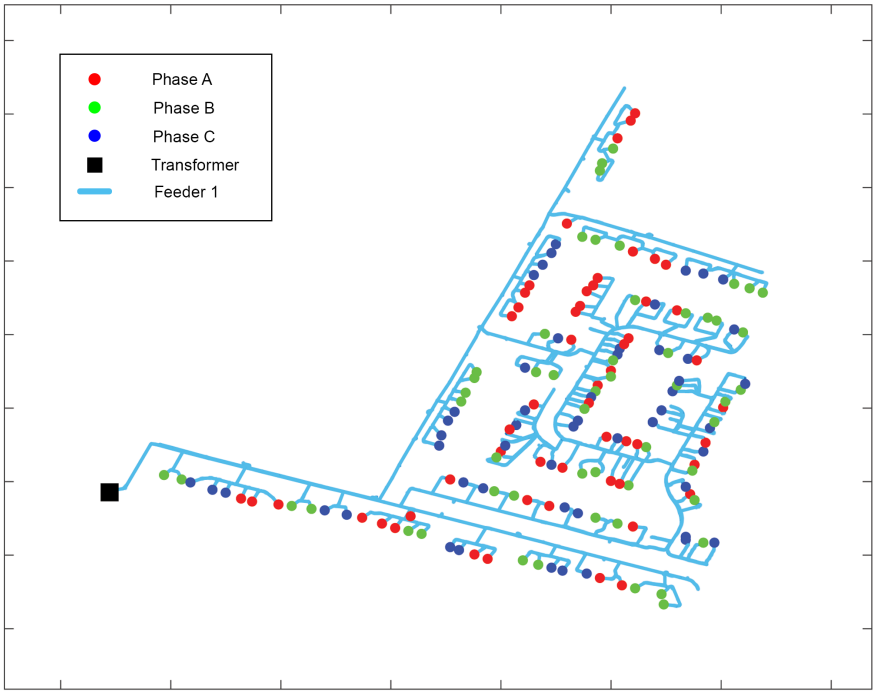

Figure 4.1: Line diagram of the low-voltage distribution network used in this study

Table 4.1: Network Constraints

Constraint	Lower Limit	Upper Limit
Node Voltage	216.2 V	253 V
Feeder Head Current	N/A	300 A
Transformer Loading	N/A	180 kVA

4.2.2 Load Profiles

A set of real load data consisting of baseload power consumption for 100 houses over a 24 hour period was provided by Electricity North West along with the distribution network model. However, considering 159 houses are present in the network, additional load data has to be created. A larger set of 1000 baseload, solar power generation and EV data profiles have been generated, see Chapter 5 for more details on the creation of these profiles. Additionally, each EV is allocated a SoC goal at its departure time, which is its desired SoC when it departs to enable it to complete the journeys it has planned for the following day.

For this P2P trading study, each house in the network has been allocated a random

baseload profile, 50% of the houses have been allocated solar PV panels and battery storage, and 50% are allocated an EV. It is not necessarily the case that every house with an EV is also equipped with solar PV panels. Solar energy generation is based on irradiance data for June, which has been chosen so that there is sufficient available solar power generated to highlight the generation and subsequent trading of NITs from this energy.

4.2.3 Study Design

This study designs a P2P trading system that operates continuously over timesteps of 10 minutes with the objective of managing load and generation on the network from baseload, EV charging and renewable energy generation, to ensure that no network power, current or voltage limits are exceeded.

A 24-hour period is modelled here, from 8:00am to 7:59am the following day, divided into 144 timesteps, each with a duration of 10 minutes, with loads assumed to be constant within each ten-minute period. The total number of timesteps is given by T, while t refers to any one of the individual timesteps, which have duration ΔT. The total number of houses in the network is K, with the set of all houses denoted as $\mathcal{K}$, and an individual house within that set, k.

It is assumed that each house is able to accurately predict its baseload power, solar PV generation and EV usage for the 24 hour period, however one advantage of the sliding window implementation is that if a house's requirements change during the day, these changes can be accommodated into the planning problem at the next timestep.

To begin with, a network initialisation stage is completed by the DSO, described in Section 4.3. This is a one-time process that involves computing power flow studies on the network, which are used to determine the network's capacity and the number of NITs and PITs each house is allocated for use and each house's Impact Value on the network. The DSO then communicates the Network and Phase Impact

Values and allocated numbers of Network and Phase Impact Tokens to each house. This stage only needs to be repeated if the power flow results would differ, for instance if the network topology or hardware changes. Once houses have received the information from the DSO, they can begin participating in P2P trading. A sliding window strategy is implemented: at every ten minute period, each house will solve a planning problem to determine its usage of the available energy resources for all timesteps from the following timestep until the end of the 24 hour period. If the house plans to purchase or sell NITs or PITs for the next timestep, it will enter the P2P market to conduct these trades. Multiple markets are completed for the trading of tokens, and the trading concludes with the house re-calculating its actual energy use for the next timestep based on the completed trading. This P2P trading process is explained in Section 4.4. Figure 4.2 represents the entire proposed process from initialisation to trading stages.

4.3 Fundamental Concepts

Before the P2P trading approach can be presented, the fundamental concepts that underpin the methodology must be introduced. This section describes the initialisation stage, which must be completed by the DSO to determine key parameters used by the houses during the P2P trading. Firstly, power flow studies are conducted to calculate the voltage and current sensitivity matrices, which are subsequently used in the calculation of the load capacity of the network. Each house's Network and Phase Impact Values are then calculated, which represent the change in load capacity of the other houses on the network or individual phase of the network as a result of a change in load at the original house, respectively. The Network Impact Tokens and Phase Impact Tokens are also introduced, corresponding to the capacity of the network and the individual three phases, and the relationship between power demand or generation and the equivalent number of tokens is explained.

It is important to note that the following initialisation procedure for determining the

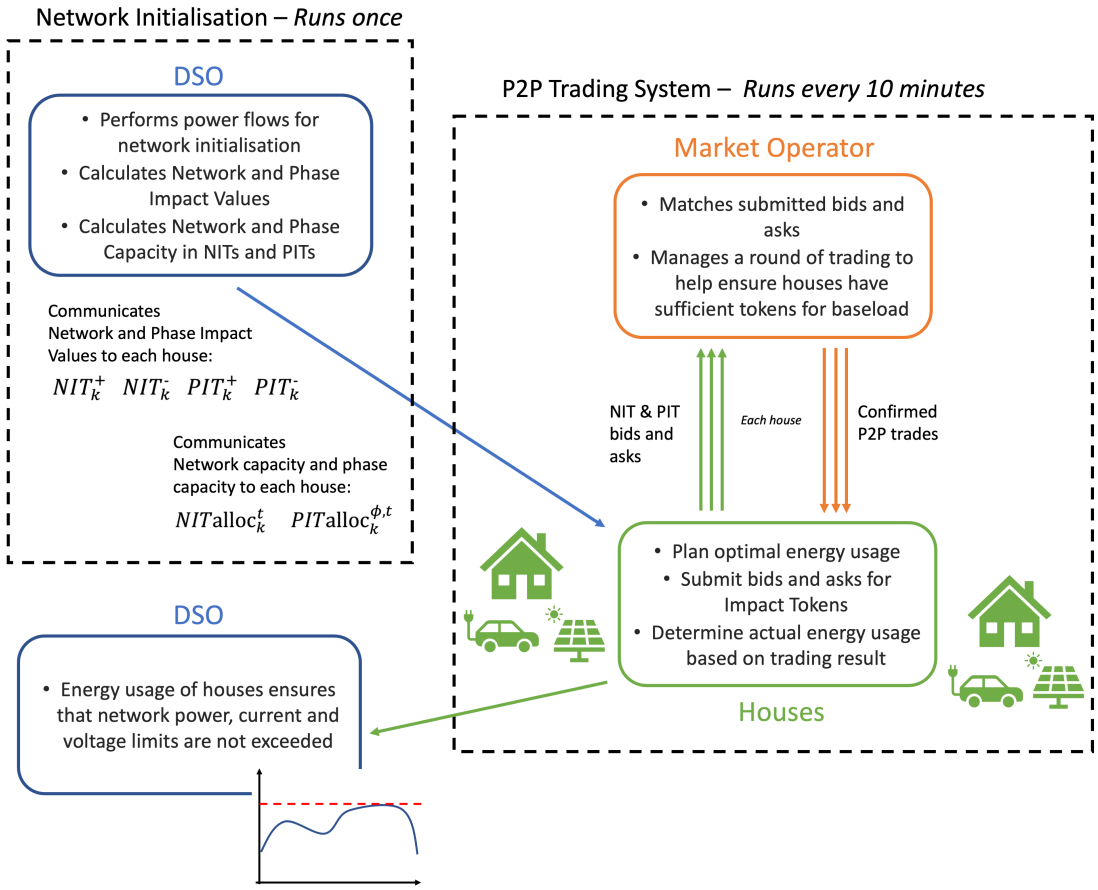

Figure 4.2: The proposed P2P trading approach of Network and Phase Impact Tokens is presented schematically, including the DSO initialisation stage and P2P trading stages

network's load capacity and subsequently the number of NITs and PITs allocated to each house and each house's Network and Phase Impact Values is time-invariant, and needs only to be completed by the DSO once, unless changes are made to the network infrastructure or topology. If no such changes are made to the network, P2P trading can occur within an unlimited time frame without having to recalculate the network capacity or Impact Values.

4.3.1 Network Initialisation and Power Flow Studies

A series of power flow studies are first performed on the network to determine a set of behaviour parameters that are subsequently used in the calculation of the load capacity of the network for determining the available PITs and NITs. No Distributed

Generation (DG - solar PV panels and battery storage) or EVs are present in the network for these studies, and the same generic baseload profile of 0.5 kW is allocated to each house at every 10-minute timestep during the day. The generic profile is arbitrarily selected to enable a power flow study to be conducted, to evaluate how the network behaves under a certain loading condition. The results of the power flow can subsequently be applied to any sets of loads and generation afterwards. This means that the power flow is time-invariant and only has to be run once for a given network topology, with the results used to estimate the effect of any load or generation in the network. The power flow studies only have to be re-run if there are changes to the network topology or hardware (e.g. line impedances or phase connections).

Sensitivity matrices are a popular way of analysing the impact of loads on a network, and are defined as the change in a network value, e.g. voltage, current or power loss, resulting from a change in power at a different node [44], [167]. Here, voltage and current sensitivity matrices are defined and the same concept is later used to calculate each house's Network and Phase Impact Values by analysing the change in load capacity. Firstly, a power flow study is run to calculate values for node voltages and line currents throughout the network based on the generic load profile. Then, for each house in turn, the generic baseload value is increased by a set margin ΔP^{+} and the power flow study is repeated, before returning the load to the original value. This step is then repeated again, but instead reducing the load at each house in turn by ΔP^{-}. From the results of each of the new power flow studies, voltage and current sensitivity matrices are calculated, which are defined as the change in node voltage at each node or change in line current in each line, as a result of a change in load at a different node [44]. The positive (increased load) and negative (decreased load) voltage sensitivity matrices are given in (4.3.1) and (4.3.2), respectively:

$$\mathbf{W}^{+}{}_{j,k+} = \left(|\hat{V}^{3\phi}_{j,k+}| - |\tilde{V}^{3\phi}_{j}|\right) \cdot \frac{1}{\Delta P^{+}} \quad \forall k, j \in \mathcal{K} \tag{4.3.1}$$

$$\mathbf{W}^{-}{}_{j,k-} = \left(|\hat{V}^{3\phi}_{j,k-}| - |\tilde{V}^{3\phi}_{j}|\right) \cdot \frac{1}{\Delta P^{-}} \quad \forall k, j \in \mathcal{K} \tag{4.3.2}$$

where ${\mathbf{W}^{+}}_{j,k+}$ is the positive voltage sensitivity matrix showing the value of the change in voltage at house j as a result of the load at house k being increased by ΔP^{+}, which is 1 kW for this study, and $\mathcal{K}$ is the set of all houses. The values of the three phase node voltages calculated in the initial power flow at house j are $\tilde{V}_{j}^{3\phi}$ and the voltages calculated in the power flow when the load at house k has been increased are $\hat{V}_{j,k+}^{3\phi}$. The nomenclature can be easily followed for the negative sensitivity matrix where the load has been decreased at house k in (4.3.2). While the power flow calculates complex values for the voltages and currents, absolute values are taken here to provide compatibility with Matlab's optimisation solvers. In the case of the line current, which can take either a positive or negative value depending on the direction of power flow in the network, care is taken to consider the phase angle of the complex values to ensure the absolute value is correctly signed.

Similarly, the current sensitivity matrices for increased loads $\mathbf{L}_{\mathbf{l},\mathbf{k}+}^{+}$ and decreased loads $\mathbf{L}_{\mathbf{l},\mathbf{k}-}^{-}$ are calculated as follows:

$$\mathbf{L}^{+}{}_{l,k+} = \left(|\hat{I}_{l,k+}^{3\phi}| - |\tilde{I}_{l}^{3\phi}|\right) \cdot \frac{1}{\Delta P^{+}} \quad \forall k \in \mathcal{K}, \forall l \in \mathcal{L} \tag{4.3.3}$$

$$\mathbf{L}^{-}{}_{l,k-} = \left(|\hat{I}_{l,k-}^{3\phi}| - |\tilde{I}_{l}^{3\phi}|\right) \cdot \frac{1}{\Delta P^{-}} \quad \forall k \in \mathcal{K}, \forall l \in \mathcal{L} \tag{4.3.4}$$

where $\tilde{I}_{l}^{3\phi}$ are line currents for each line l in the set of all lines in the network, $\mathcal{L}$, calculated in the original load flow and $\hat{I}_{l,k+}^{3\phi}$ is the line current in line l calculated resulting from an increased load at house k.

To simplify the problem, it is assumed that the network load capacity and sensitivity matrices are time-invariant, and that the calculated values are independent of the current load in the network. As a result, it is therefore assumed that the Network Impact Values and capacity of Network Impact Tokens in the network are also time-invariant. Further research could also consider the dynamic capacity of the network and how a house's impact on the network can alter with different load levels.

4.3.2 Network Load Capacity

To calculate the total load capacity of the network, the extra load capacity is first calculated based on the results of the power flow study using the generic load profile. The extra load capacity of the network is defined as the amount of additional load the network can accommodate at each node, in addition to the generic load profile, before any of the network constraints (voltage, current or power) are violated, at each timestep. The total load capacity of the network is then defined as the sum of the generic load profile and calculated extra load capacity.

The calculation of the extra load capacity is formulated as an optimisation problem to maximise the load that can be accommodated without violating the network's transformer power loading, line current and node voltage limits. Constraining this problem by these limits moves the complexity of ensuring that the network is operating within its limits from within the real-time P2P trading and network operation to this separate initialisation phase. The optimisation objective to calculate the extra load capacity at each house is given as:

$$\max_{EL} \sum_{t=1}^{T} \sum_{k=1}^{K} EL_k \tag{4.3.5}$$

where EL_k is the extra load capacity available in the network for house k. As the load capacity is assumed to be time-invariant, the value of EL_k is the same at all timesteps. A lower bound of EL is given such that $EL_k > 0$.

The voltage at house k in the network resulting from the extra load allocation is calculated by (4.3.6), and is constrained in the optimisation problem by (4.3.7).

$$V_k^{3\phi} = |\tilde{V}_k^{3\phi}| + \mathbf{W}^+{}_{k,j} \times EL_j \quad \forall j \in \mathcal{K} \tag{4.3.6}$$

$$\underline{V} \leq |V_k^{\phi}| \leq \bar{V} \quad \forall k, \phi \tag{4.3.7}$$

Similarly, the current in all three phases of line l is calculated by:

$$I_l^{3\phi} = |\tilde{I}_l^{3\phi}| + \mathbf{L}^+{}_{l,j} \times EL_j \quad \forall j \in \mathcal{K} \tag{4.3.8}$$

The line currents are implemented as a constraint in the optimisation problem through the following:

$$|I_l^\phi| \leq I_{\max_{l,\phi}} \quad \forall l, \phi \tag{4.3.9}$$

The transformer constraints are implemented here to ensure that the transformer loading does not exceed the specified limits.

$$S_{\text{trans}} = \sum_{\phi=1}^{3} |V_{\text{trans}_\phi}| \cdot I_1^\phi \tag{4.3.10}$$

$$S_{\text{trans}} \leq S_{\text{trans}_{\max}} \tag{4.3.11}$$

where I_1^ϕ is the current through the primary feeder line between the transformer and low-voltage network in phase ϕ.

A final constraint is added that sets the variance between the extra load value allocated to each house to be zero - this means that every house is allocated an equal extra load capacity for fairness. Because every house is assigned the same generic load profile, the total network capacity assigned to each house is identical.

$$EL_k - \frac{1}{K} \cdot \sum_{k=1}^{K} EL_k = 0 \tag{4.3.12}$$

where EL_k is the load capacity assigned to house k and K is the total number of houses.

The optimisation problem is then solved to calculate the values of EL at each house, referred to as $EL_{\text{var}=0,k}$. An accurate calculation of the actual extra load capacity of the network is extremely difficult, as the additional load that can be accommodated depends on the power consumption at different locations in the network. If the extra load capacity is calculated without (4.3.12), it will overestimate the extra load capacity by exploiting the strongest points of the network and allocating high extra load capacity to the one or two strongest houses and no extra load capacity to the others, while the value calculated with constraint (4.3.12) will result in an underestimation as it neither accurately represents real-world conditions, as not every house will have equal load simultaneously, nor considers that some houses

could also accommodate additional load on top of the equal amount assigned to each house without exceeding network limits.

Therefore, the optimisation problem described in equations (4.3.5) to (4.3.11) is run for a second time, but with the following lower bound on the value of the extra load.

$$EL_k \geq \frac{1}{K} \sum_{k=1}^{K} EL_{\text{var}=0,k} \tag{4.3.13}$$

This ensures that every house is at least allocated the extra load capacity calculated when all houses are allocated an equal amount of extra load capacity, but also enables some houses to accommodate a higher extra load if the network permits, which can give a better value of the total load capacity of the network.

4.3.3 Impact Values and Impact Tokens

This section introduces the concepts of Network Impact Values (NIVs), Phase Impact Values (PIVs), Network Impact Tokens (NITs) and Phase Impact Tokens (PITs). These are calculated by the network operator using the results of the extra load capacity calculations, and again are independent of any load or generation in the network, meaning that these values only have to be calculated once unless changes are made to the network topology or hardware.

Network Impact Values

Power consumption or generation at each house, depending on its location within the network, has a unique impact on the amount of extra load capacity available to the other houses in the network. The Network Impact Values quantify the impact of power consumption or generation at a house on the load capacity available to the other houses (expressed in terms of NITs), taking into account the transformer power loading and inter-phase bus voltages, i.e. how a load on one phase impacts the voltages on a different phase. For example, a large load at one house may mean that less total load could be accommodated by the network than if the load was

located elsewhere. As the load capacity of the network is constant, these different impacts are quantified using the Impact Values. The NIV for house k shows how much the available extra load capacity to the other houses is decreased or increased by resulting from a 1 kW increase in load or reduction in load at house k, respectively. Therefore, out of the total capacity of the network in terms of NITs, the house's NIV defines how many NITs each kW of load requires from the network's capacity, and how many NITs each kW of generation will add to the network. The units of NIVs are tokens/kW. A house with a higher Impact Value has greater impact on the network if adding a load, and is subsequently required to purchase a larger number of NITs to take into account this greater impact on the network.

The Network Impact Values are calculated in a similar method as the voltage and current sensitivity matrices described in Section 4.3.1. A single timestep is chosen and the following procedure is carried out to calculate the NIVs at each house:

For house $k = 1$ to K:

1. Assign generic baseload profile to all houses

2. Set upper bound of $EL_k = 0$, so that house k is not allocated any extra load capacity, and calculate the extra load capacity in network at all other houses using (4.3.5)-(4.3.13). The total extra load capacity of the network is given by:

$$EL_{\text{total}} = \sum_{\substack{j=1 \\ j \neq k}}^{K} EL_j \tag{4.3.14}$$

3. Increase load at house k by 1 kW and recalculate extra load capacity at all other houses to give:

$$EL_{k+} = \sum_{\substack{j=1 \\ j \neq k}}^{K} EL_{k+,j} \tag{4.3.15}$$

4. Calculate the change in extra load available to the other houses as a result of house k increasing its load by 1 kW

$$EL^{+}_{\Delta,k} = |EL_{\text{total}} - EL_{k+}| \tag{4.3.16}$$

5. Repeat steps 3 and 4, but instead decreasing the load at house k by 1 kW to calculate EL_{k-} and $EL^{-}_{\Delta,k}$

6. The NIVs of house k are then defined as:

$$NIV_k^+ = EL^+_{\Delta,k} \tag{4.3.17}$$

$$NIV_k^- = EL^-_{\Delta,k} \tag{4.3.18}$$

where NIV_k^+ is house k's Network Impact Value for an increased load of 1 kW and NIV_k^- is its NIV for a decreased load (or generation) or 1 kW.

The DSO will communicate to each house its two NIVs, along with the generic load profile used in the calculation of the network load capacity for the house to use in its own calculations. Because the initialisation phase only has to be completed once, the house's NIVs do not change unless the DSO has to recalculate them following a substantial change to the network topology or infrastructure.

Network Impact Tokens

Instead of expressing the network load capacity in kW, it is instead defined in terms of a quantity of Network Impact Tokens. Instead of analysing the network operation in terms of the load and generation powers through a power flow study, Network Impact Tokens (NITs) and NIVs enable the network to be analysed in terms of the impact that the loads cause on the network.

The calculated extra load capacity of the network can be equated in terms of Network Impact Tokens (NITs), which are henceforth used in all calculations instead of the extra load capacity. The extra load capacity at each house as calculated by the network operator in Section 4.3.2, is equated to a number of NITs for each house as follows. Each house is able to add loads to the network corresponding to a total number of NITs given by $NIT\text{alloc}_k^t$ without exceeding any network limits:

$$NIT\text{alloc}_k^t = (EL_k + P\text{generic}) \cdot NIV_k^+ \quad \forall t \tag{4.3.19}$$

where $NIT_{\text{alloc}_k^t}$ is the number of NITs representing the network capacity allocated to house k at time t, EL_k is the extra load capacity as calculated by the DSO, P_{generic} is the load allocated in the generic baseload profile and NIV_k^+ is the house's Network Impact Value for increasing load. The sum of $EL_k + P_{\text{generic}}$ equals the total load capacity of the network at house k. Because the load capacity is calculated in terms of the additional power that can be accommodated by the network, it must be multiplied by the NIV in order to convert it to Network Impact Tokens.

Every load that is added to the network will use up some of the network's available capacity, and therefore each load is equated to a number of NITs in order to evaluate how much of the network's capacity it will occupy. The relationship between a load power (kW) at house k and the reduction in network capacity in NITs is defined through (4.3.20). To add the load to the network, the house is required to acquire the corresponding number of Network Impact Tokens, which will ensure that the load cannot cause the network to exceed any of its limits. The link between power usage at a house and the number of NITs required is given by:

$$NIT_{\text{load},k} = P_{\text{load},k} \cdot NIV_k^+ \tag{4.3.20}$$

where $NIT_{\text{load},k}$ is the number of NITs utilised in the network as a result of a load of $P_{\text{load},k}$ kW.

If a house discharges power from its battery or EV to the network or sells power directly from its solar panels, this will generate a number of NITs that can be used by other houses to increase their load on account of the additional power that has been injected into the network. The number of NITs added to the network by power injection into the network is given by (4.3.21).

$$NIT_{\text{gen},k} = P_{\text{gen},k} \cdot NIV_k^- \tag{4.3.21}$$

where $NIT_{\text{gen},k}$ is the number of NITs generated for the network as a result of generation of $P_{\text{gen},k}$ kW at house k.

Phase Impact Values

While the Network Impact Values consider the effect of a load across the entire network, they do not take into account the behaviour and capacity of the three individual phases of the network. As each of the three phases has its own maximum line current limit, NITs alone will not ensure that each individual phase does not exceed its limit, as the NITs are generic across all phases of the network. The total quantity of NITs available will prevent the sum of the line currents of the three phases from exceeding the sum of the maximum per-phase current ratings, but if all NITs are consumed by the houses on a single phase, then the current through that particular phase will exceed the line's per-phase current rating. Therefore, Phase Impact Values and Tokens are introduced to ensure each phase of the network operates within its own limits.

Similarly to the NIVs above, the Phase Impact Values are determined for each house through the calculation of the change in extra load capacity. However, instead of analysing all houses across the network, each phase is analysed individually, and only houses connected to that phase are included in the calculation of the extra load capacity. In addition, the constraint on the transformer power (4.3.11) is not included during the PIV calculation, as the NITs ensure that this is not violated.

$$PIV_k^+ = |\sum_{\substack{j=1 \\ j\neq k}}^{K\phi} EL_j^\phi - \sum_{\substack{j=1 \\ j\neq k}}^{K\phi} EL_{k+,j}^\phi| \quad \forall\phi \tag{4.3.22}$$

$$PIV_k^- = |\sum_{\substack{j=1 \\ j\neq k}}^{K\phi} EL_j^\phi - \sum_{\substack{j=1 \\ j\neq k}}^{K\phi} EL_{k-,j}^\phi| \quad \forall\phi \tag{4.3.23}$$

where $K\phi$ is the number of houses connected to phase ϕ and EL_j^ϕ is the extra load capacity of house j on phase ϕ.

Phase Impact Tokens

Phase Impact Tokens are specific to each phase of the network, therefore the number of PITs allocated to each house are determined from the load capacities of the phase of the network to which the house is connected:

$$PIT\text{alloc}_k^{\phi,t} = \left(EL_k^{\phi} + P\text{generic}\right) \cdot PIV_k^{+} \quad \forall \phi, t \tag{4.3.24}$$

where EL_k^{ϕ} is the load capacity of the phase ϕ of the network to which house k is connected. Because PITs are specific to each phase, denoted by superscript ϕ, PITs for phase A can only bought, sold, used or generated by houses connected to phase A, and equivalently for the other two phases.

4.3.4 NITs and PITs Used in P2P Trading

The DSO uses the above method to determine the allocation of NITs and PITs to each house, with the modification that the extra load capacity used in (4.3.19) and (4.3.24) is only calculated with the variance constraint in (4.3.12) to ensure that every house is allocated equal load capacity for fairness. Because the load capacity of the network and each house's Impact Values are treated as time-invariant, the number of NITs and PITs allocated to each house is also time-invariant, and is a constant value. Therefore, once this number of NITs and PITs has been communicated to each house by the DSO, the house is able to use this number of tokens at each timestep until there is a change to the network topology or hardware requiring the initialisation stage to be recalculated.

For any load that a house wishes to add to the network, the house must possess the corresponding number of both NITs and PITs to ensure that no network or phase limit will be violated by the load. Therefore, if a house requires more NITs or PITs for their desired power consumption than they have been allocated, they must purchase additional tokens over the P2P market from other houses which are either not using all of their allocated NITs/PITs or are creating new NITs and PITs

through power injection into the network, such as discharging their battery/EV, or selling generated solar energy.

The Network and Phase Impact Tokens are subsequently divided into two categories - for baseload usage ($NIT_{\text{BL}}{}^{t}/PIT_{\text{BL}}{}^{\phi,t}$) and for EV usage ($NIT_{\text{EV}}{}^{t}/PIT_{\text{EV}}{}^{\phi,t}$), with the baseload and EV tokens traded in separate auctions. This is to ensure that houses have the opportunity to purchase the tokens required for their baseload usage before additional network capacity is used for EV charging. Baseload is treated as a non-flexible critical load, and it is essential that a house is able to use its required baseload. Therefore, the two categories of token are kept separate to ensure buyers do not try to cheat by purchasing tokens to be used for EV charging from the baseload auction, which could prohibit other houses purchasing sufficient tokens to meet their baseload requirement.

4.4 Peer-to-Peer Trading Methodology

In this section, the procedure that houses follow to determine whether to buy or sell Impact Tokens (ITs, referring to either NITs or PITs) on the P2P market and the functioning of the market itself is presented. The P2P market takes place every 10 minutes, with houses trading for ITs that are used in the following 10 minute period. For example, in the P2P market running between 10:00 - 10:10, houses will be competing to buy and sell ITs for use between 10:10 and 10:20. Each subsection describes a stage of the P2P trading process that occurs at each timestep.

Firstly, the planning problem is presented where each house must determine its optimal energy resource usage and the number of ITs that it should buy and sell at each timestep from the following 10 minute period until the end of the 24 hours. Secondly, the P2P markets are presented where houses are able to purchase ITs to enable them to use their baseload power or EV charging, with the process of submitting bids and asks through to the determination of the winning houses in the auction described. Between the P2P auctions for trading baseload ITs and EV

ITs, the market operator steps in to help ensure that all houses have sufficient ITs to permit their planned baseload, before allowing the purchase of remaining ITs for EV charging. Following the two auctions, there is a final opportunity for the sale of any remaining tokens by houses, who can offer their remaining ITs that were not sold in the previous two P2P auctions at a lower price on the seller-led market, to try to maximise their income and the utilisation of the network. This can incentivise other houses to adjust their planned energy resource usage to take advantage of these cheaper ITs, for example by increasing the EV charging that they do in the next timestep, as the cost of ITs might be lower than when they originally had planned to charge. Similarly, a buyer-led market then also takes place, where any buyers who have not been able to purchase sufficient tokens to meet baseload or EV charging requirements can incentivise sellers through higher prices to alter their planned energy usage to provide the additional ITs the buyer requires. Upon completion of all P2P trading, houses calculate their actual energy resource usage for the following timestep by again solving the original planning problem with the inclusion of all traded ITs as constraints on their resource usage. For example, if a house does not sell as many ITs as it was originally planning, then the actual battery discharging may be lower than originally planned, or more solar power will be used for EV charging so that fewer ITs are generated for sale. Similarly, if the house is not able to buy as many EV ITs as it originally bid for, then the EV charging that can no longer occur in the next timestep must be rescheduled to ensure the EV still reaches its SoC goal by departure.

4.4.1 Energy Resource Planning

To determine what ITs to buy or sell in the P2P markets, each house must first plan its optimal energy resource usage strategy for the day. This is formulated as a cost minimisation problem, and if equipped with solar PV panels, battery storage or an electric vehicle, it must determine when to charge the EV, when to store, consume or sell solar energy generation and when to discharge the EV or battery storage for

either the consumption or sale of energy. Additionally, decisions must be made on how to utilise or sell the allocated ITs and whether any additional baseload or EV ITs must be purchased. Figure 4.3 shows a flow diagram of the sources of power generation and ITs in the network along with the optimisation variables from this planning problem (middle column) and how the power/IT will be used within the network (right column). For example, power generated by a house's solar panels can be allocated to one of the following uses: to be used for the house's baseload, for charging the house's EV, to be stored in the house's battery, sold on the P2P market for other houses to use or to be curtailed if none of the above options are possible. Any generated or stored power that is sold to the grid generates additional ITs that will be sold to the other houses on the P2P market. The ITs initially allocated to the house by the network operator can be used for permitting baseload or EV consumption at that house, they could be sold on the P2P market to permit the usage of a load at another house, or may just be left unused if not all allocated ITs were either required for loads at the house or sold. This figure assumes that a house is equipped with both an EV and solar PV panels with battery storage, if a house is not equipped with one or both of these technologies, the options for generating and consuming energy and ITs will be reduced.

Resource Planning Optimisation Problem

Each house solves their own optimisation problem to determine the optimal usage of their available energy resources in the following 10 minute timestep. The optimisation objective that each house attempts to minimise is the total daily net cost of their energy, NIT and PIT usage. The results of the optimisation problem enable the house to determine their bid and asks to submit to the P2P market in the next step. Because each house is solving its own optimisation problem, the computational complexity is not affected by the number of houses in the network.

The set of optimisation variables corresponding to the usage of energy resources that the house can control, referred to as χ_{P2P}, are given along with their definitions in

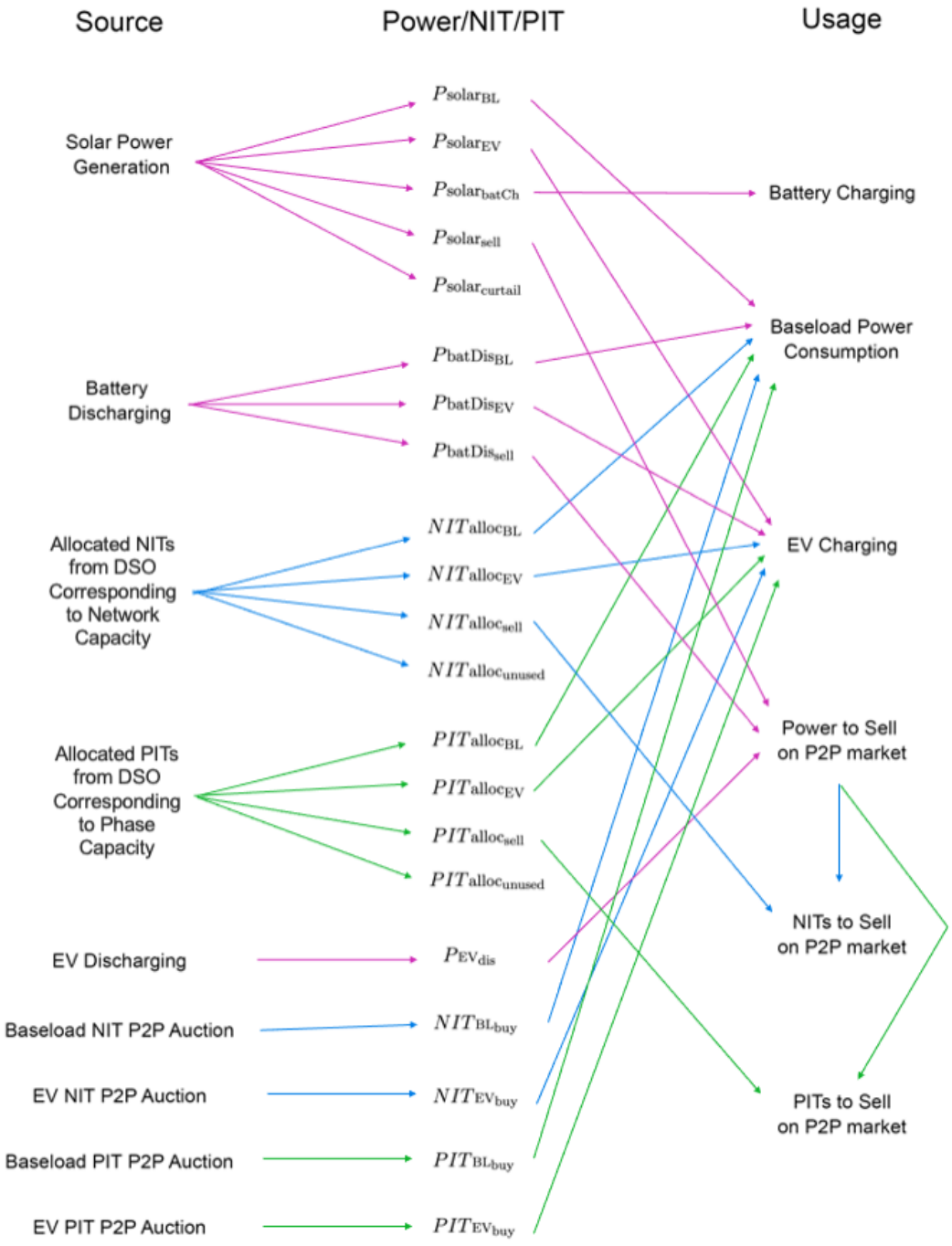

Figure 4.3: Flow diagram showing the sources and usage of each of the optimisation variables used in the energy resource planning stage. Pink lines identify variables representing power (kW), blue lines identify NITs and green lines identify PITs

Table 4.2

Each variable is of size $(T-t)\times 1$, with a value for each timestep between the current timestep t and the end of the 24 hour period when the system resets. Because the planning problem is solved a timestep ahead of the actual usage, it is assumed that to begin with the house first calculates the initial planning optimisation problem at $t=0$ for the 144 timesteps that make up the 24 hour period. All variables are constrained with a lower bound of 0. The upper bounds of the EV charging and discharging are set to 7 kW and 3 kW, respectively, when the EV is present, and 0 otherwise, so that the EV cannot charge whilst not at home. If the house has no EV, the upper bounds of all variables relating to EVs are set to 0. The upper bounds for variables relating to solar power usage and energy storage power or NITs are set to $+\infty$ if the house is equipped with these systems or is otherwise set to 0.

The house will calculate the number of NITs and PITs required to fulfil its baseload and EV charging requirements as given in (4.4.1) - (4.4.4).

$$NIT\text{REQ}_{\text{BL}}^{t} = \left(P\text{BL}^{t} - \left(P\text{solar}_{\text{BL}}^{t} + P\text{batDis}_{\text{BL}}^{t}\right)\right)\cdot NIV^{+} \quad \forall t \tag{4.4.1}$$

$$NIT\text{REQ}_{\text{EV}}^{t} = \left(P\text{EV}_{\text{ch}}^{t} - \left(P\text{solar}_{\text{EV}}^{t} + P\text{batDis}_{\text{EV}}^{t}\right)\right)\cdot NIV^{+} \quad \forall t \tag{4.4.2}$$

$$PIT\text{REQ}_{\text{BL}}^{\phi,t} = \left(P\text{BL}^{t} - \left(P\text{solar}_{\text{BL}}^{t} + P\text{batDis}_{\text{BL}}\right)\right)\cdot PIV^{+} \quad \forall t \tag{4.4.3}$$

$$PIT\text{REQ}_{\text{EV}}^{\phi,t} = \left(P\text{EV}_{\text{ch}}^{t} - \left(P\text{solar}_{\text{EV}}^{t} + P\text{batDis}_{\text{EV}}^{t}\right)\right)\cdot PIV^{+} \quad \forall t \tag{4.4.4}$$

where $P\text{BL}^{t}$ is the house's baseload power usage at time t and NIV^{+} and PIV^{+} are the house's Network Impact Value and Phase Impact Value, respectively, for increasing load on the network. Similarly, the house can calculate the number of NITs and PITs that it can offer for sale as follows:

$$NIT\text{SELL}^{t} = NIT\text{alloc}_{\text{sell}}^{t} + \left(P\text{EVDis}_{\text{sell}}^{t} + P\text{solar}_{\text{sell}}^{t} + P\text{batDis}_{\text{sell}}^{t}\right)\cdot NIV^{-} \quad \forall t \tag{4.4.5}$$

$$PIT\text{SELL}^{\phi,t} = PIT\text{alloc}_{\text{sell}}^{\phi,t} + \left(P\text{EVDis}_{\text{sell}}^{t} + P\text{solar}_{\text{sell}}^{t} + P\text{batDis}_{\text{sell}}^{t}\right)\cdot PIV^{-} \quad \forall t \tag{4.4.6}$$

where NIV^{-} and PIV^{-} are the house's Network and Phase Impact Values for generation and injecting power into the network. The actual values of $NIT\text{REQ}_{\text{BL}}$,

Table 4.2: P2P planning optimisation variables - χ_{P2P}

Variable	Definition
$P_{\text{EV}_{\text{ch}}}$	EV charging power
$P_{\text{EV}_{\text{dis}}}$	EV discharging power for V2G
$P_{\text{solar}_{\text{BL}}}$	Solar power generation used for baseload
$P_{\text{solar}_{\text{EV}}}$	Solar power generation used for EV charging
$P_{\text{solar}_{\text{batCh}}}$	Solar power generation used for battery charging
$P_{\text{solar}_{\text{sell}}}$	Solar power generation to generate NITs to be sold to other houses
$P_{\text{solar}_{\text{unused}}}$	Solar power generated that is not sold to other houses or used for loads
$P_{\text{batDis}_{\text{BL}}}$	Battery discharging power used for baseload
$P_{\text{batDis}_{\text{EV}}}$	Battery discharge power used for EV charging
$P_{\text{batDis}_{\text{sell}}}$	Battery discharging power to generate NITs to be sold to other houses
$NIT_{\text{alloc}_{\text{BL}}}$	Allocated NITs used to permit baseload power
$NIT_{\text{alloc}_{\text{EV}}}$	Allocated NITs used to permit EV charging power
$NIT_{\text{alloc}_{\text{sell}}}$	Allocated NITs sold to other houses on P2P market
$PIT_{\text{alloc}_{\text{BL}}}$	Allocated PITs used to permit baseload power
$PIT_{\text{alloc}_{\text{EV}}}$	Allocated PITs used to permit EV charging
$PIT_{\text{alloc}_{\text{sell}}}$	Allocated PITs sold to other houses on P2P market
$NIT_{\text{BL}_{\text{buy}}}$	NITs purchased from P2P market to permit baseload usage
$NIT_{\text{EV}_{\text{buy}}}$	NITs purchased from P2P market to permit EV charging
$PIT_{\text{BL}_{\text{buy}}}$	PITs purchased from P2P market to permit baseload usage
$PIT_{\text{EV}_{\text{buy}}}$	PITs purchased from P2P market to permit EV charging

$NIT\text{REQ}_{\text{EV}}$ and $NIT\text{SELL}$ corresponding to the number of NITs to buy for baseload, EV charging and to sell on the P2P market are determined through the results of the optimisation problem, along with the equivalent values of PITs.

The number of NITs required for baseload and EV charging must be met from using allocated NITs or purchasing additional baseload NITs on the P2P market as given in constraints (4.4.7) and (4.4.8). In addition, the number of allocated NITs from the network operators calculation of the network load capacity must also be consumed, sold or not used in order to balance the system and is constrained through (4.4.9).

$$NIT\text{alloc}^t_{\text{BL}} + NIT\text{BL}^t_{\text{buy}} = NIT\text{REQ}^t_{\text{BL}} \quad \forall t \tag{4.4.7}$$

$$NIT\text{alloc}^t_{\text{EV}} + NIT\text{EV}^t_{\text{buy}} = NIT\text{REQ}^t_{\text{EV}} \quad \forall t \tag{4.4.8}$$

$$NIT\text{alloc}^t_{\text{BL}} + NIT\text{alloc}^t_{\text{EV}} + NIT\text{alloc}^t_{\text{sell}} + NIT\text{alloc}^t_{\text{unused}} = NIT\text{alloc}^t \quad \forall t \tag{4.4.9}$$

Similarly, the usage of PITs is constrained as:

$$PIT\text{alloc}^{\phi,t}_{\text{BL}} + PIT\text{BL}^{\phi,t}_{\text{buy}} = PIT\text{REQ}^{\phi,t}_{\text{BL}} \quad \forall t \tag{4.4.10}$$

$$PIT\text{alloc}^{\phi,t}_{\text{EV}} + PIT\text{EV}^{\phi,t}_{\text{buy}} = PIT\text{REQ}^{\phi,t}_{\text{EV}} \quad \forall t \tag{4.4.11}$$

$$PIT\text{alloc}^{\phi,t}_{\text{BL}} + PIT\text{alloc}^{\phi,t}_{\text{EV}} + PIT\text{alloc}^{\phi,t}_{\text{sell}} + PIT\text{alloc}^{\phi,t}_{\text{unused}} = PIT\text{alloc}^{\phi,t} \quad \forall t \tag{4.4.12}$$

If the house is equipped with solar PV panels and battery storage, the amount of energy stored in the house's battery at time t is given by:

$$\begin{aligned} B^t_{\text{store}} = B^{in}_{\text{store}} + \sum_{\tau=1}^{t} (&P\text{solar}^{\tau}_{\text{batCh}} - (P\text{batDis}^{\tau}_{\text{BL}} + \\ &P\text{batDis}^{\tau}_{\text{EV}} + P\text{batDis}^{\tau}_{\text{sell}})) \cdot \Delta T \cdot \eta \end{aligned} \tag{4.4.13}$$

where B^{in}_{store} is the initial energy stored in the house's battery at time $t = 0$.

The EV's SoC at time t is given by:

$$SoC^t = SoC_{\text{in}} - SoC^t_{\text{travel}} + \sum_{\tau=1}^{t} (P\text{EVCh}^{\tau} - P\text{EVDis}^{\tau}_{\text{sell}}) \cdot \frac{\Delta T \cdot \eta}{B_{\text{EV}_{\text{cap}}}} \tag{4.4.14}$$

where SoC_{in} is the EV's initial state of charge, SoC^t_{travel} is the SoC consumed on any

journeys between timesteps $\tau = 1$ and t, η is the EV charging efficiency and $B_{\mathrm{EV_{cap}}}$ is the EV's battery capacity in kWh.

The EV is allocated a target SoC at their departure time that should be reached in order to satisfy the owner's needs. If the SoC of the EV at departure is lower than this target value, a virtual cost penalty is incurred. While not meeting the target SoC does not actually incur the owner a real cost, this virtual penalty is included in the cost based objective function to ensure that sufficient EV charging is prioritised.

$$\Pi_{\mathrm{penalty_{EV}}} = \left| SoC_{\mathrm{target}} - SoC^{T_{\mathrm{dep}}} \right| \cdot \pi_{\mathrm{EV_{penalty}}} \tag{4.4.15}$$

where $\Pi_{\mathrm{EV_{penalty}}}$ is the virtual penalty cost arising from departing with SoC $SoC^{T_{\mathrm{dep}}}$ instead of target SoC SoC_{target}. The SoC deficit is penalised at a cost of $\pi_{\mathrm{EV_{penalty}}}$ £/SoC%.

The house is subject to a cost for any NITs and PITs purchased on the P2P market as well as the cost of any electricity the house uses, but can receive income for selling NITs, PITs and energy generated from discharging of batteries or solar PV on the P2P market. Although energy is not purchased or sold specifically on the P2P market, in order to sell NITs or PITs, a house may have to inject power into the network. Rather than additional energy being sourced from the upstream grid, this injected energy is consumed locally instead, with the house that purchases the ITs generated through this power injection paying the selling house for the electricity. Therefore, while energy is effectively traded on the P2P market, it is a by-product of the trading of NITs and PITs, rather than its own specific market - a house cannot purchase energy without the purchase of NITs or PITs. Because this study focuses on the P2P trading of the NITs rather than energy, it is assumed that the cost of energy if bought via the P2P market is equivalent to the cost of energy purchased from the network operator. Therefore, the cost of baseload energy for the house is given by:

$$\Pi_{\mathrm{BL_{energy}}} = \sum_{t=1}^{T} \left(P_{\mathrm{BL}}{}^{t} - \left(P\mathrm{solar}_{\mathrm{BL}}^{t} + P\mathrm{batDis}_{\mathrm{BL}}^{t} \right) \right) \cdot \Delta T \cdot \pi_{\mathrm{energy}} \tag{4.4.16}$$

where $\Pi \text{BL}_{\text{energy}}$ is the total cost of electricity consumed for baseload, $P\text{BL}^t$ is the baseload power at time t and π_{energy} is the cost of electricity (£/kWh). Similarly, the total cost of energy for EV charging is given by:

$$\Pi \text{EV}_{\text{energy}} = \sum_{t=1}^{T} \left(P\text{EV}_{\text{ch}}^{t} - \left(P\text{solar}_{\text{EV}}^{t} + P\text{batDis}_{\text{EV}}^{t} \right) \right) \cdot \Delta T \cdot \pi_{\text{energy}} \tag{4.4.17}$$

and therefore the house's total energy cost is:

$$\Pi \text{Energy} = \Pi \text{BL}_{\text{energy}} + \Pi \text{EV}_{\text{energy}} \tag{4.4.18}$$

As all loads that are not fulfilled using self-generated energy (i.e. battery charging or solar generation, which bypass the main grid) require the corresponding number of NITs and PITs to enable their use, the house also encounters cost for purchasing any required tokens. The cost of purchasing NITs and PITs to meet the baseload requirement is given by (4.4.19) and (4.4.20),respectively.

$$\Pi \text{BL}_{\text{NIT}} = \sum_{\tau=1}^{t} \sum_{m=1}^{M} NIT\text{BL}_{\text{bought}}^{\tau,m} \cdot \Pi \text{trade}^{m} + \sum_{\tau=t+1}^{T} NIT\text{BL}_{\text{buy}}^{\tau} \cdot \pi \text{NIT}_{\text{exp}}^{\tau} \tag{4.4.19}$$

$$\Pi \text{BL}_{\text{PIT}} = \sum_{\tau=1}^{t} \sum_{m=1}^{M} PIT\text{BL}_{\text{bought}}^{\phi,\tau,m} \cdot \Pi \text{trade}^{m} + \sum_{\tau=t+1}^{T} PIT\text{BL}_{\text{buy}}^{\phi,\tau} \cdot \pi \text{PIT}_{\text{exp}}^{\tau} \tag{4.4.20}$$

where $\Pi \text{BL}_{\text{NIT}}$ is the total cost of purchasing NITs to fulfil baseload power for the 24 hour period, consisting of the cost of any baseload NITs purchased in P2P auctions during previous timesteps and the expected cost of purchasing any NITs in future timesteps. For each timestep τ between the initial timestep and the current timestep t, the number of baseload NITs purchased in each of the M trades the house has made at each timestep is given by $NIT\text{BL}_{\text{bought}}^{\tau,m}$, and the trade price of each of the M trades is given by Πtrade^{m}. The number of baseload NITs planned to be purchased in future timesteps is given by $NIT\text{BL}_{\text{buy}}^{\tau}$ and $\pi \text{NIT}_{\text{exp}}^{\tau}$ is the expected cost of purchasing a single NIT in a later timeslot. Because the price is set by the P2P auction, this expected cost cannot be known for certain in advance, and will depend on levels of supply and demand within the market. Testing found that implementing a time-of-use multiplier tariff resulted in EVs charging earlier in the day, and subsequently

more EVs departing with their desired SoC. The multipliers used were one-times between 8am and 6pm, three-times between 6pm and 10:30pm and six-times from 10:30pm until 8am. Similarly, the cost of NITs and PITs that are purchased to facilitate EV charging is given by:

$$\Pi\text{EV}_{\text{NIT}} = \sum_{\tau=1}^{t}\sum_{m=1}^{M} NIT\text{EV}_{\text{bought}}^{\tau,m} \cdot \Pi\text{trade}^{m} + \sum_{\tau=t+1}^{T} NIT\text{EV}_{\text{buy}}^{\tau} \cdot \pi\text{NIT}_{\text{exp}}^{\tau} \tag{4.4.21}$$

$$\Pi\text{EV}_{\text{PIT}} = \sum_{\tau=1}^{t}\sum_{m=1}^{M} PIT\text{EV}_{\text{bought}}^{\phi,\tau,m} \cdot \Pi\text{trade}^{m} + \sum_{\tau=t+1}^{T} PIT\text{EV}_{\text{buy}}^{\phi,\tau} \cdot \pi\text{PIT}_{\text{exp}}^{\tau} \tag{4.4.22}$$

The total cost of purchasing all required NITs and PITs on the P2P market is:

$$\Pi\text{NIT} = \Pi\text{BL}_{\text{NIT}} + \Pi\text{EV}_{\text{NIT}} \tag{4.4.23}$$

$$\Pi\text{PIT} = \Pi\text{BL}_{\text{PIT}} + \Pi\text{EV}_{\text{PIT}} \tag{4.4.24}$$

The house's energy income, NIT income and PIT income are given by (4.4.25), (4.4.26) and (4.4.27), respectively.

$$\Pi\text{Income}_{\text{Energy}} = \sum_{\tau=1}^{T} (P\text{solar}_{\text{sell}}^{\tau} + P\text{batDis}_{\text{sell}}^{\tau} + P\text{EV}_{\text{dis}}^{\tau}) \cdot \pi_{\text{energy}} \tag{4.4.25}$$

$$\Pi\text{Income}_{\text{NIT}} = \sum_{\tau=1}^{t}\sum_{m=1}^{M} NIT_{\text{sold}}^{\tau,m} \cdot \Pi\text{trade}^{m} + \sum_{\tau=t+1}^{T} NIT\text{SELL}^{\tau} \cdot \pi\text{NIT}_{\text{exp}}^{\tau} \tag{4.4.26}$$

$$\Pi\text{Income}_{\text{PIT}} = \sum_{\tau=1}^{t}\sum_{m=1}^{M} PIT_{\text{sold}}^{\tau,m} \cdot \Pi\text{trade}^{m} + \sum_{\tau=t+1}^{T} PIT\text{SELL}^{\tau} \cdot \pi\text{PIT}_{\text{exp}}^{\tau} \tag{4.4.27}$$

The total net cost of energy, NITs and PITs for the 24 hour period is therefore given by:

$$\begin{aligned}\Pi\text{total} =& \Pi\text{Energy} + \Pi\text{NIT} + \Pi\text{PIT} \\ &- (\Pi\text{Income}_{\text{Energy}} + \Pi\text{Income}_{\text{NIT}} + \Pi\text{Income}_{\text{PIT}})\end{aligned} \tag{4.4.28}$$

In addition, a virtual cost penalty is imposed to ensure that baseload usage and EV charging is prioritised in the optimisation problem, and the wasting of ITs or generated solar energy is avoided. This penalty cost does not add to the house's total real cost that it pays for energy, NITs and PITs for the 24 hour period, but is

included in the objective function of the optimisation problem.

$$\Pi\text{penalty} = \Pi_{\text{penalty}_{\text{EV}}} + \Pi_{\text{penalty}_{\text{BL}}} + \Pi_{\text{penalty}_{\text{V2G}}} + \Pi_{\text{penalty}_{\text{solar}}} + \Pi_{\text{penalty}_{\text{ITs}}} \quad (4.4.29)$$

where $\Pi_{\text{penalty}_{\text{EV}}}$ is the penalty cost associated with the house's EV not achieving its SoC goal at departure given by (4.4.15), $\Pi_{\text{penalty}_{\text{BL}}}$ is a penalty imposed if the planned baseload is less than the house's actual baseload requirement, $\Pi_{\text{penalty}_{\text{V2G}}}$ is a small cost imposed on EV discharging to account for battery degradation, $\Pi_{\text{penalty}_{\text{solar}}}$ is equal to a penalty fee multiplied by $P_{\text{solar}_{\text{unused}}}$ which accounts for any solar power generated that is neither consumed, stored or sold, and $\Pi_{\text{penalty}_{\text{ITs}}}$ is a penalty for any allocated NITs and PITs which are neither utilised or sold.

Finally, the optimisation objective can be defined as:

$$\min_{\chi_{\text{P2P}}} \ \Pi\text{total} + \Pi\text{penalty} \quad (4.4.30)$$

where χ_{P2P} is the house's controllable energy resources, and is subject to the following constraints on EV charging and battery storage:

$$0 \leq SoC^t \leq 1 \quad \forall t \quad (4.4.31)$$

$$0 \leq P_{\text{EV}_{\text{ch}}^t} \leq P_{\text{EV}_{\text{ch}_{\text{max}}}} \quad \forall t \quad (4.4.32)$$

$$0 \leq P_{\text{EV}_{\text{dis}}^t} \leq P_{\text{EV}_{\text{dis}_{\text{max}}}} \quad \forall t \quad (4.4.33)$$

The EV SoC is constrained between 0 and 1 to ensure that the battery does not charge more than its capacity or discharge further than empty. The EV charge rate is also constrained between 0 and the maximum EV charge rate, set here as 7 kW, corresponding to home charging from a dedicated charge point, and the EV discharge rate is limited between 0 and the maximum EV discharge rate, which has been chosen as 3 kW to protect the EV battery and grid.

$$0 \leq B^t_{\text{store}} \leq B_{\text{Bat}_{\text{cap}}} \quad \forall t \in T \quad (4.4.34)$$

$$0 \leq P\text{batDis}^t \leq P\text{batDis}_{\text{max}} \quad \forall t \quad (4.4.35)$$

$$P\text{batDis}^t_{\text{BL}} + P\text{batDis}^t_{\text{EV}} + P\text{batDis}^t_{\text{sell}} = P\text{batDis}^t \quad \forall t \tag{4.4.36}$$

$$P\text{solar}^t_{\text{BL}} + P\text{solar}^t_{\text{EV}} + P\text{solar}^t_{\text{batCh}} + P\text{solar}^t_{\text{sell}} + P\text{solar}^t_{\text{curtail}} = P\text{solar}^t \quad \forall t \tag{4.4.37}$$

For the included solar PV and battery storage, the energy stored in the battery must be kept between 0 and the maximum battery capacity $B\text{Bat}_{\text{cap}}$ and the battery discharge rate is constrained between 0 kW and the maximum battery discharge rate, 7 kW. Any power discharged from the battery must be allocated to either supplying power for baseload or EV or sold with NITs on the P2P market. Similarly, any solar power generated must be allocated for use for either baseload, EV charging, battery charging, sold via P2P or curtailed.

Solving of this optimisation problem will generate the house's optimal energy resource utilisation for the remaining timeslots in the 24 hour period. If the results determine that a house should buy or sell NITs or PITs for the next timestep, the house can prepare the relevant bids and asks to trade these Impact Tokens on the P2P market.

4.4.2 P2P Market Structure

At every ten-minute timestep, the P2P markets open to enable houses to buy or sell NITs and PITs in accordance with the results of their planning problem for the following timestep. As previously mentioned, two P2P markets take place, the first allowing houses to purchase any required Impact Tokens for their baseload, and the second allowing houses to purchase any tokens required for their EV charging. This ensures that any houses wishing to charge EVs that submit high bid prices do not purchase so many ITs for their EV charging such that there are not sufficient tokens remaining in the network for all houses to fulfil their baseload. As baseload power is considered a non-flexible requirement, it is imperative that all houses are able to secure sufficient NITs and PITs to accommodate this. This is achieved through having separate types of NITs/PITs that are purchased through P2P markets for baseload and EV charging, denoted $NIT_{\text{BL}}/PIT_{\text{BL}}$ and $NIT_{\text{EV}}/PIT_{\text{EV}}$, respectively. In practice, a smart EV charger will assess the quantity of NIT_{EV} and PIT_{EV} that

have been purchased, in addition to the number of allocated NITs/PITs assigned to EV charging when determining the maximum EV charge power that the device will supply. Any ITs allocated from the DSO can be used for either baseload or EV charging. Any Impact Tokens that a house wishes to sell, whether unused allocated NITs/PITs, or generated from solar power, battery discharging or V2G, can be sold to either of the two P2P auctions, so houses are expected to submit asks for all available ITs to both auctions to maximise the number of NITs and PITs they are able to sell.

The P2P market can be hosted virtually on an online platform that houses within the network have credentials to join. The entire process from each house calculating the number of NITs/PITs they plan to buy and sell at each auction and submitting these to the market platform, the market operation and determination of successful participants and the final trade price to the matching of successful buyers and sellers can be accomplished automatically through the presented algorithms. The algorithms to determine energy usage and the bids and asks to submit to the P2P market could be hosted by each house's energy management system, such as being incorporated into a smart meter. Ideally, machine learning technology can be incorporated to learn from a house's energy usage to improve the accuracy of the planning stage without requiring the user's input. Therefore, this type of system is also viable to be hosted on blockchain, with smart contracts determining the trades to be made, and ensuring appropriate actions are made by the houses to fulfil their obligations based on the results of the P2P trading.

The following sections describe the process of submitting bids and asks and the P2P market matching process to determine successful trades. These steps are repeated for both the baseload auction, and the EV auction.

4.4.3 Submitting Bids and Asks

Each house will have a private valuation for how much money they are willing to pay for NITs or PITs in the P2P auction and how much they are willing to receive for any ITs that they sell. In a truthful auction, buyers and sellers will maximise their utility from the auction by bidding their private valuation, so these private valuations for buying and selling NITs become the house's bid and ask prices, respectively.

If the result of $NIT_{\text{BL}}^{t}_{\text{buy}}$ or $NIT_{\text{EV}}^{t}_{\text{buy}}$ from the optimisation planning problem is greater than 0 for the next timestep t, then the house will submit a bid for NITs to the P2P market platform. The bid consists of four elements: the house's unique ID, the number of NITs they are bidding for ($NIT_{\text{BL}_{\text{buy}}}$ or $NIT_{\text{EV}_{\text{buy}}}$), their bid price (£/NIT) and a code to identify either NIT_{BL} or NIT_{EV}. Similarly, if $PIT_{\text{BL}}^{\phi,t}_{\text{buy}}$ or $PIT_{\text{EV}}^{\phi,t}_{\text{buy}}$ is greater than zero, the house will submit bids for the required PITs. Again, the bid consists of four elements, with the first three being identical to the NIT auction. The final identifying code represents the type and phase of the PIT, for example PIT_{BL_A}.

If the house wishes to sell surplus NITs/PITs or sell ITs created through power injection, they submit an ask to the P2P market. The ask consists of the house's ID, the number of NITs they are selling, their ask price and a value identifying the Impact Token type that is being sold. As the baseload/EV category of IT is only assigned when bought in either type of auction, the sold tokens do not require a baseload or EV designation. However, the token type, i.e. NIT or PIT is identified here, and in the case of PITs, an additional term designates the phase of the network to which the PIT belongs.

Once all houses have submitted their bids and asks to the P2P markets, the list of bids for each market can be ordered from highest bid price to lowest, and the list of asks ordered from lowest ask price to highest. As PITs are specific to a single phase of the network and can only be traded by houses on that phase, the PIT bid and ask arrays are split into separate bid and ask arrays for each of the three phases of

the network.

4.4.4 P2P Market Mechanism and Matching Result

Once the lists of bids and asks have been received, the market operator must calculate the intersection point between buyers and sellers to determine which buyers and sellers successfully trade. The following strategy is implemented to calculate the intersection point.

For each ask from ordered ask list, evaluate the two possible scenarios:

Scenario 1: Intersection occurs mid-bid

1. Check if price of ask is higher than the last successful bid
2. If so, intersection occurs at the price of the last safe bid and quantity of previous ask
3. If not, or there are not yet any successful bids recorded, test scenario 2

Scenario 2: Intersection occurs mid-ask

4. Add up ITs requested for this ask and any previous, and find number of bids required to demand this number of ITs
5. For each of these bids, check if the bid price is greater or equal to the ask price
6. If so, mark bid as successful
7. If the bid price is less than the ask price, then the intersection occurs at the quantity of final successful bid and price of current ask

If neither intersection criteria is met for the current ask, move on to the next ask from the list. The intersection point can only be found once, so once the intersection has been calculated then the loop is exited.

There are two possible intersection scenarios which must be checked, which are shown in Figure 4.4. The first occurs mid-bid, where the previous ask did not have sufficient ITs available to fulfil the bid's entire request, but the next ask is at a price higher than the bid, and the second occurs mid-ask, where the previous bids not demand the entire quantity of ITs offered by a seller, but the next bid price is below the seller's ask price. A third and fourth scenario is also possible, not shown here, where the intersection occurs at a point where the cumulative quantity of bids and asks are identical or the bid and ask price are identical, however these can be evaluated under scenarios 1 and 2, respectively.

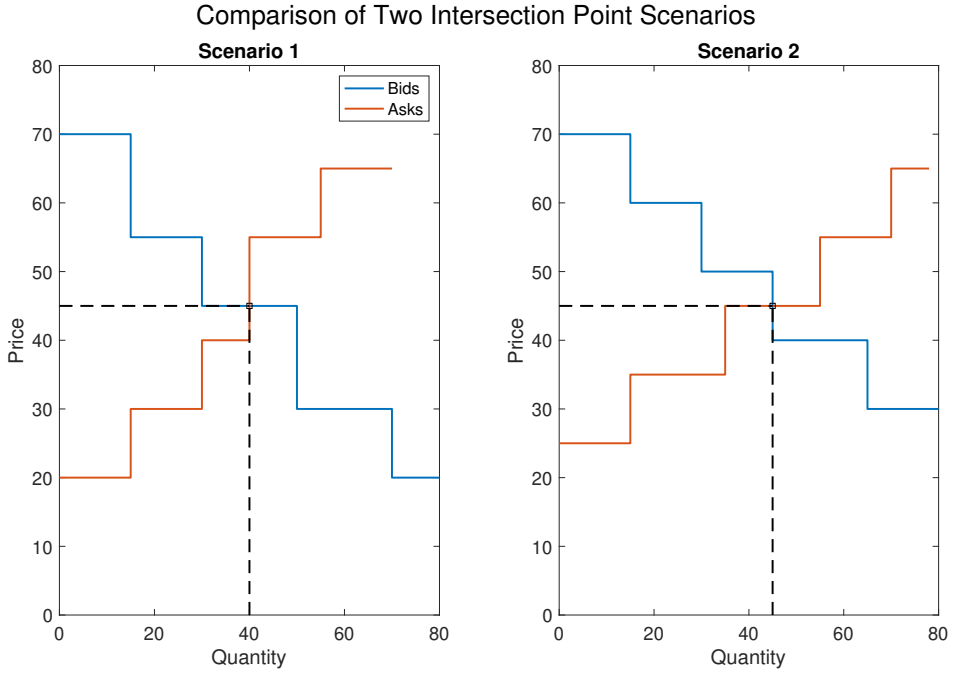

Figure 4.4: Comparison of intersection scenarios 1 and 2

To ensure that the auction is truthful, and that participants are incentivised to bid their private valuations of the ITs, McAfee's double auction mechanism is implemented here [143]. Once the intersection point in the bids and asks has been calculated, the final auction price and successful buyers and sellers are determined as follows:

1. Find the number of buyers b and number of sellers s to the left of the intersection point

2. Calculate the mean price between the $b+1^{\text{th}}$ and $s+1^{\text{th}}$ participant as

$$\pi\text{trade} = \frac{1}{2}\left(\pi_{\text{bid}_{b+1}} + \pi_{\text{ask}_{s+1}}\right) \tag{4.4.38}$$

where πtrade is the calculated trade price from the auction, $\pi_{\text{bid}_{b+1}}$ is the bid price of the $b+1^{\text{th}}$ buyer and $\pi_{\text{ask}_{s+1}}$ is the ask price of the $s+1^{\text{th}}$ seller.

3. If $\pi_{\text{bid}_b} \geq \pi\text{trade} \geq \pi_{\text{ask}_s}$, then all buyers up to and including b can trade and all sellers up to and including s are successful in the auction and can trade. The trade price is given in (4.4.38)

   If the above inequality is not satisfied, then some participants must be removed from the auction and their bid and ask prices used to set the auction price. This is done to preserve the property of truthfulness, if the auction price is set by a successful participant, they might be incentivised to alter their bid or ask price to benefit themselves

4. The final seller with the highest ask price s is then removed from the auction, along with buyer b who had the lowest bid.

5. The number of ITs available from the remaining sellers is then rechecked against the number of NITs requested from the remaining buyers to ensure that there are still sufficient ITs in the market for the final buyer to successfully purchase some of their requested ITs. In an instance where this is not the case, additional buyer(s) need to be removed. This occurs if the s^{th} seller had offered a large quantity of ITs that multiple buyers would have purchased

6. If only a single buyer and seller have to be removed, then buyers up to $b-1$ and sellers up to $s-1$ will successfully trade at the auction price given by:

$$\pi\text{trade} = \frac{1}{2}\left(\pi_{\text{bid}_b} + \pi_{\text{ask}_s}\right) \tag{4.4.39}$$

7. If n buyers are removed, then buyers up to $b-n$ and sellers up to $s-1$ are

successful and will trade at price given by:

$$\pi\text{trade} = \frac{1}{2}\left(\pi_{\text{bid}_{b-n+1}} + \pi_{\text{ask}_s}\right) \tag{4.4.40}$$

Unlike the auction matching mechanisms presented in Chapter 3, this is a many-to-many matching, meaning that each seller is able to sell ITs to multiple houses, and each buyer is able to purchase ITs from multiple sellers, which simplifies the matching mechanism considerably. The matching of buyers with sellers proceeds as follows.

For each successfully trading buyer, from highest bidding to lowest:

1. Calculate the total number of ITs purchased by the previous buyers (with higher bids) and calculate how many sellers (from lowest ask price to highest) are required to fulfil that number of NITs
2. Based on the buyer's NIT/PIT request, calculate whether the last seller to trade previously has sufficient NITs remaining to meet the buyer's request
3. If so, the buyer purchases all of their requested ITs from this seller
4. If the current seller does not have sufficient ITs remaining to meet the buyer's demand, the buyer purchases the ITs available from this seller and then moves on to the seller with the next highest ask price and looks to purchase the remainder of their required NITs from that seller. If they are still not able to acquire all ITs, they move on to the next seller again until they have done so
5. Note: The final successful buyer (with the lowest bid price) may not be able to purchase the entire quantity of ITs they originally bid for, if the total quantity of ITs offered by successful sellers is lower than the total quantity of ITs bid for by successful buyers (a scenario 1 intersection).
6. Once the buyer has had their total requested ITs matched to the sellers, each individual trade with a different seller is recorded separately, storing the buyer's

and seller's unique IDs, the total number of ITs purchased from each seller, the total cost of each separate trade based on the auction price and the number of NITs purchased on that trade and the Impact Token type identifier.

4.4.5 Market Operator Trades

A key property of McAfee's double auction mechanism is that inevitably at least one buyer and seller are excluded from trading, as their bid and ask prices are used to set the auction trade price to maintain the property of truthfulness. Therefore, such a system is guaranteed to result in at least one house that does not purchase sufficient NITs or PITs to permit the use of its baseload. Given that the usage of baseload power is considered an absolute requirement, it is necessary for the market operator to step in to help ensure that all houses acquire sufficient NITs and PITs to use their baseload before any ITs are purchased for EV charging.

Based on the submitted bids to both the baseload NIT and PIT auctions and the finalised matchings, it can be determined which houses did not purchase sufficient NITs and PITs to fulfil their baseload requirement. The total baseload NITs deficit can then be calculated by summing up the unpurchased NITs. Based on the number of NITs offered in the asks and the successfully matched trades, the percentage of unpurchased NITs to the unsold NITs is calculated, up to a maximum of 100%.

$$NIT_{\mathrm{BL_{Def\%}}} = \frac{\sum_{k=1}^{K}\left(NIT_{\mathrm{BL}_{\mathrm{buy}_k}}^{t} - NIT_{\mathrm{BL}_{\mathrm{bought}_k}}^{t}\right)}{\sum_{k=1}^{K}\left(NIT_{\mathrm{sell}_k}^{t} - NIT_{\mathrm{sold}_k}^{t}\right)} \times 100 \tag{4.4.41}$$

where $NIT_{\mathrm{BL}_{\mathrm{buy}_k}}$ is the number of NITs house k submitted in its bid to the auction, $NIT_{\mathrm{BL}_{\mathrm{bought}_k}}$ is the number of NITs that house k won in total in the auction, NIT_{sell_k} is the number of NITs that house k offered for sale in the auction and NIT_{sold_k} is the total number of NITs sold by house k in the baseload auction. The market operator then purchases $NIT_{\mathrm{BL_{Def\%}}} \times \left(NIT_{\mathrm{sell}_k}^{t} - NIT_{\mathrm{sold}_k}^{t}\right)$ NITs from each house k with unsold NITs to sell to the houses with a deficit of baseload NITs. The same calculations are done with the PITs for each of the three phases, to determine which

houses need to purchase additional PITs to meet their baseload requirement.

The price that the market operator pays the selling houses is less than the typical trade price from the P2P auction, and the price that the buying houses pay is more than the typical P2P trade price, which acts as a penalty to houses unable to sell or buy in the P2P market as their bid or ask price was less competitive than the other participants. These trades are also stored in the transaction history, along with the P2P trades, with the unique ID of the market operator (99999) used instead of the house ID as appropriate for the buyer or seller ID.

4.4.6 Transaction Log

All transactions between houses on the P2P market or transactions between houses and the market operator are recorded on a central Transaction Log to create a permanent record of agreed transactions. This log could be used to ensure that each house's actual energy resource usage in the following timestep matches the actions agreed based on the P2P trading. Each transaction between houses is recorded, so if a house sells NITs or PITs to multiple different houses, then there is a separate transaction logged for each trade. The Transaction Log consists of the unique IDs for the buying house and selling house, or market operator, the current timestep that the auction takes place during, the type of NIT or PIT being traded, the number of tokens traded and the cost of the trade to the buying house. The unique IDs allow the buying and selling houses to be identified to ensure that each house buys and sells the correct number of NITs. The current timestep is recorded to capture which auction the trade has occurred in, however the actual consumption or generation of NITs occurs in the subsequent timestep. As mentioned earlier, ITs purchased in the baseload auction cannot be used to support EV charging, so therefore the IT type is recorded for the buyer in each auction which limits the ability to use those tokens. The number of NITs or PITs traded is recorded, along with the total cost of the trade. The total cost to house k of each trade m is defined as the auction

price πtrade, calculated in (4.4.38) or (4.4.39), multiplied by the number of ITs sold in that trade. Finally, if the traded ITs had been generated by the selling house through the injection of power into the network from solar panels or battery storage, the amount of energy traded is also recorded.

The income of/cost to house k from a single trade m selling/buying baseload or EV NITs is given by:

$$\Pi\text{trade}_k^m = \pi\text{trade}^m \times NIT^m_{\text{sold, }k} \tag{4.4.42}$$

where the number of NITs traded in trade m is given by $NIT^m_{\text{sold, }k}$. For any PITs sold in a trade m, $NIT^m_{\text{sold, }k}$ is replaced with $PIT^{\phi,m}_{\text{sold, }k}$. For the buyer in this trade, the cost is recorded in the Transaction Log as a positive value, whereas for the seller, the cost is recorded as a negative value, representing income.

The total number of baseload NITs and PITs purchased by house k for timestep t is defined as:

$$NIT_{\text{BL}^t_{\text{bought}_k}} = \sum_{m=1}^{M} NIT_{\text{BL}^m_{\text{bought}_k}} \tag{4.4.43}$$

$$PIT_{\text{BL}^{\phi,t}_{\text{bought}_k}} = \sum_{m=1}^{M} PIT_{\text{BL}^{\phi,m}_{\text{bought}_k}} \tag{4.4.44}$$

where M is the total number of transactions that house k participates in, including both P2P trades and trades with the market operator. Similarly, the number of EV NITs purchased by house k is defined as:

$$NIT_{\text{EV}^t_{\text{bought}_k}} = \sum_{m=1}^{M} NIT_{\text{EV}^m_{\text{bought}_k}} \tag{4.4.45}$$

$$PIT_{\text{EV}^{\phi,t}_{\text{bought}_k}} = \sum_{m=1}^{M} PIT_{\text{EV}^{\phi,m}_{\text{bought}_k}} \tag{4.4.46}$$

The quantity of NITs and PITs sold by each house on the baseload and EV markets is given by (4.4.47):

$$NIT^t_{\text{sold, }k} = \sum_{m=1}^{M} NIT^m_{\text{sold, }k} \tag{4.4.47}$$

$$PIT^{\phi,t}_{\text{sold, }k} = \sum_{m=1}^{M} PIT^m_{\text{sold, }k} \tag{4.4.48}$$

4.4.7 Finalise Energy Resource Usage

Following completion of the P2P auctions, each house must determine its actual energy resources usage for the next timestep based on the confirmed NIT and PIT transactions. For instance, a house may have originally planned to charge their EV at a rate of 7 kW, and bid for sufficient NITs to permit that, but if it was not successful in winning those NITs in the auction, it may not have a sufficient number of NITs to permit this rate of EV charging, and would need to reduce its actual charging power.

The problem that the house solves to calculate its actual energy resource usage is very similar to the initial planning problem described in Section 4.4.1, and therefore is not described in full again in this section. The optimisation objective remains the same, however some of the optimisation variables now take known values determined by the results of the P2P trading, so the optimisation problem must account for these by adding constraints on these variables so they take the correct value. The optimisation variables corresponding to the number of NITs and PITs to purchase for EV charging, baseload usage or to sell in the next timestep, t, have values determined by the results of the now completed auctions, and are constrained as follows:

$$NIT_{\mathrm{BL}_{\mathrm{buy}}^{t}} = NIT_{\mathrm{BL}_{\mathrm{bought}}^{t}} \tag{4.4.49}$$

$$NIT_{\mathrm{EV}_{\mathrm{buy}}^{t}} = NIT_{\mathrm{EV}_{\mathrm{bought}}^{t}} \tag{4.4.50}$$

$$NIT_{\mathrm{SELL}^{t}} = NIT_{\mathrm{sold}}^{t} \tag{4.4.51}$$

$$PIT_{\mathrm{BL}_{\mathrm{buy}}^{\phi,t}} = PIT_{\mathrm{BL}_{\mathrm{bought}}^{\phi,t}} \tag{4.4.52}$$

$$PIT_{\mathrm{EV}_{\mathrm{buy}}^{\phi,t}} = PIT_{\mathrm{EV}_{\mathrm{bought}}^{\phi,t}} \tag{4.4.53}$$

$$PIT_{\mathrm{SELL}^{\phi,t}} = PIT_{\mathrm{sold}}^{\phi,t} \tag{4.4.54}$$

These constraints on the number of ITs purchased and sold force the house to recalculate its optimal energy usage given the completed trades. For instance, the constraint on $NIT_{\mathrm{SELL}^{t}}$ in (4.4.51) impacts the amount of solar generation, V2G and

battery discharging that the house will do in the next timestep to avoid generating NITs that weren't actually sold.

The number of ITs purchased by houses can also introduce a limit on the baseload and EV charging power consumption in the next timestep, however depending on the number of ITs sold, the house may be able to reallocate usage of any generated solar power or battery discharging to compensate. The actual baseload and EV power that can be used in the subsequent timestep following the P2P auction are dependent on the quantity of NITs and PITs purchased. If an insufficient quantity of one type of Impact Token has been purchased, then that will constrain the use of the load, regardless of the quantity of the other token that the house has available:

$$P_{\mathrm{BL}}{}^{t} = P\mathrm{solar}_{\mathrm{BL}}^{t} + P\mathrm{batDis}_{\mathrm{BL}}^{t} + \min\left\{\frac{1}{NIV^{+}}\left(NIT_{\mathrm{BL}_{\mathrm{buy}}}^{t} + NIT_{\mathrm{alloc}_{\mathrm{BL}}}^{t}\right),\ \frac{1}{PIV^{+}}\left(PIT_{\mathrm{BL}_{\mathrm{buy}}}^{\phi,t} + PIT_{\mathrm{alloc}_{\mathrm{BL}}}^{\phi,t}\right)\right\} \tag{4.4.55}$$

$$P_{\mathrm{EVCh}}{}^{t} = P\mathrm{solar}_{\mathrm{EV}}^{t} + P\mathrm{batDis}_{\mathrm{EV}}^{t} + \min\left\{\frac{1}{NIV^{+}}\left(NIT_{\mathrm{EV}_{\mathrm{buy}}}^{t} + NIT_{\mathrm{alloc}_{\mathrm{EV}}}^{t}\right),\ \frac{1}{PIV^{+}}\left(PIT_{\mathrm{EV}_{\mathrm{buy}}}^{\phi,t} + PIT_{\mathrm{alloc}_{\mathrm{EV}}}^{\phi,t}\right)\right\} \tag{4.4.56}$$

Otherwise, all constraints and equations remain as described in Section 4.4.1, and the optimisation problem is solved as before. The results of this optimisation problem calculate the optimal usage of the house's energy resources in the following timestep based on the outcome of the P2P trading markets and provide the house with an actual energy resource usage strategy that avoids the violation of any network limits.

4.4.8 Seller-Led Market

The inclusion of another P2P market can improve the utilisation of the network and increase the satisfaction of houses in terms of meeting their energy requirements. If houses still have unused NITs or PITs remaining following the baseload and EV P2P auctions, then there is additional network capacity that is not being fully utilised.

Therefore, efficient usage of the network is encouraged and seller income maximised through this final opportunity for sellers to sell any unused ITs. Following the determination of the final energy resource usage in the previous stage, if each house has any NITs or PITs that will be unused in the next timestep, they can submit these as an ask to this seller-led market. It is assumed that the sellers will be willing to accept a lower price for their ITs to increase the likelihood they are sold in order to maximise their income. As with the previous markets, only NITs and PITs for the next timestep t are traded.

Unlike the previous auctions, the buyers do not submit bids for the Impact Tokens. Instead, the cost minimisation problem described in Section 4.4.7 is implemented by each house to analyse the submitted asks, in order to determine if any should be accepted. Rather than operating through the auction approach, each house will individually consider all submitted asks, and if choosing to accept any, the trade price is the price submitted by the seller in the ask, which is typically lower than the trade price paid in the previous P2P auctions. The number of NITs and PITs purchased are updated as follows:

$$NIT_{\mathrm{BL}^t_{\mathrm{buy}}} = NIT_{\mathrm{BL}^t_{\mathrm{bought}}} + \sum_{k=1}^{K} NIT_{\mathrm{BL}^t_{\mathrm{accept,SM},k}} \tag{4.4.57}$$

$$NIT_{\mathrm{EV}^t_{\mathrm{buy}}} = NIT_{\mathrm{EV}^t_{\mathrm{bought}}} + \sum_{k=1}^{K} NIT_{\mathrm{EV}^t_{\mathrm{accept,SM},k}} \tag{4.4.58}$$

$$PIT_{\mathrm{BL}^{\phi,t}_{\mathrm{buy}}} = PIT_{\mathrm{BL}^{\phi,t}_{\mathrm{bought}}} + \sum_{k=1}^{K} PIT_{\mathrm{BL}^{\phi,t}_{\mathrm{accept,SM},k}} \tag{4.4.59}$$

$$PIT_{\mathrm{EV}^{\phi,t}_{\mathrm{buy}}} = PIT_{\mathrm{EV}^{\phi,t}_{\mathrm{bought}}} + \sum_{k=1}^{K} PIT_{\mathrm{EV}^{\phi,t}_{\mathrm{accept,SM},k}} \tag{4.4.60}$$

where $NIT_{\mathrm{BL}^t_{\mathrm{bought}}}$ is the number of baseload NITs that have been purchased in the previous auctions, and $NIT_{\mathrm{BL}^t_{\mathrm{accept,SM},k}}$ is an optimisation variable corresponding to the number of baseload NITs that the house is accepting from the ask submitted by house k in this seller-led market. The same nomenclature applies to the EV NITs

and both baseload and EV PITs. The value of $NIT_{\text{BL}^t_{\text{accept,SM},k}}$ is constrained as:

$$0 \leq NIT_{\text{BL}^t_{\text{accept,SM},k}} \leq NIT_{\text{BL}^t_{\text{SM},k}} \tag{4.4.61}$$

where $NIT_{\text{BL}^t_{\text{SM},k}}$ is the number of baseload NITs that house k has remaining for sale in the seller-led market.

The updated cost to the buyer of purchasing any NITs or PITs offered by the sellers in this market at the current timestep is:

$$\Pi\text{NIT}_{\text{BL}^t_{\text{updated}}} = \Pi\text{NIT}_{\text{BL}^t_{\text{traded}}} + \sum_{k=1}^{K} NIT_{\text{BL}^t_{\text{accept,SM},k}} \times \pi\text{NIT}_{\text{BL}_{\text{SM},k}} \tag{4.4.62}$$

$$\Pi\text{NIT}_{\text{EV}^t_{\text{updated}}} = \Pi\text{NIT}_{\text{EV}^t_{\text{traded}}} + \sum_{k=1}^{K} NIT_{\text{EV}^t_{\text{accept,SM},k}} \times \pi\text{NIT}_{\text{EV}_{\text{SM},k}} \tag{4.4.63}$$

$$\Pi\text{PIT}_{\text{BL}^t_{\text{updated}}} = \Pi\text{PIT}_{\text{BL}^t_{\text{traded}}} + \sum_{k=1}^{K} PIT_{\text{BL}^{\phi,t}_{\text{accept,SM},k}} \times \pi\text{PIT}_{\text{BL}_{\text{SM},k}} \tag{4.4.64}$$

$$\Pi\text{PIT}_{\text{EV}^t_{\text{updated}}} = \Pi\text{PIT}_{\text{EV}^t_{\text{traded}}} + \sum_{k=1}^{K} PIT_{\text{EV}^{\phi,t}_{\text{accept,SM},k}} \times \pi\text{PIT}_{\text{EV}_{\text{SM},k}} \tag{4.4.65}$$

where $\Pi\text{NIT}_{\text{BL}^t_{\text{updated}}}$ is the updated cost to a house of purchasing baseload NITs for timestep t, $\Pi\text{NIT}_{\text{BL}^t_{\text{traded}}}$ is the cost of any baseload NITs that have already been purchased on previous auctions and $\pi\text{NIT}_{\text{BL}_{\text{SM},k}}$ is the ask price per NIT if purchasing from house k on the seller-led market. The total updated cost to the buying house based on their transactions for purchasing NITs and PITs for timestep t is then given as:

$$\Pi^t_{\text{updated}} = \Pi\text{NIT}_{\text{BL}^t_{\text{updated}}} + \Pi\text{NIT}_{\text{EV}^t_{\text{updated}}} + \Pi\text{PIT}_{\text{BL}^t_{\text{updated}}} + \Pi\text{PIT}_{\text{EV}^t_{\text{updated}}} \tag{4.4.66}$$

By incorporating this updated cost of purchasing NITs and PITs on the seller-led market at the current timestep into the house's total daily expected cost of energy and Impact Tokens means that by minimising this value in the optimisation problem, the house will determine whether it can further decrease its total cost through the acceptance of any NIT or PIT asks on this seller-led market. Purchasing additional NITs or PITs in this seller-led market at the current timestep could also cause a change in cost at future timesteps too, as energy resource usage may change. For

instance, purchasing ITs to increase EV charging in the current timestep could mean that fewer ITs need to be purchased in future timesteps, reducing the cost.

If the house accepts any of the asks made by house k for either category of PIT or NIT, e.g. $NIT_{\mathrm{BL}_{\mathrm{accept,SM},k}} > 0$, then a trade is agreed between the buying house and house k for the Impact Tokens, and the Transaction Log is then updated to reflect this trade. Also, the quantity of Impact Tokens that house k has remaining for sale in the seller market must be decreased by the quantity traded, to avoid other houses trying to purchase tokens that have already been sold.

4.4.9 Buyer-Led Market

The final stage of the P2P trading at each timestep is the buyer-led market. This allows buyers who have not acquired sufficient NITs or PITs for their baseload or required EV charging during the previous markets to attempt to secure the necessary ITs to facilitate these loads. The approach to the buyer-led market mirrors that of the seller-led market described above, however instead of the buying house analysing the asks made by the seller, potential sellers analyse the bids submitted by the houses requiring NITs or PITs, with the seller receiving the bid price for any Impact Tokens sold. As this market is the final opportunity for buyers to acquire NITs, it is assumed that they will be willing to offer a higher price to increase the chance of winning the NITs. Therefore, once all bids have been submitted, each house will analyse the bids to determine whether by changing their planned energy resource usage in order to free up sufficient NITs or PITs to trade with the buyer, it can result in a lower total cost.

Determination of Bids in Buyer-Led Market

If a house has not purchased sufficient ITs in the baseload or seller-led markets to accommodate their required baseload, they will submit bids to this market for the number of NITs or PITs they still require. If the house has an EV, it will

assess its current planned EV charging schedule. Based on the number of timeslots that the EV will be at home for charging between the current time and the EV's next departure time, the maximum amount of energy that the EV can recharge is calculated. If the EV requires more than 70% of this maximum available energy to reach its SoC goal, the EV will bid for sufficient NITs or PITs to charge at full power in the next timeslot, provided the EV is at home. This aims to ensure that the EV is able to meet its SoC goal at departure. Depending on a house's preference between charging cost and guaranteeing sufficient EV charge, different values for the percentage of maximum charging before bids are submitted to the buyer-led market can be chosen. Choosing a lower percentage will prioritise earlier charging of the EV, but at increased cost due to the higher bid prices in this market, whereas choosing a higher percentage can reduce the cost to the house, but increases the risk that the EV will not meet its SoC goal.

Evaluation of Bids

Once bids have been submitted, houses will analyse the bids to determine whether any should be accepted in order to further reduce their total cost of energy and Impact Tokens. With the increased income for selling NITs or PITs through the buyer-led market, a house can decide to alter the amount of EV or battery charging planned, as well as changing its planned usage of allocated Impact Tokens and generated solar energy.

The house can update the number of NITs and PITs that it sells by adding an additional term to the optimisation problem which represents the number of ITs from the bids that the house chooses to accept.

$$NIT_{\text{SELL}}{}^{t} = NIT^{t}_{\text{sold}} + \sum_{k=1}^{K} \left(NIT_{\text{BL}}{}^{t}_{\text{accept,BM},k} + NIT_{\text{EV}}{}^{t}_{\text{accept,BM},k} \right) \tag{4.4.67}$$

$$PIT_{\text{SELL}}{}^{\phi,t} = PIT^{\phi,t}_{\text{sold}} + \sum_{k=1}^{K} \left(PIT_{\text{BL}}{}^{\phi,t}_{\text{accept,BM},k} + PIT_{\text{EV}}{}^{\phi,t}_{\text{accept,BM},k} \right) \tag{4.4.68}$$

where NIT^{t}_{sold} is the number of NITs already sold by the house in previous markets

for this timestep, $NIT_{\text{BL}}{}^{t}_{\text{accept,BM},k}$ is the number of NITs that the house will agree to sell to house k based on its submitted bid to the buyer-led market for baseload NITs, $NIT_{\text{EV}}{}^{t}_{\text{accept,BM},k}$ is the number of NITs from house k's bid for EV NITs that the house will agree to sell. As NIT_{SELL} and PIT_{SELL} are constrained in the optimisation problem against the use of the house's energy resources through (4.4.5) and (4.4.6), accepting any bids in this buyer-led market will reconfigure the house's planned energy resource usage in order to free up sufficient NITs or PITs to meet the accepted bids.

The total income that the house receives from selling NITs and PITs in the current timestep is given by (4.4.69) and (4.4.70), respectively:

$$\begin{aligned}\Pi\text{NIT}_{\text{SELL}}{}^{t}_{\text{updated}} = \Pi\text{NIT}^{t}_{\text{traded}} + \sum_{k=1}^{K}\Big(&\Big(NIT_{\text{BL}}{}^{t}_{\text{accept,BM},k} \times \pi\text{NIT}_{\text{BL}_{\text{BM},k}}\Big) \\ &+ \Big(NIT_{\text{EV}}{}^{t}_{\text{accept,BM},k} \times \pi\text{NIT}_{\text{EV}_{\text{BM},k}}\Big)\Big)\end{aligned} \tag{4.4.69}$$

$$\begin{aligned}\Pi\text{PIT}_{\text{SELL}}{}^{t}_{\text{updated}} = \Pi\text{PIT}^{t}_{\text{traded}} + \sum_{k=1}^{K}\Big(&\Big(PIT_{\text{BL}}{}^{\phi,t}_{\text{accept,BM},k} \times \pi\text{PIT}_{\text{BL}_{\text{BM},k}}\Big) \\ &+ \Big(PIT_{\text{EV}}{}^{\phi,t}_{\text{accept,BM},k} \times \pi\text{PIT}_{\text{EV}_{\text{BM},k}}\Big)\Big)\end{aligned} \tag{4.4.70}$$

where $\Pi\text{NIT}^{t}_{\text{traded}}$ is the income from any NITs traded on the previous P2P markets in the current timestep, $NIT_{\text{BL}}{}^{t}_{\text{accept,BM},k}$ is the number of baseload NITs accepted from house k's bid, $NIT_{\text{EV}}{}^{t}_{\text{accept,BM},k}$ is the number of EV NITs accepted from house k's bid, which together equal the number of NITs that the house will sell to house k, and $\pi\text{NIT}_{\text{BL}_{\text{BM},k}}$ and $\pi\text{NIT}_{\text{EV}_{\text{BM},k}}$ are the bid prices that house k is offering for the baseload and EV NITs, respectively.

As the house does not have to accept the entire quantity of PITs or NITs in a bid, any ITs that the house does agree to sell towards the bid must be subtracted from the bid's requested tokens in the list of bids so that other houses do not attempt to sell the same ITs.

With all P2P trading finalised, the timestep concludes with all houses re-solving the resource allocation problem to determine their actual usage of all energy resources in the next timestep.

4.4.10 Summary

The previous sections have described the entire process of the P2P trading system for a single timestep, with all houses planning their energy resource usage for subsequent timesteps and taking part in multiple P2P trading markets. All the steps described here are repeated at each timestep.

To begin, the house forms an initial plan of its resource usage for all subsequent timesteps and determines the number of baseload and EV NITs and PITs that must be purchased, and the number of NITs/PITs to be sold. A P2P auction for the trading of baseload ITs is then run using the bids and asks determined in the planning stage. As it is essential for all houses to be able to use their planned baseload, following the baseload IT auction, the market operator may step in to help ensure that houses achieve their baseload NIT/PIT requirement. A second P2P auction can then be run to enable houses to purchase ITs for the charging of their EV. If sellers still have NITs or PITs remaining following these two P2P auctions, they have the opportunity to sell these during the seller-led market to help them maximise their income. Potential buyers will analyse the submitted bids to determine whether purchasing additional ITs at a lower cost during the current timestep will reduce their total daily cost. Finally, any buyers who are in desperate need for ITs for either baseload consumption or EV charging can incentivise sellers to change their planned resource usage to sell additional ITs through the buyer-led market by offering higher bid prices. Each timestep concludes with the houses solving the energy resource allocation problem again to determine their actual usage of their energy resources in the next timestep based on the NITs and PITs traded.

4.5 Results and Discussion

This next section presents results and analysis of the Network and Phase Impact Token P2P trading system.

4.5.1 Analysis of Network Limits

One of the key contributions of the Network and Phase Impact Token approach is its ability to manage the generation and consumption of power in the network to ensure that the node voltages at each house, line currents in each phase of the main feeder and transformer power loading do not exceed their permitted limits.

To test this, three scenarios have been analysed, each consisting of a randomly allocated set of baseload profiles, EV charging requirements and DG profiles. Scenarios 1 and 3 use Summer baseload and DG data, while scenario 2 uses Winter data. All three scenarios analyse the load on the network over a 24 hour period and are shown in Figures 4.5 - 4.7.

In each figure, the top subplot displays the apparent power through the transformer as a total of all three phases, the middle subplot displays the line current in each phase of the line connecting the transformer with the rest of the network and the bottom subplot displays the voltage of each phase at the node which records the lowest voltage of that phase in the network. The solid black lines represent the limit of each signal based on the values provided in Table 4.1, including the 5% safety margin.

It can be seen that in all three scenarios, the P2P trading of NITs and PITs is extremely successful at managing the load on the network, resulting in transformer loading, line currents and node voltages being kept within their permitted limits. Although there are some excursions above the limits of transformer loading and phase currents during certain timesteps, these violations are incredibly minor, typically within $< 3\%$ of the limit and are of short duration. In addition, because the imposed limits include the 5% safety margin, the transformer power and line currents are always kept within the actual network limit. These minor violations occur for two reasons:

1. There is a small loss in accuracy from the generation of the voltage and current sensitivity matrices which are used in the computation of the NITs and PITs

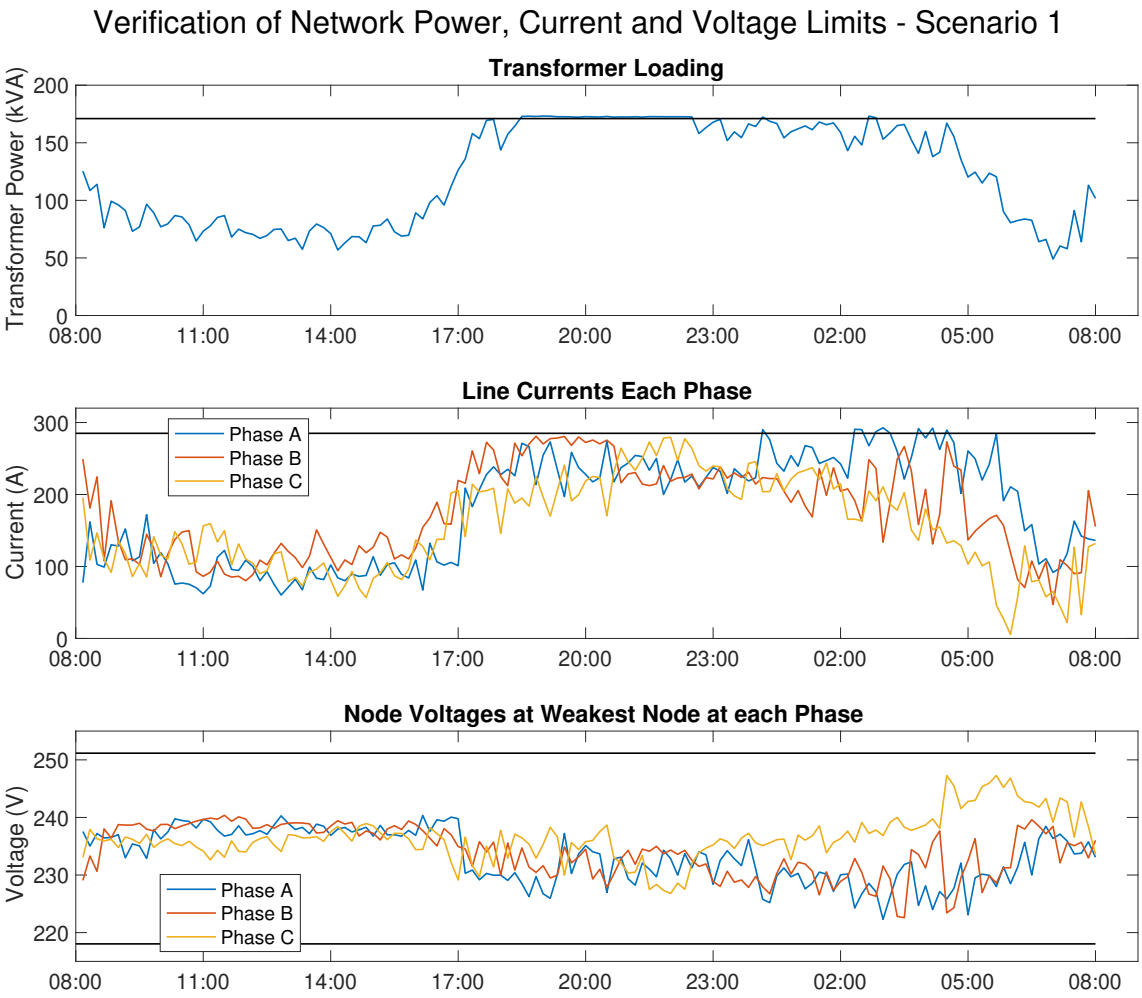

Figure 4.5: Transformer loading, line currents and node voltages from scenario 1 showing that the proposed P2P trading approach ensures that each is kept within its permitted limits

compared with the actual power flow calculation. Additionally, the sensitivity matrices and Impact Values are treated as static, when in reality they may be influenced by the real-time load on the network and exhibit dynamic behaviour

2. The P2P trading treats every load and generation as having a unity power factor. While this is accurate for EV charging and the injection of solar power or battery discharging, the baseload typically has a lagging power factor of 0.95. The inclusion of this into the power flow impacts on the results, but is not taken into account during the P2P trading

However, overall the performance of the proposed approach is excellent when evalu-

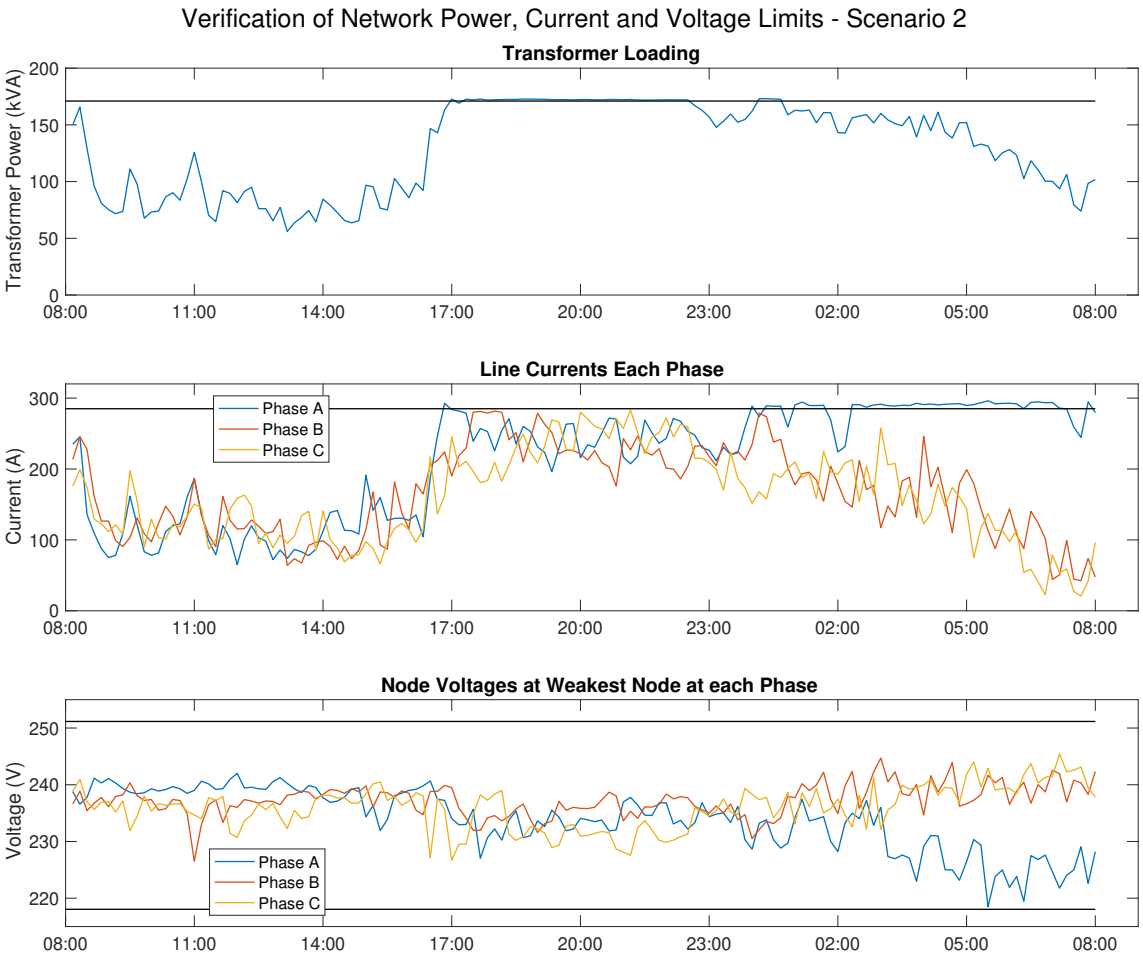

Figure 4.6: Transformer loading, line currents and node voltages from scenario 2

ating the objective of ensuring the network operates within its permitted limits.

4.5.2 Comparison with Uncontrolled Loads and Generation

The necessity of having a system to manage the load on the network is highlighted in this section. Using the data from scenario 3 above, the network power, current and voltage resulting from the P2P trading analysis is compared with a scenario where the loads and generation are uncontrolled. Identical baseload, EV and DG data is used for both the P2P scenario and uncontrolled scenario.

In the uncontrolled scenario, EV charging takes place at full power whenever an EV is at home and the EV's SoC is below its SoC goal. In addition, any solar power

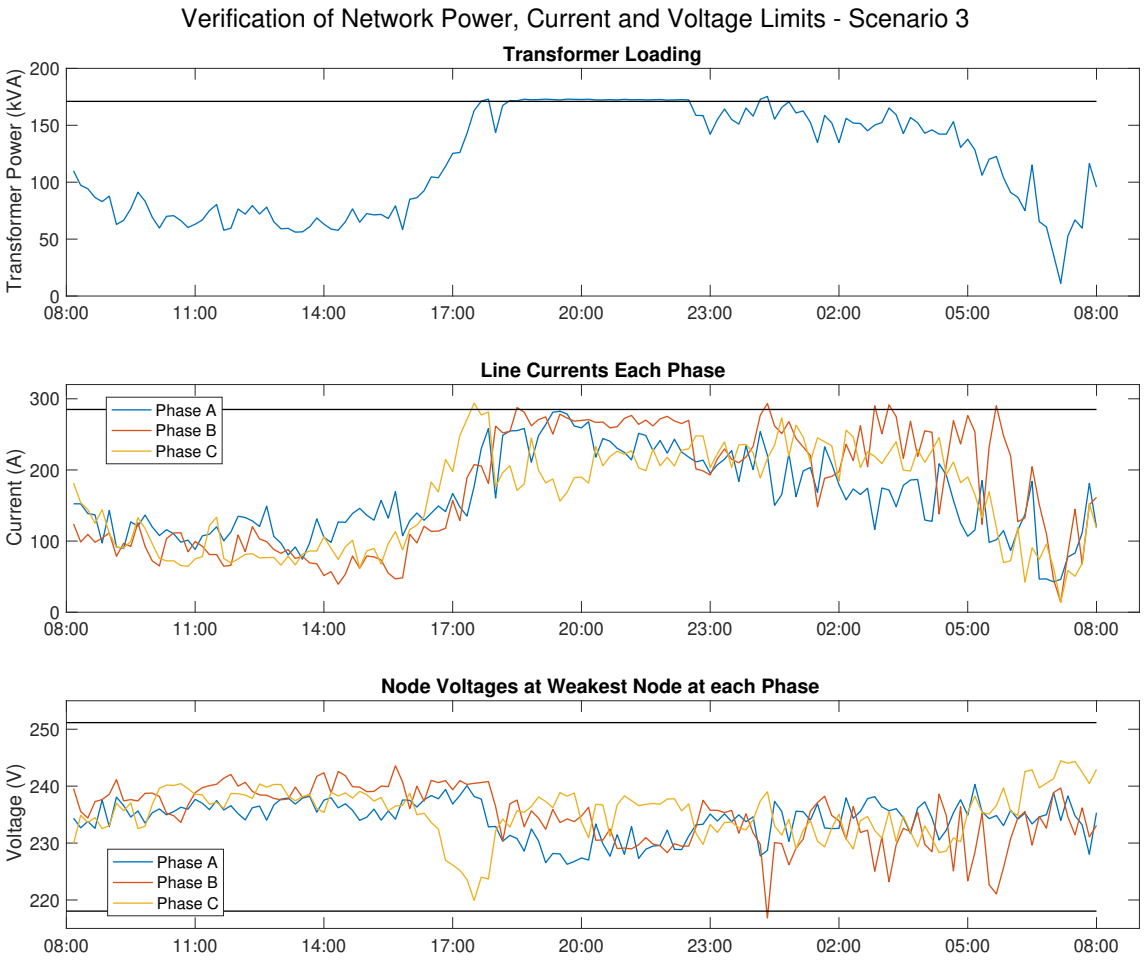

Figure 4.7: Transformer loading, line currents and node voltages from scenario 3

generated is initially used to meet the house's baseload or EV charging demand, any additional generation is stored in the house's battery if there is sufficient capacity, and the remainder is injected into the network. If the house's load is greater than its solar generation, then the battery will discharge at its maximum rate in order to meet this load.

It can be seen in Figure 4.8 that uncontrolled operation of loads and generation can cause significant violations of transformer, line current and node voltage limits. At peak load, the transformer loading exceeds its limit with the safety margin by 138%, the current in phase B is 179% above its limit and the voltage in phase B drops below its lower limit. Even when the absolute limit is considered, the transformer loading and the line current are well above their permitted limit, which would cause significant issues for the network operation and hardware. It can be seen that the

Figure 4.8: A comparison of the transformer loading, line currents and node voltages between the P2P trading of Impact Tokens and uncontrolled loads and generation, showing the importance of managing load in a network

P2P trading of NITs and PITs ensures that the network operation remains within these allowed limits. However, it should be noted that in the uncontrolled scenario, all EVs achieve their SoC goal, whereas in the P2P trading scenario, there are two EVs that depart with a SoC lower than their departure goal.

4.5.3 Load and Generation Profiles

Two scenarios are considered here, with scenario 1 using Summer baseload and PV data, and scenario 2 using Winter data, shown in the top and bottom subplots

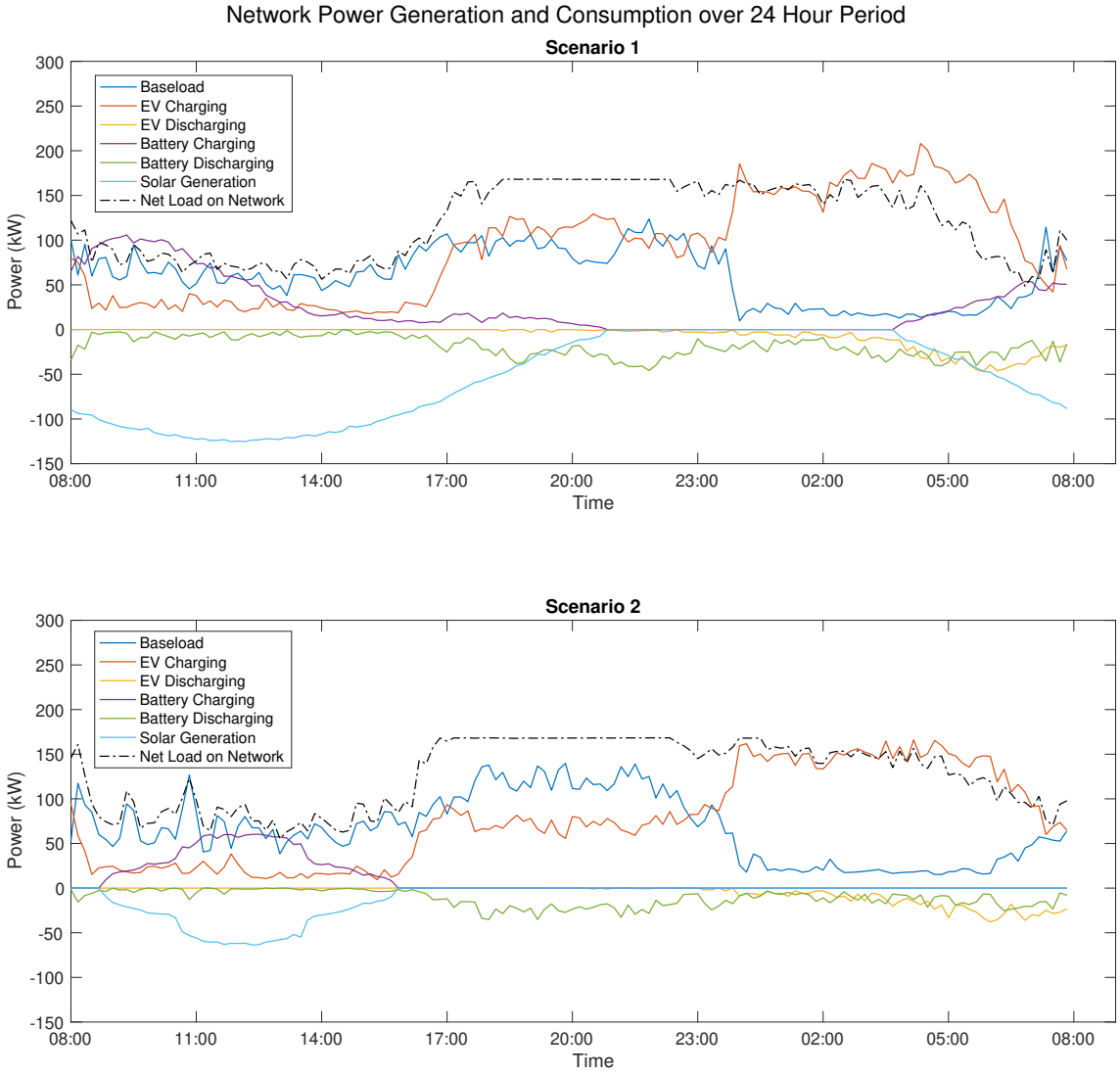

Figure 4.9: Total power generation and consumption in the network for Summer and Winter scenarios

of Figure 4.9, respectively. The total aggregate loads and generations across all houses are shown, including the baseload, EV charging, solar generation, battery charging/discharging and EV discharging. In addition, the net load on the network is shown by the black dotted line.

It can be seen in scenario 1 that the P2P trading has resulted in load flattening throughout the 24 hour period, by shifting the majority of EV charging to off-peak times during the middle of the night. In addition, the use of battery discharging and some V2G has performed peak shaving by reducing the net load on the network to below the EV charging load, enabling greater EV charging to take place than could

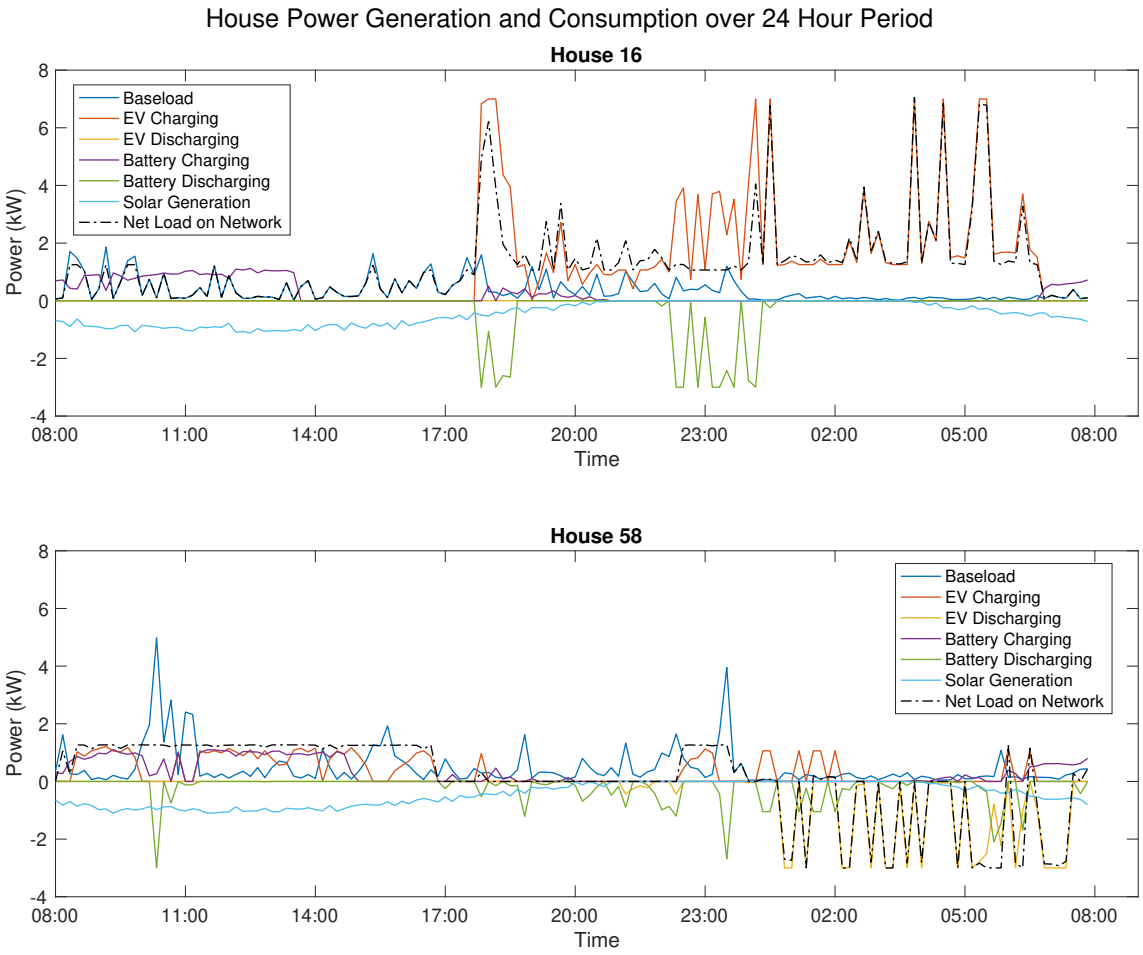

Figure 4.10: Power generation and consumption for two individual houses showing the different load profiles achieved through the P2P trading of Impact Tokens

otherwise be accommodated by the network. It can be seen that the network is at its capacity from 5:30pm, and once baseload usage decreases from 11pm, the amount of EV charging increases, with the network still operating at maximum capacity. Scenario 2 is similar, however the reduced solar energy means that not as much EV charging can take place, and fewer EVs meet their desired SoC goal at departure.

Figure 4.10 shows the individual load and generation profiles of two houses from scenario 1, with both houses equipped with an EV and solar PV panels. House 16 chooses to store its generated solar energy in its battery during the early part of the day to allow it to discharge later in the evening and early night to facilitate additional EV charging to take place during these peak times. The EV at House 58 does not make a journey during the day, and has a SoC above its departure goal,

allowing it to discharge in order to generate additional income through the sale of NITs, PITs and energy while still meeting its departure SoC.

4.5.4 Economic Analysis

This section considers the economic analysis of the cost and income to houses partaking in the P2P trading based on the three scenarios presented in Section 4.5.1. Each house is represented by a bar on the x-axis, with a positive bar denoting a net cost to the house for the NITs, PITs and energy purchased and sold during the 24 hour period, and a negative value denoting a net income (profit). Additionally, the bars have been colour coded to represent whether the house is equipped with both an EV and solar panels or just an EV or just solar, or neither, allowing any trends in the results to be interpreted based the house's available energy resources.

The cost of energy is £0.30/kWh, bid prices for Impact Tokens are randomly distributed between £0.01 and £0.02/IT and ask prices are randomly distributed between £0.005 and £0.01/IT.

With the IT trade price less than the energy price, the additional cost of purchasing ITs is negligible in comparison to the total cost of the house's energy. Figure 4.11 shows that the majority of houses have a net cost from their energy usage, however the P2P trading of ITs has enabled houses to reduce their total cost, and in some instances even make a profit. The houses with the highest daily cost are those equipped with EVs, who must pay higher costs for the increased energy and Impact Tokens required for their charging. Interestingly, some of the houses which have the highest daily cost are equipped with both DG and an EV, suggesting that the higher costs of EV charging could not be offset by revenue from selling solar energy and generated Impact Tokens. In these scenarios the participants are charged a transaction fee of £0.001/IT purchased or sold on the P2P market. The market operator subsequently receives a profit of £24.60 from scenario 1, and a profit of £22.90 from scenario 2, offering plenty of incentive to implement and host the P2P

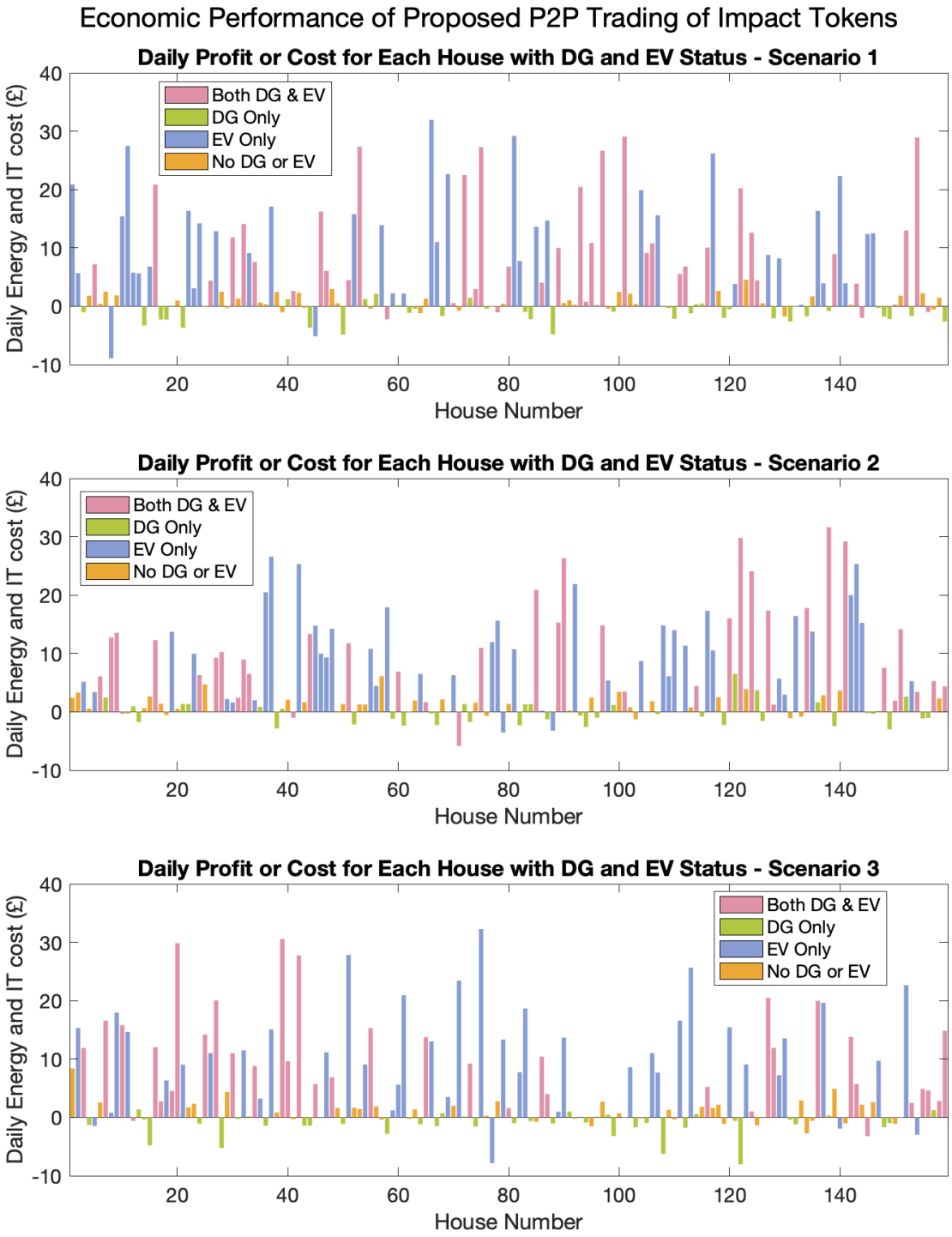

Figure 4.11: Total daily cost or income of each houses through P2P trading, with houses categorised by types of DERs

Table 4.3: EV Charging Success, With and Without Buyer- and Seller-led Markets

	Without Buyer and Seller Markets	With Buyer and Seller Market
Baseload Success	100%	100%
EV SoC Goal Success	86%	92%

trading platform.

4.5.5 Analysis of Seller-led and Buyer-led Markets

Analysing the seller-led and buyer-led markets can give a good insight into the usage of the network and the performance of the P2P trading approach.

Firstly, the percentage of EVs achieving their SoC goal by departure is compared for the P2P trading approach both with and without the use of the buyer- and seller-led markets to analyse whether these two markets are important for the performance of the proposed approach. Ten repeats were run, both with and without the buyer- and seller-led markets and the percentage of houses that were able to use their planned baseload and the percentage of EVs that depart with their desired SoC goal are calculated for all repeats, with results displayed in Table 4.3.

It can be seen that all houses are able to acquire the number of ITs they need for their planned baseload usage both with and without the buyer- and seller-led markets, however the number of EVs that depart with their desired SoC goal is increased through the inclusion of the two markets. This is because the houses have further opportunities to purchase additional ITs to allow greater EV load on the network, however even without these two markets there is still good EV charging performance.

As any unused NITs or PITs are offered by houses on the seller-led market, the comparative number of Impact Tokens traded to Impact Tokens offered for sale on the seller-led auction shows the utilisation of the network at each timestep. Similarly,

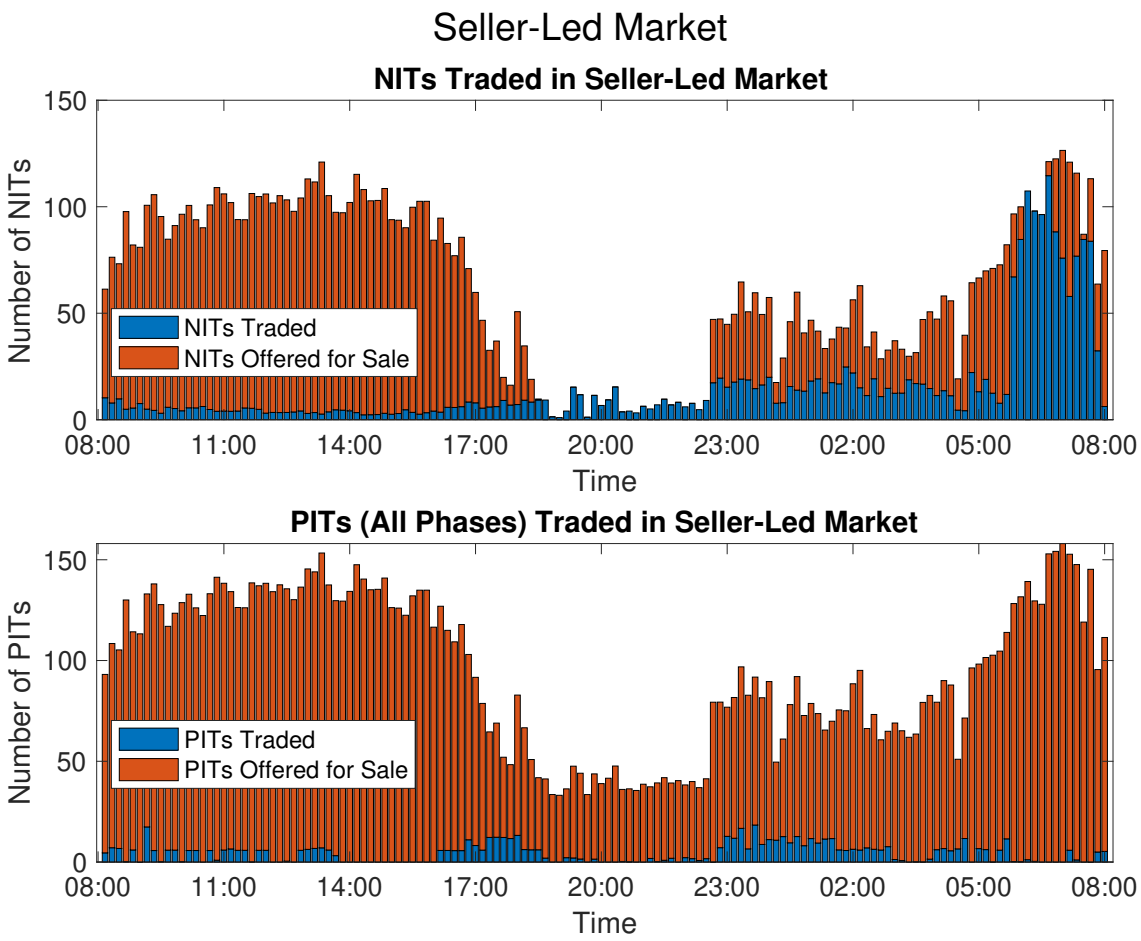

Figure 4.12: Stacked bar chart showing the number of NITs and PITs offered for sale on seller-led market and number of ITs traded at each timestep

looking at the number of Impact Tokens bid for on the buyer-led market provides insight into times of peak demand on the network, as these houses were prepared to pay more to purchase the ITs.

Figure 4.12 shows for each timestep the total number of NITs and PITs that have been offered for sale by houses on the seller-led market and the number of those tokens that are purchased by selling houses. The height of the orange bar shows the total number of Impact Tokens that are for sale, while the height of the blue bar shows the proportion which were purchased. For the PITs, the bars include the total number of PITs for all three phases. It can be seen by the height of the bars that there is significant under-utilisation of the network between 8am and 5pm, with high numbers of unused Network and Phase Impact Tokens available

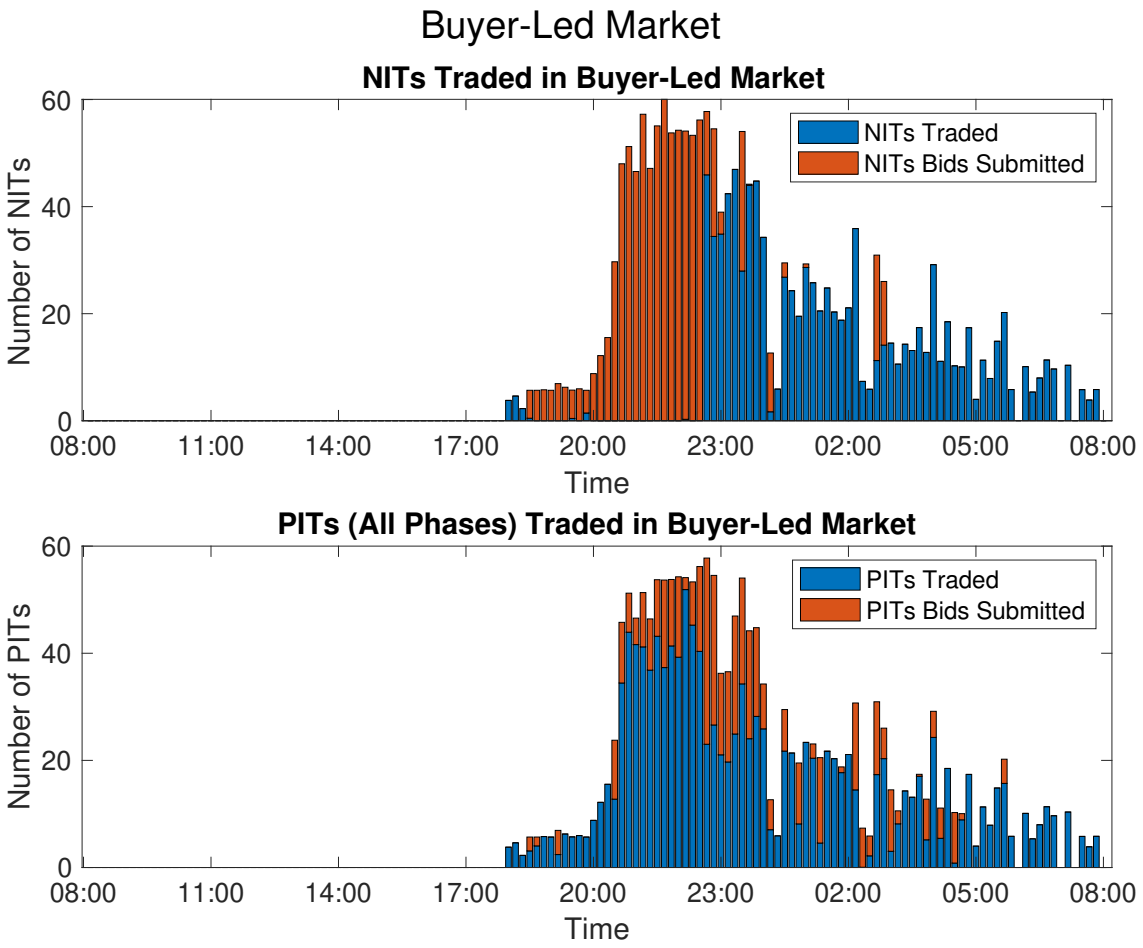

Figure 4.13: Stacked bar chart showing the number of NITs and PITs requested on buyer-led market and number of ITs traded at each timestep

in the network which could be utilised to accommodate greater loads during these times. The network is operating close to maximum capacity from 6pm to 11pm, with fewer NITs offered for sale during these hours, and the majority of the listed NITs purchased by houses to permit EV charging, and heavy usage continues until about 5am. There are significantly fewer PITs traded on the seller-led market, even during the times of high demand on the network, which shows that the overall network limit on transformer loading is the primary constraint on the network use. Despite the cheaper prices offered on the seller market, it is seen that it is hard to encourage houses to change their energy usage to add loads to the network during off-peak times, and additional incentives may be required in order to maximise the network usage.

Figure 4.13 provides the same results for the buyer-led market. Houses only enter the buyer-led market if they were not able to purchase sufficient ITs for their baseload usage on previous auctions or if their EV charging requires $> 70\%$ of the maximum charging that can be completed before its departure. As Table 4.3 shows that the buyer and seller markets are not required for acquiring sufficient ITs to permit the house's baseload, the buyer-led market activity is primarily houses purchasing NITs or PITs for EV charging, and therefore the majority of activity takes place in the evening and overnight, when most EVs are attempting to charge. Demand on the network increases between 6pm and 9pm, with increasing numbers of bids submitted for NITs and PITs. Interestingly, although there is little demand for PITs and NITs in the seller-led market, there is much higher demand in the buyer-led market. This means that houses could save money by purchasing additional PITs in the seller-led market at lower prices, so future research could also look into adapting the P2P trading methodology for houses to anticipate whether they will be able to purchase their desired quantity of ITs at times of high demand to increase the number of ITs purchased in the seller-led market rather than the buyer-led market. Also, it can be seen between 5pm and 11pm that very few NITs are traded on the buyer-led market in comparison with the number of PITs traded. Because injecting power to the network would create both PITs and NITs, the selling houses must be providing these PITs from their unused allocation, rather than changing their resource usage.

4.5.6 Successful EV Charging with Varying DG Penetration

While consumers have the opportunity to set their own energy usage schedule to attempt to minimise their daily cost of energy, there is no guarantee that they will be able to purchase sufficient NITs or PITs on the P2P market to achieve this schedule. If many houses all schedule their EV charging for the same time, there will not be sufficient network capacity to accommodate all charging, and some houses will fail

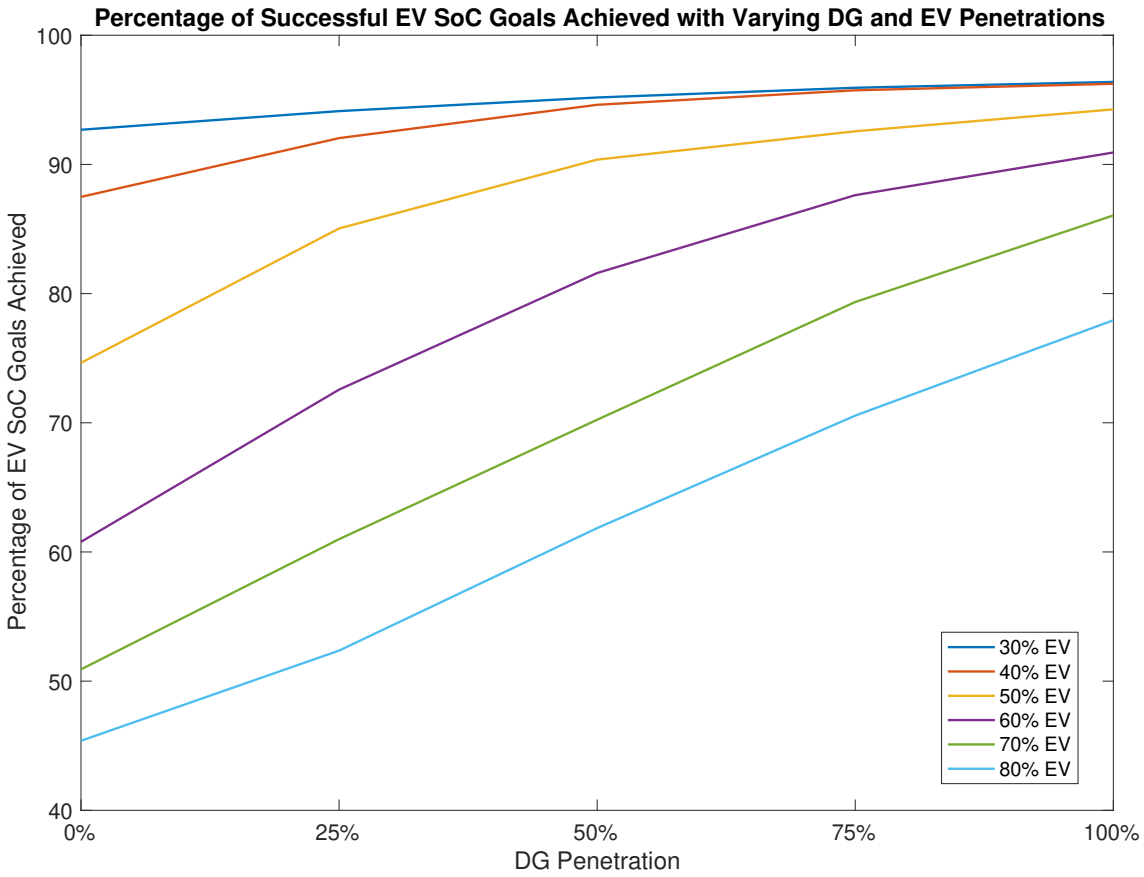

Figure 4.14: Percentage of EVs meeting their desired SoC goal at their departure with varying penetrations of EV and DG

to purchase their required number of Impact Tokens. If this occurs close to the departure time of its EV, then the EV might not be able to charge sufficiently to meet its desired SoC goal at its departure time.

Figure 4.14 shows the percentage of EVs that achieve their desired SoC goal by the EV's departure as the penetration of EVs and DG varies. For each combination of a DG and EV penetration, 25 repeats are run of the 24-hour P2P trading system, with each repeat using a random set of baseload, DG and EV profiles. For each repeat, the number of EV's that achieve their SoC goal at departure is calculated, and then this is averaged across the 25 repeats to obtain the values displayed on the graph.

As would be expected, increasing the penetration of solar DG and battery storage increases the percentage of EVs that achieve their SoC goal at departure. This is because the injection of solar power or energy discharged from battery storage will

generate additional NITs and PITs that increase the amount of EV charging load that can be accommodated through adding greater capacity to the network. At lower penetrations of EVs, the majority of EVs will depart reaching their desired SoC. At a DG penetration of 50%, at least 90% of EVs will reach their desired SoC goal with EV penetrations of up to 50%. This means that out of the 1990 EVs across the 25 repeats, 1790 will achieve their SoC goal. At higher penetrations of EV, the number of EVs departing with their desired SoC reduces significantly, as the network capacity remains the same but the EV charging demand increases. At an EV penetration of 70% and DG penetration of 50%, only 70% of EVs are able to depart at their SoC goal, which is unlikely to be satisfactory to users. At this point, network reinforcement would be required to increase the transformer power rating or maximum permitted line currents in order to accommodate a higher penetration of EVs. However, increasing the penetration of DG can have a significant impact on the number of EVs successfully charged, with over 85% meeting their SoC goal when all houses are equipped with solar PV and battery storage, even with EV penetrations of up to 70%.

Because there is no communication between houses, each house is only responsible for determining its own energy usage without any awareness of the other network users. As a result, although the seller-led market attempts to increase network utilisation, the P2P trading approach does not result in the most optimal use of the network. This means that if there was cooperation between households to increase the network utilisation, the percentage of achieved SoC goals would likely increase, however that would be at the expense of some of the benefits of the P2P trading. However, additional research can focus on how the house determines its most cost optimal energy resource usage to analyse whether there are adjustments that can be made to increase the EV charging success. For instance, scheduling the EV charging too close to departure can result in the EV departing below its target SoC if insufficient Impact Tokens could be purchased, so if EV charging is instead prioritised earlier in the day then this could be avoided.

4.5.7 Comparison with Alternative Approaches

To get a better understanding of the performance of the P2P trading approach with regards to the amount of EV charging that it enables, a comparison with two other approaches is presented in this section.

The first alternative approach is the ESPRIT monitoring and EV charging control strategy, which has also been implemented in the UK's 2013-15 My Electric Avenue project [38][168]. Current and voltage sensors at the head of the network feeder and voltage sensors at each charge point monitor the network's transformer loading, line current and node voltages in real-time. If the network is found to exceed its safety limits, then a controller will determine how many EV chargers must be disconnected in order to return the network to its allowed operating state. If the power, current or voltage later falls below a safety margin, EV chargers can be reconnected. The determination of the chargers to disconnect or reconnect is done based on their charging time, which helps to avoid privacy issues and increases the simplicity of the approach. As the ESPRIT monitoring and control strategy did not originally include the use of distributed generation and battery storage, solar PV and storage has been incorporated using the same method as the Uncontrolled Loads approach detailed in Section 4.5.2 above.

The second approach is a centralised and offline optimisation strategy. This requires full knowledge of all baseload, EV charging requirements and DG generation in advance in order to compute the optimal control strategy for all energy resources across the network with the objective of maximising the number of EVs that meet their SoC goal by departure. As all load information must be shared with the central processor computing the optimal solution, there would be significant privacy issues, and houses lose all control over the use of their loads, as they become controlled by the central operator. However, this approach will calculate the maximum number of EVs that can be accommodated, providing a true comparison for the performance of the P2P trading approach. Full details of this optimisation approach are not included

here, however the use of all energy resources are subject to the same constraints as the P2P trading resource allocation in Section 4.4.1, with the key difference being that the optimisation is solved for all houses and all timesteps, whereas the P2P trading approach only requires each house to have knowledge of its own loads and generation and solve the optimisation problem for that house individually.

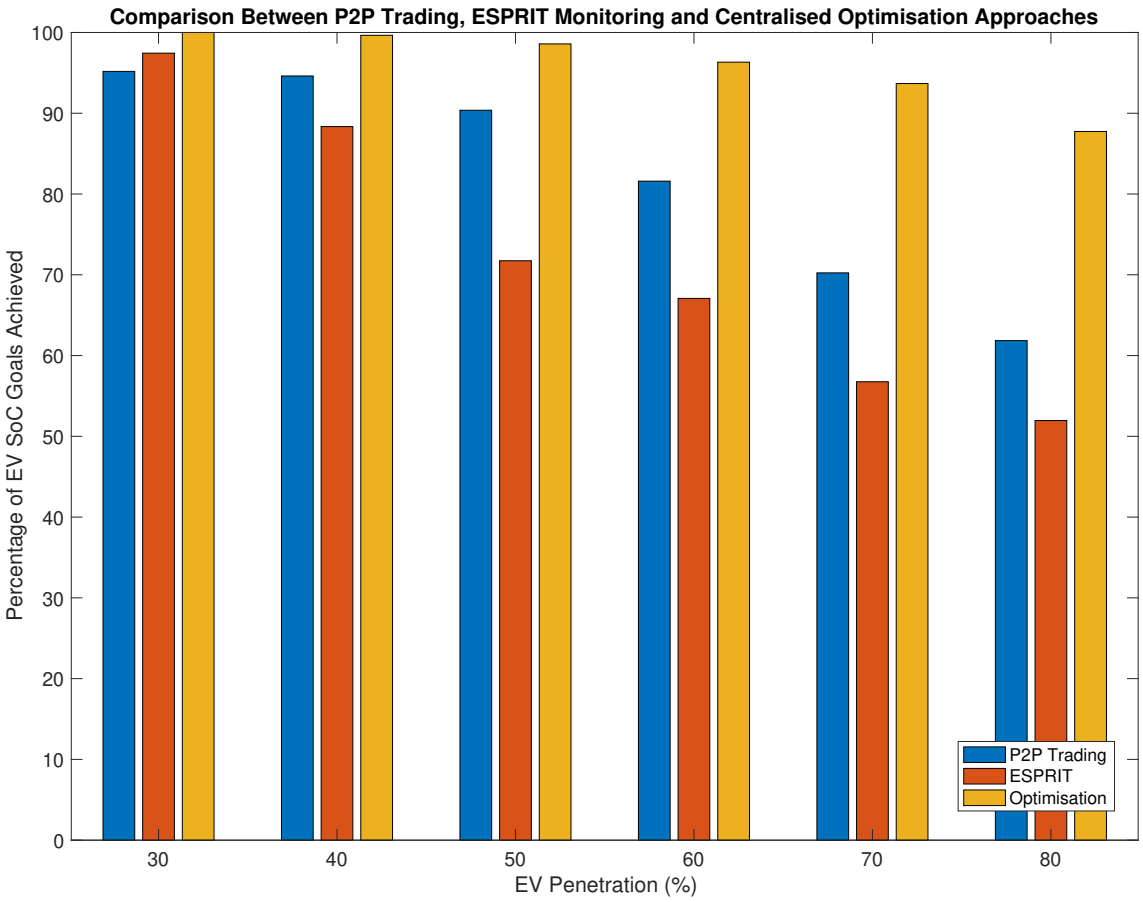

Figure 4.15: Comparison of the percentage of EVs which acheive their departure SoC as the penetration of EVs increases under three different control strategies: P2P trading of Impact Tokens, ESPRIT network monitoring and a centralised optimisation

Figure 4.15 shows the overall success rate for EV penetrations between 30-80% for the three approaches, with the P2P trading of Impact Tokens shown by the blue bar, ESPRIT monitoring shown by the red bar and the centralised optimisation result with the yellow. The EV charging success rate has been determined using the same method as in Section 4.5.6. It can be seen for all EV penetrations except 30% that the proposed P2P trading approach outperforms the ESPRIT monitoring. One

potential reason for this is that ESPRIT only considers the length of time that an EV has been charging for when determining which EVs to disconnect and reconnect, rather than taking into account how much charging each EV requires in order to achieve their SoC goal. Therefore, EVs that require additional charging to achieve their SoC goal may remain disconnected until after their departure time while EVs with later departure times are reconnected first which can result in sub-optimal network usage. As previously explained, the optimisation approach calculates the maximum number of EVs that can achieve their SoC goal, so outperforms the other two approaches for all EV penetrations. At a 50% EV penetration, the proposed P2P trading approach results in 90% of EVs achieving their SoC goal, compared with 98% of EVs under the centralised optimisation control strategy. This is a good level of performance, but shows that there is still room to improve the efficiency of the network usage with the P2P trading, particularly at higher EV penetrations. However, with the disadvantages of the centralised optimisation approach, there will likely always be a tradeoff between the sharing of information, computational complexity, autonomy of energy resource usage and network usage efficiency. To increase the percentage of EVs successfully departing at their desired SoC at higher EV penetrations, upgrades would need to be made to the network infrastructure.

4.6 Conclusion

This Chapter has presented a novel P2P trading approach for managing renewable energy generation and electric vehicle charging integration in distribution networks. Network and Phase Impact Tokens are introduced to represent the capacity of the distribution network, while all loads and sources of generation are equated to a number of Impact Tokens relative to their impact on the network's capacity through Network and Phase Impact Values. A peer-to-peer trading platform is established for the trading of NITs and PITs between houses, corresponding to the use of an equivalent amount of the network's capacity. If a house wishes to add a load to

the network, it must acquire the corresponding number of Impact Tokens to meet the impact of that load on the network's capacity, while if a house injects power into the network, additional Impact Tokens are generated that can be sold to other houses, with the power injection offsetting additional loads. The trading of the Impact Tokens ensures that all loads and generation is managed within the network, and that no power, current or voltage limits are violated.

Separate markets for trading Impact Tokens for baseload usage and EV charging help ensure that every house is able to acquire sufficient tokens to meet their baseload requirement. A seller-led market helps utilise any unused network capacity for more efficient use of the network, while a buyer-led market provides houses who urgently require Impact Tokens the chance to acquire these by incentivising selling houses to alter their energy resource usage.

The results show that the primary objective of managing EV charging and renewable energy generation within the network is successfully accomplished, with the network operating within its allowed limits for transformer power, line currents and node voltages. The P2P trading has successfully shifted EV charging to the off-peak overnight period, filling in the baseload valley, and the use of battery storage enables the discharging of solar energy and battery storage into the grid at times of peak EV charging in order to reduce the overall net load on the network. The P2P trading of NITs and PITs can help houses to reduce their total cost, and in some instances to make a profit. The proposed P2P trading system performs well in terms of the number of EVs that can be accommodated by the network, with a greater percentage of EVs achieving their SoC goal compared to the ESPRIT monitoring approach. However, the centralised offline optimisation approach shows that it is possible for the network to accommodate more EVs, although the P2P trading approach results in very good success compared with the optimisation approach up to EV penetrations of 50%, with over 90% of EVs meeting their desired departure SoC goal. A centralised system loses many of the advantages of the P2P trading regarding data privacy, control of loads and computational complexity, and therefore

is unlikely to be the best approach to managing network usage. The success of EV charging under the P2P trading approach shows it to be an extremely promising method for managing the load in networks.

Additional research could focus on methods to adapt the P2P trading of Impact Tokens to further increase the amount of EV charging that can take place. Also, it is currently assumed that all loads have a unity power factor, so the method could be further improved by incorporating loads with lagging power factors into the calculation of PITs and NITs. Finally, it is assumed that each house can accurately predict their own baseload usage and renewable generation for the 24 hour period, so additional research can focus on the implementation of the system when disparity between estimated loads and real loads occurs.

Overall, the P2P trading of Network and Phase Impact Tokens offers an extremely promising novel approach to the management of loads and generation in a low-voltage network, providing users with greater autonomy over their own power demand and generation while ensuring that the operation of the network is not compromised and avoiding the requirement for real-time monitoring or centralised control.

Chapter 5

Determining the Hosting Capacity of Electric Vehicles

Chapter Summary

Utilising the concept of Network and Phase Impact Tokens introduced in Chapter 4, a novel approach for determining the maximum hosting capacity of electric vehicles in a distribution network is presented. Taking into account EV journey and energy requirements, baseload usage, renewable energy generation, battery storage and the use of V2G, the approach enables DSOs to analyse their networks to determine their readiness for accommodating increasing numbers of EVs. A Monte Carlo approach is implemented to simulate the maximum hosting capacity caused by real-world variations in these parameters. An alternative Optimisation approach is also presented which incorporates the network constraints to verify the accuracy of the results calculated through the NIT approach. Further analysis of a network is conducted, showing how the EV hosting capacity is influenced by the number of houses equipped with solar PV and battery storage, the time of year and upgrades to network infrastructure.

5.1 Introduction

The global pursuit of decarbonisation is placing strict scrutiny on greenhouse gas emissions, and fossil-fuel based electricity generation, transportation and domestic gas heating have been identified as key areas where emissions can be cut. Rising energy costs and technological advancements are driving the uptake of electric vehicles, renewable energy generation and other low-carbon technologies at an ever increasing pace. However, these additional loads and new forms of generation are placing unprecedented demand on power systems, in particular low-voltage distribution networks, where ageing network design and infrastructure must cope with usage way beyond their original design specifications.

It is therefore important for DSOs to have methods available to them for assessing their existing network infrastructure to determine its readiness for accommodating greater numbers of electric vehicles, and any necessary hardware upgrades to further increase the EV hosting capacity. It is important to assess the hosting capacity of EVs in conjunction with other energy resources and technologies, namely distributed generation such as solar PV panels, energy storage, EV smart charging and V2G, as each will impact the amount of EV charging that can take place. The maximum EV penetration, or EV hosting capacity, is defined here as the number of EVs, expressed as a percentage of the number of houses in the network, that are able to recharge fully overnight before their departure the next morning, subject to the EVs' usage and journey requirements, and constraints on the network power, voltage and current and EV charging.

This chapter presents two approaches for determining the maximum penetration of electric vehicles that can be accommodated within a distribution network in conjunction with domestic solar PV panels, battery storage and V2G, without exceeding the network's voltage, current and power constraints. Initially, an Optimisation approach is presented to calculate the maximum EV penetration given the available solar DG, battery storage, baseload and EV charging requirements. This calculates

the maximum EV penetration such that there is no alternative EV charging strategy or usage of the other energy resources that can result in more EVs reaching full charge than has been calculated. A second approach is then presented, utilising the Network Impact Tokens (NITs) and Phase Impact Tokens (PITs) introduced in Chapter 4 in a novel approach to calculating the EV hosting capacity, while also validating the theory behind the Impact Tokens. Referred henceforth as the Network Impact Token (NIT) approach, this method is based on the initial Optimisation approach, so also calculates the absolute maximum EV penetration of the network, but offers advantages over the Optimisation approach, primarily faster computation time, increasing the practicality and usefulness of the method and allowing DSOs to determine the hosting capacity of their networks and analyse new scenarios or network upgrades.

As large variations in real-world EV energy requirements, journey times, renewable energy generation and baseload can have significant impact on the maximum EV penetration that can be accommodated by a network, a Monte Carlo simulation is used to calculate the maximum EV penetration under different values of these parameters. This means that an overall maximum penetration value can be determined for the network that reflects the likely real-world conditions that will occur.

5.2 Optimisation Approach

The maximum penetration of EVs that the network can accommodate based on a given set of load profiles can be calculated through the solving of an optimisation problem. This optimisation problem attempts to create an optimal schedule for the control of each energy resource (EV charging/discharging, battery charging/discharging, solar power consumption) to maximise the number of EVs that will depart the next morning with a full charge. This approach means that the calculated EV hosting capacity is the highest that can be accommodated by the network - there is no alternative EV charge strategy or usage of energy resources

that can result in a greater number of EVs departing fully charged. Therefore, the result of the optimisation problem can be considered an upper bound on a network's EV hosting capacity - because optimal control schedules are calculated for all energy resources, it is very unlikely that their real-world usage will correspond exactly to these optimal schedules, resulting in a lower penetration of EVs accommodated. However, this upper bound on the EV penetration could be useful to DSOs for network analysis, as it provides a consistent metric which can be applied to multiple networks and different load scenarios.

As the maximum EV penetration that a network can accommodate depends the baseload, DG energy production and EV behaviour, a Monte Carlo simulation is used to calculate the distribution of the maximum EV penetration as these parameters vary. At each repeat of the Monte Carlo, the following optimisation problem must be solved to calculate the maximum EV penetration that could be accommodated by the network based on the profiles selected in that repeat.

5.2.1 Optimisation Problem

In this section, the optimisation problem for calculating the maximum EV penetration is presented. Prior to the start of the Monte Carlo simulation and the solving of the optimisation problem, the voltage and current sensitivity matrices must be calculated for the network during the network initialisation phase described in Chapter 4, Section 4.3.1.

Optimisation Objective

The optimisation objective is to maximise the number of EVs that reach a full charge by their departure:

$$\Lambda^{EV}_{\max} = \max_{\chi_{\text{energy}}} \Lambda^{EV} \tag{5.2.1}$$

where $\Lambda^{EV}_{\max}$ is the maximum EV penetration of the network, and Λ^{EV} is the percentage of EVs that fully charge, calculated by:

$$\Lambda^{EV} = \frac{1}{K} \sum_{k \in \mathcal{K}} \Psi_k \times 100 \tag{5.2.2}$$

where Ψ_k is a binary indicator variable denoting if the EV at house k achieves full charge. The controllable set of energy resources at house k, χ_{energy}, consists of the charge and discharge rate of the EV, $P_{\text{EV}_{\text{ch},k}}$, the amount of discharging of the battery storage, P_{batDis_k}, the amount of solar energy generated at the house consumed for baseload or EV charging in the network, $P_{\text{solar}_{\text{cons},k}}$, the solar energy generated used to charge the house's battery, $P_{\text{solar}_{\text{batCh},k}}$, and Ψ_k

$$\chi_{\text{energy}} = \{P_{\text{EV}_{\text{ch},k}}, P_{\text{batDis}_k}, P_{\text{solar}_{\text{cons},k}}, P_{\text{solar}_{\text{batCh},k}}, \Psi_k\} \quad \forall k \in \mathcal{K} \tag{5.2.3}$$

Baseload

Each house in the network is assigned a real baseload profile for the 24 hour period. Because the power flow studies in the initialisation stage (Section 4.3.1) were conducted using the generic load profile, the difference in baseload between the real profile and generic profile for each house must be calculated and included in the optimisation as an additional load on the network. This enables the results of the power flow study to be applied to a different baseload within the network without having to re-run the power flow with every new set of loads.

$$P_{\text{BL}_{\Delta_k}} = P_{\text{BL}_k} - P_{\text{generic}} \tag{5.2.4}$$

Distributed Generation and Battery Storage

The penetration of distributed generation in the network, Λ^{DG}, is defined as the percentage of houses that have installed solar PV panels and battery storage. The usage of these energy resources is subject to the following constraints: Solar power produced by a house's PV panels, $P_{\text{solar}^t_k}$, can either be consumed by that house or

other houses in the network for baseload or EV charging demand, $P\text{solar}^t_{\text{cons},k}$, stored in the house's battery, $P\text{solar}^t_{\text{batCh},k}$, or must be curtailed, $P\text{solar}^t_{\text{curtail},k}$. Therefore:

$$P\text{solar}^t_k = P\text{solar}^t_{\text{cons},k} + P\text{solar}^t_{\text{batCh},k} + P\text{solar}^t_{\text{curtail},k} \tag{5.2.5}$$

The amount of energy stored in the battery at house k at time t is denoted $B^t_{\text{store}_k}$ and is initially set to 0 kWh at $t = 0$. The energy stored in the battery cannot fall below 0 kWh, or exceed the battery's capacity $B\text{Bat}_{\text{cap}}$, set here as 7 kWh.

$$0 \leq B^t_{\text{store}_k} \leq B\text{Bat}_{\text{cap}} \tag{5.2.6}$$

$$B^t_{\text{store}_k} = B^{in}_{\text{store}_k} + \sum_{\tau=1}^{t} \left(P\text{solar}^{\tau}_{\text{batCh}_k} - P\text{batDis}^{\tau}_k \right) \cdot \Delta T \cdot \eta \tag{5.2.7}$$

where $B^{in}_{\text{store}_k}$ is the initial charge in the battery, $P\text{batDis}^{\tau}_k$ is the power discharged from the battery, and η is the charging efficiency, assumed here to be 90%. It is assumed that the battery will only charge from solar power, so the maximum charge rate is the amount of solar power generated, and the maximum discharge rate is 7 kW.

$$0 \leq P\text{solar}^{\tau}_{\text{batCh}_k} \leq P\text{solar}^t_k \tag{5.2.8}$$

$$0 \leq P\text{batDis}^{\tau}_k \leq 7 \tag{5.2.9}$$

Electric Vehicles

Every house is allocated an EV, which enables any set of EVs to fully charge in the network, irrespective of their location. A set of constraints are imposed on the operation of the EVs. Firstly, EV charging and discharging is constrained as follows:

$$-3 \cdot \Psi_{\text{V2G}} \leq P^t_{\text{EV}_{\text{ch}},k} \leq 7 \cdot \Psi\text{EV}^t_{\text{present},k} \tag{5.2.10}$$

Instead of having separate variables for EV charging and discharging, $P^t_{\text{EV}_{\text{ch}},k}$ is both the charge or discharge rate of the EV at house k and Ψ_{V2G} is a binary variable indicating whether V2G is enabled or not. If V2G is enabled, $\Psi_{\text{V2G}} = 1$ and the minimum EV charge rate becomes -3 kW, denoting discharging of the EV battery.

If V2G is not enabled, $\Psi_{\mathrm{V2G}} = 0$ and the minimum charge rate is 0 kW. Another binary variable, $\Psi\mathrm{EV}^{t}_{\mathrm{present},k}$, indicates whether the EV is at home and able to be charged at time t, to ensure that EVs do not attempt to charge while they are not at home. It is assumed that this variable is equal to 1 the entirety of the time the EV is at home. The maximum charge rate has been set at 7 kW, corresponding to the latest 32 A home charge points. As V2G is a new technology with limited real-world implementation, there are no commonly defined standards on the maximum rate of discharge, so a maximum discharge speed of 3 kW has been selected here to help preserve EV battery life and to manage the power injection within the network [59].

The state of charge (SoC) of EV k at time t is given by:

$$SoC^{t}_{k} = SoC_{\mathrm{in},k} - SoC^{t}_{\mathrm{travel},k} + \sum_{\tau=1}^{t} P^{t}_{EV_{\mathrm{ch}},k} \cdot \frac{\Delta T \cdot \eta}{B_{\mathrm{EV_{cap},k}}} \tag{5.2.11}$$

where $SoC_{\mathrm{in},k}$ is the initial SoC of EV k at $t = 0$, $SoC^{t}_{\mathrm{travel},k}$ is the SoC consumed on any journeys the EV has made prior to time t, and $B_{\mathrm{EV_{cap},k}}$ is the battery capacity of the EV.

A new variable, $SoC_{\mathrm{deficit},k}$, is introduced to capture the amount of SoC that an EV is short of being fully charged at its departure time $T_{\mathrm{dep},k}$. If EV k achieves a full charge by its departure time, $SoC_{\mathrm{deficit},k}$ equals 0. Two binary indicator variables are used to indicate whether full charge has been achieved - if so, $\Psi_k = 1$ and $\Psi^{-}_{k} = 0$. The sum of Ψ for all houses forms the objective function of the maximisation problem (5.2.2).

$$SoC_{\mathrm{deficit},k} = 1 - SoC^{T_{\mathrm{dep}}}_{k} \tag{5.2.12}$$

$$SoC_{\mathrm{deficit},k} \geq -1 \cdot \Psi^{-}_{k} \tag{5.2.13}$$

$$SoC_{\mathrm{deficit},k} \leq \Psi_k \tag{5.2.14}$$

$$\Psi_k + \Psi^{-}_{k} = 1 \tag{5.2.15}$$

To prevent some EVs from fully discharging to further increase the number of fully charged EVs, a final constraint ensures that if an EV participates in V2G, it cannot

leave with a SoC lower than its arrival SoC.

$$\sum_{t=1}^{T} P^{t}_{EV_{\text{ch}},k} \geq 0 \tag{5.2.16}$$

Constraints on the Distribution Network

The operation of the distribution network is subject to a series of constraints on the maximum transformer loading, maximum line currents in each phase and upper and lower node voltages. The specific values of each constraint for both networks can be seen in Section 5.4.1. The voltage at house node k resulting from additional baseload, EV charging and DG is given by:

$$\begin{aligned} V_k^{3\phi} = |\tilde{V}_k^{3\phi}| &+ \mathbf{W}^{+}{}_{k,j} \times \left(P^{t}_{EV_{\text{ch}},j} + P\text{BL}^{t}_{\Delta_j}\right) \\ &+ \mathbf{W}^{-}{}_{k,j} \times \left(P\text{batDis}^{t}_{j} + P\text{solar}^{t}_{\text{cons}_j}\right) \quad \forall j \in \mathcal{K} \end{aligned} \tag{5.2.17}$$

Similarly, the line currents at line segment l are given by:

$$\begin{aligned} I_l^{3\phi} = |\tilde{I}_l^{3\phi}| &+ \mathbf{L}^{+}{}_{l,j} \times \left(P^{t}_{EV_{\text{ch}},j} + P\text{BL}^{t}_{\Delta_j}\right) \\ &+ \mathbf{L}^{-}{}_{l,j} \times \left(P\text{batDis}^{t}_{j} + P\text{solar}^{t}_{\text{cons}_j}\right) \quad \forall j \in \mathcal{K} \end{aligned} \tag{5.2.18}$$

The load on the transformer is given by:

$$S_{\text{trans}} = \sum_{\phi=1}^{3} |V_{\text{trans}_\phi}| \cdot I_1^{\phi} \tag{5.2.19}$$

where $\tilde{V}_k^{3\phi}$ is the voltage at house k calculated in the initialisation stage power flow, $\tilde{I}_l^{3\phi}$ is the current at line l calculated in the power flow, $\mathbf{W}^{+}$ and $\mathbf{W}^{-}$ are the voltage sensitivity matrices, $\mathbf{L}^{+}$ and $\mathbf{L}^{-}$ are the current sensitivity matrices, $V_{\text{trans}_{3\phi}}$ is the voltage at the transformer at each of the three phases and I_1^{ϕ} is the line current in the first line of the feeder for phase ϕ.

The optimisation constraints are formulated as:

$$\underline{V} \leq |V_k^{\phi}| \leq \bar{V} \quad \forall k, \phi \tag{5.2.20}$$

$$|I_l^{\phi}| \leq I_{\max_{l,\phi}} \quad \forall l, \phi \tag{5.2.21}$$

$$S_{\text{trans}} \leq S_{\text{trans}_{\text{max}}} \tag{5.2.22}$$

where $\underline{V}$ and $\bar{V}$ are the lower and upper voltage bounds of the network, -6% and +10%, respectively, $I_{\text{max}_{l,\phi}}$ is the maximum current rating of line l and $S_{\text{trans}_{\text{max}}}$ is the maximum power rating of the transformer.

Solving the Optimisation Problem

The optimisation problem can then be solved to maximise the number of EVs that can be scheduled to fully charge subject to the above constraints using Matlab's intlinprog solver.

Solving of the optimisation problem calculates a single value for the maximum EV capacity given the selected baseload, DG and EV profiles used in that repeat of the Monte Carlo simulation. Therefore, once the Monte Carlo is complete, 1000 values for the maximum EV capacity have been calculated. However, a DSO is more likely to be interested in a single value that represents the maximum EV penetration of the network considering all the scenarios evaluated during the Monte Carlo simulation, so a representative hosting capacity of the network must be determined from the 1000 individual results. There are multiple suitable approaches for this, including taking the minimum value, the mean value, the median value or other percentile, depending on how conservative the calculated value needs to be. For example, taking the median value will result in the calculated maximum penetration exceeding the allowable network limits 50% of the time, whereas taking the minimum value will be affected by outliers, and results in the network being able to accommodate more EVs 99.9% of the time. Therefore, either the 10^{th} or 20^{th} percentile is suggested as a more appropriate measure of the EV hosting capacity. For the results in this chapter, the 20^{th} percentile has been chosen, as it provides a balance between providing a conservative result, while still representing the distribution of the 1000 calculated maximum penetrations.

5.3 Network Impact Token Approach

Whilst the Optimisation approach presented in the previous section calculates an accurate value of the maximum EV penetration as a result of the inclusion of all network and energy resource usage constraints in the problem, it can be extremely slow to solve. This is because the voltage and current must be constrained at each node and line in the network, respectively. In addition, these depend on the values of every load in the network, and as EV charging load, consumption of renewable energy and battery charging/discharging are optimisation variables, this adds significant complexity to the problem, resulting in long computation times. As a result, performing sufficient repeats of a Monte Carlo simulation to calculate a reliable value for the maximum EV penetration can take several days to complete, and for larger networks, Matlab is not always able to find a solution. Therefore, a faster approach is required to enable DSOs to feasibly analyse their networks or evaluate the impact of different loading conditions and network hardware on the capacity of EVs in a reasonable time frame.

This second approach utilises the Network Impact Tokens (NITs) and Phase Impact Tokens (PITs) introduced in Chapter 4, to speed up the solving of the EV hosting capacity problem. Reformulating the problem in terms of the number of NITs and PITs available in the network and each house's impact on the network and on the phase of the network to which it is connected - its Network Impact Value (NIV) and Phase Impact Value (PIV), respectively - enables the network constraints included in the Optimisation approach in Section 5.2.1 to be removed, which speeds up to time to solve the problem considerably, whilst still ensuring the network operates within its allowed voltage, current and power limits.

5.3.1 Network and Phase Impact Tokens for Calculating the Maximum EV Penetration

Using the method presented in Chapter 4, the Network Impact Values of each house and the available quantity of Network Impact Tokens across the entire network are calculated, as well as each house's Phase Impact Value and the number of Phase Impact Tokens available in each phase of the network. The optimisation problem presented in Section 5.2.1 can then be reformulated in terms of these values, rather than the network power limits (5.2.20) - (5.2.22).

The optimisation objective remains the same for both the Optimisation and NIT approaches:

$$\Lambda^{EV}_{\max} = \max_{\chi_{\text{energy}}} \Lambda^{EV} \tag{5.3.1}$$

However the problem can be simplified from the Optimisation approach by excluding the constraints on the distribution network, and is now subject to (5.2.5) - (5.2.16). In addition, as the calculated number of NITs and PITs includes the generic profile, the actual baseload power P_{BL_k} is used instead of the difference in baseload $P_{\text{BL}_{\Delta_k}}$.

To ensure that the baseload, EV charging and usage of other energy resources does not violate any network constraints, the NITs and PITs are implemented into the optimisation problem as follows.

The consumption of NITs for loads across the network, and creation of NITs from solar PV power generation and battery discharging are given by equations (5.3.2) and (5.3.3), respectively.

$$NIT^t_{\text{load},k} = \left(P^t_{\text{EV}_{\text{ch}},k} + P\text{BL}^t_k\right) \cdot NIV^+_k \tag{5.3.2}$$

$$NIT^t_{\text{gen},k} = \left(P\text{solar}^t_{\text{cons},k} + P\text{batDis}^t_k\right) \cdot NIV^-_k \tag{5.3.3}$$

subject to:

$$\sum_{k=1}^{K} NIT^t_{\text{load},k} \leq \sum_{k=1}^{K} NIT\text{alloc}_k + \sum_{k=1}^{K} NIT^t_{\text{gen},k} \tag{5.3.4}$$

Similarly, the consumption and generation of PITs within each phase ϕ are given by:

$$PIT^{\phi,t}_{\text{load},k} = \left(P^{t}_{\text{EV}_{\text{ch}},k} + P\text{BL}^{t}_{k}\right) \cdot PIV^{+}_{k} \tag{5.3.5}$$

$$PIT^{\phi,t}_{\text{gen},k} = \left(P\text{solar}^{t}_{\text{cons},k} + P\text{batDis}^{t}_{k}\right) \cdot PIV^{-}_{k} \tag{5.3.6}$$

subject to:

$$\sum_{k=1}^{K} PIT^{\phi,t}_{\text{load},k} \leq \sum_{k=1}^{K\phi} PIT\text{alloc}^{\phi}_{k} + \sum_{k=1}^{K} PIT^{\phi,t}_{\text{gen},k} \quad \forall\phi \tag{5.3.7}$$

Again, a Monte Carlo simulation is used to calculate the maximum EV penetration, with houses allocated baseload, EV and DG profiles at each repeat as previously described. This NIT problem is solved at each repeat to calculate the maximum EV capacity based on the selected profiles. Once 1000 repeats of the Monte Carlo have been run, the overall maximum EV penetration for the network can again be calculated as the 20^{th} percentile of the individual results.

5.4 Network Models, Load Profiles and Study Parameters

5.4.1 Distribution Network Models

Two real, three-phase low-voltage distribution networks from North West England, UK, are analysed here, with each network differing in terms of the number of feeders and houses. This provides a comparison of the EV hosting capacity calculation on networks of different sizes and structures.

Network 1: IEEE Low Voltage European Test Feeder

The first network is the IEEE 2015 Low Voltage European Test Feeder [169], a single feeder low voltage network, serving 55 houses connected across three unbalanced phases. The network has a radial topology and a three-phase transformer reduces the

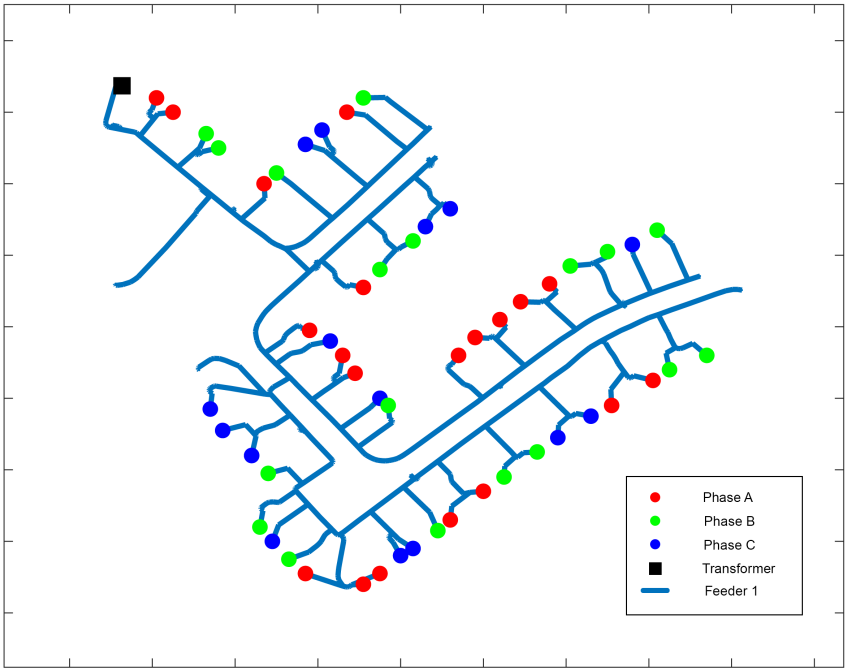

Figure 5.1: Line diagram of the IEEE Low Voltage Test Feeder

Table 5.1: Network 1 Constraints

Constraint	Lower Limit	Upper Limit
Node Voltage	216.2 V	253 V
Feeder Head Current	N/A	175 A
Transformer Loading	N/A	112.5 kVA

voltage at the head of the feeder from 11 kV to the network's nominal phase-to-phase voltage of 416 V.

The test feeder is shown in Figure 5.1, with the locations of the houses and the phase of the network that each is connected to represented by the coloured circles, and the transformer location marked with a black square.

Constraints on the node voltages, per-phase line currents and transformer loading are imposed on power networks to guarantee safe and reliable operation, with values given in Table 5.1. An additional 10% safety margin is further added to ensure the network does not operate right at its limit to avoid any risk of violations and unnecessary component aging.

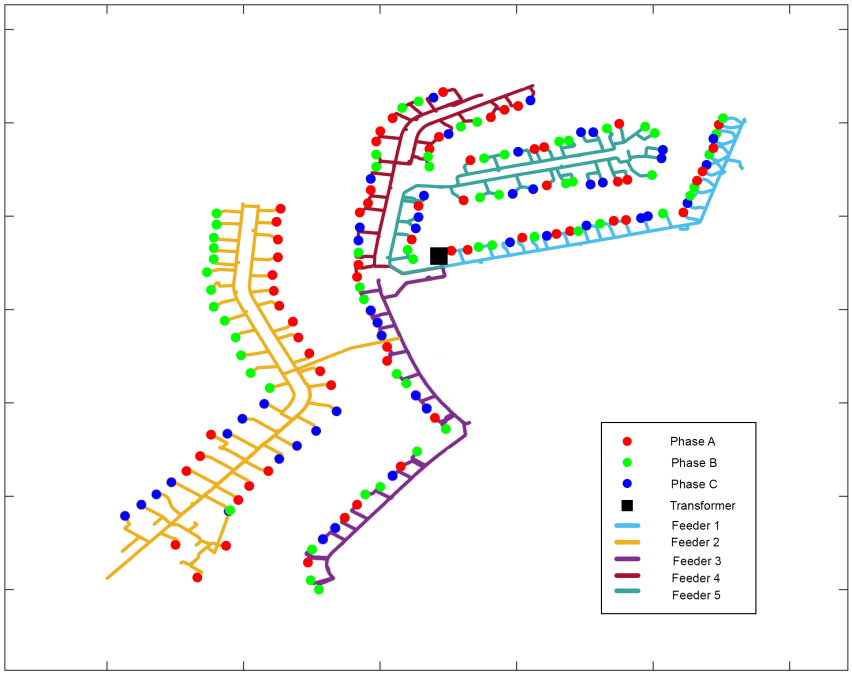

Figure 5.2: Line diagram of Network 2

Table 5.2: Network 2 Constraints

Constraint	Lower Limit	Upper Limit
Node Voltage	216.2 V	253 V
Feeder Head Current	N/A	220 A
Transformer Loading	N/A	320 kVA

Network 2: Five Feeder Distribution Network

The second network evaluated in this study is a much larger distribution network, with data provided by Electricity North West [170]. The 320 kVA, 11 kV to 416 V transformer supplies five individual three-phase feeders, with 171 houses connected across the entire network. The layout of the network is shown in Figure 5.2.

Table 5.2 gives the values of the power limits for Network 2.

5.4.2 Load Profiles

A key advantage of the proposed methodology is that any set of baseloads, renewable generation or EV profiles can be used in the study to give interesting results. For

example, a comparison could be made in the permissible EV hosting capacity between summer and winter, evaluating the impact of a higher peak baseload or different EV requirements or to evaluate the effect of higher peak baseload. The results in this chapter primarily use Summer DG and baseload profiles, as the higher solar PV generation will have the greatest impact on the maximum EV penetration, providing the most interesting results.

Based on 100 real load profiles provided by Electricity North West, an expanded set of 1000 representative baseload profiles have been created that can be used in the Monte Carlo study. It was necessary to create a larger set of profiles as Network 2 contains more houses than there are original profiles, and it also allows the Monte Carlo has to evaluate a wider range of load conditions in the network, as otherwise there would be little variation in load between repeats. Whilst these new profiles have been generated based on the provided baseload profiles, they have varying times of power usage, peak demand and overall power consumption, designed to capture the significant real-world variation in both day-to-day power consumption and varying usage between a range of users. To ensure that the set of new profiles follows the same underlying statistics as the original load profiles, and that they are representative of real-world conditions, they are generated using the following technique:

1. Calculate the probability distribution function of the daily total electricity consumption (kWh) from the 100 real profiles

2. For each new profile, generate a random number between 0 and 1 from a uniform distribution and calculate the corresponding daily electricity consumption using the inverse cumulative distribution function of the previously calculated distribution

3. From the set of 100 real profiles, randomly select N profiles, where N is an integer between 1 and 5. These profiles will form the basis of the new profile by defining the load shape and load value. Picking more profiles creates a

wider range of load values for the new profile to be created from, potentially creating new load shapes, whereas selecting fewer profiles means that the new profiles will match those original profiles more closely

4. For each timestep, calculate the maximum and minimum load value of the N profiles, and pick a random number within that range. This value will be the baseload value for the new profile at that timestep

5. Once a baseload value has been assigned at each timestep, multiply these by a factor so that the daily electricity consumption matches the target consumption calculated in step 2

A set of 1000 electric vehicle profiles have been created based on typical vehicle usage patterns. Each EV is assigned a battery capacity of 55 kWh with 20% probability, 80 kWh with 60% probability and 100 kWh with 20%, to follow recent trends of increasing battery capacity. Every EV is allocated an initial SoC randomly between 75% and 100%, as increasing EV range means that vehicles may not need to be charged every night. This initial SoC is assumed to be sufficient for all journeys that the EV will make during the day. It is assumed that the day of the study is a week day, and an EV profile has an 80% probability of going to work during the day. If an EV goes to work it is assigned a random departure time between 6am and 8:30am and a random arrival time of between 4pm and 8pm. The SoC lost on the commuting journeys is assumed to be a random number between 10% and 80% of the EV's initial SoC. If the EV is travelling to work again the next morning, it is assigned a departure time between 6am and 8:30am the following day. If the EV does not travel to work, then it can make another journey during the day instead with probability of 50%. If the EV makes this journey, it is allocated a random departure between 8am and 6pm and an arrival time before 9pm, that is at least 30 minutes after its departure. The SoC consumed on this journey is randomly selected between 10% and 80% of the EV's initial SoC.

A solar irradiance profile for the UK in June was obtained from [165] as the basis

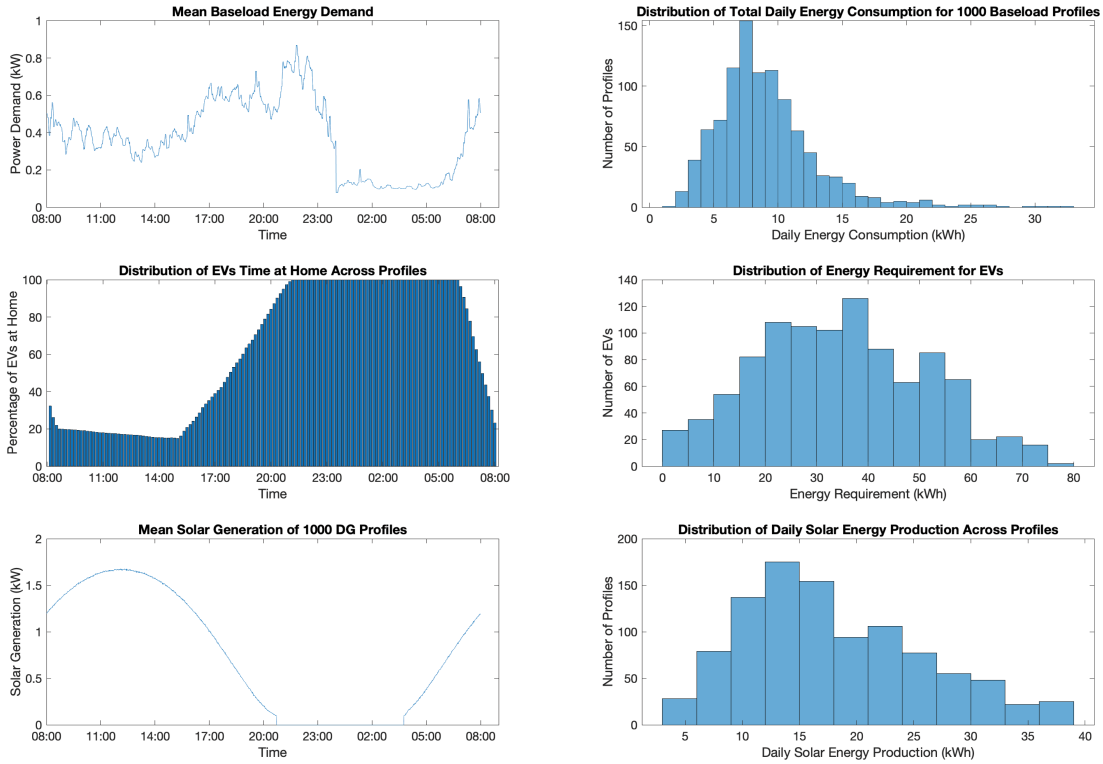

Figure 5.3: Distributions of Summer energy resource profiles

for the creation of 1000 solar PV generation profiles. Random noise was added to the profile at each timestep using Matlab's Gaussian Noise function to mimic real-world fluctuations, and the overall power production was either increased or decreased by a random percentage between -50% and +50% to account for days where weather would affect the total generation, while still ensuring the mean of the new profiles matches the original data. At each repeat of the Monte Carlo, a random selection of houses are allocated solar PV and battery storage, based on the chosen DG penetration of the study. These DG equipped houses are allocated a PV array size of either 3, 5 or 7 kWp with a random DG profile scaled in accordance to their array size, and are also equipped with a 7 kWh battery for energy storage.

As all 1000 individual baseload, EV and DG profiles cannot be shown graphically, Figure 5.3 shows some of the key summary statistics from the distributions of Summer baseload, EV and solar DG profiles. The top-left figure shows the average load from all 1000 baseload profiles at every minute, while the top-right figure is a histogram showing the number of profiles that have a total daily energy consumption given

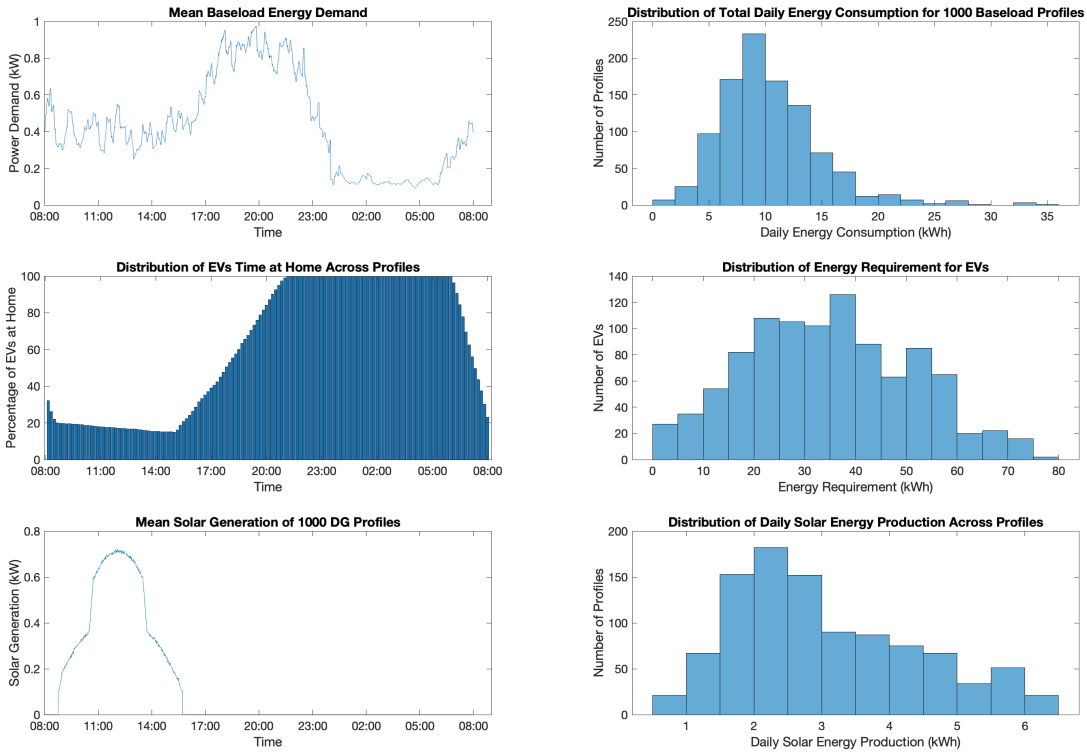

Figure 5.4: Distributions of Winter energy resource profiles

on the x-axis. The middle-left figure displays the percentage of EV profiles where the EV is at home at each minute, and the middle-right figure shows a histogram of the the number of EV profiles (again out of the 1000 created) that have the energy requirement to achieve a full charge on the x-axis. The bottom-left figure displays the average solar generation at each minute across all 1000 solar profiles, and the bottom-right figure shows the distribution of total daily solar energy production for all profiles.

Similarly a set of Winter profiles were generated using January load and solar PV data, shown in Figure 5.4, to enable a comparison in the EV hosting capacity between seasons.

5.4.3 Study Design

This study analyses a 24-hour period, from 8:00am to 7:59am the following day, which captures the full cycle of daily EV driving and charging behaviour. The EVs

depart on their daily journeys before returning home and attempting to recharge to a full SoC overnight before they are required to depart again the following morning. Every house is assigned an EV for this study, and it is assumed that all EVs want to recharge on the same day. The objective is to calculate the number of those EVs that can reach a SoC of greater than 99% (at which point they can be considered fully charged) before either their departure time the next morning, or the end of the study at 8am. This approach is chosen as it enables any set of EVs to fully charge, making the maximum penetration calculated representative of the entire network. If only some houses were allocated EVs initially then whether that penetration of EVs can be accommodated by the network will also depend on the houses that the EVs are assigned to. For instance, allocating EVs to the 28 houses (50% EV penetration on Network 1) closest to the transformer will more likely result in a successful accommodation than allocating the EVs to the 28 houses furthest downstream in the network.

The maximum EV penetration is then determined through a Monte Carlo simulation that takes into account the wide variation in energy profiles visible in Figures 5.3 and 5.4. In total, 1000 repeats of the Monte Carlo are performed, with random baseload, EV usage and PV generation profiles allocated to each house at every repeat. At each repeat of the Monte Carlo, the maximum penetration of EVs based on the chosen profiles is calculated. Following the completion of the Monte Carlo, the overall maximum EV penetration value for the network can be calculated from the 1000 results.

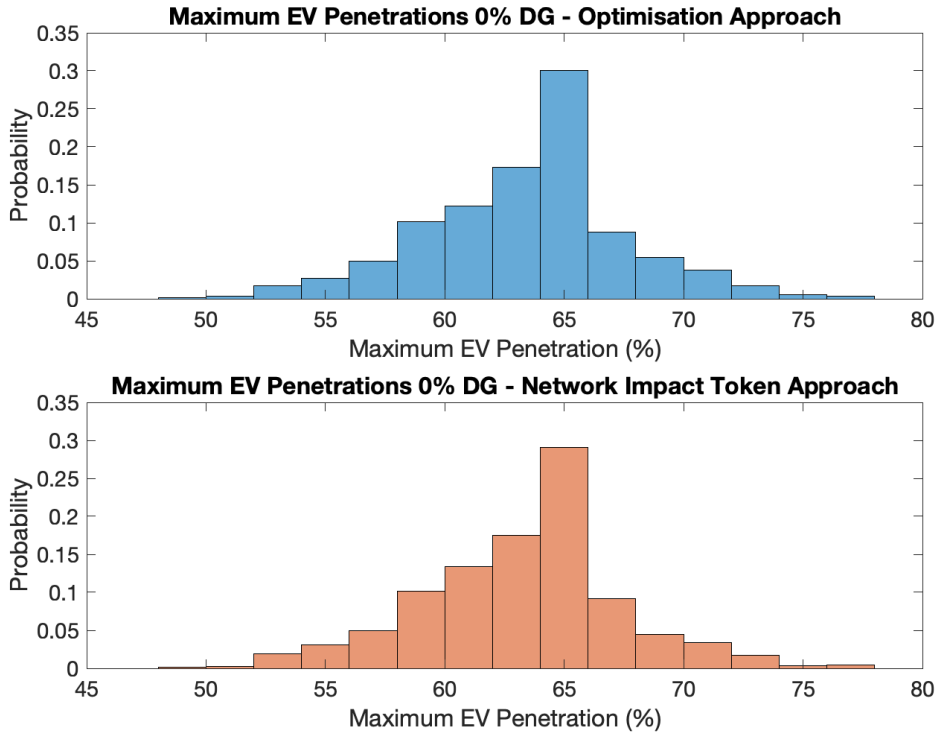

Figure 5.5: Distribution of maximum penetration of EVs calculated in Monte Carlo simulation with no houses equipped with solar PV or battery storage

5.5 Results and Discussion

5.5.1 Network 1: Verification of Network Impact Token Approach

It is important to compare the maximum EV penetration results generated from the Network Impact Token approach with the original Optimisation approach in order to verify it as a valid method for calculating the EV hosting capacity. Figures 5.5 - 5.7 show histograms comparing the distribution of the calculated EV capacity from each of the 1000 Monte Carlo repeats, for three scenarios with 0% penetration of solar PV panels and battery storage, with 50% of the houses equipped with solar panels and battery storage, along with the use of V2G, and with 100% of houses equipped with solar PV, but no V2G, respectively.

The figures show that the distribution of individual maximum penetration results

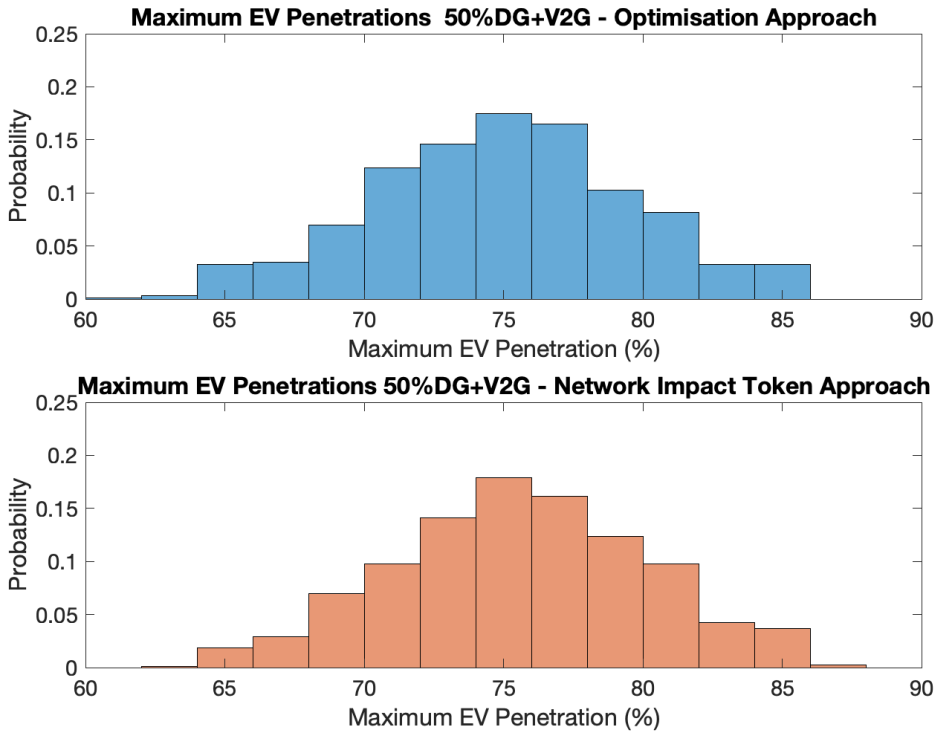

Figure 5.6: Distribution of maximum penetration of EVs with V2G enabled and 50% of houses equipped with solar PV and battery storage

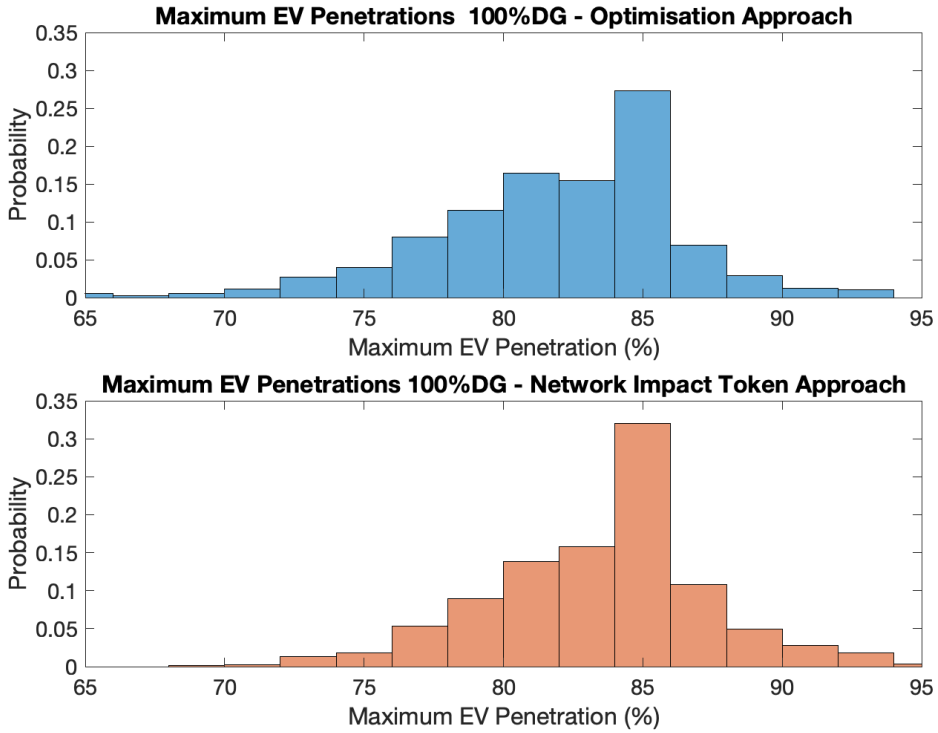

Figure 5.7: Distribution of maximum penetration of EVs with 100% of houses equipped with solar PV and battery storage

from each Monte Carlo repeat using the NIT approach matches the same results from the Optimisation approach very closely, with similar probability values of each maximum EV penetration, and almost identical distributions for all three scenarios. Additionally, it can be seen how big of an impact the selected baseload, DG and EV profiles have on the maximum EV penetration that can be accommodated by the network. There is more than 20% difference in the range of calculated penetrations from the 1000 repeats, which shows the importance of the Monte Carlo analysis to determine the representative maximum EV hosting capacity of a network.

Some of the key statistics from the four sets of results are shown in Table 5.3, which also confirm the validity of the NIT approach for estimating the maximum EV penetration of the network. Depending on the statistic used to evaluate the network's EV hosting capacity from the Monte Carlo data, the NIT approach can be seen to slightly underestimate the maximum penetration in the first scenario with 0% DG, with it typically predicting 1 fewer EV can be accommodated than Optimisation results suggest, however the mean maximum penetration calculated is very accurate. The NIT approach provides accurate results for all statistics in the second scenario considering 50% DG+V2G, with identical EV hosting capacities to the Optimisation approach calculated for the median, 10^{th} and 20^{th} percentiles. For the 100% DG scenario, the NIT approach slightly overestimates the maximum EV hosting capacity, again by around 2% (~1 EV). However, even at 0% and 100% DG, it is likely that the relatively small differences in results between the two approaches do not represent a problematic loss of accuracy. If the 30^{th} percentile is instead used to calculate the maximum penetration, then it can be seen that the NIT approach produces an identical result to the Optimisation approach for all three scenarios.

Figures 5.8 - 5.10 show the difference between the penetration calculated by the NIT and Optimisation approaches using identical baseload, DG and EV data for each of the 1000 repeats, again for the 0% DG, 50% DG+V2G and 100% DG scenarios, respectively. As identical data was used in the same repeats for both approaches, these results show the accuracy of the NIT approach on a single repeat, rather than

Table 5.3: Key statistics from EV penetration calculations

	0% DG		50% DG+V2G		100% DG	
Statistic	Opt.	NIT	Opt.	NIT	Opt.	NIT
Mean	62.9%	62.7%	74.6%	75.1%	81.3%	82.9%
Median	64%	62%	75%	75%	82%	84%
10^{th} Percentile	58%	56%	69%	69%	76%	78%
20^{th} Percentile	60%	58%	71%	71%	78%	80%
30^{th} Percentile	60%	60%	73%	73%	80%	80%

over all 1000 repeats. The x-axis shows the difference in maximum EV penetration calculated between the two approaches, while the height of each bar represents the number of repeats where that difference occurred. A positive difference shows that the NIT approach has overestimated the EV hosting capacity compared to the Optimisation result, while a negative difference represents an underestimation. For example, a +2% difference means that on a particular repeat, the NIT approach calculated a maximum EV penetration 2% higher than the Optimisation approach, for example, giving a penetration of 68% rather than 66%. The NIT approach is shown to match the Optimisation approach results exactly for the majority of repeats, with 0% difference between the two approaches, with most of the remaining results resulting in a ±2% discrepancy. It can be seen that there is a very small number of repeats where the NIT approach significantly overestimates compared to the Optimisation result, which must be down to the selected baseload, EV and DG profiles and how they interact with the network on these repeats, although the exact reason for this is not apparent. However, this does not alter the accuracy of the overall results. At higher penetrations of DG and battery storage, the NIT approach begins to overestimate the maximum EV capacity. It can be seen in Figure 5.8 that more repeats underestimate the capacity than overestimate compared to the Optimisation approach, whereas with the 50% DG+V2G scenario in Figure 5.9 and 100% DG scenario in Figure 5.10, there are more repeats that overestimate. However, it can be seen that the results still retain a high level of accuracy, with

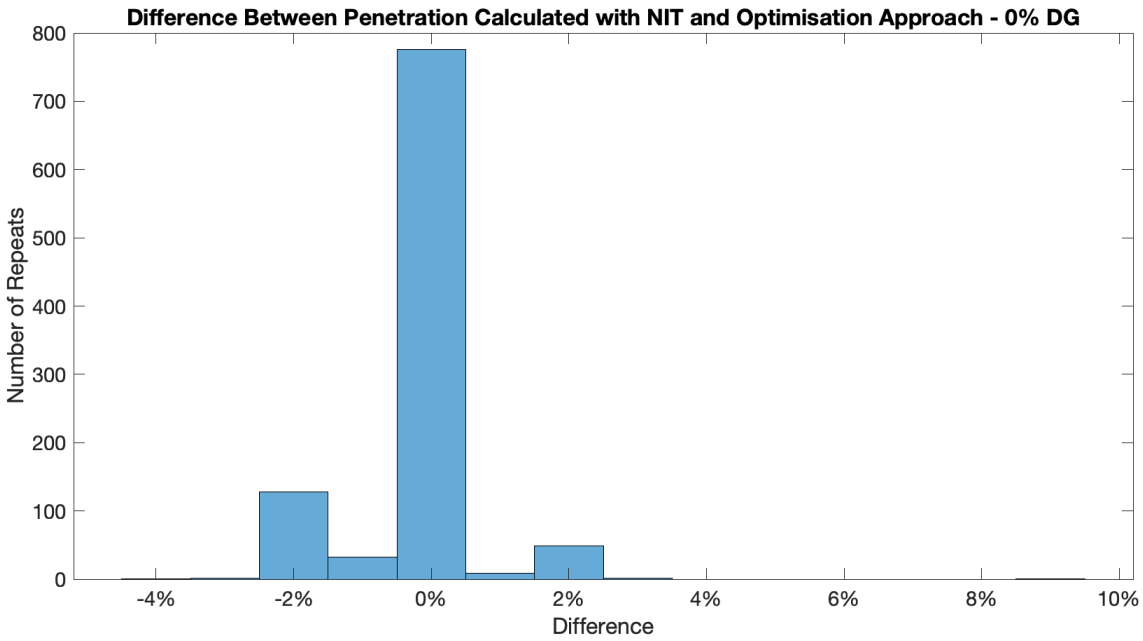

Figure 5.8: Distribution of difference in EV penetration calculated between Optimisation and NIT approaches for 0% DG scenario

80% of the results from the NIT approach being within ±2% of the Optimisation approach result. The focus of future research could be on further development of the NIT approach to further improve the accuracy of results at higher DG penetrations.

5.5.2 Network 1: Speed Comparison Between Optimisation and NIT Approaches

One of the key failings of the Optimisation approach is the time taken to calculate the results, prohibiting the use of this approach in the Monte Carlo simulation, where hundreds or thousands of repeats may be necessary to analyse the wide range of situations that the network could encounter.

The average time to calculate the maximum EV penetration for a single repeat of the Monte Carlo with one set of input data profiles is determined by running 250 Monte Carlo repeats on Durham University's Hamilton High Performance Computing cluster, and calculating the mean time that each repeat took to solve. The repeats were run in parallel over 50 CPU cores, with a total of 245 GB of RAM available.

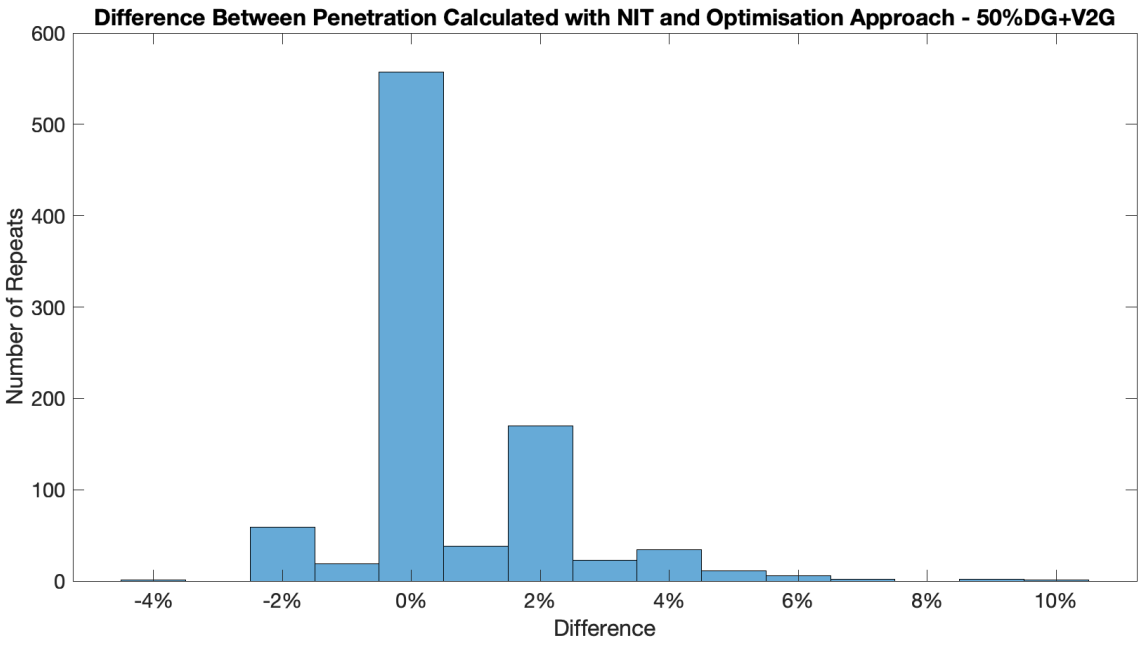

Figure 5.9: Distribution of difference in EV penetration calculated between Optimisation and NIT approaches for 50% DG & V2G scenario

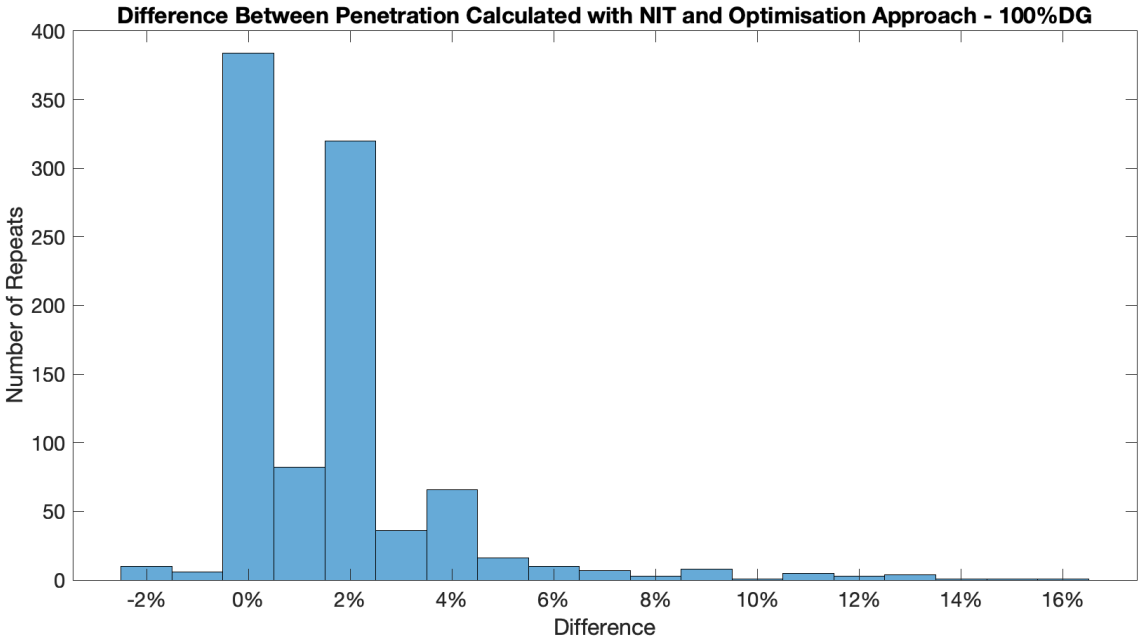

Figure 5.10: Distribution of difference in EV penetration calculated between Optimisation and NIT approaches for 100% DG scenario

Table 5.4: Average time per repeat of Monte Carlo simulation for Optimisation and NIT approaches

	Optimisation Avg. Time	NIT Avg. Time
0% DG	319.5 s	7.4 s
25% DG	1349.0 s	22.9 s
50% DG	2401.8 s	33.1 s
100% DG	3687.6 s	47.8 s
0% DG+V2G	1440.5 s	15.6 s
25% DG+V2G	2300.1 s	23.4 s
50% DG+V2G	3296.2 s	41.5 s
100% DG+V2G	4484.5 s	53.4 s

Table 5.4 shows the average time to run a single Monte Carlo repeat using the Optimisation and NIT approaches.

Depending on the penetration of DG simulated, the Network Impact Token approach can calculate a single repeat of the Monte Carlo around 40-100 times faster than the Optimisation approach, with a mean speed of between 7.4-53.4 seconds, compared to 319.5-4484.5 seconds. As many repeats of the NIT approach can be completed in the same time as a single repeat of the Optimisation approach, it significantly speeds up the time to run the entire Monte Carlo simulation, especially on hardware which is not as able to run as many threads in parallel. As would be expected, increasing the number of houses in the network equipped with solar PV panels and battery storage, or by enabling the use of V2G increases the time taken to calculate the maximum EV penetration as it increases the size of the problem with additional energy resources that must be scheduled. There can also be significant time variation between repeats, with certain selections of baseload, DG and EV profiles taking much longer to solve than others. The network constraints can play a big role in the time taken to solve, with higher transformer and line current rating making the problem easier to solve, and hence reducing the computational time. It is possible that the repeats that take the longest have baseload profiles that come closer to reaching the maximum

Table 5.5: Run time and memory usage comparison for 1000 repeat Monte Carlo simulation

	Optimisation Approach		NIT Approach	
	Run Time	Memory Usage	Run Time	Memory Usage
0% DG	21554.1 s	230.0 GB	817.9 s	75.7 GB
50% DG+V2G	100866.0 s	242.0 GB	1726.1 s	79.8 GB
100% DG	107739.2 s	235.8 GB	1574.9 s	80.7 GB

transformer power and line current before EVs are considered, making it harder to find a solution without violating these limits.

Table 5.5 gives the total run time for performing a 1000 repeat Monte Carlo simulation on Hamilton using the above CPU and RAM specs. It is again shown that the total time for running the Monte Carlo using the NIT approach is 26, 58 and 68 times faster than the Optimisation Approach for the scenarios with 0% DG, 50% DG+V2G and 100% DG, respectively. The 1000 repeat Monte Carlo finishes in 13 minutes, 28 minutes and 26 minutes using the NIT approach for the three scenarios, compared with 6 hours, 28 hours and 30 hours using the Optimisation approach, which makes the NIT approach suitable for use by a DSO for rapid evaluation of their networks, as well quickly being able to analyse changes to network parameters or loads. In addition, the memory usage of the NIT approach is considerably lower than the Optimisation approach, which increases the feasibility of the approach when running on standard computer hardware. Hamilton's compute nodes have a 250 GB memory limit, which prohibits the usage of more than 50 CPU cores simultaneously for the the Optimisation approach, which means at most 50 repeats can be run simultaneously. However, the lower memory usage of the NIT approach can allow more than 50 CPU cores to be run simultaneously, which would further decrease the total run time from that given in Table 5.5. The high memory consumption of the Optimisation Approach can mean that standard PC hardware can struggle to solve the optimisation problem, with the solver failing to find a solution for some repeats, whereas the NIT approach can be easily solved.

5.5.3 Network 1: Comparison in EV Hosting Capacity Calculation Methods

This section provides a comparison of the network's maximum EV penetration calculated through three different approaches that are commonly analysed in the current literature. The EV hosting capacity calculated by the Network Impact Token approach is compared with the maximum EV capacity with uncontrolled EV charging and the maximum capacity calculated in the worst-case scenario, with simultaneous charging at peak load. In all three approaches, a Monte Carlo simulation is performed to calculate the maximum EV penetration, using the same methods and data as previously presented in this chapter.

To calculate the maximum EV penetration with uncontrolled EV charging, every house is allocated an EV, and the charge profile for each EV is calculated such that the EV will charge at maximum power as soon as the EV is at home until full SoC is achieved. Based on these charge profiles, an optimisation problem is solved to maximise the number of EVs that could be accommodated by the network without violating any voltage, current or power constraints for each repeat.

The EV hosting capacity with simultaneous charging at peak load is found by solving an optimisation problem at the time of peak baseload to maximise the number of houses that could accommodate an EV charger operating at the maximum 7 kW charge rate without violating any network constraints.

In the uncontrolled EV charging case, every EV's primary objective is to charge as soon as possible, and as a result the use of V2G is incompatible with this goal, therefore, V2G is not used in this comparison.

Figure 5.11 shows the maximum EV capacity calculated for the network with each of the three methods as the penetration of solar PV and battery storage increases.

The Network Impact Token approach calculates the absolute maximum penetration of EVs that can be accommodated within the network, and as a result is guaranteed

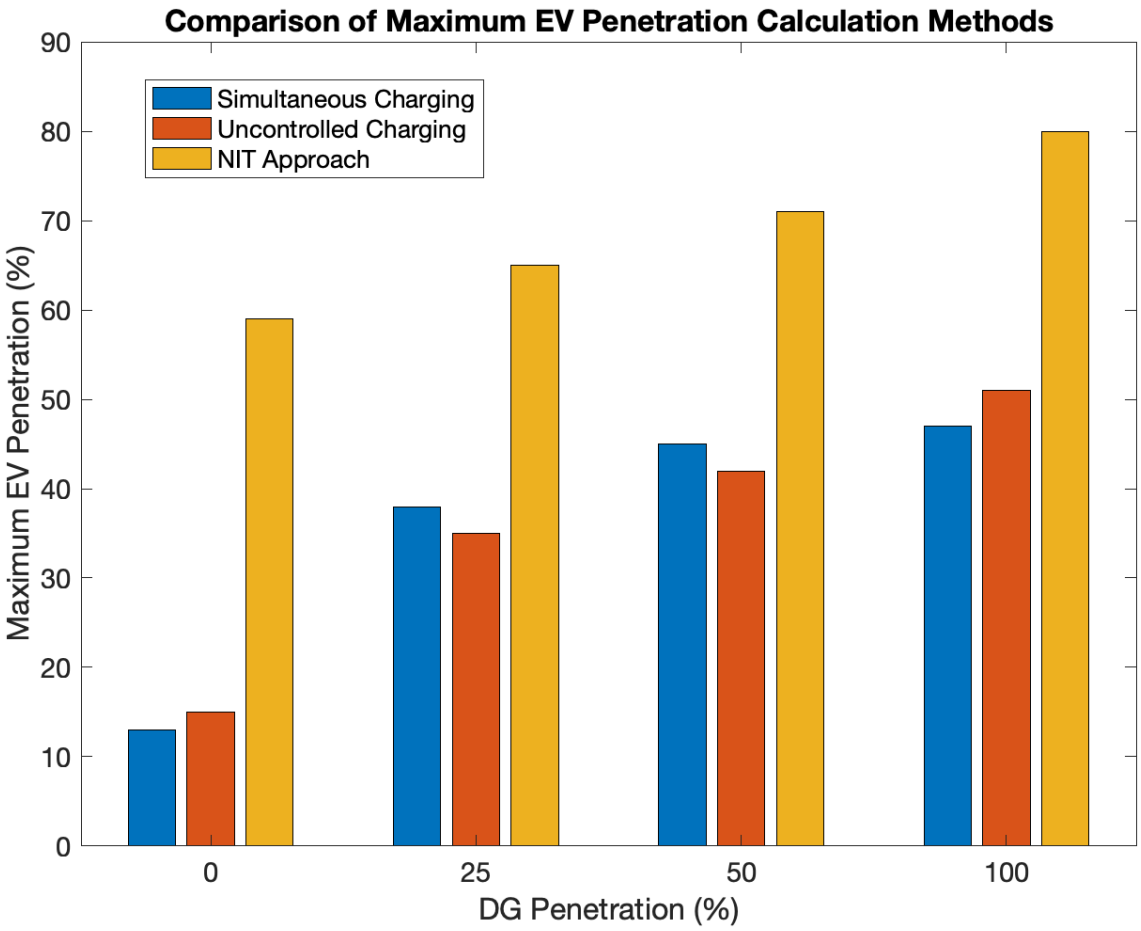

Figure 5.11: The maximum EV penetration of the network calculated using three different methods is compared for increasing levels of DG penetration

to calculate a maximum EV penetration higher than the other two approaches. The simultaneous charging and uncontrolled charging strategies also result in inconsistency - for some DG penetrations the simultaneous charging approach calculated a higher EV capacity than uncontrolled charging, for other DG penetrations it calculated a lower hosting capacity.

The discharging of the houses' batteries can have a big impact on the maximum EV penetration. For example, if the house's battery is allowed to discharge at its maximum allowable rate during the timeslot analysed in the simultaneous charging approach, then a higher maximum EV penetration would be calculated than if the battery was not able to discharge, as a result of the additional energy available in the network. As each house will have its own strategy for operating the charging

and discharging of its battery throughout the day, there are no guarantees that all houses in the network would all be able to discharge their batteries at maximum power at the time of peak load under normal operation, which means this method can calculate a maximum EV penetration higher than would realistically be achieved. Additionally, if a house discharges its battery at peak load, then it is not able to discharge at another timestep, so the network could only accommodate a lower penetration of EVs during another timestep as a result of the lower power discharged from the batteries. This issue is avoided in the NIT and uncontrolled charging methods, as the entire 24 hour period is analysed, with the charging and discharging of the battery constrained by the minimum and maximum battery storage capacity, charging and discharging rates.

Therefore, the results have been repeated in Figure 5.12 with varying penetrations of solar PV but no battery storage, which can provide a fairer comparison between the methods. However, it can be seen that removing the battery storage has a significant impact on the maximum penetration of EVs that can be accommodated in both the simultaneous and uncontrolled charging approaches, with half the number of EVs able to be accommodated under certain DG penetrations. Combined with the inconsistency in the calculated results, there is lower confidence in the results of these two approaches compared with the NIT approach, which is guaranteed to calculate the maximum EV capacity every time. Therefore, it can be concluded that the NITs is a more suitable and reliable approach for calculating the maximum EV penetration of a network.

5.5.4 Network 1: Other Results

The calculation of the maximum EV penetration can be used in many different ways for interesting analysis of the network. This section uses the NIT approach for calculating the EV hosting capacity and presents a selection of different results that could be of interest to a DSO evaluating their networks.

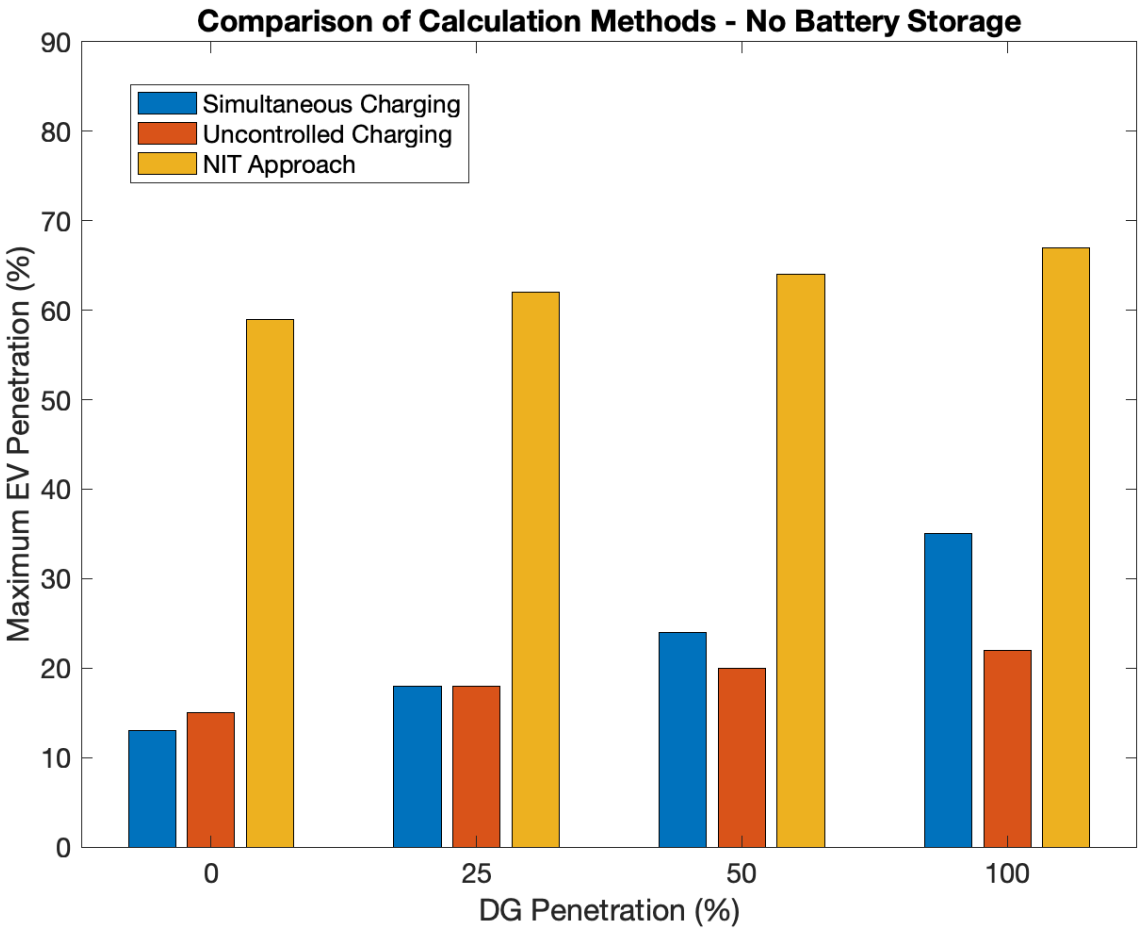

Figure 5.12: Comparison of the maximum EV penetration calculated through the three approaches with increasing penetration of solar PV but no battery storage

Firstly, Figure 5.13 shows the maximum EV hosting capacity of the network as the penetration of houses equipped with solar PV panels and battery storage increases. The results were calculated using Summer solar generation data to show the greatest impact on the EV hosting capacity caused by increasing the DG penetration. As would be expected, higher penetrations of houses equipped with solar PV and battery storage increases the number of EVs that can be accommodated by increasing the amount of power available in the network for EV charging. It is found that raising the DG penetration from 0% to 100% increases the EV capacity from 58% to 80%, a 38% increase in the number of EVs that can be accommodated. V2G has the potential to increase the maximum EV penetration by allowing some EVs to act as battery storage to discharge energy enabling other EVs to charge at times when additional energy is not available from the grid. However, the use of V2G is found

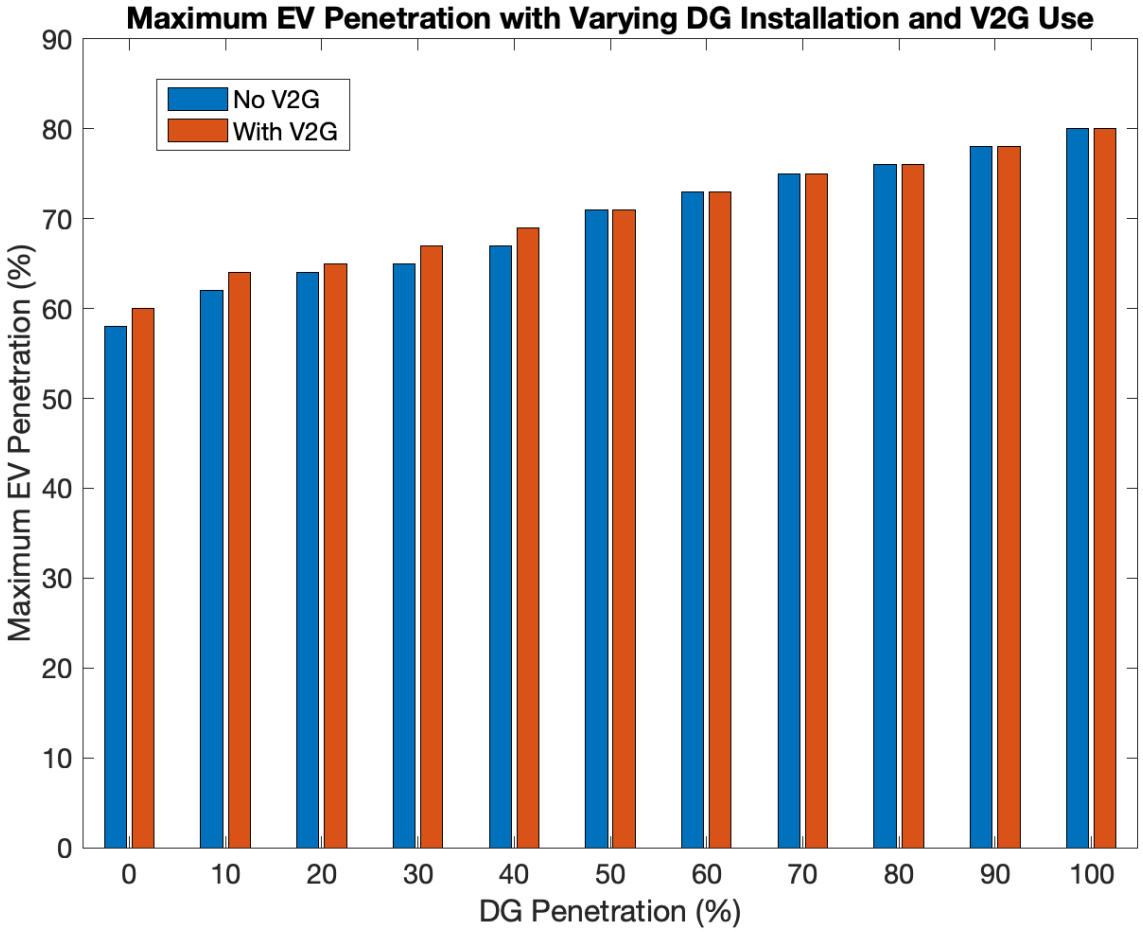

Figure 5.13: The maximum EV penetration for the network is calculated as the penetration of houses equipped with solar PV and battery storage increases from 0% to 100%, both with and without the use of V2G

to have a much less significant impact on the maximum EV penetration, with it resulting in at most a 2% increase (1 additional EV) in EV hosting capacity at any given DG penetration compared with the scenario without V2G.

As these results were calculated using Summer baseload and solar PV generation data, it would be expected that higher penetrations of DG would not be able to accommodate as many EVs in Winter when solar PV generation is lower. Figure 5.14 shows the difference in maximum EV penetration calculated for each penetration of DG when using Winter baseload and solar PV profiles compared with Summer profiles. There is a minor difference in EV capacity between Summer and Winter when no solar PV and battery storage is installed in the network, which likely results from the higher baseload power usage in Winter months. It can be seen that higher

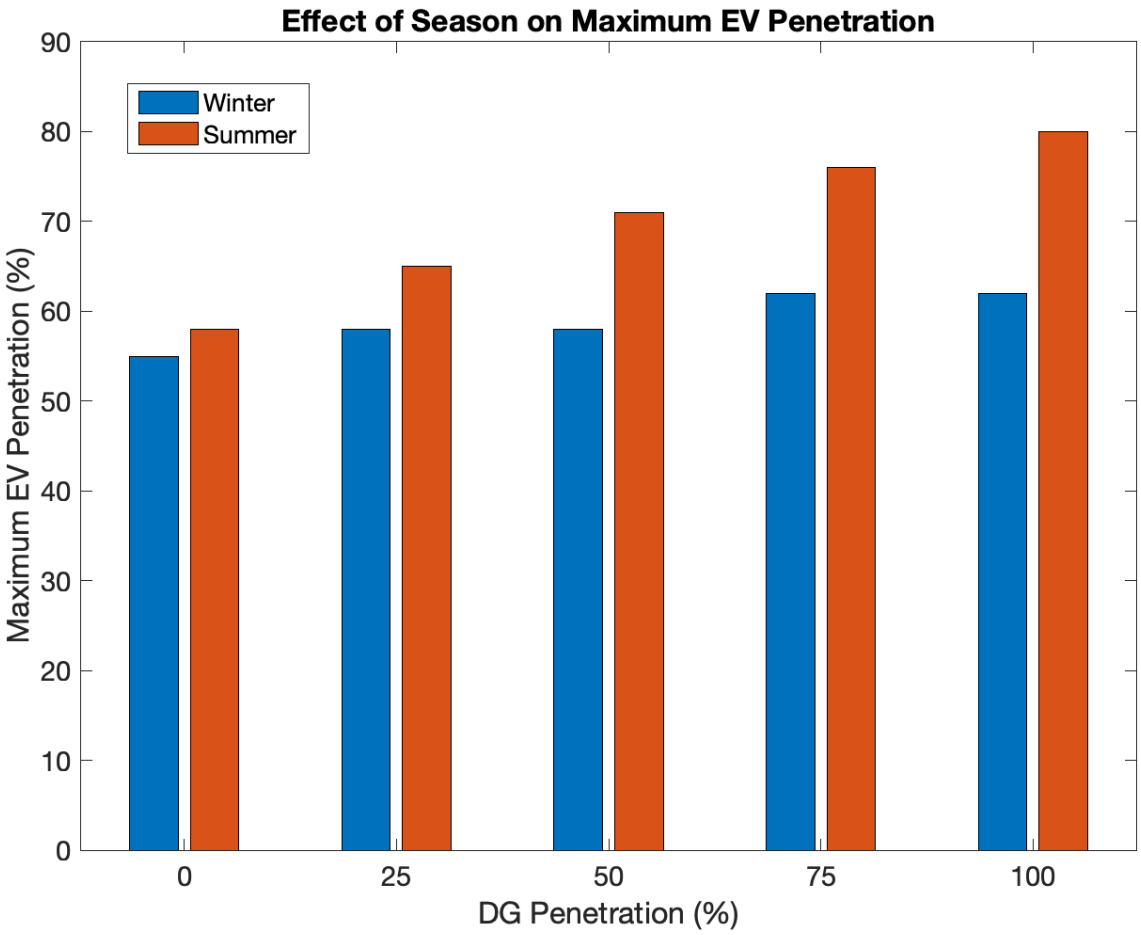

Figure 5.14: The maximum EV penetration for the network is calculated for both Summer and Winter load and PV data as the penetration of houses equipped with solar PV and battery storage increases

penetrations of DG in Winter do not have the same effect on increasing the EV hosting capacity as in Summer. Even with all houses equipped with solar PV and battery storage (100% penetration), the maximum EV penetration in Winter is 65% compared with 80% in Summer. Therefore, Winter remains the weakest period for low-voltage distribution networks, with it hardest to increase the hosting capacity of EVs in these months. Alternative renewable energy generation sources, such as micro wind turbines may be required to facilitate higher EV capacities in Winter.

For the houses equipped with solar PV panels and battery storage, the energy storage capacity of the battery can have a big impact on the number of electric vehicles that can be accommodated in the network. Six different battery capacities have been analysed: 0 kWh (no battery storage), 3 kWh, 7 kWh (the standard battery

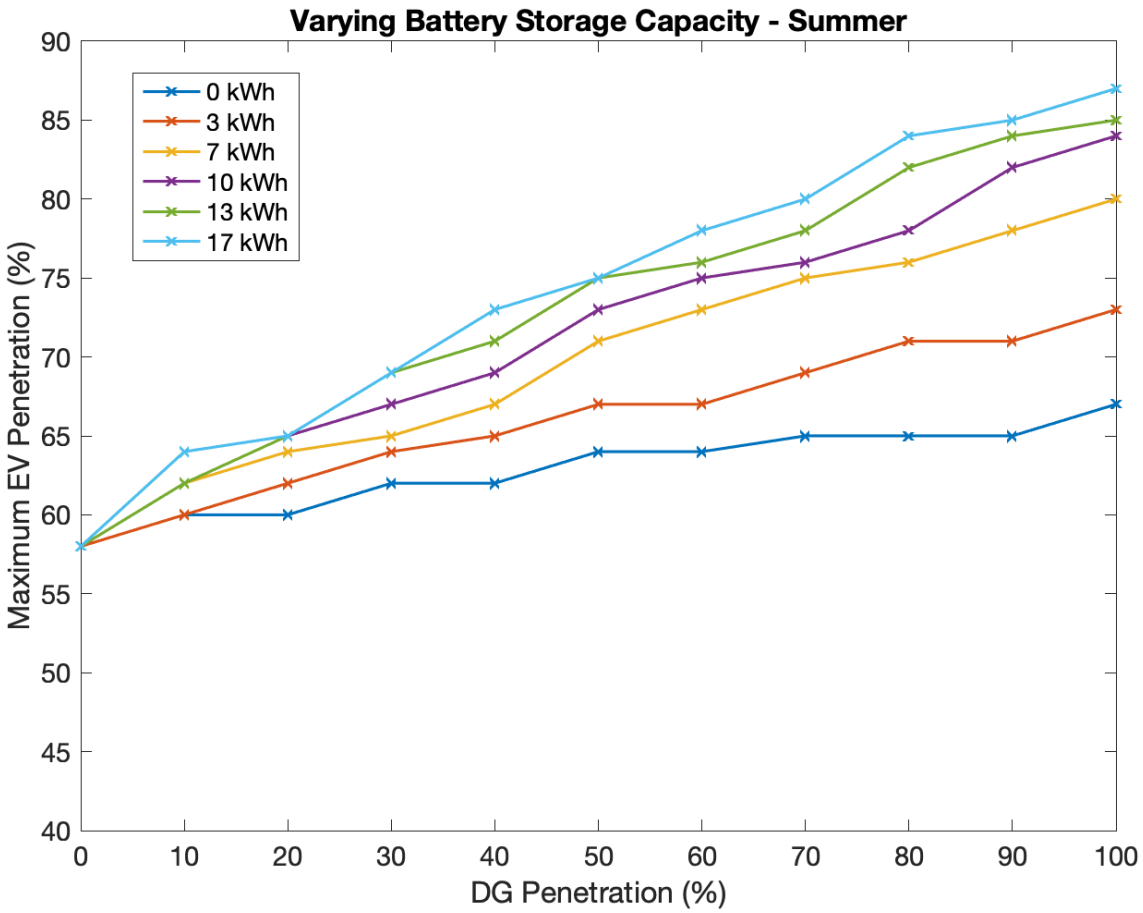

Figure 5.15: Varying the capacity of the house's installed battery if equipped with solar PV panels can have a big impact on the maximum EV hosting capacity in Summer

capacity used in other results), 10 kWh, 13 kWh and 17 kWh. Figures 5.15 and 5.16 show the calculated EV hosting capacity for the network as the installed battery capacity and DG penetration varies for Summer and Winter solar generation profiles, respectively. Increasing the installed battery capacity enables more of the generated solar power to be stored for later consumption, leading to a greater utilisation rate of the renewable energy and therefore a higher EV maximum penetration. In Summer, at 100% penetration of solar PV, the EV hosting capacity is increased from 67% with no battery storage to 87% with 17 kWh batteries, however there appears to be diminishing returns as the battery capacity increases - there is greater improvement in the EV hosting capacity going from 3 kWh to 7 kWh batteries than there is going from 13 kWh to 17 kWh.

The battery capacity plays a much smaller role in increasing the EV capacity in

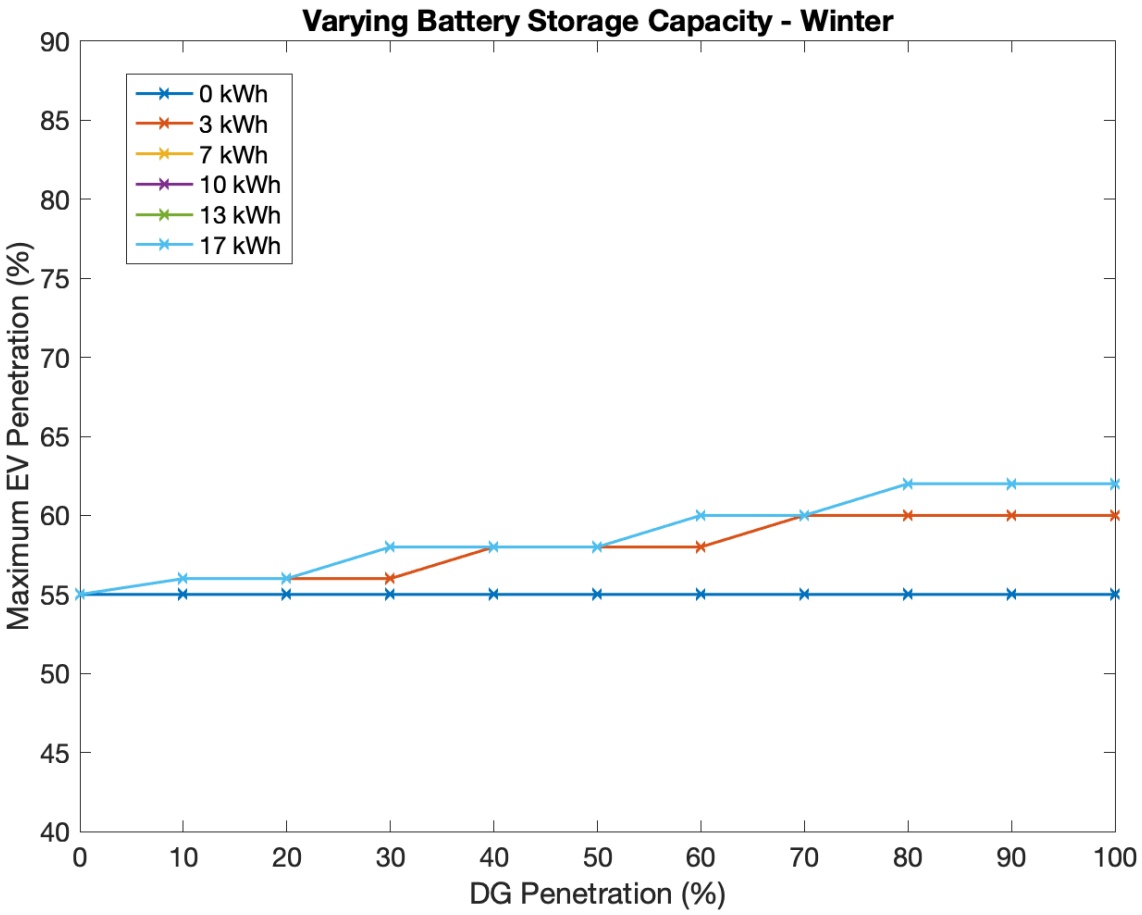

Figure 5.16: With Winter solar energy generation, the benefit of increasing the house's battery capacity on the EV capacity is reduced

Winter, as the lower solar energy production requires less storage for full utilisation of the energy, and as a result increasing the battery capacity beyond this has no benefit as all solar energy has already been consumed. It can be seen in Figure 5.16 that battery capacities of 7 kWh and above result in the same maximum EV penetration, while without any battery storage (0 kWh), the maximum EV penetration does not increase, even with 100% DG penetration. Further cost-benefit analysis would be required to determine the optimal battery capacity for the entire year - a large battery will have unused capacity in Winter, while a smaller battery cannot provide full benefit in Summer.

A DSO will also be interested in the network infrastructure impact on the maximum EV penetration. The first result analyses the effect of changing the transformer power and maximum line current ratings on the EV hosting capacity. This type of

study allows a DSO to analyse potential changes and upgrades to their network, and establish the most cost-effective upgrades that can be made in order to have greatest impact on the maximum EV penetration.

Figure 5.17 shows the maximum EV penetration, expressed as a percentage, as the line current limit and transformer power limits were increased. These results were calculated using Summer baseload and DG data with 50% of the houses equipped with solar PV panels and battery storage. Both the transformer and line current limits were increased from the original values in Section 5.4.1 by 25%, 50%, 100% and 200%, and the maximum EV penetration was calculated. It is shown that substantial increases in the EV hosting capacity can be achieved through upgrades to the network infrastructure, however both transformer and line current upgrades are required together to maximise the benefit of the upgrades. For example, if there is no increase in the maximum line current, even increasing the transformer rating by 200% only results in a 2% increase in EV hosting capacity. However, if both the transformer and current ratings are increased by 200%, the maximum penetration is increased by 25% to allow an EV capacity of 96% to be accommodated, enabling nearly all houses to fully charge an EV.

Finally, the locations of successful EV charging in the network are analysed. With a DG penetration of 50% and V2G, 1000 repeats of the Monte Carlo are run. At each repeat, the houses where EVs successfully reach a full SoC are recorded. Following completion of the Monte Carlo simulation, the number of repeats where each house's EV achieved a full charge is calculated. This enables the DSO to assess whether there are certain houses or stronger parts of the network which are always successful in charging their EV and whether the opposite is true and if there are weaker parts of the network which struggle to charge their EVs.

Figure 5.18 shows the layout of Network 1, with the locations of the houses marked by circles. The colour of each circle represents the percentage of the 1000 Monte Carlo repeats where the EV at that house was able to charge, as given in the key. It shows that the EV charging is distributed fairly evenly throughout the network,

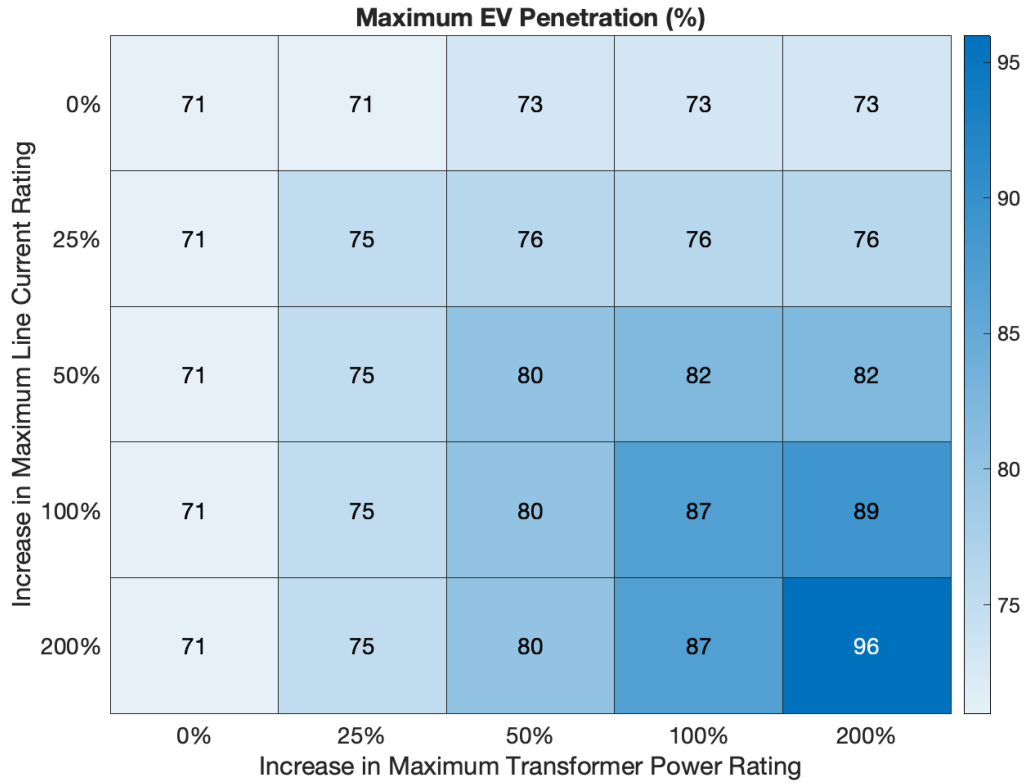

Figure 5.17: Increasing the maximum transformer power and line current ratings can have a substantial impact on the maximum EV penetration

with all houses achieving a full EV charge on at least 69% of the repeats, while the house with the highest EV charging success rate achieving full charge on 84% of the repeats. Comparing this with Figure 5.1 reveals that the houses with the lowest EV charging success are all connected to phase A of the network, and the houses with the highest charging success are those connected to phase C. This indicates potential unbalance between the phases, and a network operator may wish to repeat this analysis by modelling different phase connections to certain houses to see if this can further improve the network's EV hosting capacity.

5.5.5 Network 2: NIT Verification Results

Network 2 tests the performance of the proposed NIT approach for the EV hosting capacity calculation on a larger, multi-feeder network. The key result for this

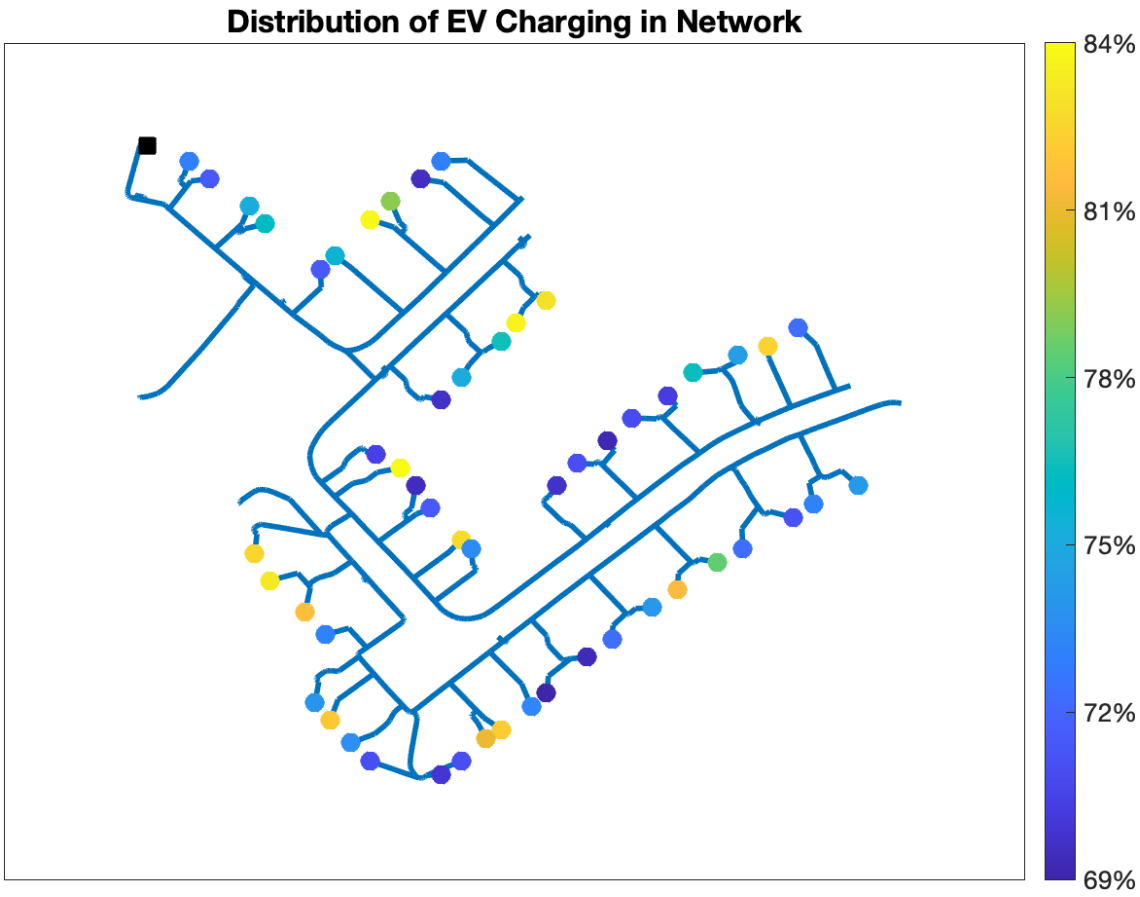

Figure 5.18: Colour coded map of Network 1 highlighting the houses with highest and lowest EV charging success from Monte Carlo simulation

network is the verification of the NIT approach results with those calculated by the Optimisation approach, as this accuracy underpins any subsequent analysis. While further analysis of the network can be carried out, as presented for Network 1 above, this section focuses solely on the verification results. For this multi-feeder network, the Network Impact Tokens and Network Impact Values are calculated across all houses on all feeders, whereas the Phase Impact Tokens and Phase Impact Values are calculated for houses on the individual phases of each feeder.

Figures 5.19-5.21 show histograms comparing the probability distribution of the calculated maximum EV penetration from 1000 repeats of the Monte Carlo simulation with 0%, 50% and 100% of houses equipped with solar PV and battery storage, respectively, in addition to the use of V2G in the 50% DG scenario. It can be seen that there is good accuracy between the Optimisation and NIT approaches,

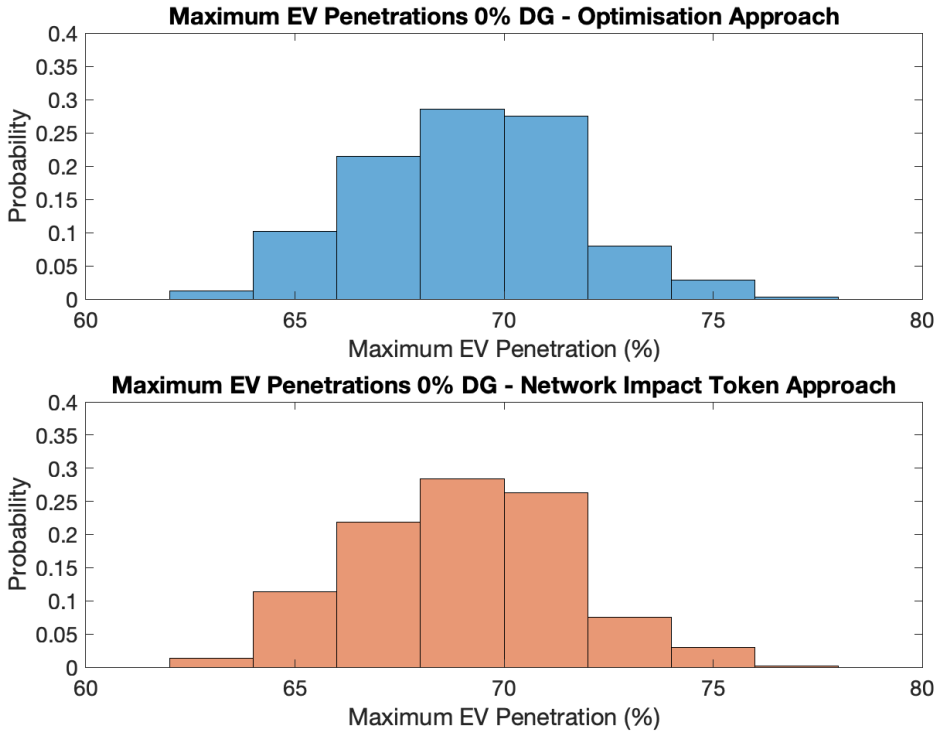

Figure 5.19: Distribution of maximum EV penetrations from Monte Carlo simulation for Network 2 without solar PV and battery storage

especially at lower penetrations of DG. Figure 5.19 shows that the NIT approach calculates almost identical maximum penetrations at each repeat of the Monte Carlo simulation as the Optimisation approach at 0% DG, however at 100% DG in Figure 5.21 there is minor overestimation of the maximum penetration.

Table 5.6 provides values of the overall maximum EV penetration calculated at each percentage of DG for both the Optimisation and Network Impact Token approaches. The data confirms that the NIT approach is most accurate at low penetrations of DG and overestimates at higher penetrations. This is similar to the behaviour with Network 1, however it appears more pronounced with this larger network. Despite this, the results maintain a good level of accuracy, with at most 2 percentage points difference between the two solutions, e.g. 83% vs 85% at 100% DG, although the results with V2G at the same penetration of DG are slightly less accurate. For this network, there is very similar accuracy in the results for both the 20^{th} and 30^{th} percentiles. Overall, this level of accuracy is likely to be sufficient for much of the

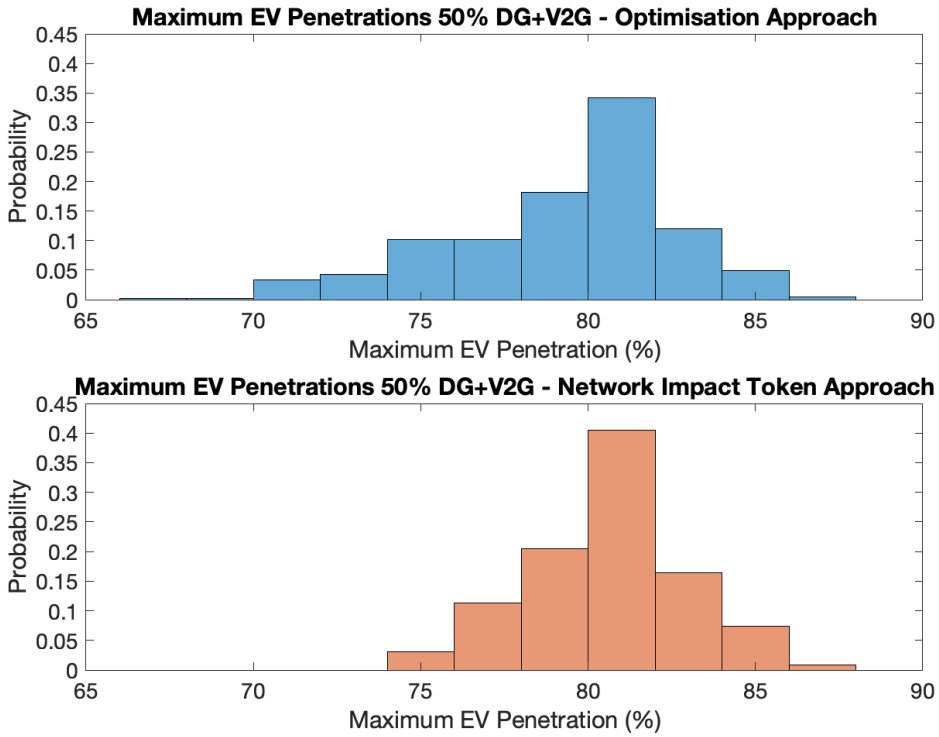

Figure 5.20: Distribution of maximum EV penetrations for Network 2 with 50% of houses equipped with solar PV, battery storage and the use of V2G

analysis that a network operator may wish to conduct, although future research could be conducted to improve the accuracy at these higher penetrations.

5.6 Conclusion

This chapter has introduced an optimisation problem that can accurately calculate the maximum EV hosting capacity of a low-voltage distribution network, while considering the integration of solar PV, battery storage, V2G and smart charging. Calculating the absolute maximum EV penetration results in a reliable and repeatable value that can be used for analysis and comparison, with there being no possible way that more EVs could be accommodated than is calculated here. A Monte Carlo simulation is used to simulate the maximum EV penetration under a wide variation of baseload, solar PV generation and EV charging conditions, which enables a reliable determination of the maximum EV penetration under real-world conditions.

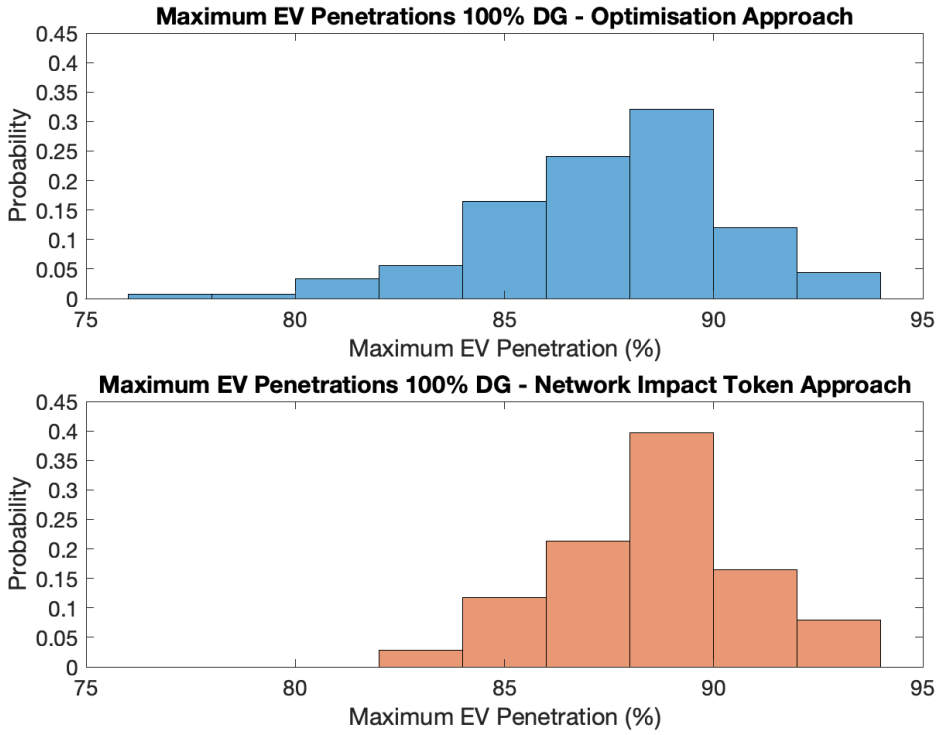

Figure 5.21: Distribution of maximum EV penetrations for Network 2 with 100% of houses equipped with solar PV and battery storage

The concept of Network Impact Tokens and Phase Impact Tokens introduced in Chapter 4 is then implemented here as an alternative to solving the voltage, current and power constraints in the original Optimisation problem. This approach ensures that the maximum EV penetration is calculated while adhering to the network limits, but moves the complexity of ensuring these constraints are met to the problem initialisation phase rather than the optimisation problem, dramatically increasing the time in which the maximum EV penetration can be calculated. It is shown that a 1000 repeat Monte Carlo on Network 1 with 50% of houses equipped with DG and the use of V2G can be solved 58 times faster using the NIT approach than the original Optimisation approach.

Comparison of the maximum EV penetration results calculated through the original Optimisation approach with those calculated by the NIT approach shows good levels of accuracy, especially at low-to-mid penetrations of solar panels and battery storage, although the NIT approach overestimates slightly at higher penetrations

Table 5.6: Network 2 verification of maximum EV penetration calculated by NIT approach

		Mean	Median	10^{th} PCTL	20^{th} PCTL	30^{th} PCTL
0% DG	Opt.	68.6%	68%	65%	67%	67%
	NIT	68.6%	68%	65%	67%	67%
25% DG	Opt.	74.1%	74%	71%	72%	73%
	NIT	74.1%	74%	71%	72%	73%
50% DG	Opt.	79.0%	79%	75%	77%	78%
	NIT	79.2%	79%	76%	77%	78%
100% DG	Opt.	86.9%	87%	83%	85%	86%
	NIT	88.1%	88%	85%	86%	87%
0% DG+V2G	Opt.	69.7%	70%	67%	68%	69%
	NIT	69.9%	70%	67%	68%	68%
25% DG+V2G	Opt.	75.0%	75%	72%	73%	74%
	NIT	75.3%	75%	72%	73%	74%
50% DG+V2G	Opt.	78.3%	80%	74%	76%	77%
	NIT	80.1%	80%	77%	78%	79%
100% DG+V2G	Opt.	85.6%	86%	81%	83%	84%
	NIT	88.5%	88%	85%	87%	87%

of DG. However, there is still close agreement between the results of both methods, which validates the NIT approach as a suitable and highly effective method for calculating the EV hosting capacity. This has been confirmed on both a small, single feeder network (Network 1), and also on a larger, multi-feeder network (Network 2), showing the reliability of the approach for DSOs to use on different types of network. Whilst the accuracy of the results shows the NIT approach is a valid method for calculating the maximum EV capacity, additional research into why overestimation at higher DG penetrations occurs could further improve the accuracy and confidence of the NIT approach.

The NIT approach enables fast calculation of a wide range of results for detailed analysis of the readiness of a network to host increasing numbers of EVs. These

include analysis of the effects of differing baseloads and solar generation between Summer and Winter on the EV capacity and the effect of increasing the number of houses equipped with solar PV, battery storage and V2G or battery storage capacity on the maximum EV penetration. The network hardware can also be assessed, with the change in EV penetration resulting from an increase in transformer power or maximum line current rating calculated. This can enable a DSO to perform cost-benefit analysis by identifying the most cost effective solutions to provide the greatest impact in EV hosting capacity. In addition, the Monte Carlo simulation can help identify the strongest and weakest parts of the network depending on the percentage of repeats in which each house is able to fully charge their EV. This can be useful in planning more targeted network upgrades to ensure every house receives fair access to the network.

Chapter 6

Conclusions

Adapting to the rapid increases in the uptake of electric vehicles and distributed renewable energy generation in low-voltage networks requires novel solutions in order to maximise both the benefits of these low-carbon technologies and their integration in existing networks. The primary contributions of this thesis are novel P2P trading approaches designed to increase the amount of renewable energy used for EV charging, and the amount of charging that can be accommodated in a distribution network.

Chapter 3 analyses P2P auction matching mechanisms for trading between houses and EVs for the scenario of matching visiting EVs to houses equipped with charge points and solar energy generation. As an EV does not wish to move once parked, and a house only has a single charge point, one-to-one matching is enforced, which means that the quality of the matching can have a significant impact on the EV charging completed using renewable energy, particularly as any future EV arrivals are not known.

Chapter 4 uses the load capacity of a network to introduce Network and Phase Impact Tokens. Adding a load to the network requires a house to possess a number of NITs and PITs, whereas adding generation will create new tokens. A P2P trading system is established between houses on the network to trade NITs and PITs, which manages the use of the network to ensures that it operates within its allowed power, current and voltage limits.

The Network Impact Token approach is further utilised in Chapter 5 as the fundamentals of an analytical tool for DSOs to evaluate the maximum EV penetration that their distribution networks can accommodate with the inclusion of solar PV generation, battery storage and V2G. The results are verified by an optimisation approach for two separate networks. Detailed analysis of one network is conducted, with the maximum EV hosting capacity found for a number of scenarios, including as the penetration of DG and battery storage capacity varies, for different seasons and with upgrades to the network hardware.

6.1 Achieved Research Goals

This section highlights the specific research objective from each chapter of this Thesis and the key contributions that have been made to achieve these goals.

6.1.1 Chapter 3

With the majority of EV charging taking place at home, significant numbers of home charge points are installed but are unused during the day when the home's own EV is away. Additionally, peak solar generation around mid-day typically coincides with the times of lowest baseload, meaning that expensive battery storage is required for a house to maximise the use of the renewable energy it generates. As public charge points cannot be booked by visiting EVs, home charge points offer a promising alternative, allowing EVs to guarantee charging in addition to a parking spot, which can be in high demand in urban centres. The visiting EVs can then benefit from the surplus solar generation produced during the day for the charging of their vehicle, while the home owner benefits by receiving income from the EV for the energy consumed and use of its charge point.

This scenario is presented as a matching problem for a P2P trading platform running every 15 minutes where the visiting EVs submit bids detailing the amount of charging

they require and the price they are willing to pay, and houses submit asks, consisting of their renewable energy generation forecast and the price they are willing to accept for the energy and use of their charge point. One-to-one matching is enforced as EVs do not wish to move once they are parked, and each house is only equipped with a single charge point. It is further assumed that the houses cannot sell energy amongst themselves on the grid. Under these conditions, once a house and EV have committed to a trade, the house cannot accept any more EV bids until the first EV has departed. As a result, the matching mechanism can have a significant impact on the performance of the system in terms of the amount of EV charging that can be fulfilled using solar energy and the overall consumption of the renewable energy.

The key research objectives were:

- To explore the use of vacant EV home charge points and surplus home solar energy generation to provide renewable energy charging for visiting EVs
- To maximise the amount of EV charging that is accomplished using renewable energy under the scenario where there is greater EV charging demand than renewable energy generation
- To develop an improved one-to-one matching mechanism that results in superior EV charging performance without any knowledge of future EV arrivals or energy requirements

A novel double auction matching mechanism, called Closest Energy Matching is proposed, which considers all bids and asks in the market to match each bid with the seller whose predicted solar generation provided the closest amount of energy to the EV's request and whose ask price was lower than the buyer's bid. This helps ensure that EVs receive the energy they need to complete their charging, while houses with greater predicted solar energy generation will increase their chance of being matched with an EV which will utilise more of their available energy.

The Closest Energy Matching mechanism is compared with four alternative double auction matching mechanisms and was found to enable the highest percentage of

EVs departing with their desired SoC from solar energy alone, and achieved up to a 70% reduction in grid energy required to fully charge the EVs, which is important when trying to maximise the number of EVs that could be accommodated in existing network infrastructure. In addition, greater consumption of solar energy resulted in the highest profit for sellers and lowest cost for buyers compared with the four other mechanisms.

6.1.2 Chapter 4

The rapid uptake of EVs is putting increasing pressure on low-voltage distribution networks to accommodate their charging. If left uncontrolled, the high power demand of EV charging can overwhelm networks, especially at peak times, such as when EV owners return from work and plug in their vehicles in the evening. In addition, the deployment of more distributed energy resources such as solar PV panels and battery storage can also problems for the grid through increased power injection. The operation of these new loads and generation resources can lead to networks exceeding their transformer power, line current and node voltage limits, which causes unsafe operation of the network and accelerated infrastructure failure.

The key research objectives of this Chapter were:

- To develop a method for quantifying the impact of different loads and energy generation on a distribution network
- To ensure that EV charging and renewable energy generation are managed without exceeding the network's power, current or voltage limits
- To present a decentralised approach for this network load and generation management that enables houses to retain autonomy over the use of their energy, without loss of privacy or the requirement of real-time monitoring or data collection

- To increase the number of EVs that are able to successfully charge within a distribution network

The impact of increasing power demand or generation at each house on both the entire network and the phase of the house is calculated by analysing the change in load capacity resulting from the change in demand or generation, with each house subsequently assigned Network and Phase Impact Values. Additionally, the total load capacity of the network and each phase before any limits are violated is calculated and expressed in terms of Network Impact Tokens and Phase Impact Tokens, respectively. Equating loads and generation to NITs and PITs through each house's Impact Values provides a method for quantifying the impact of energy demand or generation at each house on its phase and the entire network.

As houses must acquire the number of Impact Tokens equivalent to the load they wish to add to the network, the power demand from EV chargers and baseload can be managed. With the number of Impact Tokens available in the network equal to the amount of load that the network can accommodate, it is ensured that the power demand at any timestep does not exceed the permitted capacity of the network. Houses that inject power into the network through solar PV integration or battery discharging generate additional Impact Tokens for their phase and the network, which could permit further loads to be added.

A peer-to-peer trading platform is proposed which enables houses to trade the Network and Phase Impact Tokens that they are initially allocated corresponding to the network capacity and any new tokens created through energy generation amongst themselves. The markets run every ten minutes, giving houses the chance to purchase or sell Impact Tokens for use in the next timeslot. The predetermined quantity of allocated NITs and PITs and the consideration of the impact on the network of any energy generation and the corresponding number of generated Impact Tokens ensures that the network operates without exceeding the transformer power, line current or node voltage limits. This P2P trading approach provides houses

with more autonomy over the use of their loads, as if they wish to charge their EV sooner, they can purchase more Impact Tokens through the market to facilitate this. Additionally, even during times of high energy prices, houses are able to reduce their net cost or make profit through the trading of these Impact Tokens.

The approach is decentralised as houses make their own decisions about how to partake in the auction, and privacy is preserved as no load data needs to be shared. While bids and asks for Impact Tokens must be submitted, the entire process from the house determining its optimal energy usage strategy, submitting the bids or asks for any NITs or PITs, to the determination of successful trades in the market can be automated, which enables the bids and asks to be kept secret, and also provides simpler implementation. As the management of the network limits is achieved through the trading of Impact Tokens, no real-time monitoring or sensors are required to ensure that the network does not exceed its limits.

6.1.3 Chapter 5

With EVs set to push low-voltage distribution networks to their limits, it is important that network operators have the tools available to analyse their networks to determine their readiness for accommodating increasing numbers of EVs and plan upgrade programs to determine the most cost-effective ways to improve the hosting capacity of their networks. As renewable energy generation, battery storage and V2G can all impact the number of EVs that are able to recharge, it is important that these are all taken into account when assessing the maximum EV penetration that the network can accommodate.

The key research objectives of this Chapter were:

- To provide a novel approach to allow DSOs to assess the EV hosting capacity of their networks in conjunction with the use of renewable energy generation, battery storage and V2G

- To verify the accuracy and usefulness of the concept of NITs and PITs through their utilisation in determining the EV hosting capacity

Initially, an Optimisation approach was introduced to calculate the maximum penetration of EVs that could fully recharge in a distribution network, taking into account the generation and storage of solar energy. This approach provides an accurate result for the maximum EV penetration through inclusion of all energy resources and grid limits into the optimisation problem, however the complex constraints on the grid limits make this problem incredibly slow to solve. For rapid analysis of their networks under different conditions, DSOs would require a much faster approach.

By re-framing the optimisation problem in terms of the Impact Values and Impact Tokens, the complexity of ensuring that the grid operation remains within its allowable power, current and voltage limits is shifted to the initialisation stage where the network capacity is calculated, rather than during the calculation of the maximum EV penetration, which dramatically increases the speed at which the EV hosting capacity is calculated.

A Monte Carlo simulation is used to analyse the network under a variety of baseload conditions, EV energy and journey requirements and renewable energy generation profiles to calculate a more representative hosting capacity for the network that reflects real-world behaviour.

Comparison of the results calculated between the Optimisation approach and Network Impact Token approach for two different networks shows that the NIT approach generates accurate results which helps to verify the legitimacy of the Network and Phase Impact Token approach. Full analysis of one network is conducted to demonstrate how the NIT approach can be used to evaluate the maximum EV hosting capacity as the penetration of DG and battery storage capacity varies, the effect of different seasons and how the network can be analysed to identify the strongest phases and the impact of upgrading the transformer or lines on the maximum EV penetration to help inform the most cost-effective upgrades.

6.2 Future Research

6.2.1 Inclusion of Reactive Power into Impact Values/Tokens

The approach for calculating the Network Impact Values and subsequently the determination of the network capacity in terms of NITs and PITs currently assumes that all loads and generation operate at a unity power factor, without reactive power. While this assumption is accurate for modelling the injection of renewable energy generation or battery discharging to the grid and the charging of EVs, domestic baseload is typically modelled with a lagging power factor of around 0.95. In addition, a number of studies have examined the potential of EV chargers to operate at a non-unity power factor to provide voltage support to the network.

The process for determining the Network and Phase Impact Values could be expanded to include the voltage and current sensitivity matrices resulting from both active and reactive loads and generation in the network, and add additional Impact Values to include reactive generation and reactive load. Research would be needed to see whether this inclusion of loads and generation with different power factors has a significant impact on the performance and accuracy compared with treating all loads and generation as having a unity power factor. If implemented, the reactive power compensation that EV charge points can provide could also be considered in the NIT approach for calculating the maximum EV penetration of a network alongside DG and battery storage in Chapter 5.

6.2.2 Further Improvement to EV Charging Success in P2P Impact Token Approach

In the resource planning stage of the P2P trading of PITs and NITs, each house must determine its optimal usage of the available energy resources and when to

purchase NITs and PITs on the P2P market. This is done through the house determining the expected cost of NITs and PITs at each timestep to use in the cost minimisation problem. A time-of-use price signal was used in this study, with a three-times multiplier in price between 6pm and 10:30pm, and a six-times multiplier from 10:30pm until 7am. This was chosen to encourage houses to schedule EV charging earlier in the day when demand on the network is lower. Otherwise, most EV charging is scheduled to take place overnight, with the total demand exceeding the network capacity, preventing some EV charging from taking place and resulting in fewer EVs achieving their departure SoC goal. Implementing the ToU virtual price scheme has increased the number of EVs that achieve their SoC goal. Therefore, it is likely that additional changes could also increase the success rate of EV charging. Additional research into a machine learning technique for houses to learn from previous days trading the times when they are likely to be successful purchasing Impact Tokens and more accurate prices could further increase the success rate of EV charging.

6.2.3 Implementation of P2P Trading of Impact Tokens in Multi-Feeder Networks

Currently, the P2P trading of Network and Phase Impact Tokens has been implemented between houses on a single feeder distribution network. However, in reality, most networks consist of multiple feeders connected to the same transformer. Therefore, adaptations must be made to the approach to take into account that the total transformer loading is the sum of the load on all feeders. The calculation of the number of Network Impact Tokens available for the network based on the transformer loading capacity must be done including all feeders, and the trading of Network Impact Tokens would need to be conducted between all houses across all feeders, whereas the Phase Impact Tokens remain unique to each phase of each feeder, so separate markets would be necessary for each feeder.

6.2.4 Dealing with Error in Energy Usage Prediction and Missed Communication

It is assumed that each house is able to accurately predict its baseload, EV usage and renewable generation for the 24 hour period covered by the P2P trading scenario. While the sliding-window approach allows the house to alter their planned usage throughout the day if required, it is assumed that the following timestep is accurate. However, future research must give consideration to the situation that arises if a house agrees to sell a certain number of NITs or PITs in the next timestep but does not actually generate sufficient renewable energy to fulfil this, or if the house's baseload is actually different to its predicted value. Additionally, it is assumed that all communication between the house and the P2P market platform happens successfully, with houses able to compute their bids and asks in time for the respective auctions, whereas in reality the situation may exist where there is a loss of communication between the two entities, which could have a significant impact on the house's ability to use energy in the next timestep.

6.2.5 Improving the Accuracy of the NIT Approach for Calculating the Maximum EV Penetration at Higher Penetrations of DG

In Chapter 5 it is seen that the results calculated by the NIT approach are most accurate at lower penetration of DG when comparing to the Optimisation approach results, with it typically overestimating the maximum EV penetration at higher penetrations of DG. Further research is required to understand why this overestimation occurs, and adapt the approach to improve the accuracy at all penetrations of DG.

Bibliography

[1] Ofgem. (May 2021). One in four consumers plan to buy an electric car in next five years according to Ofgem reserach, https://www.ofgem.gov.uk/publications/one-four-consumers-plan-buy-electric-car-next-five-years-according-ofgem-research.

[2] UK Government. (Nov. 2020). Government takes historic step towards net-zero with end of sale of new petrol and diesel cars by 2030, https://www.gov.uk/government/news/government-takes-historic-step-towards-net-zero-with-end-of-sale-of-new-petrol-and-diesel-cars-by-2030.

[3] Deloitte Insights, 'Electric vehicles: Setting a course for 2030', Deloitte, Jul. 2020, https://www2.deloitte.com/us/en/insights/focus/future-of-mobility/electric-vehicle-trends-2030.html.

[4] Intergovernmental Panel on Climate Change (IPCC), 'Summary for policymakers', in *Climate Change 2021: The Physical Science Basis. Contribution of Working Group I to the Sixth Assessment Report of the Intergovernmental Panel on Climate Change*, Cambridge University Press, Aug. 2021.

[5] A. Mobius and J. Kroll. (Feb. 2021). How do greenhouse gases trap heat in the atmosphere?,

https://climate.mit.edu/ask-mit/how-do-greenhouse-gases-trap-heat-atmosphere.

[6] Our World in Data. (Aug. 2020). Co_2 and greenhouse gas emissions, https://ourworldindata.org/co2-and-other-greenhouse-gas-emissions.

[7] Department for Transport, 'Transport and environment statistics - 2021 annual report', UK Government, May 2021, https://www.gov.uk/government/statistics/transport-and-environment-statistics-2021.

[8] D. Hirst, J. Winnett and S. Hinson, 'Electric vehicles and infrastructure', House of Commons Library, Jun. 2021, https://commonslibrary.parliament.uk/research-briefings/cbp-7480/.

[9] G. Bieker, 'A global comparison of the life-cycle greenhouse gas emissions of combustion engine and electric passenger cars', The International Council on Clean Transportation, Jul. 2021.

[10] Ofgem. (Jul. 2021). Wholesale market indicators, https://www.ofgem.gov.uk/energy-data-and-research/data-portal/wholesale-market-indicators.

[11] UNFCCC, 'Paris agreement', Framework Convention on Climate Change, 2015.

[12] Climate Change Committee, 'Sixth carbon budget', CCC, Dec. 2020, https://www.theccc.org.uk/publication/sixth-carbon-budget/.

[13] Reuters. (Jan. 2021). Electric cars rise to record 54% market share in Norway in 2020, Reuters, https://www.reuters.com/world/europe/electric-cars-rise-record-54-market-share-norway-2020-2021-01-05/.

[14] Mercedes Benz. (2021). The New EQS from Mercedes EQ, https://www.mercedes-benz.co.uk/passengercars/mercedes-benz-cars/models/eqs/saloon-v297/pad/stage.module.html.

[15] Department for Transport, 'Transport Statistics: Great Britain 2019', Dec. 2019, https://www.gov.uk/government/statistics/transport-statistics-great-britain-2019.

[16] Office for National Statistics. (Jan. 2019). Table a47: Percentage of households with ars by income group, tenure and household composition, https://www.ons.gov.uk/peoplepopulationandcommunity/personalandhouseholdfinances/expenditure/datasets/percentageofhouseholdswithcarsbyincomegrouptenureandhouseholdcompositionuktable

[17] Department for Transport, 'Statistical dataset - veh1153: Cars registered for the first time by propulsion and fuel type: Great Britain and United Kingdom', UK Government, Jul. 2021, https://www.gov.uk/government/statistical-data-sets/vehicle-licensing-statistics-data-tables.

[18] ——, 'Statistical Dataset - VEH0203: Licensed cars by propulsion or fuel type: Great Britain and United Kingdom', UK Government, May 2021.

[19] BloombergNEF. (Dec. 2020). Batteries for electric cars speed toward a tipping point, https://www.bloomberg.com/news/articles/2020-12-16/electric-cars-are-about-to-be-as-cheap-as-gas-powered-models.

[20] T. Wills, 'The UK's transition to electric vehicles', Climate Change Committee, Dec. 2020.

[21] ALD Automotive. (Mar. 2018). Over three quarters of daily journeys could be completed using an electric car, https://www.aldautomotive.co.uk/news/over-three-quarters-of-daily-journeys-could-be-completed-using-an-electric-car.

[22] Department for Transport, 'Statistical Dataset - NTS0308a: Average number of trips by trip length and main mode: England, from 2002', UK Government, Aug. 2020, https://www.gov.uk/government/collections/national-travel-survey-statistics.

[23] Competition and Markets Authority. (Aug. 2021). Electric vehicle charging: CMA finds more needs to be done, https://competitionandmarkets.blog.gov.uk/2021/08/04/electric-vehicle-charging-cma-finds-more-needs-to-be-done/.

[24] Energy Saving Trust, 'Charging electric vehicles: Getting the best out of electric vehicle batteries, home and public chargepoints and maximising savings', Apr. 2019.

[25] Office for Zero Emission Vehicles, 'Electric vehicle homecharge scheme: Guidance for customers', UK Government, Mar. 2021, https://www.gov.uk/government/publications/customer-guidance-electric-vehicle-homecharge-scheme.

[26] Department for Transport, 'Statistical Dataset - NTS0901: Annual mileage of cars by ownership and trip purpose: England since 2002', UK Government, Aug. 2020, https://www.gov.uk/government/statistical-data-sets/nts09-vehicle-mileage-and-occupancy.

[27] A. D. S. Jennings R. Parkin, 'Charging ahead!', PWC, Apr. 2018, https://www.pwc.co.uk/industries/power-utilities/insights/electric-vehicle-infrastructure-report-april-2018.html.

[28] Oxford City Council. (Nov. 2019). Oxford trials world's first residential 'pop-up' on-street electric vehicle charging points, https://www.oxford.gov.uk/news/article/1246/oxford_trials_world_s_first_residential_pop-up_on-street_electric_vehicle_charging_points.

[29] Siemens. (Mar. 2020). Siemens unveils UK's first converted 'Electric Avenue', https://news.siemens.co.uk/news/siemens-unveils-uks-first-converted-electric-avenue.

[30] Co Charger. (2021). Co Charger, https://co-charger.com.

[31] BEAMA, 'A guide to electric vehicle infrastructure', Apr. 2015, https://www.beama.org.uk/resourceLibrary/beama-guide-to-electric-vehicle-infrastructure.html.

[32] International Electrotechnical Commission, 'IEC 61851-1:2017', Feb. 2017.

[33] A. Tomaszewska, Z. Chu, X. Feng *et al.*, 'Lithium-ion battery fast charging: A review', *eTransportation*, vol. 6, p. 100 011, Nov. 2020.

[34] National Grid ESO. (2021). Frequency response services, https://www.nationalgrideso.com/industry-information/balancing-services/frequency-response-services.

[35] National Grid. (2021). Network and infrastructure, https://www.nationalgrid.com/uk/electricity-transmission/network-and-infrastructure.

[36] M. Liu, P. K. Phanivong, Y. Shi and D. S. Callaway, 'Decentralized charging control of electric vehicles in residential distribution networks', *IEEE Transactions on Control Systems Technology*, vol. 27, no. 1, pp. 266–281, Jan. 2019.

[37] J. de Hoog, T. Alpcan, M. Brazil, D. A. Thomas and I. Mareels, 'A market mechanism for electric vehicle charging under network constraints', *IEEE Transactions on Smart Grid*, vol. 7, no. 2, pp. 827–836, Mar. 2016.

[38] J. Quirós-Tortós, L. F. Ochoa, S. W. Alnaser and T. Butler, 'Control of EV charging points for thermal and voltage management of LV networks', *IEEE Transactions on Power Systems*, vol. 31, no. 4, pp. 3028–3039, Jul. 2016.

[39] S. Khushalani, J. M. Solanki and N. N. Schulz, 'Development of three-phase unabalanced power flow using PV and PQ models for distributed generation and study of the impact of DG models', *IEEE Transactions on Power Systems*, vol. 22, no. 3, pp. 1019–1025, Aug. 2007.

[40] M. F. Shaaban and E. F. El-Saadany, 'Accommodating high penetrations of PEVs and renewable DG considering uncertainties in distribution systems', *IEEE Transactions on Power Systems*, vol. 29, no. 1, pp. 259–270, Jan. 2014.

[41] P. Papadopoulos, S. Skarvelis-Kazakos, I. Grau, L. M. Cipcigan and N. Jenkins, 'Electric vehicles' impact on British distribution networks', *IET Electrical Systems in Transportation*, vol. 2, pp. 91–102, Mar. 2012.

[42] T. Gönen, *Modern power system analysis*. Wiley-Interscience, 1987.

[43] W. H. Kersting, *Distribution system modeling and analysis*. CRC Press, 2001.

[44] X. Luo and K. W. Chan, 'Real-time scheduling of electric vehicles charging in low-voltage residential distribution systems to minimise power losses and improve voltage profile', *IET Generation, Transmission & Distribution*, vol. 8, no. 3, pp. 516–529, May 2014.

[45] S. Deb, A. K. Goswami, P. Harsh, J. P. Sahoo, R. L. Chetri, R. Roy and A. S. Shekhawat, 'Charging coordination of plug-in electric vehicle for congestion management in distribution system integrated with renewable energy sources', *IEEE Transactions on Industry Applications*, vol. 56, no. 5, pp. 5452–5462, Oct. 2020.

[46] EPRI. (2008). The green grid: Energy savings and carbon emissions reductions enabled by a smart grid, `https://www.epri.com/research/products/1016905`.

[47] Western Power, 'DNO transition to DSO', Feb. 2020.

[48] V. Behravesh, R. Keypour and A. A. Foroud, 'Control strategy for improving voltage quality in residential power distribution network consisting of roof-top photovoltaic-wind hybrid systems, battery storage and electric vehicles', *Solar Energy*, vol. 182, pp. 80–95, Apr. 2019.

[49] L. Novoa and J. Brouwer, 'Dynamics of an integrated solar photovoltaic and battery storage nanogrid for electric vehicle charging', *Journal of Power Sources*, vol. 399, pp. 166–178, Sep. 2018.

[50] M. J. E. Alam, K. M. Muttaqi and D. Sutanto, 'An approach for online assessment of rooftop solar PV impacts on low-voltage distribution networks', *IEEE Transactions on Sustainable Infrastructure*, vol. 5, no. 2, pp. 663–672, Apr. 2014.

[51] S. M. Ismael, S. H. E. A. Aleem, A. Y. Abdelaziz and A. F. Zobaa, 'State-of-the-art of hosting capacity in modern power systems with distributed generation', *Renewable Energy*, vol. 130, pp. 1002–1020, Jan. 2019.

[52] S. Faddel and O. A. Mohammed, 'Automated distributed electric vehicle controller for residential demand side management', *IEEE Transactions on Industry Applications*, vol. 55, no. 1, pp. 16–25, Feb. 2019.

[53] A. Dubey and S. Santoso, 'Electric vehicle charging on residential distribution systems: Impacts and mitigations', *IEEE Access*, vol. 3, pp. 1871–1893, 2015.

[54] M. H. K. Tushar, C. Assi, M. Maier and M. F. Uddin, 'Smart microgrids: Optimal joint scheduling for electric vehicles and home appliances', *IEEE Transactions on Smart Grid*, vol. 5, no. 1, pp. 239–250, Jan. 2014.

[55] N. G. Paterakis, O. Erdinç, I. N. Pappi, A. G. Bakirtzis and J. P. S. Catalão, 'Coordinated operation of a neighborhood of smart households comprising electric vehicles, energy storage and distributed generation', *IEEE Transactions on Smart Grid*, vol. 7, no. 6, pp. 2736–2747, Nov. 2016.

[56] M. R. Mozafar, M. H. Moradi and M. H. Amini, 'A simultaneous approach for optimal allocation of renewable energy sources and electric vehicle charging stations in smart grids based on improved GA-PSO algorithm', *Sustainable Cities and Society*, vol. 32, pp. 627–637, Jul. 2017.

[57] RAC. (Jun. 2020). Electric car owners were just paid to charge their cars with excess power, `https://www.rac.co.uk/drive/news/motoring-news/electric-car-owners-were-just-paid-to-charge-their-cars-with-excess-power/`.

[58] M. J. E. Alam, K. M. Muttaqi and D. Sutanto, 'A controllable local peak-shaving strategy for effective utilization of PEV battery capacity for distribution network support', *IEEE Transactions on Industry Applications*, vol. 51, no. 3, pp. 2030–2037, May 2015.

[59] E. L. Karfopoulos and N. D. Hatziargyriou, 'Distributed coordination of electric vehicles providing V2G services', *IEEE Transactions on Power Systems*, vol. 31, no. 1, pp. 329–338, Jan. 2016.

[60] Y. Mu, J. Wu, J. Ekanayake, N. Jenkins and H. Jia, 'Primary frequency response from electric vehicles in the great british power system', *IEEE Transactions on Smart Grid*, vol. 4, no. 2, pp. 1142–1150, Jun. 2013.

[61] V. Monteiro, B. Exposto, J. C. Ferreira and J. L. Alfonso, 'Improved vehicle-to-home (iV2H) operation mode: Experimental analysis of the electric vehicle as off-line UPS', *IEEE Transactions on Smart Grid*, vol. 8, no. 6, pp. 2702–2711, Nov. 2017.

[62] M. Carrión, R. Zárate-Miñano and R. Domínguez, 'Integration of electric vehicles in low-voltage distribution networks considering voltage management', *Energies*, vol. 13, pp. 4125–4147, 2020.

[63] EA Technology, 'My electric avenue: Summary report', My Electric Avenue, 2016.

[64] Electric Nation, 'Summary of the findings of the Electric Nation smart charging trial', 2019.

[65] M. H. Mobarak and J. Bauman, 'Vehicle-directed smart charging strategies to mitigate the effect of long-range EV charging on distribution transformer aging', *IEEE Transactions on Transportation Electrification*, vol. 5, no. 4, pp. 1097–1111, Dec. 2019.

[66] UK Government, *Automated and electric vehicles act 2018*, 2018, `https://www.legislation.gov.uk/ukpga/2018/18/contents/enacted`.

[67] C. S. Antúnez, J. F. Franco, M. J. Rider and R. Romero, 'A new methodology for the optimal charging coordination of electric vehicles considering vehicle-to-grid technology', *IEEE Transactions on Sustainable Energy*, vol. 7, no. 2, pp. 596–607, Apr. 2016.

[68] J. Hu, S. You, M. Lind and J. Østergaard, 'Coordinated charging of electric vehicles for congestion prevention in the distribution grid', *IEEE Transactions on Smart Grid*, vol. 5, no. 2, pp. 703–711, Mar. 2014.

[69] W. Sun, F. Neumann and G. P. Harrison, 'Robust scheduling of electric vehicle charging in LV distribution networks under uncertainty', *IEEE Transactions on Industry Applications*, vol. 56, no. 5, pp. 5785–5795, Oct. 2020.

[70] R. Mehta, D. Srinivasan, A. M. Khambadkine, J. Yang and A. Trivedi, 'Smart charging strategies for optimal integration of plug-in electric vehicles within existing distribution system infrastructure', *IEEE Transactions on Smart Grid*, vol. 9, no. 1, pp. 299–312, Jan. 2018.

[71] N. I. Nimalsiri, C. P. Mediwaththe, E. L. Ratnam, M. Shaw, D. B. Smith and S. K. Halgamuge, 'A survey of algorithms for distributed charging control of electric vehicles in smart grid', *IEEE Transactions on Intelligent Transportation Systems*, vol. 21, no. 11, pp. 4497–4515, Nov. 2020.

[72] S. Faddel, T. Youssef, A. T. Elsayed and O. A. Mohammed, 'An automated charger for large-scale adoption of electric vehicles', *IEEE Transactions on Transportation Electrification*, vol. 4, no. 4, pp. 971–984, Dec. 2018.

[73] S. Pal and R. Kumar, 'Electric vehicle scheduling strategy in residential demand response programs with neighbor connection', *IEEE Transactions on Industrial Informatics*, vol. 14, no. 3, pp. 980–988, Mar. 2018.

[74] Y. He, B. Venkatesh and L. Guan, 'Optimal scheduling for charging and discharging of electric vehicles', *IEEE Transactions on Smart Grid*, vol. 3, no. 3, pp. 1095–1105, Sep. 2012.

[75] E. R. Muñoz, G. Razeghi, L. Zhang and F. Jabbari, 'Electric vehicle charging algorithms for coordination of the grid and distribution transformer levels', *Energy*, vol. 113, pp. 930–942, 2016.

[76] H. Xing, M. Fu, Z. Lin and Y. Mou, 'Decentralized optimal scheduling for charging and discharging of plug-in electric vehicles in smart grids', *IEEE Transactions on Power Systems*, vol. 31, no. 5, pp. 4118–4126, Sep. 2016.

[77] O. Beaude, S. Lasaulce, M. Hennebel and I. Mohand-Kaci, 'Reducing the impact of EV charging operations on the distribution network', *IEEE Transactions on Smart Grid*, vol. 7, no. 6, pp. 2666–2679, Nov. 2016.

[78] M. R. Sarker, M. A. Ortega-Vazquez and D. S. Kirschen, 'Optimal coordination and scheduling of demand response via monetary incentive', *IEEE Transactions on Smart Grid*, vol. 6, no. 3, pp. 1341–1352, May 2015.

[79] L. Hua, J. Wang and C. Zhou, 'Adaptive electric vehicle charging coordination on distribution network', *IEEE Transactions on Smart Grid*, vol. 5, no. 6, pp. 2666–2675, Nov. 2014.

[80] B. Sun, Z. Huang, X. Tan and D. H. K. Tsang, 'Optimal scheduling for electric vehicle charging with discrete charging levels in distribution grid', *IEEE Transactions on Smart Grid*, vol. 9, no. 2, pp. 624–634, Mar. 2018.

[81] H. N. T. Nguyen, C. Zhang and M. A. Mahmud, 'Optimal coordination of G2V and V2G to support power grids with high penetration of renewable energy', *IEEE Transactions on Transportation Electrification*, vol. 1, no. 2, pp. 188–195, Aug. 2015.

[82] Y. Mou, H. Xing, Z. Lin and M. Fu, 'Decentralized optimal demand-side management for PHEV charging in a smart grid', *IEEE Transactions on Smart Grid*, vol. 6, no. 2, pp. 726–735, Mar. 2015.

[83] A. Bilh, K. Naik and R. El-Shatshat, 'A novel online charging algorithm for electric vehicles under stochastic net-load', *IEEE Transactions on Smart Grid*, vol. 9, no. 3, pp. 1787–1799, May 2018.

[84] L. Gan, U. Topcu and S. H. Low, 'Optimal decentralized protocol for electric vehicle charging', *IEEE Transactions on Power Systems*, vol. 28, no. 2, pp. 940–951, May 2013.

[85] M. S. Islam, N. Mithulananthan and K. Y. Lee, 'Development of impact indices for performing charging of a large EV population', *IEEE Transactions on Vehicular Technology*, vol. 67, no. 2, pp. 866–880, Feb. 2018.

[86] R. Lamedica, A. Geri, F. M. Gatta, S. Sangiovanni, M. Maccioni and A. Ruvio, 'Integrating electric vehicles in microgrids: Overview on hosting capacity and new controls', *IEEE Transactions on Industry Applications*, vol. 55, no. 6, pp. 7338–7346, Dec. 2019.

[87] T. Morstyn, A. Teytelboym and M. D. McCulloch, 'Matching markets with contracts for electric vehicle smart charging', in *2018 IEEE Power Energy Society General Meeting (PESGM)*, Portland, OR, USA, Aug. 2018, pp. 1–5.

[88] L. Zhang, F. Jabbari, T. Brown and S. Samuelsen, 'Coordinating plug-in electric vehicle charging with electric grid: Valley filling and target load following', *Journal of Power Sources*, vol. 267, pp. 584–597, 2014.

[89] L. Wang, S. Sharkh and A. Chipperfield, 'A*-based optimal coordination of vehicle-to-grid batteries and renwable generators in a distribution network', in *2017 IEEE 26th International Symposium on Industrial Electronics (ISIE)*, Edinburgh, UK, Jun. 2017.

[90] S. Xie, W. Zhong, K. Xie, R. Yu and Y. Zhang, 'Fair energy scheduling for vehicle-to-grid networks using adaptive dynamic programming', *IEEE Transactions on Neural Networks and Learning Systems*, vol. 27, no. 8, pp. 1697–1707, Aug. 2016.

[91] R. Wang, P. Wang and G. Xiao, 'Two-stage mechanism for massive electric vehicle charging involving renewable energy', *IEEE Transactions on Vehicular Technology*, vol. 65, no. 6, pp. 4159–4171, Jun. 2016.

[92] F. Rassaei, W.-S. Soh and K.-C. Chua, 'Distributed scalable autonomous market-based demand response via residential plug-in electric vehicles in smart grids', *IEEE Transactions on Smart Grid*, vol. 9, no. 4, pp. 3281–3290, Jul. 2018.

[93] M. R. Islam, H. Lu, M. J. Hossain and L. Li, 'Optimal coordination of electric vehicles and distributed generators for voltage unbalance and neutral current compensation', *IEEE Transactions on Industry Applications*, vol. 57, no. 1, pp. 1069–1080, Feb. 2021.

[94] J. Wang, G. R. Bharati, S. Puadyal, O. Ceylan, B. P. Bhattarai and K. S. Myers, 'Coordinated electric vehicle charging with reactive power support to distribution grids', *IEEE Transactions on Industrial Informatics*, vol. 15, no. 1, pp. 54–63, Jan. 2019.

[95] M. Mazumder and S. Debbarma, 'EV charging stations with a provision of V2G and voltage support in a distribution network', *IEEE Systems Journal*, vol. 15, no. 1, pp. 662–671, Mar. 2021.

[96] Z. Xie, W. Qi, C. Huang and H. Li, 'Effect analysis of EV optimal charging on DG integration in distribution network', in *2019 IEEE 8th International Conference on Advanced Power System Automation and Protection (APAP)*, Xi'an,China, Oct. 2019.

[97] D. van der Meer, G. R. C. Mouli, G. M.-E. Mouli, L. R. Elizondo and P. Bauer, 'Energy management system with PV power forecast to optimally charge EVs at the workplace', *IEEE Transactions on Industrial Informatics*, vol. 14, no. 1, pp. 311–320, Jan. 2018.

[98] Y. Zhang and L. Cai, 'Dynamic charging scheduling for EV parking lots with photovoltaic power system', *IEEE Access*, vol. 6, pp. 56 995–57 005, Oct. 2018.

[99] H. Turker and S. Bacha, 'Optimal minimization of plug-in electric vehicle charging cost with vehicle-to-home and vehicle-to-grid concepts', *IEEE Transactions on Vehicular Technology*, vol. 67, no. 11, pp. 10 281–10 292, Nov. 2018.

[100] J.-H. Teng, S.-H. Liao and C.-K. Wen, 'Design of a fully decentralized controlled electric vehicle charger for mitigating charging impact on power grids', *IEEE Transactions on Industry Applications*, vol. 53, no. 2, pp. 1497–1505, Apr. 2017.

[101] S. Shao, M. Pipattanasomporn and S. Rahman, 'Grid integration of electric vehicles and demand response with customer choice', *IEEE Transactions on Smart Grid*, vol. 3, no. 1, pp. 543–550, Mar. 2012.

[102] L. Wang, J. Kwon, O. Verbas, A. Rousseau and Z. Zhou, 'Charging station planning to maximize extra load hosting capacity in unbalanced distribution system', in *2020 IEEE Power & Energy Society General Meeting (PESGM)*, Montreal, QC, Canada, Aug. 2020.

[103] G. Ravarino, A. Galati, C. A. Baquedano, L. Consiglio and G. Licasale, 'Distribution planning methodology for network integration of EV', in *CIRED Porto Workshop 2022: E-mobility and power distribution systems*, Porto, Portugal, Jun. 2022, pp. 142–146.

[104] V. Aravinthan and W. Jewell, 'Controlled electric vehicle charging for mitigating impacts on distribution assets', *IEEE Transactions on Smart Grid*, vol. 6, no. 2, pp. 999–1009, Mar. 2015.

[105] A. Zaidi, K. Sunderland and M. Conlon, 'Impact assessment of high-power domestic EV charging proliferation of a distribution network', *IET Generation, Transmission & Distribution*, vol. 14, no. 24, pp. 5918–5926, Dec. 2020.

[106] C. Dimas, G. Ramos, L. Caro and A. C. Luna, 'Parallel computing and multicore platform to assess electric vehicle hosting capacity', *IEEE Transactions on Industry Applications*, vol. 56, no. 5, pp. 4709–4717, Oct. 2020.

[107] J. Zhao, J. Wang, Z. Xu, C. Wang, C. Wan and C. Chen, 'Distribution network electric vehicle hosting capacity maximization: A chargeable region optimization model', *IEEE Transactions on Power Systems*, vol. 32, no. 5, pp. 4119–4130, Sep. 2017.

[108] A. S. B. Humayd and K. Bhattacharya, 'A novel framework for evaluating maximum PEV penetration into distribution systems', *IEEE Transactions on Smart Grid*, vol. 9, no. 4, pp. 2741–2751, Jul. 2018.

[109] P. Paudyal, S. Ghosh, S. Veda, D. Tiwari and J. Desai, 'EV hosting capacity analysis on distribution grids', in *2021 IEEE Power & Engineering Society General Meeting (PESGM)*, Washington DC, USA, Jul. 2021.

[110] S. Cundeva, A. K. Mateska and M. H. J. Bollen, 'Hosting capacity of LV residential grid for uncoordinated EV charging', in *2018 18th International*

Conference on Harmonics and Quality of Power (ICHQP), Ljubljana, Slovenia, May 2018.

[111] M. F. Shaaban, Y. M. Atwa and E. F. El-Saadany, 'PEVs modeling and impacts mitigation in distribution networks', *IEEE Transactions on Power Systems*, vol. 28, no. 2, pp. 1122–1131, May 2013.

[112] E. C. da Silva, O. D. Melgar-Dominguez and R. Romero, 'Simultaneous distributed generation and electric vehicles hosting capacity assessment in electric distribution systems', *IEEE Access*, vol. 9, pp. 110 927–110 939, Aug. 2021.

[113] Q. Deng, Y. Wang, F. Wen, W. Zheng, P. Dai and Y. Zhang, 'Investigation on the accommodation capability of a distribution system for electric vehicles considering system flexibility', in *2019 IEEE PES Innovative Smart Grid Technologies Asia*, Chengdu, China, May 2019, pp. 3663–3668.

[114] A. Rabiee, A. Keane and A. Soroudi, 'Enhanced transmission and distribution network coordination to host more electric vehicles and PV', *IEEE Systems Journal*, vol. 16, no. 2, Jun. 2022.

[115] M. Kamruzzaman, X. Zhang, M. Abdelmalak, M. Benidris and D. Shi, 'A method to evaluate the maximum hosting capacity of power systems to electric vehicles', in *2020 International Conference on Probabilistic Methods Applied to Power Systems (PMAPS)*, 2020.

[116] W. Tushar, T. K. Saha, C. Yuen, D. Smith and H. V. Poor, 'Peer-to-peer trading in electricity networks: An overview', *IEEE Transactions on Smart Grid*, vol. 11, no. 4, pp. 3185–3200, Jul. 2020.

[117] S. Wang, A. F. Taha, J. Wang, K. Kvaternik and A. Hahn, 'Energy crowdsourcing and peer-to-peer energy trading in blockchain-enabled smart grids', *IEEE Transactions on Systems, Man, and Cybernetics: Systems*, vol. 49, no. 8, pp. 1612–1623, Aug. 2019.

[118] P. Shamsi, H. Xie, A. Longe and J.-Y. Joo, 'Economic dispatch for an agent-based community microgrid', *IEEE Transactions on Smart Grid*, vol. 7, no. 5, pp. 2317–2324, Sep. 2016.

[119] E.ON Energy. (2021). Smart export guarantee, `https://www.eonenergy.com/smart-export-guarantee.html`.

[120] M. R. Alam, M. St-Hilaire and T. Kunz, 'Peer-to-peer energy trading among smart homes', *Applied Energy*, vol. 238, pp. 1434–1443, Mar. 2019.

[121] N. Liu, X. Yu, C. Wang, C. Li, L. Ma and J. Lei, 'Energy-sharing model with price-based demand response for microgrids of peer-to-peer prosumers', *IEEE Transactions on Power Systems*, vol. 32, no. 5, pp. 3569–3583, Sep. 2017.

[122] N. Liu, X. Yu, C. Wang and J. Wang, 'Energy sharing management for microgrids with PV prosumers: A stackleberg game approach', *IEEE Transcations on Industrial Informatics*, vol. 13, no. 3, pp. 1088–1098, Jun. 2017.

[123] A. Paudel, K. Chaudhari, C. Long and H. B. Gooi, 'Peer-to-peer energy trading in a prosumer-based community microgrid: A game-theoretic model', *IEEE Transactions on Industrial Electronics*, vol. 66, no. 8, pp. 6087–6097, Aug. 2019.

[124] H. Liu, J. Li, S. Ge, X. He, F. Li and C. Gu, 'Distributed day-ahead peer-to-peer trading for multi-microgrid systems in active distribution networks', *IEEE Access*, vol. 8, pp. 66 961–66 976, Mar. 2020.

[125] T. Morstyn, A. Teytelboym and M. D. McCulloch, 'Bilateral contract networks for peer-to-peer energy trading', *IEEE Transactions on Smart Grid*, vol. 10, no. 2, pp. 2026–2035, Mar. 2019.

[126] M. Khorasany, Y. Mishra and G. Ledwich, 'A decentralized bilateral energy trading system for peer-to-peer electricity markets', *IEEE Transactions on Industrial Electronics*, vol. 67, no. 6, pp. 4646–4657, Jun. 2020.

[127] T. AlSkaif, J. L. Crespo-Vazquez, M. Sekuloski, G./ van Leeuwen and J. P. S. Catalão, 'Blockchain-based fully peer-to-peer energy trading strategies for residential energy systems', *IEEE Transactions on Industrial Informatics*, vol. 18, no. 1, pp. 231–241, Jan. 2022.

[128] J. Guerrero, A. C. Chapman and G. Verbič, 'Decentralized p2p energy trading under network constraints in a low-voltage network', *IEEE Transactions on Smart Grid*, vol. 10, no. 5, pp. 5163–5173, Sep. 2019.

[129] M. Yan, M. Shahidehpour, A. Paaso, L. Zhang, A. Alabdulwahab and A. Abusorrah, 'Distribution network-constrained optimization of peer-to-peer transactive energy trading among multi-microgrids', *IEEE Transactions on Smart Grid*, vol. 12, no. 2, pp. 1033–1047, Mar. 2021.

[130] H. Yao, Y. Xiang, S. Hu, G. Wu and J. Liu, 'Optimal prosumers' peer-to-peer energy trading and scheduling in distribution networks', *IEEE Transactions on Industry Applications*, vol. 58, no. 2, pp. 1466–1477, Mar. 2022.

[131] Y. Jia, C. Wan, P. Yu, Y. Song and P. Ju, 'Security constrained P2P energy trading in distribution network: An integrated transaction and operation model', *IEEE Transactions on Smart Grid*, vol. 13, no. 6, pp. 4773–4786, Nov. 2022.

[132] L. Affolabi, M. Shahidehpour, W. Gan, M. Yan, B. Chen, S. Pandey, A. Vukojevic, E. A. Paaso, A. Alabdulwahab and A. Abusorrah, 'Optimal transactive energy trading of electric vehicle charging stations with on-site PV generation in constrained power distribution networks', *IEEE Transactions on Smart Grid*, vol. 13, no. 2, pp. 1427–1440, Mar. 2022.

[133] L. P. M. I. Sampath, A. Paudel, H. D. Nguyen, E. Y. S. Foo and H. B. Gooi, 'Peer-to-peer energy trading enabled optimal decentralized operation of smart distribution grids', *IEEE Transactions on Smart Grid*, vol. 13, no. 1, pp. 654–666, Jan. 2022.

[134] J. Yang, T. Wiedmann, F. Luo, G. Yan, F. Wen and G. H. Broadbent, 'A fully decentralized hierarchical transactive energy framework for charging EVs with local DERs in power distribution systems', *IEEE Transactions on Transportation Electrification*, vol. 8, no. 3, pp. 3041–3055, Sep. 2022.

[135] W. Hua and H. Sun, 'A blockchain-based peer-to-peer trading scheme coupling energy and carbon markets', in *2019 International Conference on Smart Energy Systems and Technologies (SEST)*, Porto, Portugal, Sep. 2019.

[136] C. Liu, K. K. Chai, X. Zhang, E. T. Lau and Y. Chen, 'Adaptive blockchain-based electric vehicle participation scheme in smart grid platform', *IEEE Access*, vol. 6, pp. 25 657–25 665, 2018.

[137] D. Li, Q. Yang, D. An and X. Yang, 'Towards double auction for assisting electric vehicles demand response in smart grid', in *2017 13th IEEE Conference on Automation Science and Engineering (CASE)*, Xi'an, China, Aug. 2017, pp. 1604–1609.

[138] A. Yassine, S. Hossain, G. Muhammad and M. Guizani, 'Double auction mechanisms for dynamic autonomous electric vehicles energy trading', *IEEE Transactions on Vehicular Technology*, vol. 68, no. 8, pp. 7466–7476, Aug. 2019.

[139] J. Kang, R. Yu, X. Huang, S. Maharjan, Y. Zhang and E. Hossain, 'Enabling localized peer-to-peer electricity trading among plug-in hybrid electric vehicles using consortium blockchain', *IEEE Transactions on Industrial Informatics*, vol. 13, no. 6, pp. 3154–3164, Dec. 2017.

[140] S. Thakur, B. P. Hayes and J. G. Breslin, 'Distributed double auction for peer to peer energy trade using blockchains', in *2018 5th International Symposium on Environmentally-Friendly Energies and Applications*, Rome, Italy, Sep. 2018.

[141] A. E. Roth and M. A. O. Sotomayor, *Two-Sided Matching: A Study in Game-Theoretic Modeling and Analysis*. Cambridge University Press, 1990.

[142] S. Parsons and M. Marcinkiewicz, 'Everything you wanted to know about double auctions, but were afraid to (bid or) ask', Jan. 2006.

[143] R. P. McAfee, 'A dominant strategy double auction', *Journal of Economic Theory*, vol. 56, no. 2, pp. 434–450, Apr. 1992.

[144] A. Hahn, R. Singh, C.-C. Liu and S. Chen, 'Smart contract-based campus demonstration of decentralized transactive energy auctions', in *2017 IEEE Power & Energy Society Innovative Smart Grid Technologies Conference (ISGT)*, Washington, DC, USA, Apr. 2017.

[145] C. Long, J. Wu, C. Zhang, L. Thomas, M. Cheng and N. Jenkins, 'Peer-to-peer energy trading in a community microgrid', in *2017 IEEE Power Energy Society General Meeting*, Chicago, IL, USA, Jul. 2017.

[146] R. Rana, S. Bhattacharjee and S. Mishra, 'Energy trading framework for electric vehicles: An assignment matching-theoretic game', *IET Smart Grid*, vol. 2, no. 3, pp. 371–380, Sep. 2019.

[147] H. Liu, Y. Zhang, S. Zheng and Y. Li, 'Electric vehicle power trading mechanism based on blockchain and smart contract in V2G network', *IEEE Access*, vol. 7, pp. 160 546–160 558, Nov. 2019.

[148] W. Zhong, K. Xie, Y. Liu, C. Yang and S. Xie, 'Topology-aware vehicle-to-grid energy trading for active distribution systems', *IEEE Transactions on Smart Grid*, vol. 10, no. 2, pp. 2137–2147, Mar. 2019.

[149] F. Luo, Z. Y. Dong, G. Liang, J. Murata and Z. Xu, 'A distributed electricity trading system in active distribution networks based on multi-agent coalition and blockchain', *IEEE Transactions on Power Systems*, vol. 34, no. 5, pp. 4097–4108, Sep. 2019.

[150] Z. Zhang, R. Li and F. Li, 'A novel peer-to-peer local electricity market for joint trading of energy and uncertainty', *IEEE Transactions on Smart Grid*, vol. 11, no. 2, pp. 1205–1215, Mar. 2020.

[151] H. T. Doan, J. Cho and D. Kim, 'Peer-to-peer energy trading in smart grid through blockchain: A double auction-based game theoretic approach', *IEEE Access*, vol. 9, pp. 49 206–49 218, Apr. 2021.

[152] D. Schürmann, J. Timpner and L. Wolf, 'Cooperative charging in residential areas', *IEEE Transactions on Intelligent Transportation Systems*, vol. 18, no. 4, pp. 834–846, Apr. 2017.

[153] S. Hashimoto, R. Kanamori and T. Ito, 'Auction-based parking reservation system with electricity trading', in *2013 IEEE 15th Conference on Business Informatics*, Vienna, Austria, Jul. 2013, pp. 33–40.

[154] Y. Zhang, Q. Yang, W. Yu, D. An, D. Li and W. Zhao, 'An online continuous progressive second price auction for electric vehicle charging', *IEEE Internet of Things Journal*, vol. 6, no. 2, pp. 2907–2921, Apr. 2019.

[155] Y. Zhao, X. Jia, Q. Yang, D. Li and D. An, 'Towards incentive compatible auction mechanism for electric vehicles bidding in microgrids', in *2018 33rd Youth Academic Annual Conference of Chinese Association of Automation (YAC)*, Nanjing, China, May 2018, pp. 334–339.

[156] J. Bornstein and T. Bain, 'Hurry up and... wait: The opportunities around electric vehicle charge points in the UK', Deloitte, 2019.

[157] JustPark. (2023). JustPark - The Parking App, `https://www.justpark.com/`.

[158] YourParkingSpace. (2023). Your Parking Space, `https://www.yourparkingspace.co.uk/`.

[159] Park on My Drive. (2023). Park on My Drive, `https://www.parkonmydrive.com/`.

[160] Zap-Map. (2021). EV charging stats 2021, `https://www.zap-map.com/statistics`.

[161] Y.-B. Son, J.-H. Im, H.-Y. Kwon, S.-Y. Jeon and M.-K. Lee, 'Privacy-preserving peer-to-peer energy trading in blockchain-enabled smart grids using functional encryption', *Energies*, vol. 13, pp. 1321–1342, 2020.

[162] W. Zhong, K. Xie, C. Yang and S. Xie, 'Auction mechanisms for energy trading in multi-energy systems', *IEEE Transactions on Industrial Informatics*, vol. 14, no. 4, pp. 1511–1521, Apr. 2018.

[163] W. J. Han and S. L. Seaman, 'The winner's curse and optimal auction bidding strategies', *Graziadio Business Review*, vol. 12, no. 2, 2009.

[164] M. Zeng, S. Leng, S. Maharjan, S. Gjessing and J. He, 'An incentivized auction-based group-selling approach for demand response management in V2G systems', *IEEE Transactions on Industrial Informatics*, vol. 11, no. 6, pp. 1554–1563, Dec. 2015.

[165] European Commission, 'Photovoltaic Geographic Information System', 2019, `https://re.jrc.ec.europa.eu/pvg_tools/en/tools.html`.

[166] UK Power, 'Compare energy prices per kWh', 2019, `https://www.ukpower.co.uk/home_energy/tariffs-per-unit-kwh`.

[167] C. Feng, B. Liang, Z. Li, W. Liu and F. Wen, 'Peer-to-peer energy trading under network constraints based on generalized fast dual ascent', *IEEE Transactions on Smart Grid*, 2022.

[168] J. S. Sinclair, 'Power demand management on a low voltage network with a plurality of intelligent sockets', WO/2012/146907, Nov. 2012.

[169] IEEE, *IEEE PES Test Feeders*, 2015, `https://cmte.ieee.org/pes-testfeeders/resources/`.

[170] Electricity North West, *Low Voltage Network Solutions (LVNS)*, 2015, `https://www.enwl.co.uk/go-net-zero/innovation/smaller-projects/low-carbon-networks-fund/low-voltage-network-solutions/`.